Ionic liquids of active pharmaceutical ingredients:

A novel platform addressing solubility challenges of poorly water soluble drugs

Dissertation zur Erlangung des naturwissenschaftlichen Doktorgrades der

Julius-Maximilians-Universität Würzburg

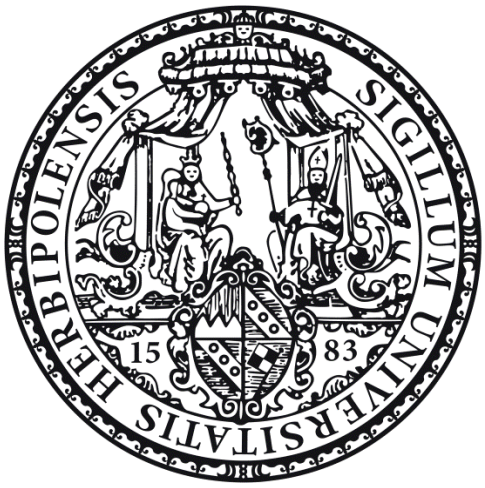

vorgelegt von

Anja Balk

aus Roding

Würzburg 2015

Eingereicht bei der Fakultät für Chemie und Pharmazie am

Gutachter der schriftlichen Arbeit

1. Gutachter:

2. Gutachter:

Prüfer des öffentlichen Promotionskolloquiums

1. Prüfer:

2. Prüfer:

3. Prüfer:

Datum des öffentlichen Promotionskolloquiums

Doktorurkunde ausgehändigt am

Die vorliegende Arbeit wurde in der Zeit von Januar 2012 bis Juni 2015 am Institut für Pharmazie und Lebensmittelchemie der Bayerischen Julius-Maximilians-Universität Würzburg unter der Anleitung von Herrn Prof. Dr. Dr. Lorenz Meinel angefertigt.

Table of contents

Summary

Starting in the late 1990s ionic liquids (ILs) gained momentum both in academia as well as industry. ILs are defined as organic salts with a melting point below 100 °C. Active pharmaceutical ingredients (APIs) may be transferred into ILs by creating salts with a bulky counterion with a soft electron density. ILs have demonstrated the potential to tune important pharmaceutical features such as the solubility and the dissolution rate, particularly addressing the challenge of poor water soluble drugs (PWSD). Due to the tunability of ILs, modification of physico-chemical properties of APIs may be envisioned without any modifications of the chemical structure.

In the first chapter the potential as well as the limitation of ILs are discussed. The chapter commences with an overview of preparation and characterization of API-ILs. Moreover, examples for pharmaceutical parameters are presented which may be affected by IL formation, including the dissolution rate, kinetic solubility or hygroscopicity as well as biopharmaceutical performance and toxicology. The impact of IL formation on those pharmaceutically relevant features is highlighted, resulting in a blueprint for a novel formulation concept to overcome PWSD challenges without the need for structural changes of the API.

Within the second chapter the IL concept is detailed for one specific API - counterion combination. A poorly water soluble acidic API against migraine attacks was transformed into an IL in an effort to minimize the time to maximum plasma concentration (t_{max}) and optimize the overall bioavailability. These studies were conducted in parallel to a prodrug of the API for comparison of the IL strategy versus a strategy involving modification of the API's structure. A significantly longer duration of API supersaturation and a 700 fold faster dissolution rate of the IL in comparison to the free acid were obtained and the underlying mechanism was elucidated. The transepithelial absorption was determined using Caco-2 cell layers. For the IL about 3 times more substance was transported in comparison to the prodrug when substances were applied as suspensions, despite the higher permeability of the prodrug, as increased solubility of the IL exceeded this effect. Cytotoxicity of the counterion was assessed in hepatic, renal and macrophage cell lines, respectively, and IC50 values were in the upper µM / lower mM range. The outcome of the study suggested the IL approach instrumental for tuning biopharmaceutical properties, without structural changes of the API as required for preparation of prodrugs. Thus the toolbox for formulation strategies of poorly water soluble drugs could be extended by an efficient concept.

The third chapter focuses on the effect of different counterions on the physico-chemical properties of an API-IL, in particular to overcome the challenge of poor water solubility. Therefore, the same poorly water soluble acidic API against migraine attacks mentioned above was combined with 36 counterions resulting in ILs and low lattice enthalpy salts (LLES). Depending on the counterions,

different dissolution rates, durations of supersaturation and hygroscopicities were obtained and release profiles could be tailored from immediate to sustained release. Besides, in vitro the cytotoxicity of the counterions was assessed in three cell lines. Using molecular descriptors such as the number of hydrophobic atoms, the graph theoretical diameter and the number of positive charges of the counterion, the dissolution rate, supersaturation and hygroscopicity as well as the cytotoxicity of counterions could be adequately modeled, rendering it possible to predict properties of new LLESs.

Within the forth chapter different poorly water soluble APIs were combined with the counterion tetrabutylphosphonium (TBP) studying the impact on the pharmaceutical and physical properties of the APIs. TBP-ILs and low lattice enthalpy salts were prepared of the acidic APIs Diclofenac, Ibuprofen, Ketoprofen, Naproxen, Sulfadiazine, Sulfamethoxazole and Tolbutamide. NMR and IR spectroscopy, DSC, XRPD, DVS and dissolution rate measurements, release profiles and saturation concentration measurements were used to characterize the free acids and TBP salts as compared to the corresponding sodium salts. The TBP salts as compared to the free acids displayed lower melting points and glass transition temperatures and up to 1000 times higher dissolution rates. The increase in the dissolution rate directly correlated with the salts' hygroscopicity, an aspect which is critically discussed in terms of pharmaceutical translation challenges. In summary TBP ILs of solid salts were proved instrumental to approach the challenge of poor water solubility. The outcome profiled tailor-made counterions as a powerful formulation strategy to address poor water solubility, hence bioavailability and ultimately therapeutic potential of challenging APIs.

In summary, a plethora of ILs and LLESs were prepared by combination of different acidic APIs and counterions. The IL and LLESs concept was compared to conventional salt and prodrug strategies. By choice of the counterion, biopharmaceutical relevant parameters were deliberately modified and release profiles were tuned ranging from immediate to prolonged release. The impact of distinct structural counterion features controlling the dissolution, supersaturation, hygroscopicity and counterion cytotoxicity were identified, correlations were presented and predictive models were built. ILs and LLESs could be proven to be a powerful concept for the formulation of poorly water soluble acidic APIs.

Zusammenfassung

Seit etwa 1990 haben Ionische Flüssigkeiten (IL) großes Interesse sowohl in der universitären als auch in der industriellen Forschung geweckt. ILs werden als organische Salze definiert, die einen Schmelzpunkt von unter 100 °C aufweisen. Arzneistoffe können in ILs umgewandelt werden, indem man Salze herstellt, mit einem voluminösen Gegenion mit delokalisierter Elektronendichte. ILs ermöglichen es wichtige pharmazeutische Eigenschaften wie Löslichkeit und Auflösungsgeschwindigkeit bewusst zu verändern, und im Besonderen stellen sie eine Möglichkeit dar, die Herausforderung, die schwer wasserlösliche Arzneistoffe mit sich bringen, zu bewältigen. Aufgrund der Variabilität von ILs, wird die Anpassung von physikochemischen Eigenschaften von Wirkstoffen denkbar, ohne die chemische Struktur des Stoffes zu modifizieren.

Im ersten Kapitel werden die Potentiale aber auch die Grenzen von ILs dargestellt. Zu Beginn des Kapitels wird eine Übersicht über die Herstellung und Charakterisierung von ILs gegeben. Des Weiteren werden pharmazeutisch relevante Parameter gezeigt, die durch die IL Herstellung beeinflusst werden können, wie beispielsweise die Auflösungsgeschwindigkeit, die kinetische Löslichkeit oder die Hygroskopizität. Daneben können biopharmazeutische Größen und die Toxizität modifiziert werden. Der Einfluss der IL Bildung auf diese pharmazeutisch relevanten Parameter wird zusammengefasst und ein Formulierungskonzept aufgezeigt, um die schlechte Wasserlöslichkeit von Arzneistoffen zu überwinden ohne den Wirkstoff strukturell zu verändern.

Im zweiten Kapitel wird das IL Konzept für eine spezifische Wirkstoff-Gegenion Kombination gezeigt. Ein schwer wasserlöslicher Arzneistoff gegen Migräne wird in ein IL umgewandelt, um eine schnellere und bessere Bioverfügbarkeit im Vergleich zu einem Prodrug zu erreichen. Eine signifikant verlängerte Übersättigung des Wirkstoffes und eine 700-fach schnellere Auflösung des ILs im Vergleich zur freien Säure wurden gemessen und der zugrunde liegende Mechanismus aufgeklärt. Die transepitheliale Aufnahme wurde anhand von Caco-2 Zellen untersucht. Vom IL wurde 3mal mehr Substanz transportiert als von dem Prodrug, wenn Suspensionen der Substanzen appliziert wurden und dies trotz der höheren Permeabilität des Prodrugs, da die verbesserte Löslichkeit des ILs hier überwog. Die Zytotoxizität des Gegenions wurde in einer Leber- und einer Nierenzellinie und in Makrophagen getestet und die IC50 Werte lagen im oberen µM- und unteren mM-Bereich. Die Ergebnisse der Untersuchungen legen dar, dass das IL Konzept hilfreich sein kann, um biopharmazeutische Eigenschaften zu variieren, ohne strukturelle Veränderung des Arzneistoffes, wie es für ein Prodrug nötig ist. Entsprechend konnten die Strategien, um schwer wasserlösliche Arzneistoffe zu formulieren, um ein neues und effizientes Konzept ergänzt werden.

Der Fokus des dritten Kapitels liegt auf dem Einfluss von verschiedenen Gegenionen auf die physikochemischen Eigenschaften von Arzneistoff-ILs, insbesondere um Probleme aufgrund von

schlechter Wasserlöslichkeit zu lösen. Dazu wurde der bereits im zweiten Kapitel genannte, saure und schwer wasserlösliche Arzneistoff gegen Migräne mit 36 Gegenionen kombiniert, wodurch ILs und Salze mit einer geringen Gitterenthalpie (LLES) erhalten wurden. In Abhängigkeit vom Gegenion wurden verschiedene Auflösungsgeschwindigkeiten, Übersättigungsdauern und Hygroskopizitäten erhalten. Durch Verändern des Gegenions konnte sowohl eine sofortige als auch verzögerte Freisetzung des Arzneistoffs erreicht werden. Daneben wurde in vitro die Zytotoxizität in drei Zelllinien bestimmt. Mittels zwei-dimensionaler Deskriptoren, wie der Anzahl der hydrophoben Atomen, dem graphentheoretischen Durchmesser und der Anzahl an positiven Ladungen des Gegenions, konnten die Auflösungsgeschwindigkeit, die Übersättigung und die Hygroskopizität sowie die Zytotoxizität des Gegenions berechnet werden, wodurch es gleichzeitig möglich wird, diese Eigenschaften für neue LLES vorherzusagen.

Im vierten Kapitel werden verschiedene schwer wasserlösliche Arzneistoffe mit dem Gegenion Tetrabutylphosphonium (TBP) kombiniert und der Einfluss auf die pharmazeutischen und physikochemischen Eigenschaften des Wirkstoffes untersucht. TBP-ILs und Salze mit niedrigem Schmelzpunkt wurden von den sauren Arzneistoffen Diclofenac, Ibuprofen, Ketoprofen, Naproxen, Sulfadiazin, Sulfamethoxazol und Tolbutamid hergestellt. NMR- und IR-Spektroskopie, DSC, XRPD, DVS und Auflösungsgeschwindigkeitsmessungen wurden verwendet, um die freien Säuren und die TBP-Salze im Vergleich zu den entsprechenden Natrium-Salzen zu untersuchen. Die TBP-Salze zeigten im Vergleich zu den freien Säuren niedrigere Schmelzpunkte und Glasübergangstemperaturen und eine bis zu 1000-fach schnellere Auflösungsgeschwindigkeit. Ein Nachteil der Salze, die eine schneller Auflösungsrate zeigten, war die damit einhergehende erhöhte Hygroskopizität. Zusammenfassend lässt sich sagen, dass die Herstellung von flüssigen und festen TBP-Salzen hilfreich sein kann, um die Wasserlöslichkeit von Arzneistoffen zu verbessern. Die Untersuchungen lassen den Schluss zu, dass durch maßgeschneiderte Gegenionen neue Formulierungsstrategien für schlecht wasserlösliche Arzneistoffe zugänglich werden, wodurch die Bioverfügbarkeit und der therapeutische Nutzen optimiert werden kann.

Insgesamt wurde eine Vielzahl von ILs und LLESs durch die Kombination von verschiedenen sauren Arzneistoffen und Gegenionen hergestellt. Das IL- und LLES-Konzept wurde mit der klassischen Salz– und Prodrug-Strategie verglichen. Durch die Wahl des Gegenions konnten biopharmazeutisch Parameter bewusst verändert werden und die Freisetzungsprofile von sofortiger bis hin zu verzögerter Freisetzung gewählt werden. Die strukturellen Merkmale der Gegenionen, die entscheidend für die Auflösungsgeschwindigkeit, die Übersättigung, die Hygroskopizität und die Gegenionen-Zytotoxizität waren, konnten gezeigt werden und Berechnungen dazu wurden präsentiert. Abschließend lässt sich sagen, dass die Herstellung von ILs und LLESs ein wirkungsvolles Konzept ist, um schwer wasserlösliche, saure Arzneistoffe zu formulieren

Chapter 1: ‘Pro et contra’ ionic liquid drugs - Challenges and opportunities for pharmaceutical translation

Anja Balk, Ulrike Holzgrabe, Lorenz Meinel*

Institute for Pharmacy, Am Hubland, University of Würzburg,
DE-97074 Würzburg, Germany

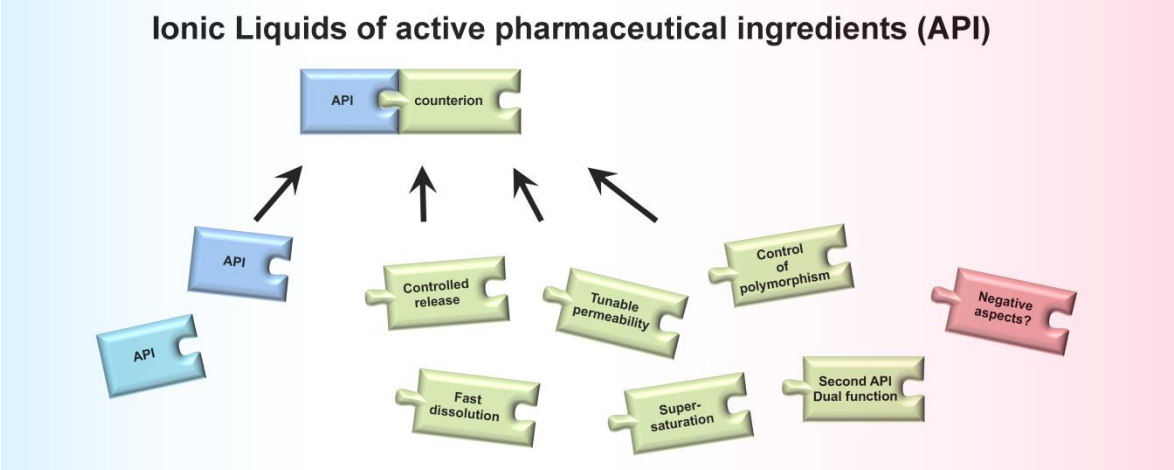

This chapter was originally published in European journal of pharmaceutics and biopharmaceutics, ahead of print 2015; DOI: 10.1016/j.ejpb.2015.05.027, with permission of Elsevier.

Introduction

Starting in the late 1990s the research on ionic liquids (ILs) has attracted rising interest in academia as well as industry [1, 2]. ILs are defined as liquids composed of ionized species with melting points (MP) or glass transition temperatures (TG) below 100 °C [3-5]. Those ILs being liquid at ambient conditions are referred to as room temperature ILs (RT-ILs) [6]. As ions can be deliberately exchanged, a huge number of ILs are easily amenable, offering a plethora of application possibilities [1, 7-9]. It is for this flexibility and variability, that within the chemical applications (solvents), ILs were called ‘designer solvents’[9]. According to their properties and characteristics ILs were classified into three generations [4]. Initially, ILs were particularly interesting as solvents due to their desirable physico-chemical properties, including improved thermal and chemical stability, negligible vapor pressure, non-flammable properties, and a wider liquid range as compared to molecular solvents [2]. The second generation focused on the deliberate tuning of physico-chemical characteristics of ILs for adaptation of properties to a specific task. ILs were designed for use as reaction media and catalysts [2, 8, 10, 11], for separations and extractions [2, 12-15], as electrolytes for electrochemistry [2, 16] application in nanotechnology [17-19], biotechnology [2, 20, 21], engineering [15], lubricants [22, 23], magnetic fluids [24-26], propellants [27, 28] or hydraulic fluids [29]. With increasing insight into their toxicity and biocompatibility ILs were discussed as a formulation concept for active pharmaceutical ingredients (APIs), forming the third generation of ILs and expanding into pharmaceutical application [4]. The third generation has considerably branched to date, ranging from ILs serving as solvents for APIs to APIs which were transformed into ILs themselves by means of creating appropriate salts (API-ILs). One application was the use of ILs as tunable solvents for the dissolution of APIs and replacing common organic solvents [8, 30, 31]. This includes the use for synthesis of APIs [1, 8, 32], as well as analytical approaches [33, 34]. Besides this ILs were used as solvents for proteins [35, 36] or poorly water soluble APIs [30, 37-39] or as excipients for the preparation of microemulsions [40-42].

The focus of this review is on API-ILs and their potential application for medicines of tomorrow. An overview of the metathesis and characterization of API-ILs is presented. Furthermore, ILs are discussed in comparison to typical crystalline salts, focusing on poorly water soluble APIs, which form one of the major technical challenges in the pharmaceutical industry today. This review builds off previous articles reporting on the research and use of API-ILs [6, 8, 31, 43], however, with a particular focus on pharmaceutical *‘pro et contra’* of these formulations and challenges and opportunities of translating them into pharmaceutical and ultimately clinical application.

Classification of ionic liquids

ILs are organic salts composed of ionized species with a MP or TG lower than 100 °C. Depending on the degree of ionization and TG or MP a distinction is made between the following species [5] (**Figure 1**): Salts are considered to be solid crystalline (MP > 100 °C) substances consisting of two

	Ionized ⟶		Neutral
Solid	Salt	Ionic co-crystal Salt solvates	Co-crystal
Liquid (MP<100°C)	Ionic liquid	Oligomeric Ionic liquids	Liquid co-crystal Hydrogen bonded complex Low melting eutectic Deep eutectic mixture

Figure 1: Classification of ionic liquids.

completely ionized oppositely charged molecules (*vide infra*). On the contrary, co-crystals consist of two neutral molecules crystallizing simultaneously without covalent interactions [44]. In between those two extremes are combinations of ionized salts and neutral molecules as ionic co-crystals, hence co-crystals of the API salt and a neutral organic molecule [45]. Similarly, salt solvates, consisting of the API salt and neutral (residual) solvent are between the two extremes of the pure salts and pure co-crystals [5]. The liquid equivalents of salts are ILs, stoichiometric combinations of completely ionized anions and cations. The term IL is somewhat loosely defined such that crystalline and amorphous salts with a melting point below 100 °C also fulfill the definition of ILs. The liquid equivalents to co-crystals are low melting eutectics, deep eutectic mixtures or liquid co-crystals. An example for a liquid co-crystal is the complex of lidocaine and fatty acids [5, 46] as well as the liquid complex of lidocaine and ibuprofen [47]. In both cases proton transfer between acid and base was not determined but a hydrogen bonded complex with strong ion pairing was demonstrated. Liquid intermediates between ILs and liquid co-crystals are oligomeric ILs. Oligomeric ILs are prepared by combining a salt with an excess of free acid or base, resulting in oligomeric ions, which are complexes of ionized and unionized form, sharing a delocalized proton. Examples for oligomeric ILs are tetrabutylphosphonium or lidocainium with the counterion being a complex of salicylic acid and salicylate [48]. Further examples for oligomeric ILs are salicylate combined with a complex of lidocaine and lidocainium or N-methylpyrrolidine with a complex of acetic acid and acetate [48, 49]. The degree of ionicity is

critical for the pharmaceutically relevant properties and fundamental for classification as outlined [5]. We like to direct the reader to excellent previous reviews and manuscripts regarding co-crystals [46, 50] as well as non-stoichiometric liquid salts [48] and focus on API-ILs [8, 31, 43] (**Table 1**).

API	Counterion	Interesting features	Reference
Acetylsalicylic acid	Lidocainium Cetylpyridinium Benzethonium Tramadolium	Dual functional ILs, moisture sensitive	[51]
Amantadine	Benzoate	Dual functional ILs	[50, 52]
Amitriptylin	Dodecyl sulfate (from SDS)	Self-assembly into vesicles , controlled release, better bioavailability	[53]
Ampicillin	Tetraethylammonium Cholinium 1-Ethyl-3-methylimidazolium Cetylpyridinium Trihexyltetradecylphosphonium	Counterion lipophilicity reduses solublilty and increases permeability	[54-56]
Ampicillin	1-Hexadecyl-3-methylimidazolium 1-Hexadecyl-2,3-dimethylimidazolium Cetylpyridinium	ILs with improved antibacterial activity compared to sodium salt	[57]
Bupivacaine	Salicylate Flurbiprofen Diclofenac Saccharinate Acesulfame Docusate Flufenamic acid	Dual functional ILs	[58]
Carvedilol	Phosphate	ILs of small counterions	[59]
Ethambutol	Dibenzoate	Trimorphic IL	[60]
Ethambutol	Adipate	Hygroscopic IL	[61]
Gentisic acid	Tuaminoheptane Amantadine 2-Pyrrolidinoethanol	Dual functional ILs	[50, 52]
Ibuprofen	1-Methyl-3-butylimidazoium	Short alkyl chain→low toxicity, viscous liquid, solid silica particles	[62]
Ibuprofen	Tetrabutylphosphonium	Viscous liquid, ionogels	[47, 63]
Ibuprofen	Bromhexidinium	Formation of hydrogen bonded clusters	[52]
Ibuprofen	1-Butyl-3-methyl-imidazolium 1-Hexyl-3-methyl-imidazolium 1-Octyl-3-methyl-imidazolium	Dependence of micells on chain length of counterions	[64]
Ibuprofen	Didecyldimethylammonium	RT-IL	[4, 7]
Ibuprofen	Benzalkonium	Dual functional IL	[7]
Lidocaine	Salicylate Flurbiprofen Diclofenac	Dual functional ILs	[58]

	Saccharinate Acesulfam Docusate Flufenamic acid		
Lidocaine	Hydrochloride	IL with small counterion	[65]
Lidocaine	Docusate	Controlled release Enhanced bioactivity	[4, 7]
Lidocaine	Ibuprofen	Faster permeation than classical salt through artifical membrane due to ion pairing	[47]
Metformin	Docusate	Dual functional IL	[58]
Penicillin G	Benzalkonium Didecyldimethylammonium Hexadecylpyridinium	Dual functional ILs	[66]
Piperacillin	Hexadecylpyridinium Didecyldimethylammonium Benzalkonium	Dual functional ILs	[66]
Phenazone	Gentisic acid	Dual functional IL	[8, 10]
Prilocaine	Docusate	Dual functional IL	[58]
Procaine	Acetate	RT-IL, crystalline dihydrate	[67]
Procaine	Hydrochloride	IL with small counterion	[59]
Propantheline	Acesulfamate p-toluenesulfonate	RT-ILs	[68]
Pyridostigmine	Saccharinate	RT-IL	[68]
Ranitidine	Docusate	Solution to polymorphism	[4, 7]
Salicylic acid	Didecyldimethylammonium	Dual functional IL	[66]
Salicylic acid	Tuaminoheptane Amantadine 2-Pyrrolidinoethanol	Dual functional ILs	[50, 52]
Salicylic acid	Tetrabutylphosphonium Cetylpyridinium Benzethonium Benzalkonium Hexetidinium Lidocainium Tramadolium Procainium Procainamidium	Dual functional ILs	[31, 51]
Salicylic acid	Cetylpyridinium Benzalkonium 1-ethyl-3-methylimidazolium	Surface actibity, protein binding, membrane permeability	[69]
Sulfacetamide	Benzalkonium	Dual functional IL	[7]
Sulfacetamide	Didecyldimethylammonium Hexadecylpyridinium	Dual functional ILs	[66]
Tetracycline	Docusate	Reduced solublilty and increased logP and liposome –water partition coefficient	[70]
Tuaminoheptane	Benzoic acid	Dual functional ILs	[50, 52]

Table 1: API-ILs in the literature.

Salt metathesis of ionic liquids

The ultimate goal of most if not all efforts for the preparation of liquid salts is establishing low lattice forces between the API and the counterion. This can be effectively achieved by choosing bulky counterions with soft electron density and a minimal number of potential H-bonds among molecules. Typical counterions are monovalent and asymmetric and possess flexible alkyl chains, causing steric inhibition among the salt components [71, 72]. These geometric features increase the degree of rotational freedom resulting in an entropy gain, hence reduction of the free enthalpy of the salt formation process [50]. Entropic changes are confined to a view of the components of the IL itself, as no other molecules are present such as water or other solvents. The counterions must not necessarily be pharmaceutically inert. In fact, some APIs possess IL counterion requirements (e.g. bulky, voluminous side chains, functional groups) and can be the starting point to build ILs together with other APIs, an approach which has been previously referred to as dual functional ILs [73]. Examples for this approach include lidocaine hydrochloride, carvedilol phosphate and procaine hydrochloride [59, 65]. In most pharmaceutical applications, ILs result from proton transfer (Brønsted) which is sometimes specified as protic ILs [50, 74]. API-ILs are usually synthesized by metathesis reactions [43, 58]. Typically the components (API and counterion) are obtained as a certain salt, dissolved in a suitable solvent (e.g. methanol, ethanol, water) within which the IL readily forms at room temperature or upon heating. Unavoidable counterions of the IL components (e.g. the hydroxide counterion of tetrabutylphosphonium and the chloride of procaine hydrochloride, etc.) are eliminated through additional organic solvent, resulting in the precipitation of the inorganic salt impurities or by extracting the ILs in an adequate solvent. Within the pharmaceutical context, these solvents must be carefully chosen, as organic or inorganic residuals are to be minimized during reaction or removed by proper purification. One approach to minimize impurity related challenges is to proceed with plain acid base reactions for the generation of ILs [51], which may require an additional preceding ion exchange step to obtain the free forms of the API and the counterion, respectively [75, 76]. One caveat during acid base reactions are possible pH changes during manufacture, challenging this approach e.g. for acid-labile APIs. One study addressed such stability challenges for the hydrolysis-sensitive acetylsalicylic acid under basic conditions by dissolving the anionic API and the hydrochloride form of the cationic counterion followed by discontinuous addition of $NaHCO_3$ at 0 °C and extraction of the resulting IL into an organic solvent [51]. A solvent free metathesis by melting the free form of the API and counterion was described for salicylate ILs [51] or ethambutol adipate [61].

The exhaustive preparation of protic ILs typically demands a sufficient pKa difference among the API and the counterion, leading to effective proton transfer and complete ionization of the resulting ion pair. Therefore the pka difference (Δ pka) has to be considered for IL preparation. Typical

technical recommendations suggest a Δ pka of 10 for efficient proton transfer / ionization, which is hardly possible for most APIs [77]. However, ionization does not only depend on the pka difference but on structural features of the API and counterion as well [50, 58]. Exemplarily, for procaine diclofenac the Δ pka of 3.9 resulted in 99% of the API being ionized while for lidocaine diclofenac the same Δ pka of 3.9 led only to 6% of ionized API [58]. This discrepancy is at least in part a result of the experimental approach for the determination of pka values in dilute aqueous solutions. These examples demonstrated, that Δ pka values are valuable qualitative predictors for solid or liquid salts but must not be taken as sole parameters when assessing the ionization potential [5]. Therefore with smaller Δ pka than 10 – as typically present for common pharmaceuticals - proton transfer might well be complete. On the contrary, lidocaine (free base) reacted with a fatty acid with Δ pKa ~ 3 resulting in a liquid product, however, without demonstrated proton transfer, indicating that the product was not a salt hence no IL. The components were attracted by hydrogen bonds, such that the product was classified as a liquid analogue of a co-crystal, another interesting approach for liquefaction of pure APIs [46]. These examples demonstrate that the experimental characterization of the degree of ionization is critical for the characterization of ILs and may not be derived theoretically in a reliable fashion.

Characterization of ionic liquids

Deploying API-ILs requires a critical assessment to which extent existing analytical methods are sufficient and exhaustive to guarantee pharmaceutical quality and whether complementary methods need to be developed. API-ILs have not been approved by regulatory authorities to date, hence, this discussion is of pivotal importance in the absence of successful precedence let alone regulatory guidelines [78]. Characterization of pharmaceutical ILs typically includes a qualitative characterization of the proton transfer as a key part of IL science, purity of the product and generally relevant pharmaceutical characteristics of ILs [4, 51, 54, 55, 63, 68, 69, 73, 79, 80]. Since the chemical shift of ^{1}H, ^{13}C, and ^{15}N is closely related to the electron density in Nuclear Magnetic Resonance (NMR) spectroscopy, it can be utilized to monitor the proton transfer from a Brønsted acid to a Brønsted base in a protic IL and to determine the degree of proton transfer and thus whether the substance is ionized or hydrogen bonded complexes are present [58, 81]. Especially ^{15}N atoms show a rather pronounced migration of the chemical shift upon protonation of an amine, which is counterbalanced by its low natural abundance [82]. Moreover, the effective charges of the ions in solvents of different polarity can be measured by means of diffusion and electrophoretic NMR experiments [83]. ^{1}H and ^{13}C NMR spectroscopy can be deployed to monitor reactions and to assess the occurrence of by- and degradation products by simple integration of a pure signal of either compound [84]. Correspondingly, the stoichiometry of cations and anions of an IL containing hydrogens and carbon atoms can be determined, either in solution (when the formation

of the IL is confirmed by the changes of the chemical shift upon proton transfer related to the IL formation) or in solid phase NMR experiments [85]. Information about the structure of the IL complexes might be available by means of 2-dimensional (intermolecular) Nuclear Overhauser Enhancement (NOE) experiments, such as NOESY, ROESY and HOESY [86, 87]. In order to rule out the influence of the solvent, ^{1}H and ^{13}C NMR spectra of pure ionic liquids can be measured in a simple NMR tube (with an insert containing the deuterated solvent). Especially the ^{1}H NMR reflects differences in interaction between ions of varying size and differences in hydrogen bonding interactions. This has been shown for imidazolium ILs with various anions [88]. Infrared spectroscopy (IR) is also instrumental to qualitatively assess the proton transfer and impurities. Thermal analysis (differential scanning calorimetry (DSC) or thermal gravimetric analysis (TGA)) is applied for the assessment of the glass transition temperature or melting point. Besides, the water content (Karl-Fischer titration) is determined and hygroscopicity (during storage) is assessed by dynamic vapor sorption. Halide analyses are performed to detect inorganic impurities from metathesis. X-ray-diffraction (XRD) of single crystals or powders (XRPD) is applied to assess the crystallinity. Solubility and dissolution rate directly impact the bioavailability and are typically tested in water, organic solvents and simulated gastrointestinal fluids. As ILs or the free form of the API may recrystallize from solution, by simultaneous measurements of both liquid-state and solid-state NMR spectra as a function of time a better insight into the crystallization process could be gained [89]. Permeability is assessed by transport of API-ILs through cell layers (Caco-2 cells) or artificial membranes (silicone, hexadecylphosphocholine) [52-54, 85]. Besides, electrospray ionization mass spectrometry (ESI-MS) and conductivity and viscosity measurements (Walden plots) are quite frequently used to determine aggregate formation of cation and anion [90-92] and NMR may also be used to address aggregates by measurement of concentration-dependent ^{1}H NMR spectra on the one hand [93-95] and NOESY experiments on the other hand, resulting in critical aggregation concentration and aggregation numbers [85]. These aggregates are of particular interest within the pharmaceutical context, as these phenomena may impact membrane transport and, therefore, bioavailability (*vide infra*) [52]. Another challenge is storage stability (shelf-life) and few studies are available assessing the physico-chemical properties as a function of stressed storage conditions. In particular, for solid amorphous ILs recrystallization may occur as they may be present as supercooled amorphous glassy phases. By running several heating and cooling cycles by DSC, the original state of the IL may be determined from the first heating cycle. The cooling cycle is instrumental for the assessment to which extent the IL recrystallizes and from the second heating cycle the formation of a supercooled phase can be assessed, e.g. if a melting point was detected during the first heating cycle but a glass transition temperature during the second cycle [68]. In case of recrystallization, crystallinity should be assessed by XRPD in comparison to the original substance. The specification must be a stability of at least 2 years upon manufacture [96].

Other considerations akin to any new pharmaceutical salt include the assessment of the potency as appropriate [56, 73] and the protein binding of ILs to determine the impact of the counterion on API binding and whether the complex of API and counterion binds to the protein or whether there is a competitive binding of API and counterion after partial dissociation [69]. Further studies on API-ILs include biological activity assessment and cytotoxicity experiments (*vide infra*). Few animal trials and no human trials are reported to date.

Ionic liquids as pharmaceutical salts

Approximately 50% of all APIs are administered as salts [97]. These salts typically have melting points far exceeding 100 °C (which when below would qualify them as ILs) and one of the main drivers for the high melting points is the need for sustained stability during storage – a specification posing an inherent challenge to amorphous APIs, molecular dispersion drug products, or polymorphs not being in the lowest free enthalpy state [98]. Salt formation or ‘salification’ is motivated by positive impact on API stability, kinetic solubility, dissolution rate and ultimately bioavailability as compared to the free form of the API [99]. Consequently, new APIs enter a broad salt selection program in pharmaceutical development before larger toxicological studies or even first in man studies commence. The impact of appropriate salts is indirectly reflected by means of the possibility to generate new intellectual property for API salts if those were not addressed in the initial patent covering the novel API. This is occasionally referred to as “secondary patents” as these typically come after innovation on the API itself or, more specifically, when these contain secondary claims only, “independent secondary patents”. It has been estimated, that independent patents on salt claims (or polymorphs, isomers, products, etc.) add an average of 6.3 years of patent life to a chemical compound patent [100]. Thereby, ionic liquid approaches with rather uncommon or novel counterions may substantially contribute to the “evergreening”/life cycle management of pharmaceutical patent portfolios aiming to foster their monopoly status [101]. Similarly, new salts of an API may be recognized as new chemical entities by the Food and Drug Administration (FDA) agency and other health authorities. Salt preparation for ionizable drugs, and in particular for poorly water soluble drugs (PWSD) is one of or perhaps the most effective and developable approach to optimize pharmaceutical parameters including kinetic solubility and dissolution rate [99]. The challenge of PWSD has constantly grown as a result of research strategies, which due to high-throughput screening for lead identification, tend to identify lipophilic molecules with high molecular weight which are typical molecular features of PWSDs. Approximately 70% of the new APIs found today belong to this category [102]. This development fueled the need for rather complex drug formulations which in return increase the risk of the overall development plan. This risk is not only problematic from a technical perspective (challenge of upscaling of complex forms; potential by- and degradation products of several excipients required for these formulations and

associated analytical challenges; purity and batch-to-batch homogeneity of starting materials; up-scaling challenges; missing know-how in companies or driving the dependency of companies to specialist know-how, etc.) but unknown pharmaceutical dosage forms may easily translate into fluctuating pharmacokinetics and safety and efficacy profiles. Surprises are what most pharmaceutical development programs encounter at one or more stages of their development cycle but obviously, these must be minimized to the maximum possible extent. Consequently, one of the arising needs is to find pharmaceutically acceptable approaches to tackle the challenge posed by the increasing presence of PWSDs while avoiding the need for complex drug products. One of the alternatives is to complement current standard salt screening programs [97] by tailored counterions for new APIs failing expectations after routine screenings. One of the frequent oppositions by formulation scientists is the potential toxicity of novel counterions which might require some balance in light of the known safety issues of several excipients in complex formulations, which are so readily used today. Manufacturing ability is another driver for salt screening tailoring aspects such as compressibility and friability. However, also negative consequences have been reported for salt formation. For example, an increase in water sorption has been described as a result of the changed polarity of surface chemical groups of the salt as compared to the free form of the API [103]. Another drawback is the increase in molecular mass particularly when larger counterions are used. This aspect is of importance when indications/APIs requiring high doses are targeted and/or situations for which volume limitations exist at the site of administration.

As mentioned before, many APIs enter salt screenings to increase physical stability during storage and pharmaceutical properties for manufacture, storage, and treatment alike [97]. For exhaustive salification the API and counterion pKa as well as the pH of maximum solubility (pH_{max}) and the solubility product (K_{sp}) of the salt are considered, as effective salt formation is limited to the salt plateau [99]. In general, pKa values of API and counterion should differ by at least 3 log units for effective proton transfer [104]. As most APIs being weak acids or bases their solubility is a function of the environmental pH. If a basic (monoprotic) API or the corresponding salt is dissolved in water the concentrations of base [B] and salt [BH^+] can be calculated from $K_a = \frac{[B][H_3O^+]}{[BH^+]}$. Similarly, for an acidic (monoprotic) API (A) the correlation is $K_a = \frac{[AH]}{[A^-][H_3O^+]}$. If the solution is saturated the pH-solubility profile of drugs can be described by two independent curves, one for which an excess of the free form is present and one for which the corresponding salt is present (**Figure 2**). The pH_{max} is the pH value where both the free form and the salt coexist and which separates the two curves. Recrystallization of the free form occurs, if the pH of the solution exceeds the pH_{max} value (**Figure 2**).

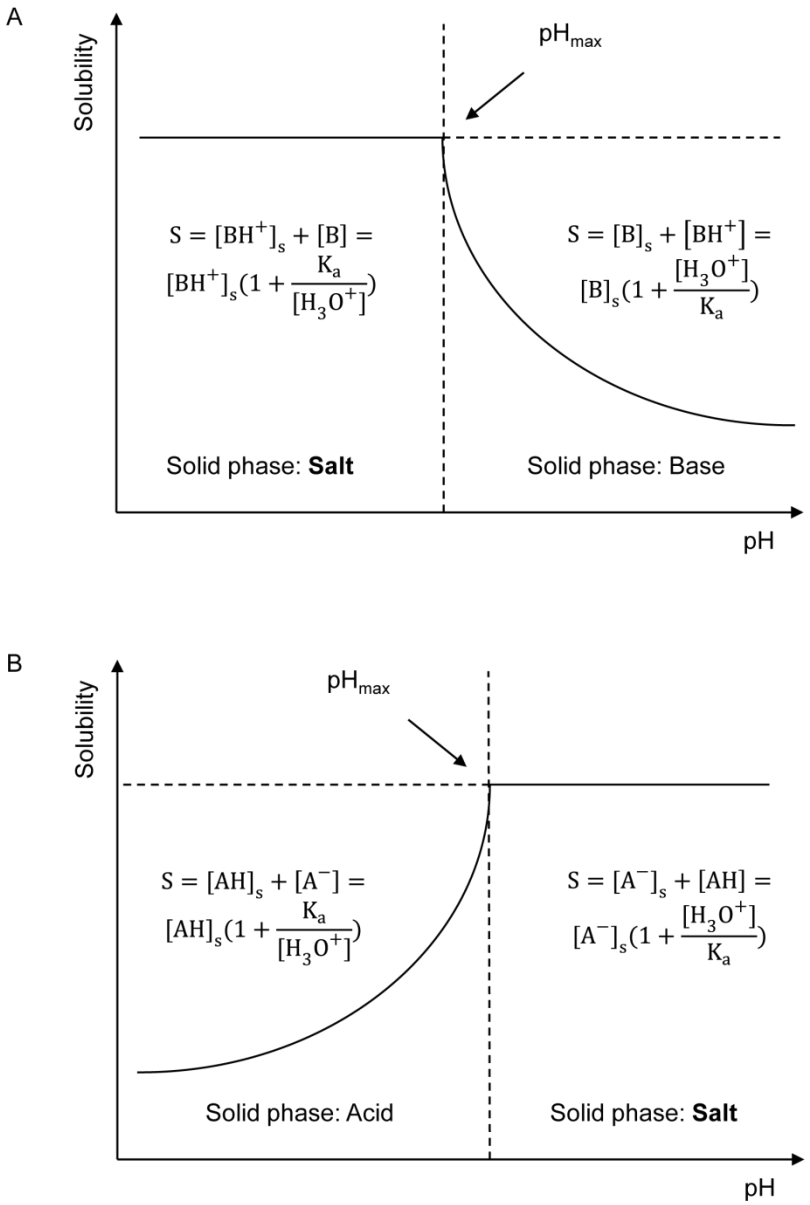

Figure 2: Solubility of salts of weak acids and bases as a function of the pH.

At pH < pH$_{max}$ a basic API is mainly ionized (salt form) and in a saturated solution. Addition of further acid will almost completely convert the API into the salt. The pH will not change until all solid substance is transformed into the salt. The total solubility S at that pH can be expressed by

$$S(base; pH < pH_{max}) = [BH^+]_s + [B] = [BH^+]_s(1 + \frac{K_a}{[H_3O^+]})$$

The subscript 's' indicates that saturation concentration is reached. From the equation it can be derived that at pH < pka only very low amounts of free base are present in solution and the total solubility mainly depends on the saturation solubility of the salt. Therefore, a plateau is reached. In the plateau region the solid phase is completely converted to the salt form and this is why salt

formation (metathesis) is done in this pH region. Within the second part of the curve for pH > pH_{max}, the substance is present as free base as solid excess substance. The total solubility can be calculated by

$$S(base; pH > pH_{max}) = [B]_s + [BH^+] = [B]_s(1 + \frac{[H_3O^+]}{K_a})$$

With increasing pH the amount of the ionized form decreases and the solid substance is the free base. Therefore this pH region is not suitable for salt preparation. For acidic compounds (A) similar calculations are applicable:

$$S(acid; pH < pH_{max}) = [AH]_s + [A^-] = [AH]_s(1 + \frac{K_a}{[H_3O^+]})$$

$$S(acid; pH > pH_{max}) = [A^-]_s + [AH] = [A^-]_s(1 + \frac{[H_3O^+]}{K_a})$$

The plateau region is reached at pH > pH_{max} and this region is suitable for salt preparation for acidic APIs [99]. Therefore, the pH_{max} value is important to decide at which pH a salt can be prepared. Furthermore, the pH_{max} defines the pH range when the dissolved salt will considerably commence its conversion into the free form and, therefore, potentially crystallize or precipitate from solution. One challenge from this consideration applies for acidic API salts, which in acidic gastric fluids may convert to the free form, increasing the risk of precipitation and reduced bioavailability. Therefore, for acidic API salts low pH_{max} values are needed and salts should typically be protected from the gastric pH e.g. by enterically coated tablets with the ultimate goal that API release from the tablet is prevented at sites with pH values lower than the pH_{max}. The pH_{max} is calculated from the pKa of the API, the intrinsic solubility S_0 and the solubility product K_{sp} [99] by

$pH_{max} = pK_a + log\frac{S_0(Base)}{\sqrt{K_{sp}}}$ for bases and by $pH_{max} = pK_a + log\frac{\sqrt{K_{sp}}}{S_0(Acid)}$ for acids.

The API's solubility is directly impacted by its lipophilicity and melting point [105]. Once the API and counterion are ionized their lipophilicity is rather low, favoring their solubility in polar solvents. By combination of one API with different counterions to a salt, the counterions' size and lipophilicity impact the overall solubility of the API [106]. Besides, the melting point is indirectly related to the overall solubility product (K_{sp}) [106]. Therefore, both lipophilicity and melting point are important for rationale selection of a counterion. As a rule of the thumb, the larger the counterion, the lower is the melting point and the higher is the kinetic solubility [106, 107]. The lower the melting point, the higher is the possibility that an ionic liquid is obtained.

Typically, small inorganic counterions are used for salt preparation including sodium, potassium and calcium for acidic APIs and chloride, sulfate, bromide and phosphate for bases [108, 109]. Notably, the K_{sp} affects the total kinetic solubility of a salt. For example, if chloride is chosen as counterion, the gastric and intestinal chloride concentration is affecting the K_{sp} on top of the chloride counterion. Thereby, precipitation of the salt may occur - an observation referred to as the “common ion effect”. The common ion effect is relevant at the salt plateau, e.g. in cases in which the environmental pH is above or below pH_{max} for bases and acids, respectively (irrelevant for bases *in vivo*, as pH exceeding 7.4 is rarely found) [97, 99]. Other commonly used counterions, which are listed by the FDA as ‘generally regarded as safe’ substances (GRAS), include “larger” organic anions like mesylate, maleate, citrate tartrate and aceteate or cations like N-methylglucamine [109]. However organic counterions pose an additional risk of side reactions during metathesis. Safety challenges were reported for the genotoxic alkylmesylates in mesylate salts, due to impurities of the methane sulfonic acid used for salt preparation [110, 111]. As ILs are liquid salts the above considerations are also applicable for API-ILs. Thus the pka of the API and counterion is not only important for the degree of ionization but may critically impact the recrystallization of API or counterion at different pH values. As mentioned for salts, enteric coating is necessary for ILs with pH_{max} values below gastric pH.

Ionic liquids of active pharmaceutical ingredients

Impact on kinetic solubility and release profiles

The formation of ionic liquids combines the concept of salification (*vide supra*) and the reduction of the melting point to increase the dissolution rate and the solubility. Detailed reports on API-ILs solubility have been published [4, 54, 57, 70, 71, 80, 112]. For example, one study reported on several acidic APIs for which salts were formed with tetrabutylphosphonium (TBP). These salts displayed a decreased melting point as compared to the free form and corresponding sodium salts. Moreover, the TBP salts (whether ILs or crystalline salts) had a higher kinetic solubility and faster dissolution rate than the free API forms. However, in comparison to the sodium salts no unanimous (in a sense of increasing) effect on solubility was reported among the tested API-ILs [80]. Furthermore, and in spite of the overall MP reduction for all reported TBP salts not all of these displayed an improvement on the dissolution rate when compared to the sodium salts. These data demonstrated that a robust comparison of the IL counterions to small inorganic and conventional counterions (sodium, chloride, etc.) is important. Correspondingly, for 4 choline API-ILs an improved solubility in comparison to the free form was reported, but the data set did not include a comparison to conventional small and inorganic salts [112]. A reduced kinetic solubility upon replacement of conventional counterions by bulky counterions was observed for several API-ILs

[4, 55, 57, 70, 71]. For example, creating ampicillin ILs with pyridinium or imidazolium counterions resulted in a 100 to 150 fold reduced kinetic solubility as compared to the sodium salt [57] and the use of trihexyltetradecylphosphonium transformed ampicillin into a water insoluble liquid [55]. In other studies the formation of ampicillin ILs with tetraethylammonium (TEA) and 1-ethyl-3-methylimidazoium (C_2MIM) as counterions resulted in lower kinetic solubilities as compared to the sodium salt, while 1-hydroxy-ethyl-3-methylimidazolium (C_2OHMIM) and choline based ILs displayed comparable kinetic solubilities. This high kinetic solubility of C_2OHMIM was linked to the additional hydroxyl group of the counterion and the resulting impact on polarity and hydrogen bonding capacity. Besides, the TEA IL was less soluble than the C_2MIM IL which was attributed to the more exposed charge of the imidazolium in comparison to the rather shielded charge of the TEA [54]. Furthermore, an indirect correlation between the counterions’ lipophilicity - as determined by octanol-water partition - and solubility was observed for these 4 ampicillin preparations [54]. Similarly, for tetracycline docusate the less than half kinetic solubility as compared to its hydrochloride salt was linked to the three times higher lipophilicity, as assessed by octanol-water partition [70]. One of the conclusions from these studies is that successful kinetic solubility improvement by means of IL preparation is a balancing act of melting point reduction (supporting kinetic solubility) and counterion lipophilicity (reducing kinetic solubility). Predictive models are currently developed.

The molecular mechanisms leading to an improvement of kinetic solubility for APIs/counterions are quite instrumental in shaping a strategy for the salt program. This has been demonstrated in a study, focusing on solubility and supersaturation of an API-IL [85]. The prolonged supersaturation of the IL in comparison to the potassium salt was linked to the aggregates formed of the API and counterion as determined by NMR. The acidic API with a pKa of 6.7 was prone to recrystallize as the free form in neutral aqueous solutions. In contrast to the potassium ion the counterion tetrabutylphosphonium (TBP) interacted with the API and stabilized its ionized state, thereby keeping it at a much higher kinetic solubility. At this supersaturated state, observed amorphous precipitates of the IL were composed of anionic TBP and cationic counterion. One of the consequences was that, the ratio of the dissolution rate in comparison to the precipitation rate was significantly increased for the IL as compared to the potassium salt, thereby fueling the kinetic solubility of the IL in contrast to the potassium salt.

In addition to affecting the state of protonation at supersaturated states, the counterion may impact the kinetic solubility by API solubilization upon dissolution. IL counterions are charged and typically have an apolar side chain, rendering them amphiphilic and therefore micelles can be formed. The API in solubilized state may integrate into or onto these micelles, improving kinetic solubility. This will be particularly the case for amphiphilic counterions, and solubilization is a

quite frequently discussed mechanism for chemical applications (e.g. solvent properties) but less frequently discussed from a pharmaceutical point of view [113-115]. For APIs, some studies deployed surface active quaternary ammonium counterions for IL formation, molecules which are pharmaceutically known as penetration enhancers through biological membranes [73]. Besides, micelle formation was reported for three salicylate API-ILs [69]. For ibuprofen ILs the mechanism was analyzed in more detail with a focus on the impact of the alkyl chain length on micelle structure. 1-Alkyl-3-methyl-imidazolium derivative (C_nMIm) counterions with alkyl chain lengths of n = 4, 6, or 8 were used to prepare ILs. The interesting article detailed the impact of the counterion’s alkyl chain on stoichiometry of the resulting micelles and provided another example to which extent physical-pharmaceutical properties can be tailored by counterion design [64]. In fact, the design space within which API properties can be adapted is extending beyond kinetic solubility considerations or dissolution rates, as controlled release profiles can be targeted as well. Controlled release in a strict sense is present, if dissolution from the solid state is the rate limiting event in a chain of others, typically ending with the pharmacokinetic profile, i.e. the concentration profile of the API in the circulation. In cases in which the dissolution is retarded to an extent that API uptake from the site of injection or transport through the biological barrier is faster, the absorption kinetics are controlled by the pharmaceutical formulation. If the dissolution rate is slower than the metabolism of the API, the entire pharmacokinetic profile is controlled by the IL, a feature, which is typically less relevant for oral but for parenteral administration. Practical limitations for oral application are due to the duration of gastrointestinal exposure to the API, with sustained release profiles being particularly intriguing for rather fast metabolized APIs (less than 6 hours). A general constraint of any retarded as compared to instantaneous availability is the dampening impact on the maximal concentration of the pharmacokinetic profile, which is frequently accommodated for by increasing the dose. Further concerns apply for APIs with narrow absorption windows for which retardation of release translates into a substantial reduction in bioavailability. One example reported sustained release for the API-IL of amitriptyline and the counterion sodium dodecyl sulfate (SDS), which resulted in retarded release as compared to the hydrochloride salt. By using SDS as a counterion, self-assembling vesicles were formed. This was linked to electrostatic interaction between the API and the counterion leading to a retarded release from the vesicles for the IL. Furthermore, the hemolytic toxicity of the amitriptyline IL was determined (surfactants may damage cell membranes) but no increased toxicity was detected following IL formation [53]. Amitriptyline’s half-life is well beyond 6 hours and, therefore, the controlled release profile following potential oral use is of less pharmaceutical interest. However, the study outlined the potential to tailor API release kinetics when released from different salt forms, a feature which typically requires more complex dosage forms than amenable through simple salt formation. Therefore, IL formation offers an interesting possibility to deliberately tune

dissolution rate, stabilization of IL in solution and API release by choice of the counterion. Similarly, the approach has been deployed before for absorption from other sites, e.g. a reduced dissolution of the topically applied lidocaine docusate IL as compared to its hydrochloride salt was linked to longer residence time on the skin and potential longer effect [71].

In summary, rationally designed counterions are instrumental to tailor the kinetic solubility and dissolution rate of API salts. Furthermore, a balance has to be achieved between desired properties (e.g. in most situations increased kinetic solubility or faster dissolution rate) and undesired properties (e.g. in most situations decreased kinetic solubility or slower dissolution rate), which are introduced by the respective counterions. In some situations, the slower dissolution rate might be interesting for controlling API release as long as overall bioavailability is not compromised. In this case, extremely simple salts may challenge the use of complex pharmaceutical controlled release dosage forms, with positive impact on the complexity of technical development, analytics, and production. The counterion may also act as a solubilizing agent upon release, which is relevant for amphiphilic molecules with longer alkyl chains. In essence, the proper design of a counterion can tailor both, the pass over rate of API-counterion aggregates from the solid into the liquid state and API concentration profiles in solution.

Permeability and absorption

The movement through membranes is described by the term drug transport, summarizing processes and transport systems facilitating uptake. Drug transport is among other factors mainly impacted by the physico-chemical properties of the API salts. Proper counterion choice is instrumental to tune the overall physico-chemical properties. Providing passive transport only hydrophilic ionized APIs hardly permeate intact lipid membranes of an epithelial barrier unless they are small enough to pass ‘aqueous pores’ [116, 117]. A design strategy for these APIs can aim for modulating their overall lipophilicity in an effort to increase trans-epithelial transport in those cases in which drug transport through these barriers is rate limiting. This increase in overall lipophilicity may come at the expense of a reduced dissolution rate and care is warranted that the rate limitation would not flip from the permeation to the dissolution. With increased permeation, the overall bioavailability can be improved for the API. The approach to increase the lipophilicity by counterion mediated charge shielding of the API, resulting in neutral aggregates has been reported before and was assessed by increased partitioning into an apolar octanol phase [72, 118]. Improved drug transport into red blood cells of whole blood, as a more biorelevant model, was demonstrated for polar anions after pairing with lipophilic ammonium cations [119]. However, it was not assessed to which extent dissociation of the salt occurred before permeation, to which extent the counterion is absorbed and whether a permeation enhancement due to surface activity of the counterion had an impact on the

result. Similarly, for ampicillin ILs with ammonium and imidazolium counterions ion pairing was reported to increase hexadodecylphosphocholine membrane transport, while surface activity was determined for the counterion at the same time [54]. Likewise, ion pairing was stated for three salicylate API-ILs using the surface active molecules cetylpyridinium, benzalkonium and 1-ethyl-3-methyl-imidazolium as counterions, respectively [69]. The reported data demonstrate improved partitioning and membrane transport, however, the existence of ion pairs simultaneously permeating the membrane has to date not been demonstrated directly, such that one could differentiate the impact of a possible undissociated ion pair *versus* dissociated ion pairs for which the surface activity of the (dissociated) counterion was the reason for an enhanced API permeability. Future studies e.g. using PAMPA membranes, Caco-2 monolayers and *in vivo* pharmacokinetic studies including blood partitioning should aim at detailing this important aspect.

Nevertheless, some insight has been provided. For example, the transformation of ampicillin into an IL using the apolar counterion cetylpyridinium increased the permeability and antibacterial activity, while highly polar small cations like choline displayed no improved effect [56]. Likewise for an IL of the rather polar counterion tetrabutylphosphonium membrane transport was not improved as compared to the free API in a Caco-2 cell permeation assay [85]. These studies provide preliminary evidence, that the lipophilicity of the counterions is a relevant driver for API permeation but cannot elucidate to which extent incomplete dissociation or counterion surface activity upon dissociation lead to this observation. The same applies for the improved membrane transport, demonstrated in a parallel artificial membrane permeation assay (PAMPA) for the API-IL amitriptyline dodecylsulfate which was linked to results in rabbits for which a higher absorption was observed after oral administration. It has to be considered that dodecylsulfate is a surface active molecule and thus may influence drug absorption [53]. Arguably, the “ion pair” hypothesis (i.e. incomplete dissociation renders the salt more hydrophobic, hence supporting passive transport across lipophilic membranes) finds support in another study for the ampicillin ILs of cetylpyridinium (CP) and hexadecyldimethylimidazolium ($C_{16}M_2Im$) for which improved bactericidal activity was described as compared to its sodium salt or to a mixture of the ampicillin sodium salt and bromide salt of the bulky counterion for IL preparation. Thus it was demonstrated that the supplementation with the counterion had no solubilizing effect affecting membrane permeability of the sodium salt. Therefore, enhanced efficacy was attributed to the increased lipophilicity of the API-counterion aggregate, resulting in a more effective perturbation of the bacterial walls [57]. Other studies linked ion pair formation to improved membrane permeability. For example, ion pairs of salicylate combined with 2-amino heptane as counterion (N_TH_3Sal) crossed a silicon membrane as rapidly as the unionized neutral salicylic acid and 10 times better than the sodium salt. Disruption of aggregate formation of N_TH_3Sal by propylenglycol reduced permeation to the level of the sodium salt [73]. Similarly, the complex of ibuprofen and lidocaine

([Lid][Ibu]) resulted in a simultaneous membrane transport of both APIs with a faster rate as compared to the corresponding crystalline sodium and hydrochloride salts [109]. However, both N_TH_3Sal and [Lid][Ibu] were hydrogen bonded complexes rather than ILs (*vide supra*). In summary, IL formation may substantially increase drug transport. The mechanism may depend on the counterions and needs to be further studied to assess the extent of ion pair formation and the stability in biorelevant fluids with a focus on the dissociation pattern of aggregates before and after permeating the membrane. One straightforward approach would be through *in vivo* data to assess the amount of absorbed API and concomitantly of the counterion. Tailor-made counterions may be an intriguing strategy to modulate transport kinetics across membranes, particularly as by formation of relatively stable ion pairs, "apparent" physico-chemical properties of APIs can be transiently modified for passage. This feature is far beyond of what even complex pharmaceutical formulations are able to accomplish, which upon release of the API molecule cannot impact uptake – unless often problematic membrane disruptive excipients are co-administered. Future studies must detail this exciting potential on drug transport in light of the ability to tailor – in a transient way – the physico-chemical properties of an API by counterion design.

Control of Polymorphism

One of the frequently cited advantages of room temperature ILs (RT-IL) is the principle inability to form solid structures, including different crystal forms or polymorpis. Polymorphism may result in different physico-chemical properties for each crystalline form of the API. These different forms may relevantly affect manufacture, stability, solubility, and bioavailability [8, 31, 120-122]. Obviously, only RT-ILs offer the advantage of polymorphism control whereas ILs with MP/TG exceeding RT may not. For instance, three polymorphs were found for the solid IL ethambutol dibenzoate [60]. The strategy to overcome the challenge of different crystalline forms was impressively demonstrated for ranitidine hydrochloride, which is existing in at least two different forms [123]. Transforming ranitidine into an RT-IL by the use of the counterion docusate effectively addressed the challenge of polymorphism for this H2 receptor antagonist [4]. Similar successes were reported for propantheline bromide - a muscarinic acetylcholine receptor antagonist – which resulted in a RT-IL by using the counterions acesulfamate or p-toluenesulfonate [68, 71]. Other efforts aimed at the ibuprofen sodium polymorphism [124], naproxen sodium pseudo-polymorphism [125], or the polymorphism of the free naproxen acid [126], which were transformed into stable RT-IL with tetrabutylphosphonium (TBP) [63, 80] and for ibuprofen also with 1-alkyl-3-methylimidazolium [127]. In conclusion, transforming APIs into RT-ILs is an appropriate approach to address polymorphism challenges.

Expanded application options

Liquid RT-ILs can be a desirable API form in cases in which solid particles are problematic. One aspect is manufacturing and analytical control, thereof. Generally for characterization of an API powder the particle size, particle morphology and size distribution are key parameters affecting dissolution, solubility, powder fluidity, miscibility compressibility and further process parameters. With liquid APIs these parameters are largely irrelevant [31]. Besides, certain applications demand particle-free formulations. For example, for eye ointments or application on skin particle size should be smaller than 100 µm to avoid irritation. Especially for poorly soluble substances or if high concentrations are required a liquid API could facilitate the preparation of an adequate formulation. These challenges may be met at times by transforming APIs in RT-ILs. One example was suggested for transdermal drug delivery [128]. The study detailed the disruptive role on biofilms of the IL, thereby enhancing the drug transport of the antibiotic API into the bacteria. Four ILs were prepared, which were proved to be effective against biofilm-forming gram-negative pathogens, *Pseudomonas aeruginosa* and *Salmonella enterica*. Among them the use of two counterions, tetraalkylphosphonium oleate (TAPO) and tetraalkylphosphonium hexanoate (TAPH), facilitated the transport of the respective IL with the model “API” mannitol into skin. For the TAPO IL, mannitol delivery was increased into the superficial layers of the skin while TAPH shuttled mannitol even into deeper tissue layers. Moreover, the ability of the two ILs to enhance skin penetration was assessed using the model antibiotic cefadroxil. ILs from cefadroxil/TAPH and cefadroxil/TAPO delivered 15-20% of the applied API dose, which was approximately fivefold better as compared to cefadroxil itself [128]. Furthermore, the ILs had a low skin irritation potential in spite of demonstrated irritation in response to the individual components (TAPH or TAPO).

Within the context of expanding therapeutic application of APIs, RT-ILs may offer exciting novel options. Successes have been demonstrated for RT-ILs which facilitated intra- and transdermal delivery of APIs, and better efficacy was determined for antibiotics. One study demonstrated a reduced skin irritation for an API transformed into an RT-IL, however, robust toxicity studies are required to corroborate these initial findings (e.g. Magnusson and Kligman test on the allergenic potential [129], repeated daily topical administration for 4 weeks, and Vinson & Borselli test on the photosensibilizing potential [130]).

However, the resulting RT-ILs are typically viscous fluids which may pose specific handling challenges (e.g. pumping) in manufacture or quite hygroscopic posing challenges for dosing accuracy, impacting the stability of the surrounding dosage form (e.g. a hard gelatin capsule may dry out and break) or film coatings (cracks may form jeopardizing film integrity) as well as required environmental demands during manufacture, filling, and storage.

Translating API-ILs into pharmaceutical manufacturing

Liquid instead of solid salts

ILs are extensively used in chemistry, replacing volatile organic solvents or for electro-chemical applications. However, application as a formulation principle is still in its infancy. The challenge particularly applies for RT-ILs, as liquid and viscous images cannot be processed or pose substantial engineering hurdles. One of the approaches to overcome this challenge is to adsorb RT-ILs on solid carriers. Such immobilization of ILs was demonstrated on mesoporous silica, resulting in free flowing powders of TBP ibuprofenate and lidocainium-ibuprofenate with drug loads up to 20% and complete drug release was demonstrated within 5 minutes [63]. Another example for immobilization of an IL is the preparation of Ionogels, using tetramethoxysilane alone or together with methyltrimethoxysilane [62, 131]. For the API-IL imidazolium ibuprofenate the preparation of an Ionogel achieved drug loads of about 50%. Release kinetics were retarded as compared to the pure API, demonstrating the potential of Ionogels for controlled release [62]. However, these approaches result in a mass increase; hence, the same API dose requires substantially higher masses of the API-IL-hydrogel or API-IL/particle complexes. At times, this may be critical in instances in which only low volumes may be applied.

Besides, a typical approach for liquid or semi-solid preparations for oral application is the encapsulation into soft gelatin capsules or sealed hard gelatin capsules [132, 133]. In both cases the IL may be directly filled into the capsules, however, the water content of the filling has to be controlled carefully. As moisture from the capsule shell may migrate into the filling and *vice versa* the shell may lose water and become brittle or moisture increase may cause softening of the shell. It has to be assured that water content of the shell and the filling as well as the humidity during storage results in an equilibrium state with the capsule shell containing the desired percentage of water. Models for prediction of the optimal initial moisture contents for the empty capsule and the filling were reported before, offering more guidance for formulation scientists [134].

Counterion toxicity

Many counterions are bulky with lipophilic parts while charged at the same time, features typically resulting in surface activity and a potential risk of skin or mucosa irritation. However, by now many interesting approaches for IL preparation were made with counterions ‘generally recognized as safe’ (GRAS) and listed by the FDA as such [9, 68, 128]. A common example is docusate which was reported to form ILs with lidocaine, ranitidine and propantheline [4, 72]. Further counterions of this list are quaternary ammonium counterions, choline, p-toluenesulfonate or artificial sweeteners including saccharinate, acesulfamate and cyclamate [31, 68]. Other harmless options

include naturally occurring amino acids [75, 76, 135] or fatty acids [38]. Novel counterions require toxicological profiling, likely alone and as salts with the respective API at question. Cytotoxicity has been frequently assessed for some counterions, e.g. imidazolium counterions, and quantitative structure–activity relationship models (QSAR models) were postulated [136-139]. Aquatic toxicity was correlated with counterion lipophilicity [140]. Cell viability in mouse macrophages (J774) for choline phosphate ILs was profiled and the EC_{50} values were linked to anion mass size and the presence of moderately long and / or branched alkyl chains of the counterion [141]. An analogous correlation was reported from studies using the human breast cancer cell line MCF7 and the counterions pyridinium, pyrrolidinium, piperidinium and imidazolium with different alkyl chain lengths [142]. One possible mechanism linking counterion lipophilicity to cytotoxicity is that for the more apolar molecules the interaction with the aqueous environment is reduced such that partitioning of the counterion into lipophilic cell membranes increases. Similar argumentation was given for those IL ion pairs for which an increase in cytotoxicity was observed, with uncharged pairs partitioning into the lipophilic cell membranes leading to more effective cell membrane penetration [141].

In conclusion, ILs can be prepared from naturally occurring molecules or from counterions generally recognized as safe. New counterions must be toxicologically profiled. However, the general assumption that counterions themselves or IL in general are less safe than the pure API or common salts of the API is wrong. The demonstrated versatility in counterions, as well as demonstrated successes in which the proper choice of the counterion resulted in safer application as compared to conventional salts clearly demand an unbiased and scientifically justified view on ILs.

Hygroscopicity

Hygroscopicity is critically challenging pharmaceutical use. The water content affects thermal and chemical stability, powder flow, compressibility, dosage accuracy and dissolution rate [51, 103, 143, 144]. Most if not nearly all ILs are hygroscopic at ambient conditions [145-147]. The impact for some ILs is illustrated for lidocaine, typically a rather lipophilic drug. When transformed into an IL, lidocaine docusate reaches a water content of 9.6% after saturation [4]. Another group of APIs transformed into TBP-ILs exposed to 80% r.h resulted in water contents ranging from 3% to 27% [80]. The consequences of water absorption are different. API-ILs typically liquefy with water sorption but may as well crystallize. For example, water sorption by procaine acetate (RT-IL) resulted in transformation of the IL into a crystalline dihydrate (MP = 52 °C) [67]. In consequence, one would exchange the counterion to prevent this effect. Water sorption is particularly high for amorphous and liquid APIs, as water can easily permeate into the bulk of the liquid or solid substance in contrast to crystalline APIs for which water sorption is limited to the surface of the

substance [143]. Absorbed water in amorphous substances serves as a plasticizer and reduces the TG in accordance with the Kelley-Büche equation.

$$TG_{mix} = [(w_1 * TG_1) + (K * w_2 * TG_2)]/[w_1 + (K * w_2)] \text{ with } K = (\rho_1 * \Delta\alpha_2)/(\rho_2 * \Delta\alpha_1)$$

TG is the glass transition temperature, w the weight fraction, Δα the change in thermal expansivity and ρ is the true density [148, 149]. Thus water sorption can result in significant changes of the consistency and the physical properties of an IL, as the TG of water is at <136 K [150]. Thereby, even small amounts of water lead to a substantial depression of the TG. Therefore, the facilitated water absorption of amorphous ILs or RT-ILs is particularly challenging due to hygroscopicity related stability issues. Nevertheless, hygroscopicity can be tailored. As hygroscopicity depends on the interaction of water and the IL there is a strong correlation between solubility and water sorption. Factors impacting the propensity for hygroscopicity introduced by a counterion depend on its overall surface charge, localization of the charge (localized or delocalized), coordination of water, size, and overall lipophilicity, quite often driven by the length of alkyl chains in many counterions. Increasing charge strengthens IL-water interactions while with increasing size of the counterions the charge may be more delocalized and the resulting interaction is weaker [146, 147, 151, 152]. From these insights, one can design ILs with reduced hygroscopicity – knowingly introducing a challenge to other pharmaceutical parameters including dissolution rate and solubility. An acceptable compromise has to be identified, balancing the needs for a successful pharmaceutical product. Another approach may be the reproducible annealing of water to precondition the IL for manufacturing, an approach which may be viable in instances in which water absorption is similar across larger relative humidity states of the manufacturing environment. However, this approach will require special primary packaging (e.g. aluminium blister) to ensure constant water conditions throughout storage. Another study addressed the challenge of hygroscopicity by incorporating vancomycin hydrochloride (not an IL but a hygroscopic salt) into a polyethylene glycol matrix, with the formulation resulting in comparable *in vivo* pharmacokinetics as the corresponding API solution [132]. Further alternatives may be derived from pyridostigmine bromide, which rapidly transforms from solid to liquid state under ambient conditions as a result of water annealing. To address this challenge, pyridostigmine bromide was encapsulated into Avicel pH 102 – a water-insoluble excipient - by extrusion–spheronization and water uptake was prevented [153]. Other studies deployed porous calcium silicate for formulation of very hygroscopic drugs [154].

These exemplarily selected formulation strategies addressing the challenge of hygroscopicity might form interesting approaches to meet a potential increase in hygroscopicity of ILs as compared to crystalline, conventional salts of the APIs, however, further studies are required to prove that these

approaches are a reasonable concept for ILs. Beside, lipophilic counterions reduce the propensity for water annealing of the API-counterion pair, however, likely affect other pharmaceutical parameters such as the dissolution rate or kinetic solubility. It is the task of the formulation scientist to balance these factors such that an optimal drug product is formulated.

Physical, chemical and biological stability

For a pharmaceutical application ILs have to meet strict requirements concerning stability. Nevertheless, a paucity of studies addresses this issue and detailed long term stability data for API-ILs are rarely found. Physical stability needs to be tested in early stage stress tests in order to assure that the IL is in its thermodynamically most stable form and no recrystallization may occur during storage. In accordance with the guideline ‘Stability Testing of New Drug Substances and Products’ by the International Conference on Harmonisation of Technical Requirements for Registration of Pharmaceutics for human use (ICH) [155], ILs might be stored at a defined temperature and r.h. over a certain period of time, followed by detailed characterization using XRPD and DSC and determining conductivity, viscosity, density or the dissolution pattern [156-158]. Furthermore, due to their hygroscopic nature, viscosity, density and water content, should be monitored during the stability studies of API-ILs under storage conditions, in particular as molecular mobility is an important factor for chemical API and counterion stability of amorphous pharmaceuticals and may change with water absorption (*vide supra*) [159]. Pharmaceutical ILs should be chemically and physically stable at ambient conditions, a fact which was addressed by the first air and water stable ethyl-methylimidazolium based ILs in 1992 [160], and followed by subsequent studies detailing a general stability of imidazolium counterions in water and under oxidative conditions at ambient temperature [15]. Chemical stability for ILs is typically assessed from thermal stability in the form of degradation temperature, determined by TGA and differential thermal analysis (DTA). A general trend was postulated regarding thermal stability with phosphonium cations being most stable, followed by imidazolium and ammonium cations [161]. Quaternary ammonium and phosphonium as well as imidazolium salts decomposed through a reverse Menschutkin reaction and by Hofmann elimination and their decomposition is a function of the nucleophilicity of the anion. The study further detailed, that an increase in the lengths of the straight alkyl chains of imidazolium counterions results in an increased thermal stability [161]. Hygroscopicity may arguably lead to a microbiological challenge throughout storage. Residual water may be sufficient to allow for bacterial growth which may require supplementation with preservatives. In this context the preparation of ILs with counterions displaying antimicrobial activity is suggested. Antimicrobial alkylimidazolium, choline-like quaternary ammonium ILs and quaternary phosphonium ILs demonstrated a broad anti-bacterial activity comparable to the preservative benzalkonium chloride [162-165]. For quaternary ammonium counterions QSAR analysis revealed that lipophilicity (logP)

was the main important factor for antimicrobial activity such that efficacy was boosted by increasing the alkyl chain length and introducing two instead of one long chain lipophilic substituent [162]. Based on these findings, ILs with antimicrobial or antibacterial activity were prepared using TBP, cetylpyridinium, benzethonium, benzalkonium and hexetidinium as counterions [51]. A similar correlation between alkyl chain lengths/lipophilicity and antimicrobial activity was demonstrated for ILs using imidazolium and pyridinium derivatives as counterions [138], or for ß-lactam antibiotics for which imidazolium- and pyridinium ILs displayed increased antimicrobial activity as compared to the respective sodium salt [57].

In conclusion, the physical and chemical stability of ILs is an inherent concern to any amorphous or liquid formulation. Previously demonstrated formulation successes for hygroscopic APIs must be extended to ILs, such that hygroscopicity challenges can be adequately addressed, simultaneously reducing the propensity for bacterial contamination. In summary, physical, chemical and biological stability can be effectively controlled by proper choice of the counterion.

Conclusion

API-ILs have a fascinating potential for pharmaceutical application for medicines of tomorrow (**Table 2**). They offer a minimalistic yet highly controlled approach potentially supplementing or in selected cases replacing complex formulations. This strategy is in fact leading to enhanced salt screening programs including the design, metathesis, and application of tailor-synthesized counterions allowing access to a large pharmaceutical design space (tailored parameters include kinetic solubility, dissolution rate, controlled release, stability, hygroscopicity, manufacturing, biopharmaceutical properties) with efficient use of resources (straightforward manufacture with conventional equipment, low risk technical development and production due to minimal process steps reducing out of specification batches, facilitating analytics and release due to the absence of complex excipient mixtures as present in drug product formulations, low scale-up risk, etc.). As a result of their quite frequent amorphous character or crystalline nature with a low melting point, ILs are readily absorbing water and this is potentially one of the main caveats for pharmaceutical use. The formulation scientist can tailor the degree of hygroscopicity but as true for regular salts, one will unlikely achieve conditions in which this phenomenon can be entirely neglected. However, proper choice of the counterion has been instrumental to address this challenge typically leading to more lipophilic ionic pairs. In turn, this lipophilicity increase reduces the dissolution rate and quite frequently the kinetic solubility. This is exactly the point at which the formulation scientist needs to balance the phenomena against each other in an effort to find the most desirable compromise among interfering parameters. The incomplete dissociation of the API and the

Strengths	**Weaknesses**
• Possibility to tune pharmaceutical properties without structural changes of the API • Immediate and modified release • Tunable permeability through biological barriers • Control of polymorphism by RT-IL	• Hygroscopicity • Increased molecular weight by large counterions • Ionizable APIs prerequisite
Opportunities	**Threats**
• Avoiding complex formulations • Novel administration routes (e.g. transdermal) • Portfolio expansion /Life cycle management • Avoid structural changes of API (e.g. prodrug) • Rapid and simplified development program • Dual function of IL (e.g. biofilm disruptive counterion for antibiotics or preservative as counterion to meet microbiological challanges) • Replace counterions with safety concerns (e.g. mesylate)	• Toxicology challenge for some counterions • Impurities in newly synthesized counterions • High viscosity, requiring specialized equipment for manufacture

Table 2: ‘Pro et contra’ ionic liquids for pharmaceutical application.

counterion upon dissolution introduces intriguing possibilities for biopharmaceutical development and several studies reported enhanced transport of the ion pair across membranes. One exciting direction – however, still in its infancy – is the application of IL strategies with the ultimate goal to enhance transmembrane transport to an extent, such that intra- or transdermal delivery becomes feasible. Future studies must demonstrate to which extent these exciting insights can be deployed for advanced pharmaceutical application. Similarly, the strategy of reducing the melting point / glass transition temperature to an extent such that liquid API are obtained at room temperature in an effort to remove polymorphism challenges is a topic demanding careful experiments before implementing this into critical path activities. The boundaries of this approach are readily visible to date, with processing of typically highly viscous liquids being one challenge and the aforementioned hygroscopicity with associated stability challenges being another. Future studies should aim at optimizing the rheological features of RT-ILs as well as addressing the challenge of water sorption or other dynamics during storage. ILs are typically linked to safety issues, ignoring the unlimited structural space of the counterions, the broad pharmaceutical design space which can be approached by this strategy as well as the simplicity of this extrapolation, which to a large extent rests on experiences from using ILs as solvents. *De facto*, toxicology can be designed as the other

parameters can. One question which arises for ILs in a pharmaceutical setting is the arbitrary definition for the melting point / glass transition temperature at 100 °C. Obviously, the pharmaceutical advantage overrides the need to develop salts with a TG/MP smaller than 100 °C. This is why the term “low lattice force salts” may better describe the aim at improving or adapting pharmaceutical properties by the strategies outlined here within than the term IL does.

As pointed out, the formulation scientist gets a novel tool to tailor the physico-chemical properties of the API in solid state, upon dissolution, and to some extent as a result of incomplete dissociation of the ion pairs for drug transport across membranes. From a high-level perspective and in simplified terms, one is modulating the overall API lipophilicity but not by changing the API structure itself. Instead, this modulation is achieved by formation of incompletely dissociating ion pairs with properly chosen counterions. Thereby, and in contrast to many current approaches introducing changes to the API structure in an effort to meet pharmaceutical demands, much faster, resource effective and straightforward approaches may readily become feasible. Following this strategy, the future promises pharmaceutical design spaces for key pharmaceutical parameters for APIs by simply presenting these as salts with a suite of counterions. To build this future, well-characterized (metathesis, stability, purity, toxicity) counterion libraries must be built for both basic and acidic APIs. Equally important are studies on IL carriers, with the focus on overcoming hygroscopicity or viscosity challenges of RT-ILs. Lastly, analytical and salification platforms should be designed, such that automatic, semi- or high throughput pharmaceutical characterization allows rapid and reliable screening of large API-counterion combinations.

Acknowledgments

We thank the DFG (SFB 630) and the Bayerische Forschungsstiftung (“Springs and parachutes”) for financial support. DAAD support within the program “PAJAKO - Partnerschaften mit Japan und Korea” is gratefully acknowledged.

References

[1] S. V. Malhotra, *Ionic Liquid Applications: Pharmaceuticals, Therapeutics, and Biotechnology* vol. 1038. Washington, DC: American Chemical Society, 2010.

[2] M. Freemantle, *An Introduction to Ionic Liquids*. Cambridge: Royal Society of Chemistry, 2010.

[3] R. D. Rogers and K. R. Seddon, "Chemistry. Ionic liquids--solvents of the future?," *Science,* vol. 302, pp. 792-3, Oct 31 2003.

[4] W. L. Hough, M. Smiglak, H. Rodriguez, R. P. Swatloski, S. K. Spear, D. T. Daly, *et al.*, "The third evolution of ionic liquids: active pharmaceutical ingredients," *New Journal of Chemistry,* vol. 31, pp. 1429-1436, 2007.

[5] S. P. Kelley, A. Narita, J. D. Holbrey, K. D. Green, W. M. Reichert, and R. D. Rogers, "Understanding the Effects of Ionicity in Salts, Solvates, Co-Crystals, Ionic Co-Crystals, and Ionic Liquids, Rather than Nomenclature, Is Critical to Understanding Their Behavior," *Crystal Growth & Design,* vol. 13, pp. 965-975, Mar 2013.

[6] R. Ferraz, L. C. Branco, C. Prudencio, J. P. Noronha, and Z. Petrovski, "Ionic liquids as active pharmaceutical ingredients," *ChemMedChem,* vol. 6, pp. 975-85, Jun 6 2011.

[7] W. L. Hough and R. D. Rogers, "Ionic liquids then and now: From solvents to materials to active pharmaceutical ingredients," *Bulletin of the Chemical Society of Japan,* vol. 80, pp. 2262-2269, Dec 15 2007.

[8] I. M. Marrucho, L. C. Branco, and L. P. Rebelo, "Ionic liquids in pharmaceutical applications," *Annu Rev Chem Biomol Eng,* vol. 5, pp. 527-46, 2014.

[9] P. M. Dean, J. M. Pringle, and D. R. MacFarlane, "Structural analysis of low melting organic salts: perspectives on ionic liquids," *Phys Chem Chem Phys,* vol. 12, pp. 9144-53, Aug 28 2010.

[10] V. Kumar and S. V. Malhotra, "Ionic Liquids as Pharmaceutical Salts: A Historical Perspective," *Symposium A Quarterly Journal In Modern Foreign Literatures,* vol. 1038, pp. 1-12, 2010.

[11] D. R. MacFarlane, J. M. Pringle, K. M. Johansson, S. A. Forsyth, and M. Forsyth, "Lewis base ionic liquids," *Chem Commun (Camb),* pp. 1905-17, May 14 2006.

[12] B. Tang, W. Bi, M. Tian, and K. H. Row, "Application of ionic liquid for extraction and separation of bioactive compounds from plants," *J Chromatogr B Analyt Technol Biomed Life Sci,* vol. 904, pp. 1-21, Sep 1 2012.

[13] D. Han and K. H. Row, "Recent applications of ionic liquids in separation technology," *Molecules,* vol. 15, pp. 2405-26, Apr 2010.

[14] H. Zhao, S. Xia, and P. Ma, "Use of ionic liquids as ‘green’ solvents for extractions," *Journal of Chemical Technology & Biotechnology,* vol. 80, pp. 1089-1096, 2005.

[15] S. Sowmiah, V. Srinivasadesikan, M. C. Tseng, and Y. H. Chu, "On the chemical stabilities of ionic liquids," *Molecules,* vol. 14, pp. 3780-813, 2009.

[16] M. Armand, F. Endres, D. R. MacFarlane, H. Ohno, and B. Scrosati, "Ionic-liquid materials for the electrochemical challenges of the future," *Nat Mater,* vol. 8, pp. 621-9, Aug 2009.

[17] M. Palacio and B. Bhushan, "A Review of Ionic Liquids for Green Molecular Lubrication in Nanotechnology," *Tribology Letters,* vol. 40, pp. 247-268, Nov 2010.

[18] T. Ichikawa, M. Yoshio, A. Hamasaki, T. Mukai, H. Ohno, and T. Kato, "Self-organization of room-temperature ionic liquids exhibiting liquid-crystalline bicontinuous cubic phases: formation of nano-ion channel networks," *J Am Chem Soc,* vol. 129, pp. 10662-3, Sep 5 2007.

[19] Y. Jiang and Y.-j. Zhu, "Microwave-assisted synthesis of sulfide M2S3 (m = Bi, Sb) nanorods using an ionic liquid," *The journal of physical chemistry. B,* vol. 109, pp. 4361-4, 2005.

[20] F. van Rantwijk and R. A. Sheldon, "Biocatalysis in ionic liquids," *Chem Rev,* vol. 107, pp. 2757-85, Jun 2007.

[21] M. Erbeldinger, A. J. Mesiano, and A. J. Russell, "Enzymatic catalysis of formation of Z-aspartame in ionic liquid - An alternative to enzymatic catalysis in organic solvents," *Biotechnol Prog,* vol. 16, pp. 1129-31, Nov-Dec 2000.
[22] L. Weng, X. Liu, Y. Liang, and Q. Xue, "Effect of tetraalkylphosphonium based ionic liquids as lubricants on the tribological performance of a steel-on-steel system," *Tribology Letters,* vol. 26, pp. 11-17, 2006.
[23] M. D. Bermudez, A. E. Jimenez, J. Sanes, and F. J. Carrion, "Ionic liquids as advanced lubricant fluids," *Molecules,* vol. 14, pp. 2888-908, 2009.
[24] Y. Yoshida and G. Z. Saito, "Influence of structural variations in 1-alkyl-3-methylimidazolium cation and tetrahalogenoferrate(III) anion on the physical properties of the paramagnetic ionic liquids," *Journal of Materials Chemistry,* vol. 16, pp. 1254-1262, 2006.
[25] M. Okuno, H. O. Hamaguchi, and S. Hayashi, "Magnetic manipulation of materials in a magnetic ionic liquid," *Applied Physics Letters,* vol. 89, pp. 132506-1 - 132506-2, Sep 25 2006.
[26] S. Shang, L. Li, X. Yang, and L. Zheng, "Synthesis and characterization of poly(3-methyl thiophene) nanospheres in magnetic ionic liquid," *J Colloid Interface Sci,* vol. 333, pp. 415-8, May 1 2009.
[27] S. Schneider, T. Hawkins, M. Rosander, G. Vaghjiani, S. Chambreau, and G. Drake, "Ionic liquids as hypergolic fuels," *Energy & Fuels,* vol. 22, pp. 2871-2872, Jul-Aug 2008.
[28] S. Schneider, T. Hawkins, Y. Ahmed, M. Rosander, L. Hudgens, and J. Mills, "Green bipropellants: hydrogen-rich ionic liquids that are hypergolic with hydrogen peroxide," *Angew Chem Int Ed Engl,* vol. 50, pp. 5886-8, Jun 20 2011.
[29] T. Predel, E. Schlücker, P. Wasserscheid, D. Gerhard, and W. Arlt, "Ionic Liquids as Operating Fluids in High Pressure Applications," *Chemical Engineering & Technology,* vol. 30, pp. 1475-1480, 2007.
[30] H. Mizuuchi, V. Jaitely, S. Murdan, and A. T. Florence, "Room temperature ionic liquids and their mixtures: potential pharmaceutical solvents," *Eur J Pharm Sci,* vol. 33, pp. 326-31, Apr 23 2008.
[31] J. L. Shamshina, P. S. Barber, and R. D. Rogers, "Ionic liquids in drug delivery," *Expert Opin Drug Deliv,* vol. 10, pp. 1367-81, Oct 2013.
[32] T. Siodmiak, M. P. Marszall, and A. Proszowska, "Ionic Liquids: A New Strategy in Pharmaceutical Synthesis," *Mini-Reviews in Organic Chemistry,* vol. 9, pp. 203-208, May 2012.
[33] R. J. Soukup-Hein, M. M. Warnke, and D. W. Armstrong, "Ionic liquids in analytical chemistry," *Annu Rev Anal Chem (Palo Alto Calif),* vol. 2, pp. 145-68, 2009.
[34] P. Sun and D. W. Armstrong, "Ionic liquids in analytical chemistry," *Anal Chim Acta,* vol. 661, pp. 1-16, Feb 19 2010.
[35] K. Fujita, D. R. MacFarlane, and M. Forsyth, "Protein solubilising and stabilising ionic liquids," *Chem Commun (Camb),* vol. 70, pp. 4804-6, Oct 14 2005.
[36] X. W. Chen, J. W. Liu, and J. H. Wang, "Ionic liquids in the assay of proteins," *Analytical Methods,* vol. 2, pp. 1222-1226, Sep 2010.
[37] V. Jaitely, A. Karatas, and A. T. Florence, "Water-immiscible room temperature ionic liquids (RTILs) as drug reservoirs for controlled release," *Int J Pharm,* vol. 354, pp. 168-73, Apr 16 2008.
[38] P. D. McCrary, P. A. Beasley, G. Gurau, A. Narita, P. S. Barber, O. A. Cojocaru, *et al.*, "Drug specific, tuning of an ionic liquid's hydrophilic–lipophilic balance to improve water solubility of poorly soluble active pharmaceutical ingredients," *New Journal of Chemistry,* vol. 37, pp. 2196-2202, 2013.
[39] H. D. Williams, Y. Sahbaz, L. Ford, T. H. Nguyen, P. J. Scammells, and C. J. Porter, "Ionic liquids provide unique opportunities for oral drug delivery: structure optimization and in vivo evidence of utility," *Chem Commun (Camb),* vol. 50, pp. 1688-90, Feb 18 2014.

[40] J. Eastoe, S. Gold, S. E. Rogers, A. Paul, T. Welton, R. K. Heenan, *et al.*, "Ionic liquid-in-oil microemulsions," *Journal of the American Chemical Society*, vol. 127, pp. 7302-7303, May 25 2005.
[41] M. Moniruzzaman, M. Tamura, Y. Tahara, N. Kamiya, and M. Goto, "Ionic liquid-in-oil microemulsion as a potential carrier of sparingly soluble drug: characterization and cytotoxicity evaluation," *Int J Pharm*, vol. 400, pp. 243-50, Nov 15 2010.
[42] M. Moniruzzaman, N. Kamiya, and M. Goto, "Ionic liquid based microemulsion with pharmaceutically accepted components: Formulation and potential applications," *J Colloid Interface Sci*, vol. 352, pp. 136-42, Dec 1 2010.
[43] C. P. Frizzo, I. M. Gindri, A. Z. Tier, and L. Buriol, "Pharmaceutical Salts: Solids to Liquids by Using Ionic Liquid Design," K. Jun-ichi, Ed., ed: InTech, 2013, pp. 557-579.
[44] J. W. Steed, "The role of co-crystals in pharmaceutical design," *Trends Pharmacol Sci*, vol. 34, pp. 185-93, Mar 2013.
[45] S. L. Childs, L. J. Chyall, J. T. Dunlap, V. N. Smolenskaya, B. C. Stahly, and G. P. Stahly, "Crystal engineering approach to forming cocrystals of amine hydrochlorides with organic acids. Molecular complexes of fluoxetine hydrochloride with benzoic, succinic, and fumaric acids," *J Am Chem Soc*, vol. 126, pp. 13335-42, Oct 20 2004.
[46] K. Bica, J. Shamshina, W. L. Hough, D. R. MacFarlane, and R. D. Rogers, "Liquid forms of pharmaceutical co-crystals: exploring the boundaries of salt formation," *Chem Commun (Camb)*, vol. 47, pp. 2267-9, Feb 28 2011.
[47] H. Wang, G. Gurau, J. Shamshina, O. A. Cojocaru, J. Janikowski, D. R. MacFarlane, *et al.*, "Simultaneous membrane transport of two active pharmaceutical ingredients by charge assisted hydrogen bond complex formation," *Chemical Science*, vol. 5, pp. 3449-3456, Sep 2014.
[48] K. Bica and R. D. Rogers, "Confused ionic liquid ions-a "liquification" and dosage strategy for pharmaceutically active salts," *Chem Commun (Camb)*, vol. 46, pp. 1215-7, Feb 28 2010.
[49] K. M. Johansson, E. I. Izgorodina, M. Forsyth, D. R. MacFarlane, and K. R. Seddon, "Protic ionic liquids based on the dimeric and oligomeric anions: [(AcO)xH(x-1)]," *Phys Chem Chem Phys*, vol. 10, pp. 2972-8, May 28 2008.
[50] J. Stoimenovski, P. M. Dean, E. I. Izgorodina, and D. R. MacFarlane, "Protic pharmaceutical ionic liquids and solids: aspects of protonics," *Faraday Discuss*, vol. 154, pp. 335-352, 2012.
[51] K. Bica, C. Rijksen, M. Nieuwenhuyzen, and R. D. Rogers, "In search of pure liquid salt forms of aspirin: ionic liquid approaches with acetylsalicylic acid and salicylic acid," *Phys Chem Chem Phys*, vol. 12, pp. 2011-7, Feb 28 2010.
[52] J. Stoimenovski and D. R. MacFarlane, "Enhanced membrane transport of pharmaceutically active protic ionic liquids," *Chem Commun (Camb)*, vol. 47, pp. 11429-31, Nov 7 2011.
[53] L. Zhang, J. Liu, T. Tian, Y. Gao, X. Ji, Z. Li, *et al.*, "Pharmaceutically active ionic liquid self-assembled vesicles for the application as an efficient drug delivery system," *Chemphyschem*, vol. 14, pp. 3454-7, Oct 21 2013.
[54] C. Florindo, J. M. Araujo, F. Alves, C. Matos, R. Ferraz, C. Prudencio, *et al.*, "Evaluation of solubility and partition properties of ampicillin-based ionic liquids," *Int J Pharm*, vol. 456, pp. 553-9, Nov 18 2013.
[55] R. Ferraz, L. C. Branco, I. M. Marrucho, J. M. M. Araujo, L. P. N. Rebelo, M. N. da Ponte, *et al.*, "Development of novel ionic liquids based on ampicillin," *Medchemcomm*, vol. 3, pp. 494-497, Apr 2012.
[56] R. Ferraz, V. Teixeira, E. Rodrigues, R. Fernandes, C. Prudencio, J. P. Noronha, *et al.*, "Antibacterial activity of Ionic Liquids based on ampicillin against resistant bacteria," *Rsc Advances*, vol. 4, pp. 4301-4307, 2014.
[57] M. R. Cole, M. Li, B. El-Zahab, M. E. Janes, D. Hayes, and I. M. Warner, "Design, synthesis, and biological evaluation of beta-lactam antibiotic-based imidazolium- and pyridinium-type ionic liquids," *Chem Biol Drug Des*, vol. 78, pp. 33-41, Jul 2011.

[58] D. N. Moreira, N. Fresno, R. Pérez-Fernández, C. P. Frizzo, P. Goya, C. Marco, *et al.*, "Brønsted acid–base pairs of drugs as dual ionic liquids: NMR ionicity studies," *Tetrahedron,* vol. 71, pp. 676-685, 2015.
[59] Z. Wojnarowska, C. M. Roland, K. Kolodziejczyk, A. Swiety-Pospiech, K. Grzybowska, and M. Paluch, "Quantifying the Structural Dynamics of Pharmaceuticals in the Glassy State," *Journal of Physical Chemistry Letters,* vol. 3, pp. 1238-1241, May 17 2012.
[60] S. Cherukuvada and A. Nangia, "Polymorphism in an API ionic liquid: ethambutol dibenzoate trimorphs," *Crystengcomm,* vol. 14, pp. 7840-7843, 2012.
[61] S. Cherukuvada and A. Nangia, "Salts and Ionic Liquid of The Antituberculosis DrugS,S-Ethambutol," *Crystal Growth & Design,* vol. 13, pp. 1752-1760, 2013.
[62] L. Viau, C. Tourne-Peteilh, J. M. Devoisselle, and A. Vioux, "Ionogels as drug delivery system: one-step sol-gel synthesis using imidazolium ibuprofenate ionic liquid," *Chem Commun (Camb),* vol. 46, pp. 228-30, Jan 14 2010.
[63] K. Bica, H. Rodriguez, G. Gurau, O. A. Cojocaru, A. Riisager, R. Fehrmann, *et al.*, "Pharmaceutically active ionic liquids with solids handling, enhanced thermal stability, and fast release," *Chem Commun (Camb),* vol. 48, pp. 5422-4, Jun 4 2012.
[64] C. Tourne-Peteilh, B. Coasne, M. In, D. Brevet, J. M. Devoisselle, A. Vioux, *et al.*, "Surfactant behavior of ionic liquids involving a drug: from molecular interactions to self-assembly," *Langmuir,* vol. 30, pp. 1229-38, Feb 11 2014.
[65] Z. Wojnarowska, K. Grzybowska, L. Hawelek, A. Swiety-Pospiech, E. Masiewicz, M. Paluch, *et al.*, "Molecular dynamics studies on the water mixtures of pharmaceutically important ionic liquid lidocaine HCl," *Mol Pharm,* vol. 9, pp. 1250-61, May 7 2012.
[66] R. D. Rogers, D. T. Daly, R. P. Swatloski, W. L. Hough, J. H. Davis, M. Smiglak, *et al.*, "Multi-functional ionic liquid compositions for overcoming polymorphism and imparting improved properties for active ingredients," WO2007044693, 2007.
[67] O. A. Cojocaru, S. P. Kelley, G. Gurau, and R. D. Rogers, "Procainium Acetate Versus Procainium Acetate Dihydrate: Irreversible Crystallization of a Room-Temperature Active Pharmaceutical-Ingredient Ionic Liquid upon Hydration," *Crystal Growth & Design,* vol. 13, pp. 3290-3293, Aug 2013.
[68] P. M. Dean, J. Turanjanin, M. Yoshizawa-Fujita, D. R. MacFarlane, and J. L. Scott, "Exploring an Anti-Crystal Engineering Approach to the Preparation of Pharmaceutically Active Ionic Liquids," *Crystal Growth & Design,* vol. 9, pp. 1137-1145, Feb 2009.
[69] P. C. A. G. Pinto, D. M. G. P. Ribeiro, A. M. O. Azevedo, V. Dela Justina, E. Cunha, K. Bica, *et al.*, "Active pharmaceutical ingredients based on salicylate ionic liquids: insights into the evaluation of pharmaceutical profiles," *New Journal of Chemistry,* vol. 37, pp. 4095-4102, 2013.
[70] F. Alves, F. S. Oliveira, B. Schroder, C. Matos, and I. M. Marrucho, "Synthesis, characterization, and liposome partition of a novel tetracycline derivative using the ionic liquids framework," *J Pharm Sci,* vol. 102, pp. 1504-12, May 2013.
[71] J. Stoimenovski, D. R. MacFarlane, K. Bica, and R. D. Rogers, "Crystalline vs. ionic liquid salt forms of active pharmaceutical ingredients: a position paper," *Pharm Res,* vol. 27, pp. 521-6, Apr 2010.
[72] A. S. Prakash, "The counter ion: expanding excipient functionality," *J. Excipients and Food Chem.*, vol. 2, pp. 28-40, 2011 2011.
[73] W. L. Hough-Troutman, M. Smiglak, S. Griffin, W. M. Reichert, I. Mirska, J. Jodynis-Liebert, *et al.*, "Ionic liquids with dual biological function: sweet and anti-microbial, hydrophobic quaternary ammonium-based salts," *New Journal of Chemistry,* vol. 33, pp. 26-33, 2009.
[74] H. Nakamoto and M. Watanabe, "Bronsted acid-base ionic liquids for fuel cell electrolytes," *Chem Commun (Camb),* pp. 2539-41, Jun 28 2007.
[75] K. Fukumoto, M. Yoshizawa, and H. Ohno, "Room temperature ionic liquids from 20 natural amino acids," *J Am Chem Soc,* vol. 127, pp. 2398-9, Mar 2 2005.
[76] H. Ohno and K. Fukumoto, "Amino acid ionic liquids," *Acc Chem Res,* vol. 40, pp. 1122-9, Nov 2007.

[77] M. Yoshizawa, W. Xu, and C. A. Angell, "Ionic liquids by proton transfer: vapor pressure, conductivity, and the relevance of DeltapKa from aqueous solutions," *Journal of the American Chemical Society,* vol. 125, pp. 15411-9, 2003.
[78] J. L. Shamshina and R. D. Rogers, "Overcoming the problems of solid state drug formulations with ionic liquids," *Therapeutic delivery,* vol. 5, pp. 489-91, 2014.
[79] L. Kumar, A. Amin, and A. K. Bansal, "An overview of automated systems relevant in pharmaceutical salt screening," *Drug Discov Today,* vol. 12, pp. 1046-53, Dec 2007.
[80] A. Balk, J. Wiest, T. Widmer, B. Galli, U. Holzgrabe, and L. Meinel, "Transformation of acidic poorly water soluble drugs into ionic liquids," *Eur J Pharm Biopharm,* vol. 94, pp. 73-82, May 11 2015.
[81] K. Noack, P. S. Schulz, N. Paape, J. Kiefer, P. Wasserscheid, and A. Leipertz, "The role of the C2 position in interionic interactions of imidazolium based ionic liquids: a vibrational and NMR spectroscopic study," *Phys Chem Chem Phys,* vol. 12, pp. 14153-61, Nov 14 2010.
[82] G. L. Burrell, I. M. Burgar, F. Separovic, and N. F. Dunlop, "Preparation of protic ionic liquids with minimal water content and (15)N NMR study of proton transfer," *Phys Chem Chem Phys,* vol. 12, pp. 1571-7, Feb 21 2010.
[83] M. Giesecke, G. Meriguet, F. Hallberg, Y. Fang, P. Stilbs, and I. Furo, "Ion association in aqueous and non-aqueous solutions probed by diffusion and electrophoretic NMR," *Phys Chem Chem Phys,* vol. 17, pp. 3402-8, Feb 7 2015.
[84] U. Holzgrabe, I. Wawer, and B. Diehl, *NMR spectroscopy in drug development and analysis*. Weinheim: VCH Wiley, 1999.
[85] A. Balk, T. Widmer, J. Wiest, H. Bruhn, J. C. Rybak, P. Matthes, *et al.*, "Ionic liquid versus prodrug strategy to address formulation challenges," *Pharm Res,* vol. 32, pp. 2154-67, Jun 2015.
[86] S. Khatun and E. W. Castner, Jr., "Ionic Liquid-Solute Interactions Studied by 2D NOE NMR Spectroscopy," *J Phys Chem B,* Nov 26 2014.
[87] S. Gabl, O. Steinhauser, and H. Weingartner, "From short-range to long-range intermolecular NOEs in ionic liquids: frequency does matter," *Angew Chem Int Ed Engl,* vol. 52, pp. 9242-6, Aug 26 2013.
[88] T. Cremer, C. Kolbeck, K. R. Lovelock, N. Paape, R. Wolfel, P. S. Schulz, *et al.*, "Towards a molecular understanding of cation-anion interactions--probing the electronic structure of imidazolium ionic liquids by NMR spectroscopy, X-ray photoelectron spectroscopy and theoretical calculations," *Chemistry,* vol. 16, pp. 9018-33, Aug 9 2010.
[89] C. E. Hughes, P. A. Williams, and K. D. Harris, ""CLASSIC NMR": an in-situ NMR strategy for mapping the time-evolution of crystallization processes by combined liquid-state and solid-state measurements," *Angew Chem Int Ed Engl,* vol. 53, pp. 8939-43, Aug 18 2014.
[90] D. R. MacFarlane, M. Forsyth, E. I. Izgorodina, A. P. Abbott, G. Annat, and K. Fraser, "On the concept of ionicity in ionic liquids," *Phys Chem Chem Phys,* vol. 11, pp. 4962-7, Jul 7 2009.
[91] R. Bini, O. Bortolini, C. Chiappe, D. Pieraccini, and T. Siciliano, "Development of cation/anion "interaction" scales for ionic liquids through ESI-MS measurements," *J Phys Chem B,* vol. 111, pp. 598-604, Jan 25 2007.
[92] K. J. Fraser, E. I. Izgorodina, M. Forsyth, J. L. Scott, and D. R. MacFarlane, "Liquids intermediate between “molecular” and “ionic” liquids: Liquid Ion Pairs?," *Chem Commun,* pp. 3817-3819, 2007.
[93] Y. Zhao, S. Gao, J. Wang, and J. Tang, "Aggregation of ionic liquids [C(n)mim]Br (n = 4, 6, 8, 10, 12) in D2O: a NMR study," *J Phys Chem B,* vol. 112, pp. 2031-9, Feb 21 2008.
[94] S. R. LaPlante, R. Carson, J. Gillard, N. Aubry, R. Coulombe, S. Bordeleau, *et al.*, "Compound aggregation in drug discovery: implementing a practical NMR assay for medicinal chemists," *J Med Chem,* vol. 56, pp. 5142-50, Jun 27 2013.
[95] S. R. LaPlante, N. Aubry, G. Bolger, P. Bonneau, R. Carson, R. Coulombe, *et al.*, "Monitoring drug self-aggregation and potential for promiscuity in off-target in vitro

pharmacology screens by a practical NMR strategy," *J Med Chem*, vol. 56, pp. 7073-83, Sep 12 2013.
[96] K. C. Waterman and R. C. Adami, "Accelerated aging: prediction of chemical stability of pharmaceuticals," *Int J Pharm*, vol. 293, pp. 101-25, Apr 11 2005.
[97] P. H. Stahl, C. G. Wermuth, and I. U. o. P. a. A. Chemistry, *Handbook of pharmaceutical salts : Properties, Selection, and Use*, 2nd ed. Zurich: VHVA; Weinheim:Wiley-VCH, 2011.
[98] L. Yu, S. M. Reutzel, and G. A. Stephenson, "Physical characterization of polymorphic drugs: an integrated characterization strategy," *Pharmaceutical Science & Technology Today*, vol. 1, pp. 118-127, Jun 1998.
[99] A. T. Serajuddin, "Salt formation to improve drug solubility," *Adv Drug Deliv Rev*, vol. 59, pp. 603-16, Jul 30 2007.
[100] A. Kapczynski, C. Park, and B. Sampat, "Polymorphs and prodrugs and salts (oh my!): an empirical analysis of "secondary" pharmaceutical patents," *PLoS One*, vol. 7, p. e49470, 2012.
[101] P. W. Grubb and P. R. Thomsen, *Patents for Chemicals, Pharmaceuticals, and Biotechnology: Fundamentals of Global Law, Practice, and Strategy.*, 5 ed. Oxford: Oxford University Press, 2010.
[102] Y. Kawabata, K. Wada, M. Nakatani, S. Yamada, and S. Onoue, "Formulation design for poorly water-soluble drugs based on biopharmaceutics classification system: basic approaches and practical applications," *Int J Pharm*, vol. 420, pp. 1-10, Nov 25 2011.
[103] A. W. Newman, S. M. Reutzel-Edens, and G. Zografi, "Characterization of the "hygroscopic" properties of active pharmaceutical ingredients," *J Pharm Sci*, vol. 97, pp. 1047-59, Mar 2008.
[104] R. J. Bastin, M. J. Bowker, and B. J. Slater, "Salt selection and optimisation procedures for pharmaceutical new chemical entities," *Organic Process Research & Development*, vol. 4, pp. 427-435, Sep-Oct 2000.
[105] N. Jain, G. Yang, S. G. Machatha, and S. H. Yalkowsky, "Estimation of the aqueous solubility of weak electrolytes," *Int J Pharm*, vol. 319, pp. 169-171, Aug 17 2006.
[106] B. D. Anderson and R. A. Conradi, "Predictive relationships in the water solubility of salts of a nonsteroidal anti-inflammatory drug," *J Pharm Sci*, vol. 74, pp. 815-20, Aug 1985.
[107] P. L. Gould, "Salt Selection for Basic Drugs," *International Journal of Pharmaceutics*, vol. 33, pp. 201-217, Nov 1986.
[108] D. A. Haynes, W. Jones, and W. D. Samuel Motherwell, "Occurrence of pharmaceutically acceptable anions and cations in the Cambridge Structural Database," *J Pharm Sci*, vol. 94, pp. 2111-20, Oct 2005.
[109] S. M. Berge, L. D. Bighley, and D. C. Monkhouse, "Pharmaceutical salts," *J Pharm Sci*, vol. 66, pp. 1-19, Jan 1977.
[110] D. J. Snodin, "Residues of genotoxic alkyl mesylates in mesylate salt drug substances: real or imaginary problems?," *Regul Toxicol Pharmacol*, vol. 45, pp. 79-90, Jun 2006.
[111] D. I. Robinson, "Control of genotoxic impurities in active pharmaceutical ingredients: a review and perspective," *Org. Process Res. Dev*, vol. 14, pp. 946-959, 2010.
[112] J. M. M. Araújo, C. Florindo, A. B. Pereiro, N. S. M. Vieira, A. A. Matias, C. M. M. Duarte, *et al.*, "Cholinium-based ionic liquids with pharmaceutically active anions," *RSC Advances*, vol. 4, pp. 28126-28132, 2014.
[113] J. Bowers, C. P. Butts, P. J. Martin, M. C. Vergara-Gutierrez, and R. K. Heenan, "Aggregation behavior of aqueous solutions of ionic liquids," *Langmuir*, vol. 20, pp. 2191-8, Mar 16 2004.
[114] Z. Miskolczy, K. Sebok-Nagy, L. Biczok, and S. Gokturk, "Aggregation and micelle formation of ionic liquids in aqueous solution," *Chemical Physics Letters*, vol. 400, pp. 296-300, Dec 21 2004.
[115] M. Blesic, M. H. Marques, N. V. Plechkova, K. R. Seddon, L. P. N. Rebelo, and A. Lopes, "Self-aggregation of ionic liquids: micelle formation in aqueous solution," *Green Chemistry*, vol. 9, pp. 481-490, May 2007.

[116] P. H. Stahl, C. G. Wermuth, and I. U. o. P. a. A. Chemistry, *Handbook of Pharmaceutical Salts Properties, Selection, and Use*, 2 ed. Zürich: VHVA; Weinheim:Wiley-VCH, 2011.
[117] S. D. Kramer, "Absorption prediction from physicochemical parameters," *Pharm Sci Technolo Today*, vol. 2, pp. 373-380, Sep 1999.
[118] E. K. Esbjorner, P. Lincoln, and B. Norden, "Counterion-mediated membrane penetration: cationic cell-penetrating peptides overcome Born energy barrier by ion-pairing with phospholipids," *Biochim Biophys Acta*, vol. 1768, pp. 1550-8, Jun 2007.
[119] S. P. Vincent, J. M. Lehn, J. Lazarte, and C. Nicolau, "Transport of the highly charged myo-inositol hexakisphosphate molecule across the red blood cell membrane: a phase transfer and biological study," *Bioorg Med Chem*, vol. 10, pp. 2825-34, Sep 2002.
[120] S. R. Vippagunta, H. G. Brittain, and D. J. Grant, "Crystalline solids," *Adv Drug Deliv Rev*, vol. 48, pp. 3-26, May 16 2001.
[121] B. Rodriguez-Spong, C. P. Price, A. Jayasankar, A. J. Matzger, and N. Rodriguez-Hornedo, "General principles of pharmaceutical solid polymorphism: a supramolecular perspective," *Adv Drug Deliv Rev*, vol. 56, pp. 241-74, Feb 23 2004.
[122] J. Bauer, S. Spanton, R. Henry, J. Quick, W. Dziki, W. Porter, *et al.*, "Ritonavir: an extraordinary example of conformational polymorphism," *Pharm Res*, vol. 18, pp. 859-66, Jun 2001.
[123] S. Agatonovic-Kustrin, T. Rades, V. Wu, D. Saville, and I. G. Tucker, "Determination of polymorphic forms of ranitidine-HCl by DRIFTS and XRPD," *J Pharm Biomed Anal*, vol. 25, pp. 741-50, Jul 2001.
[124] G. G. Zhang, S. Y. Paspal, R. Suryanarayanan, and D. J. Grant, "Racemic species of sodium ibuprofen: characterization and polymorphic relationships," *J Pharm Sci*, vol. 92, pp. 1356-66, Jul 2003.
[125] P. Di Martino, C. Barthelemy, G. F. Palmieri, and S. Martelli, "Physical characterization of naproxen sodium hydrate and anhydrate forms," *Eur J Pharm Sci*, vol. 14, pp. 293-300, Dec 2001.
[126] J. S. Song and Y. T. Sohn, "Crystal forms of naproxen," *Arch Pharm Res*, vol. 34, pp. 87-90, Jan 2011.
[127] C. Tourné-Péteilh, J.-M. Devoisselle, A. Vioux, P. Judeinstein, M. In, and L. Viau, "Surfactant properties of ionic liquids containing short alkyl chain imidazolium cations and ibuprofenate anions," *Physical chemistry chemical physics : PCCP*, vol. 13, pp. 15523-9, 2011.
[128] M. Zakrewsky, K. S. Lovejoy, T. L. Kern, T. E. Miller, V. Le, A. Nagy, *et al.*, "Ionic liquids as a class of materials for transdermal delivery and pathogen neutralization," *Proc Natl Acad Sci U S A*, vol. 111, pp. 13313-8, Sep 16 2014.
[129] B. Magnusson and A. M. Kligman, "The Identification of Contact Allergens by Animal Assay. the Guinea Pig Maximization Test1," *Journal of Investigative Dermatology*, vol. 52, pp. 268-276, 1969.
[130] L. J. Vinson and V. F. Borselli, "A Guinea Pig Assay of the Photosensitizing Potential of," *J. Soc. Cosmetic Chemists*, vol. 17, pp. 123-130, 1966.
[131] M.-A. Néouze, J. L. Bideau, P. Gaveau, S. Bellayer, and A. Vioux, "Ionogels, New Materials Arising from the Confinement of Ionic Liquids within Silica-Derived Networks," *Chemistry of Materials*, vol. 18, pp. 3931-3936, 2006.
[132] E. T. Cole, D. Cade, and H. Benameur, "Challenges and opportunities in the encapsulation of liquid and semi-solid formulations into capsules for oral administration," *Adv Drug Deliv Rev*, vol. 60, pp. 747-56, Mar 17 2008.
[133] R. P. Gullapalli, "Soft gelatin capsules (softgels)," *J Pharm Sci*, vol. 99, pp. 4107-48, Oct 2010.
[134] R. K. Chang, K. S. Raghavan, and M. A. Hussain, "A study on gelatin capsule brittleness: moisture tranfer between the capsule shell and its content," *J Pharm Sci*, vol. 87, pp. 556-8, May 1998.

[135] J. Kagimoto, K. Fukumoto, and H. Ohno, "Effect of tetrabutylphosphonium cation on the physico-chemical properties of amino-acid ionic liquids," *Chem Commun (Camb)*, pp. 2254-6, Jun 4 2006.
[136] A. García-Lorenzo, E. Tojo, J. Tojo, M. Teijeira, F. J. Rodríguez-Berrocal, M. P. González, *et al.*, "Cytotoxicity of selected imidazolium-derived ionic liquids in the human Caco-2 cell line. Sub-structural toxicological interpretation through a QSAR study," *Green Chemistry*, vol. 10, pp. 508-516, 2008.
[137] B. Jastorff, R. Störmann, J. Ranke, K. Mölter, F. Stock, B. Oberheitmann, *et al.*, "How hazardous are ionic liquids? Structure–activity relationships and biological testing as important elements for sustainability evaluationThis work was presented at the Green Solvents for Catalysis Meeting held in Bruchsal, Germany, 13–16th October 2002," *Green Chemistry*, vol. 5, pp. 136-142, 2003.
[138] K. M. Docherty and C. F. Kulpa, "Toxicity and antimicrobial activity of imidazolium and pyridinium ionic liquids," *Green Chemistry*, vol. 7, pp. 185-189, 2005.
[139] M. Petkovic, J. L. Ferguson, H. Q. N. Gunaratne, R. Ferreira, M. C. Leitão, K. R. Seddon, *et al.*, "Novel biocompatible cholinium-based ionic liquids—toxicity and biodegradability," *Green Chemistry*, vol. 12, pp. 643-649, 2010.
[140] S. Stolte, M. Matzke, J. Arning, A. Boschen, W. R. Pitner, U. Welz-Biermann, *et al.*, "Effects of different head groups and functionalised side chains on the aquatic toxicity of ionic liquids," *Green Chemistry*, vol. 9, pp. 1170-1179, 2007.
[141] K. D. Weaver, H. J. Kim, J. Z. Sun, D. R. MacFarlane, and G. D. Elliott, "Cyto-toxicity and biocompatibility of a family of choline phosphate ionic liquids designed for pharmaceutical applications," *Green Chemistry*, vol. 12, pp. 507-513, 2010.
[142] R. A. Kumar, N. Papaiconomou, J. M. Lee, J. Salminen, D. S. Clark, and J. M. Prausnitz, "In vitro cytotoxicities of ionic liquids: effect of cation rings, functional groups, and anions," *Environ Toxicol*, vol. 24, pp. 388-95, Aug 2009.
[143] C. Ahlneck and G. Zografi, "The Molecular-Basis of Moisture Effects on the Physical and Chemical-Stability of Drugs in the Solid-State," *International Journal of Pharmaceutics*, vol. 62, pp. 87-95, Jul 31 1990.
[144] G. Zografi, "States of Water Associated with Solids," *Drug Development and Industrial Pharmacy*, vol. 14, pp. 1905-1926, 1988.
[145] F. D. Francesco, N. Calisi, M. Creatini, B. Melai, P. Salvo, and C. Chiappe, "Water sorption by anhydrous ionic liquids," *Green Chemistry*, vol. 13, pp. 1712-1717, 2011.
[146] Y. Cao, Y. Chen, X. Sun, Z. Zhang, and T. Mu, "Water sorption in ionic liquids: kinetics, mechanisms and hydrophilicity," *Phys Chem Chem Phys*, vol. 14, pp. 12252-62, Sep 21 2012.
[147] S. Cuadrado-Prado, M. Dominguez-Perez, E. Rilo, S. Garcia-Garabal, L. Segade, C. Franjo, *et al.*, "Experimental measurement of the hygroscopic grade on eight imidazolium based ionic liquids," *Fluid Phase Equilibria*, vol. 278, pp. 36-40, Apr 15 2009.
[148] F. N. Kelley and F. Bueche, "Viscosity and glass temperature relations for polymer-diluent systems," *Journal of Polymer Science*, vol. 50, pp. 549-556, 1961.
[149] B. Hancock and G. Zografi, "The Relationship Between the Glass Transition Temperature and the Water Content of Amorphous Pharmaceutical Solids," *Pharmaceutical Research*, vol. 11, pp. 471-477, 1994/04/01 1994.
[150] K. Amann-Winkel, C. Gainaru, P. H. Handle, M. Seidl, H. Nelson, R. Bohmer, *et al.*, "Water's second glass transition," *Proc Natl Acad Sci U S A*, vol. 110, pp. 17720-5, Oct 29 2013.
[151] M. Klahn, C. Stuber, A. Seduraman, and P. Wu, "What determines the miscibility of ionic liquids with water? Identification of the underlying factors to enable a straightforward prediction," *J Phys Chem B*, vol. 114, pp. 2856-68, Mar 4 2010.
[152] M. G. Freire, C. M. Neves, P. J. Carvalho, R. L. Gardas, A. M. Fernandes, I. M. Marrucho, *et al.*, "Mutual solubilities of water and hydrophobic ionic liquids," *J Phys Chem B*, vol. 111, pp. 13082-9, Nov 15 2007.

[153] Y. T. Huang, T. R. Tsai, C. J. Cheng, T. M. Cham, T. F. Lai, and W. H. Chuo, "Formulation design of a highly hygroscopic drug (pyridostigmine bromide) for its hygroscopic character improvement and investigation of in vitro/in vivo dissolution properties," *Drug Dev Ind Pharm,* vol. 33, pp. 403-16, Apr 2007.
[154] N. Hirai, K. Ishikawa, and K. Takahashi, "Improvement of the agitation granulation method to prepare granules containing a high content of a very hygroscopic drug," *J Pharm Pharmacol,* vol. 58, pp. 1437-41, Nov 2006.
[155] "Stability Testing of New Drug Substances and Products Q1A(R2)," vol. 68, ed. US FDA Federal Register: International Conference on Harmonisation (ICH), 2003, pp. 65717-18.
[156] B. C. Hancock and G. Zografi, "Characteristics and significance of the amorphous state in pharmaceutical systems," *J Pharm Sci,* vol. 86, pp. 1-12, Jan 1997.
[157] A. N. Ghebremeskel, C. Vemavarapu, and M. Lodaya, "Use of surfactants as plasticizers in preparing solid dispersions of poorly soluble API: stability testing of selected solid dispersions," *Pharm Res,* vol. 23, pp. 1928-36, Aug 2006.
[158] A. A. Ambike, K. R. Mahadik, and A. Paradkar, "Stability study of amorphous valdecoxib," *Int J Pharm,* vol. 282, pp. 151-62, Sep 10 2004.
[159] S. Yoshioka and Y. Aso, "Correlations between molecular mobility and chemical stability during storage of amorphous pharmaceuticals," *J Pharm Sci,* vol. 96, pp. 960-81, May 2007.
[160] J. S. Wilkes and M. J. Zaworotko, "Air and Water Stable 1-Ethyl-3-Methylimidazolium Based Ionic Liquids," *Journal of the Chemical Society-Chemical Communications,* pp. 965-967, Jul 1 1992.
[161] P. J. Scammells, J. L. Scott, and R. D. Singer, "Ionic liquids: The neglected issues," *Australian Journal of Chemistry,* vol. 58, pp. 155-169, 2005.
[162] J. Pernak and P. Chwała, "Synthesis and anti-microbial activities of choline-like quaternary ammonium chlorides," *European Journal of Medicinal Chemistry,* vol. 38, pp. 1035-1042, 2003.
[163] J. Pernak, I. Goc, and I. Mirska, "Anti-microbial activities of protic ionic liquids with lactate anion," *Green Chemistry,* vol. 6, pp. 323-329, 2004.
[164] J. Pernak, K. Sobaszkiewicz, and I. Mirska, "Anti-microbial activities of ionic liquids," *Green Chemistry,* vol. 5, pp. 52-56, 2003.
[165] A. Cieniecka-Rosłonkiewicz, J. Pernak, J. Kubis-Feder, A. Ramani, A. J. Robertson, and K. R. Seddon, "Synthesis, anti-microbial activities and anti-electrostatic properties of phosphonium-based ionic liquids," *Green Chemistry,* vol. 7, pp. 855-862, 2005.

Chapter 2: Ionic liquid *versus* prodrug strategy to address formulation challenges

Anja Balk[1,§], Toni Widmer[1,2,§], Johannes Wiest[1], Heike Bruhn[3], Jens-Christoph Rybak[1], Philipp Matthes[4], Klaus Müller-Buschbaum[4], Anastasios Sakalis[1], Tessa Lühmann[1], Jörg Berghausen[2], Ulrike Holzgrabe[1], Bruno Galli[2] and Lorenz Meinel[1,*]

[1]Institute for Pharmacy, Am Hubland, University of Würzburg, DE-97074 Würzburg, Germany, [2]Novartis Pharma AG, Lichtstraße 35, CH-4002 Basel, Switzerland, [3]Institute for Molecular Infection Biology, Josef-Schneider-Straße 2, DE-97080 Würzburg, Germany, [4]Institute for Inorganic Chemistry, Am Hubland, University of Würzburg, DE-97074 Würzburg, Germany.

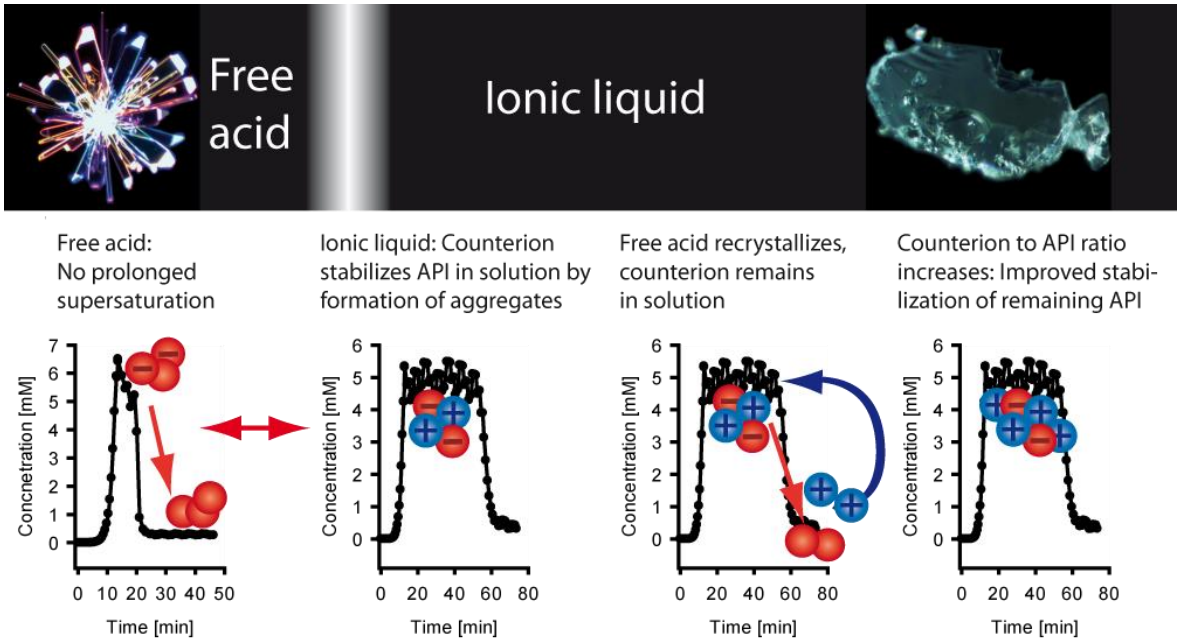

This chapter was originally published in Pharmaceutical Research, vol. 32, pp. 2154-67, 2015; DOI:10.1007/s11095-014-1607-9, with permission of Springer, License number 3638780454628 and 3638780932292.

Introduction

Improper solubility jeopardizes biopharmaceutical impact of pharmaceuticals and ultimately delays relief to the suffering. This problem is aggravated in pharmaceutics today as a result of high throughput screening (HTS) based research strategies for lead identification. By HTS preferentially lipophilic and high molecular weight molecules are selected, posing an additional developmental challenge, for these molecules are typically less soluble in water [1, 2]. To overcome the low bioavailability, the concept of transforming an active pharmaceutical ingredient (API) into an ionic liquid (IL) is presented in this manuscript. ILs are organic salts with a melting point below 100 °C and are dissociated to some extent into ions [3, 4] and have been developed to address e.g. solubility challenges[5]. Another improvement of permeability and / or solubility may be by converting a parent drug into a prodrug [6]. The prodrug concept is well established, however, challenging from a drug regulatory perspective as it constitutes a new API.

We compared the IL strategy to a prodrug concept with the aim to improve the biopharmaceutical properties of a new, orally active α-amino-3-hydroxy-5-methyl-4-isoxazolepropionic acid receptor (AMPA) antagonist [7-9], which was administered to patients with acute migraine attacks at a dose of 250 mg before [10]. We identified the physical-chemical mechanism to achieve improved biopharmaceutical properties of the IL in comparison to the free acid, its potassium salt, and an acetylated prodrug. These interpretations were based on structural information collected in the solid (single crystal, NMR, DSC) and liquid state (NMR), including a precise characterization of ion pairing (NMR, ESI-MS), solubility patterns (acid-base titration experiments), dissolution and precipitation kinetics at the supersaturated and equilibrium phase, respectively. Counterion toxicity was tested in three cell lines of hepatic and renal origin and in macrophages [11]. Data sets from the physical-chemical characterization were correlated to transport kinetics through relevant jejunal *in vitro* model system.

Results

Structure and physical characteristics

The structural formula of N-[7-isopropyl-6-(2-methyl-2H-pyrazol-3-yl)-2,4-dioxo-1,4-dihydro-2*H*-quinazolin-3-yl]-methanesulfonamide (referred to as ‘free acid’) and its prodrug (acetylated at the methylenesulfonamido group; referred to as ‘prodrug’) are provided (**Figure 1A**; formula of the counterion tetrabutylphosphonium is not shown). The free acid crystallized in an orthorhombic space group (*Pbca*) and molecules were arranged in layers (**Figure 1B; Supplementary Figure 1A**). Within each layer, one molecule was connected to four neighboring molecules via hydrogen

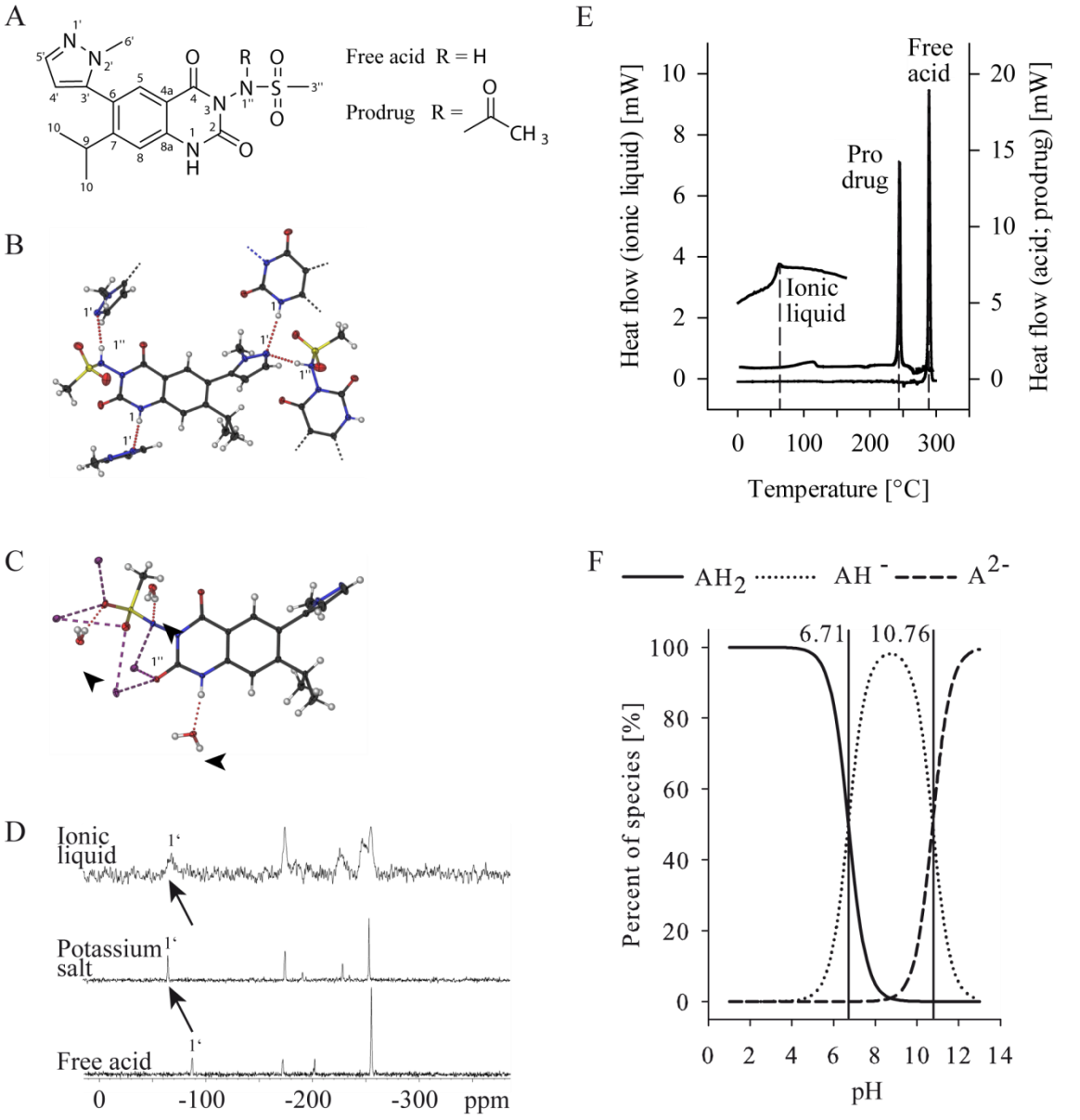

Figure 1: (**A**) Structural formula of the free acid and the prodrug. Crystal structure of the (**B**) free acid and (**C**) the potassium salt of the free acid (a monohydrate) and as determined by single crystal diffractometry. Crystal water is highlighted by arrowheads and the interaction of the potassium cation with the acid is illustrated by dashed rods. (**D**) Solid state ^{15}N NMR spectra displaying the high field shift of the N-1´ signal of the ionic liquid and the potassium salt in comparison to the free acid. (**E**) Glass transition temperature (ionic liquid) and melting points of the prodrug and the free acid, respectively, and as determined by dynamic scanning calorimetry. (**F**) Distribution of species as a function of pH as determined potentiometrically.

bonds. In particular, the unsubstituated nitrogen atom of the pyrazole ring interacted with the hydrogen atom in the sulfonamide group and the hydrogen atom at the unsubstituated nitrogen atom in the 2,4-quinazolindione ring (**Figure 1B**; **Supplementary Figure 1A**; **Table 1**).The potassium salt crystallized as a monohydrate in the monoclinic space group $P2_1/c$ (**Figure 1C**, **Table 1**). In this crystal structure, potassium ions (K^+-ions) formed layers in the crystallographic

	Free acid ($C_{16}H_{19}N_5O_4S$) M_r = 377.43	K^+ salt ($C_{16}H_{20}N_5O_5SKCl$) M_r = 433.53
Crystal system	orthorhombic	monoclinic
Space group	Pbca	$P2_1/c$
a [Å]	15.0318 (10)	22.8265 (6)
b [Å]	12.0212 (8)	5.8993 (2)
c [Å]	19.5095 (13)	15.3597 (4)
α [°]	90	90.00
β [°]	90	104.2530 (10)
γ [°]	90	90.00
Volume [$Å^3$]	3525.4(4)	2004.67 (10)
Z value	8	4
D_{calc} [g/cm^3]	1.4221	1.436

Table 1: Single crystal X-ray data of the free acid and the potassium salt, respectively.

bc-plane with the acid anions placed atop and below the K^+ ions (**Supplementary Figure 1B**). The atomic distances between K^+-ions and nitrogen and oxygen atoms (**Supplementary Figure 1B, Table 1**) suggested ionic interactions between the K^+-ion and four partners, (i) the oxygen atoms and the (ii) nitrogen atom of the sulfonamide group as well as to (iii) one oxygen atom of the quinazolindione ring and to (iv) one crystal water molecule, respectively (**Figure 1C, Supplementary Figure 1B**). In contrast to the crystal structure of the free acid, no direct hydrogen bonds were observed between the organic molecules (**Figure 1C**, **Supplementary Figure 1B**). The free acid, its potassium salt and the prodrug were crystalline whereas the IL was amorphous as determined by XRPD (**Supplementary Figure 2A**) and no birefringence was observed by polarized light microscopy (data not shown). Solid state ^{15}N NMR spectra were recorded for all three forms, the IL, the free acid and the potassium salt (see **Figure 1D**). The nitrogen signals were assigned by long-range ^{1}H-^{15}N HMBC, HSQC and INEPT experiments in solution at room temperature and -70 °C (data not shown) with the N-1´ to δ at -87.2 ppm and N-2´ to δ at -172.1 ppm, respectively. Interestingly, the N-1´ signal was shifted to δ= -64.1 ppm in the spectrum of the IL and to δ= -64.8 ppm in the potassium salt. In the IR spectrum of the free acid, characteristic stretching vibrations were observed at 3146 cm^{-1} for the N-H (1''), and for the sulfonamide group at 1343 cm^{-1} and 1150 cm^{-1}, respectively. For the potassium salt no stretching vibration of N-H (1'') at 3146 cm^{-1} was detected and the absorption band was shifted to 1247 cm^{-1} and 1107 cm^{-1} indicating the deprotonation of the API. In analogy to the observations for the potassium salt, the IL produced no signal of N-H (1'') at 3146 cm^{-1} and the stretching vibration for the sulfonamide group was shifted to 1243 cm^{-1} and 1104 cm^{-1} (**Supplementary Figure 2C**). The melting point for the prodrug and the free acid were read from endothermic peak 244 °C and 290 °C, respectively, and the glass transition temperature of the IL was observed at about 57 °C (**Figure 1E**). A broad

endothermic peak with an onset at 150 °C and a concomitant mass loss of about 4% was observed for the potassium salt (monohydrate), indicating the loss of hydrate water at that temperature (corresponding TGA data **Supplementary Figure 2B**). No melting was detected before degradation onset at about 275 °C. Two pKa values were found for the free acid at 6.7 and 10.8 (**Figure 1F**) linked to the N-1´´ (6.7; as a result of a high-field shift of the methyl group of the methylenesulfonamide group in the ^{1}H NMR spectrum observed at pH 7.6) and to the nitrogen in position 1 of the quinazolinedione ring (10.8; as a result of the high-field signal shift of the aromatic hydrogen H-8 and to a lesser extent of H-5 observed at pH 11.75) (**Supplementary Figure 3A**, **Supplementary Figure 3C**). After storage of the IL for 18 month *in vacuo* no crystallinity was detected by XRPD (date not shown). Furthermore, no changes in ^{1}H NMR spectrum were observed and the glass transition temperature was unaltered (data not shown) as compared to baseline.

Dissolution rate, duration of supersaturation, solubility, precipitation rate and formation of supramolecular aggregates

Drug substance dissolution rate in PBS buffer pH 6.8 was more than 700 fold higher for the IL, as compared to the free acid and twice as high as compared to the potassium salt (**Figure 2**).

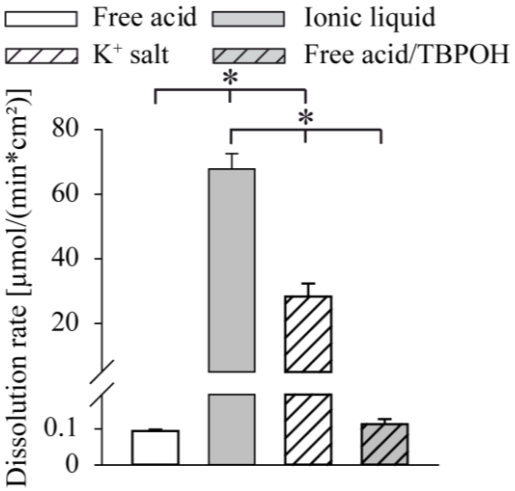

Figure 2: Dissolution rate of the bulk qualities of the free acid, ionic liquid, potassium salt and an equimolar blend of the free acid and the counterion in dissolution medium.

The dissolution rate of the free acid was not different as compared to the blend of the free acid with tetrabutylphosphonium added to the dissolution medium. The duration of supersaturation, calculated from the concentration *versus* time profiles determined by potentiometric titration [12], was for the free acid (10 ± 2 minutes) < potassium salt (12 ± 1 minute) < blend of the free acid and the counterion (22 ± 6 minutes) < IL (35 ± 15 minutes) (**Figure 3A, B**). The duration observed for

the IL and the blend (free acid and counterion) was significantly longer as compared to the free acid and its potassium salt ($p < 0.05$). The duration of supersaturation was further measured by real-time precipitation experiments, complementing these accelerated potentiometric titrations (**Figure 3C, D**). In these, the IL did not demonstrate a pH shift with the solution remaining clear throughout 12 hours (end of experiment). In contrast, a significant pH shift and precipitation was observed after about 12 minutes (± 1 minute) for the potassium salt (**Figure 3C, D**). The dissolution rates for the IL or the free acid were comparable in acetate buffer (data not shown).

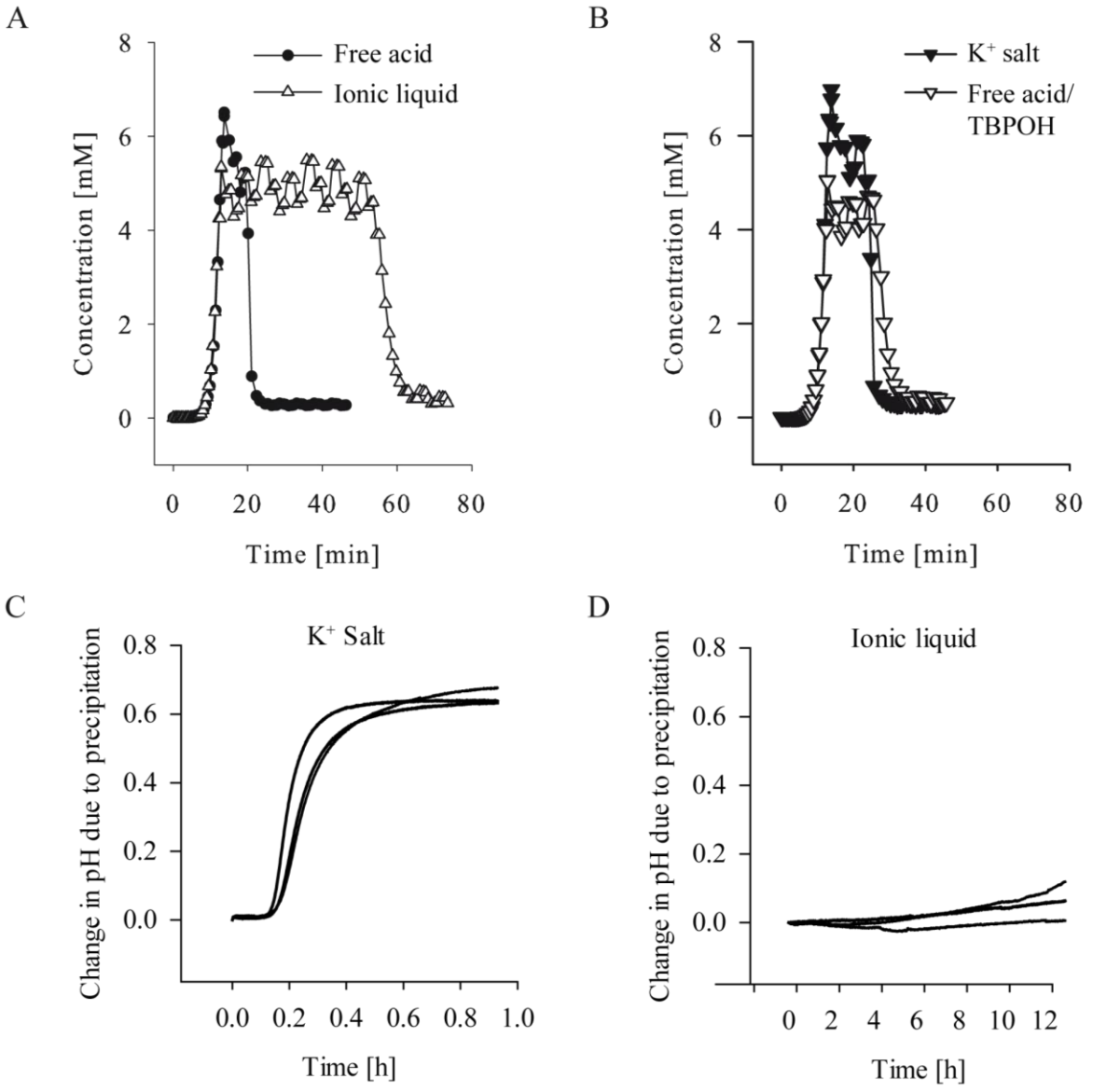

Figure 3: API concentration [mM] – time [minutes] profile for the (**A**) free acid, ionic liquid, (**B**) potassium salt and an equimolar blend of the free acid and the counterion, respectively. Change in pH due to precipitation – time [h] profile of (**C**) potassium salt and (**D**) ionic liquid.

The peak concentration during the supersaturation phase (kinetic solubility), determined by potentiometric titration, was typically higher for the free acid or its potassium salt in comparison to

the IL or the blend of the free acid and the counterion (**Figure 3A, 3B, 4A**). The kinetic solubility recorded for the potassium salt was significantly higher as compared to all other groups ($p < 0.05$), followed by the free acid, which had a higher kinetic solubility as compared to the IL and the blend (free acid and counterion; $p < 0.05$) the latter two groups of which demonstrating equal kinetic solubility (**Figure 4A**). The intrinsic solubility (equilibrium solubility) was generally an order of magnitude lower as compared to the kinetic solubility for all groups (**Figure 4B**). The ratio of the dissolution rate and the precipitation rate measured from the precipitates at supersaturation, was significantly higher for the IL in comparison to the free acid and the potassium salt ($p < 0.05$) and equal for the free acid and the potassium salt, respectively (**Figure 4C)**. In contrast, no differences among groups were observed in the rates observed at equilibrium (**Figure 4C)**.

The IL was further characterized for the presence of soluble supramolecular aggregates when dissolved in water. At a concentration of 1 mM, the electrospray ionization mass spectrum (ESI-MS) in the positive ion mode revealed peaks corresponding to an aggregate formation following the general pattern of $[A_n]^-$ (with signals for n from 1 to 5) and $[A_nK]^-$ (with signals for n from 1 to 7; **Supplementary Figure 3B**) [13]. Lower API concentrations did not show these aggregates (data not shown). Analogous studies following dissolution of the free acid in 30% or 70% acetonitrile in water, respectively, exhibited an increasingly complex association pattern for the free acid as compared to pure water, following $[A_nK_o]^-$, with the index n being an integer between 1 – 6 and o between 1 to 4 for the 70% acetonitrile in water solution (data not shown). The supramolecular association of the API in solution was further analyzed by a ^{1}H NMR based aggregation assay [14] . The superimposition of the ^{1}H NMR spectra collected in the supersaturated and the equilibrium phase exhibited a clear high field shift of all signals in the supersaturated phase with the overall number of signals remaining constant **(Figure 4D).** The signal intensity of the API was substantially reduced when comparing the supersaturated and the equilibrium phase and in comparison to those of the counterion, which was concluded by comparing the H-5' signal of the pyrazole moiety and the terminal methyl group signal of the counterion, respectively (**Figure 4D**). This suggested the precipitation of the IL as the free acid with the counterion remaining in solution.

The duration of supersaturation was exponentially related to supersaturation ratio, following a general trend as approximated by duration of supersaturation $= 206 * e^{-0,16*S}$ ($r^2 = 0.62$), with S being the supersaturation ratio as calculated by dividing the kinetic by the equilibrium solubility, respectively (**Figure 4E**). The duration of supersaturation was linearly correlated to the ratio of the counterion and the free acid by duration of supersaturation $= 10 + 10 * \text{ratio}$ ($r^2 = 0.98$), with the ratio being the molar amount of the counterion divided by the amount of free acid (**Figure 4F**).

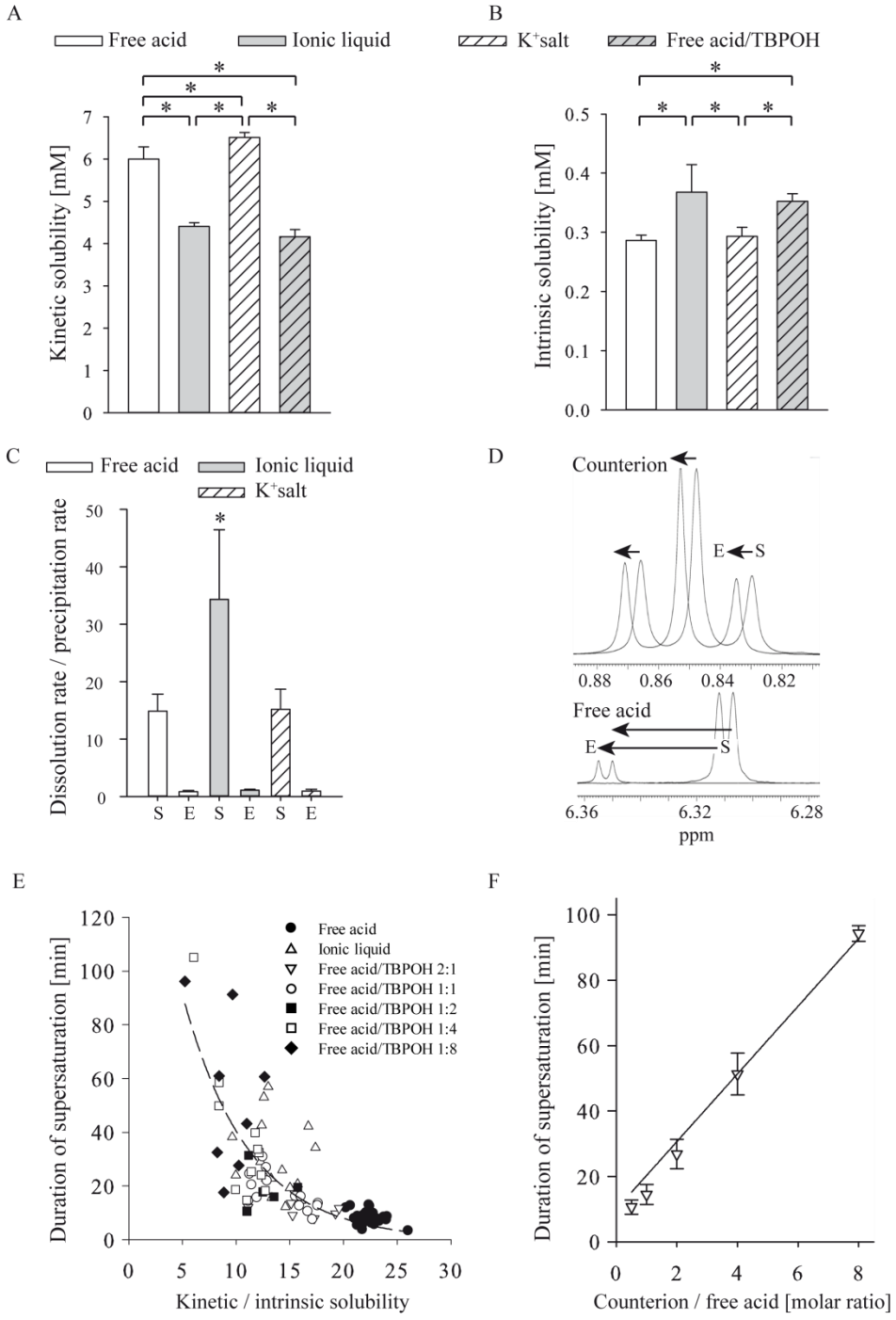

Figure 4: (**A**) Kinetic solubility [mM] and (**B**) intrinsic solubility [mM] of the APIs and blend of free acid and counterion. (**C**) Ratio of the dissolution rate over the precipitation rate of the precipitate in the supersaturated phase (S) and at equilibrium (E) for the free acid, ionic liquid and the potassium salt, respectively. Asterisks indicate statistically significant differences among groups ($p < 0.05$). (**D**) Superimposition of expansions from NMR spectra of the supersaturated phase (S) and in the equilibrium phase (E). The signals of the terminal methyl group of the counterion (tetrabutylphosphonium) at $\delta \sim 0.85$ ppm and H-5' of the pyrazole ring at $\delta \sim 6.3 - 6.4$ ppm are displayed. (**E**) Overview of the duration of the supersaturation phase [minutes] as a function of the ratio of kinetic solubility over equilibrium solubility (supersaturation ratio) for the free acid, the ionic liquid and different blends of the free acid and the counterion. (**F**) Duration of supersaturation [minutes] as a function of different blends of the free acid and the counterion.

Characterization of precipitates in supersaturated and equilibrium state

Time lapsed diffractometric studies on precipitates collected from the supersaturated phase and the equilibrium phase analyzed under gradual drying, revealed different crystallization kinetics for the free acid and the IL (**Figure 5**). The precipitate of the free acid was amorphous in the supersaturated phase and this state was maintained for up to 14 minutes throughout the continuous diffractometric monitoring (**Figure 5A**). However, after 21 minutes the reflection of the potassium chloride – as present from the solubility experiments which were conducted in presence of potassium chloride and from which the precipitates were collected – was observed at about 28° (**Figure 5A**) along with reflections of the free acid (**Supplementary Figure 2A**). Similar to the free acid, the precipitate collected from the supersaturated phase of the IL displayed an amorphous structure at the beginning of the time-lapsed measurements (**Figure 5B**). After 14 minutes, the potassium chloride reflection was observed at about 28°, with the IL still being in amorphous form – a state, which was maintained up to 42 minutes after which the experiment was stopped. In contrast, precipitates collected from the free acid and the IL collected in the equilibrium phase had identical reflections.

Furthermore, the precipitates were analyzed by ^{1}H NMR measurements. The precipitate of the IL collected from the supersaturated phase (dissolved in DMSO-d_6) was measured and the hydrogens attached to the N-1 and N-1'' showed one broad signal (δ = 10 – 12.5 ppm; **Figure 5C**) indicating a single deprotonation (assignment of deprotonation to N-1 and N-1'' was verified by EXSY experiments at room temperature and -70 °C due to rapid proton exchange among groups). In contrast, two resonances were seen in the precipitate harvested from the equilibrium phase indicating that both groups, the N-1'' and the N-1 were protonated and supporting that precipitation occurred as the free acid (**Figure 5C**) as both signals were also observed for the free acid in equilibrium state (**Figure 5C**). The counterion was present in the precipitates collected from the supersaturated phase (**Figure 5C**, arrows; δ = 0.5 – 4 ppm), with an estimated ratio of the API to the counterion of about 6 : 1 as calculated from the integrals of the ^{1}H NMR signals. In contrast, the precipitates harvested from the equilibrium phase showed only traces of the counterion and yielded almost identical spectra as obtained for the free acid (**Figure 5C**). ^{1}H NMR measurements of the precipitate of the free acid collected from the supersaturated state displayed the same broad signal as observed for the IL (data not shown), however no tetrabutylphosphonium signals were detected. After equilibrium state was reached precipitates displayed the same ^{1}H NMR spectra as the bulk substance.

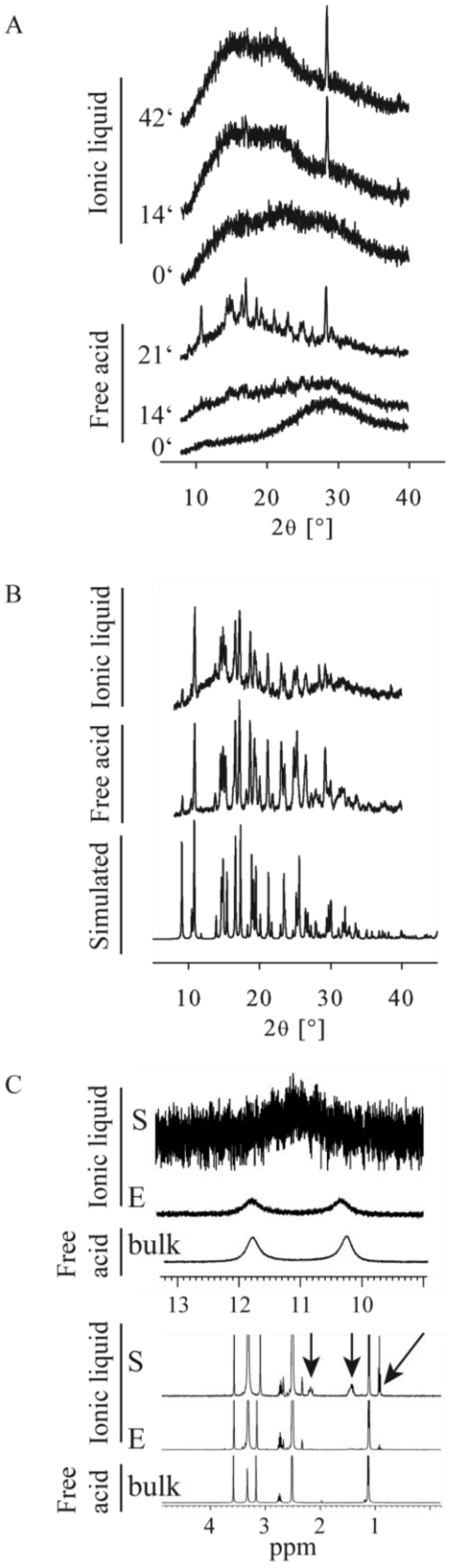

Figure 5: Time lapsed powder diffractograms. Numbers within charts indicate the time [minutes] after the set of experiments commenced. Suspensions gradually dried under ambient conditions within the diffractometer and during measurement. Representative diffractograms of precipitates collected from the supersaturation phase of the (**A**) ionic liquid and the free acid. (**B**) Representative diffractograms of precipitates collected from the equilibrium phase of the ionic liquid and the free acid. A simulated diffractogram as calculated from the single crystal data of the free acid is provided. (**C**) 1H NMR of the precipitates collected in the supersaturated phase (S) and in the equilibrium phase (E) for the free acid and the ionic liquid, respectively (precipitates were re-dissolved in DMSO after collection and right before measurement). Spectra of the bulk free acid are given for comparison (bulk). The upper set of three spectra shows the signal of the hydrogen bound to the methylenesulfonamide group (H-1’’). The lower set of three spectra shows the region within which signals by the counterion are detected and as highlighted by the arrowheads.

In vitro permeability through the Caco-2 cell monolayer model

Caco-2 cell monolayers were characterized before use. All monolayers had TEER values of at least 600 Ω*cm^2 and paracellular permeability and monolayer tightness was demonstrated by sodium fluorescein transport with mean P_{app} values < 10^{-7} cm/s (apical to basolateral; data not shown) [15]. Furthermore, the monolayers were morphologically characterized for the location and distribution of cell nuclei through DAPI stain (blue) and tight junctions were labeled by e-cadherin staining (**Figure 6A**). In a first experiment, API were applied as *solutions* to the apical compartment, resulting in comparable normalized molar amounts found basolaterally over time for the IL and the free acid while the amount of transported prodrug was significantly higher ($p < 0.05$; **Figure 6B**). In a second experiment, a *suspension* of the API was used in the apical compartment instead of the API solution applied in the previous set-up (**Figure 6C, D**). The concentration in the apical chamber of the free acid was approximately three times higher than the concentration observed for the prodrug ($p < 0.05$) and four times lower than the concentration of the IL ($p < 0.05$; **Figure 6C**). The molar API amounts analyzed within the basolateral compartment over time were significantly and typically 5 times higher for the IL as compared to the free acid or the prodrug (**Figure 6D**).

Counterion cytotoxicity

Cytotoxicity of tetrabutylphosphonium chloride was analyzed *in vitro* in three cell lines with an AlmarBlue based assay. IC_{50} values were 712 ± 14 µM for HepG2 cells, 248 ± 48 µM in HEK 293T cells and >1000 µM for J774.1 cells.

Discussion

We defined the IL based on the observed glass transition below 100 °C (**Figure 1E**) and the ionic nature determined by solid state ^{15}N NMR (**Figure 1D**) and IR spectroscopy (**Supplementary Figure 2C**). For both the IL and the potassium salt, the N-1´ signal of the pyrazole nitrogen was shifted almost identically in contrast to the high field shift of this signal for the free acid (**Figure 1D**). Crystal structure data detailed these findings to the deprotonation of the methylenesulfonamide group of the potassium salt (**Figure 1C**). While the proton of the methylenesulfonamide group of the acid is part of a hydrogen bond to the pyrazole nitrogen N-1´, no such interaction is possible for the deprotonated potassium salt, resulting in a shifted N-1´ signal to higher field. In the IR spectra an identical shift of the methylenesulfonamide group after deprotonation for both the potassium salt and IL was observed (**Supplementary Figure 2C**). Therefore, the solid state ^{15}N NMR and IR spectroscopy data confirmed the ionic nature of the IL in solid state. Stored *in vacuo* the IL was stable for 18 month, with no recrystallization and no shift in glass transition temperatures occurring throughout the storage period, an important yet

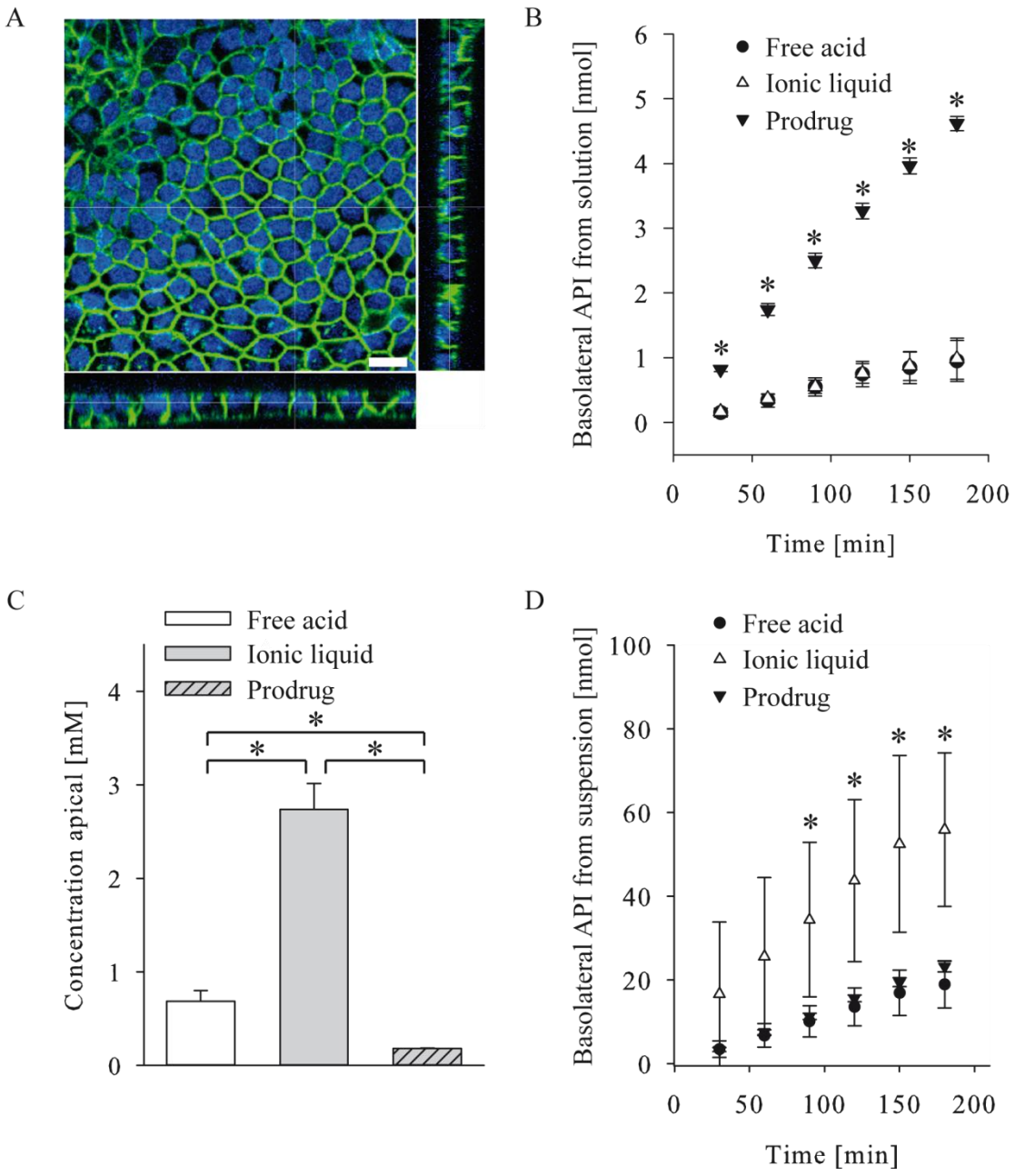

Figure 6: Transport studies through an *in vitro* Caco-2 cell culture model of the human small intestinal mucosa and grown on a cell culture insert filter. (**A**) Representative confocal microscopy image after immunohistological staining of cell-cell contacts (e-cadherin, green) and cell nuclei (DAPI, blue). Bar length = 20 µm. (**B**) Amount of API [nmol] as measured from samples taken from the basolateral chamber at different time points [minutes]. Solutions of the free acid, the ionic liquid and the prodrug were administered to the apical chamber, respectively. (**C**) Amounts of dissolved API when applied as suspension to the apical chamber for the free acid, the ionic liquid and the prodrug, respectively. (**D**) Amount of API [nmol] as measured from samples taken from the basolateral chamber at different time points [minutes]. Suspensions of the free acid, the ionic liquid and the prodrug were administered to the apical chamber, respectively. Asterisks indicate statistically significant differences among groups ($p < 0.05$).

preliminary finding regarding drug substance stability. Further studies including stress tests are required to detail the stability under real life or accelerated conditions.

The drug substance dissolution rate of the IL exceeded the potassium salt and even more the free acid (**Figure 2**). The faster dissolution of the IL and the potassium salt in comparison to the free acid is likely a result of the ionization whereas the differences of the (amorphous) IL in comparison to the (crystalline) potassium salt are attributed to the different lattice forces.

A prolonged supersaturation was observed for the IL (**Figure 3A**). The observation for the IL matched the classical nucleation theory [16, 17], linking the rate of crystal formation J exponentially to the supersaturation ratio and given by $J = Ae^{(-\frac{B}{ln^2 S})}$. A and B are typically regarded as constants with $\frac{B}{ln^2 S} = W/kT$ representing a dimensionless energy barrier for the formation of nuclei and S being the supersaturation ratio [16]. The pre-exponential term A represents the molecular kinetics of the formation of nuclei. According to the Szilard-Farkas model, the formation of nuclei is a stochastic process of consecutive attachment and detachment events of single molecules, yielding clusters of different sizes in the supersaturated solution [18]. The frequency of attachment of unit blocks to a nucleus (f^*) is assumed to be the rate limiting step of nucleus formation [19]. The precise assessment of f^* is challenging [16], yet our data provided evidence, that the ratio of the attachment and detachment kinetics of precipitates, obtained from previously dissolved API through pH adaptation in the supersaturated phase was significantly higher for the IL as compared to the other groups tested (**Figure 4C**). This suggested that the extended duration of supersaturation is at least in part driven by the counterion's impact on nucleus formation. This interpretation is supported by the linear dependency observed for the duration of supersaturation and the ratio of the counterion and the API (**Figure 4F**). These solubility profiles obtained by potentiometric titration are determined using an accelerated method of measuring the duration of supersaturation and, therefore, real-time precipitation experiments were additionally performed (**Figure 3C, D**). In these real-time experiments, the potassium salt recrystallized within 12 minutes counteracting the positive effect of increased dissolution and questioning a sensible use *in vivo*. In contrast, the IL was stable in solution throughout 12 hours (end of experiment), providing a more promising profile for further development. Nevertheless, more details are required to elucidate the broader impact of the IL, e.g. building off previous elegant studies detailing crystal growth dynamics of Theophylline by using crystal seeds [20]. In analogy, the impact of crystal growth on seeds prepared from the free acid can be profiled in solutions of the IL or the free acid.

Time lapsed diffractometric studies of the free acid and the IL detailed the crystalline status of precipitates formed in the supersaturated and the equilibrium phase generated from initially

dissolved API by pH adaptation (**Figure 5A, B**). A faster collapse of the supersaturated phase was found for the free acid as compared to the IL, with precipitates from both groups being amorphous in the supersaturated phase and deprotonated at the sulfonamide group (**Figure 5C**). The term amorphous is used in a sense that crystallinity was not detected based on interpretation of the diffractograms. However, we cannot exclude that other mesophases were present, which were not detected by XRPD [21]. Interestingly, the IL precipitated in the supersaturated phase together with the counterion (**Figure 5C**), whereas the precipitate collected at equilibrium was composed of the free acid (**Figure 5B**) indicating a different molecular association of the counterion and the API at supersaturated and equilibrium state, respectively. To elucidate the underlying mechanism, the API was further characterized in solution. The stable number and the chemical shifts of the signals measured by ^{1}H NMR at concentrations spanning from 0.125 mM to 4 mM (**Supplementary Figure 4**) and at 8 mM (**Figure 4D**) suggested a concentration dependent formation of soluble associates, and the concentration effect on association was corroborated by mass spectrometry (data not shown). By ^{1}H NMR a striking change in peak intensity (and a signal shift) was observed at the supersaturated and equilibrium phase, respectively (**Figure 4D**) as a result of precipitation and supported by the solubility measurements (**Figure 3A, B**). In contrast, this intensity change observed for the API was not observed for the counterion. In conclusion, these experiments demonstrated that the counterion prolonged supersaturation by stabilizing the deprotonated state of the API. The moment the counterion fails in doing so, the API is precipitating as the free acid. This is further supported by the decrease of the API concentration with a stable concentration of the counterion in solution at equilibrium. Therefore, the mechanism is characterized by a constant increase of the counterion to API ratio in the supersaturated state as a result of the advancing precipitation of the API while the counterion does not precipitate (API precipitates as free acid; counterion remains in solution). This increase of the counterion to free acid ratio correlated to prolonged supersaturation (**Figure 4F**) and, thereby, a self-stabilizing loop is closed leading to long-lasting supersaturation of the API. Furthermore, the IL may be formulated into a gastro-protective to prevent rapid collapse of the free acid in the gastric environment with high proton concentrations.

Solubility and / or permeability challenges are typically addressed by the synthesis of prodrugs, rapidly metabolizing entities leading to the parent drug already during or shortly after uptake. The acetylation of the sulfonamide group yielded a prodrug with a 5 times enhanced permeability through Caco-2 monolayers (**Figure 6B**) but 4 times reduced solubility (**Figure 6C**) as compared to the free acid. In contrast, the increased solubility of the IL, translated into an increased amount of absorbed substance as compared to the free acid or the prodrug. *In vivo* studies are needed to substantiate this first evidence for better bioavailability of the IL.

We conclude that the formation of an IL positively impacted the permeability through Caco-2 cell layers in terms of dissolution rate and time of supersaturation potentially widening the window for API uptake within the GIT.

Previous studies link the counterion to a skin irritation potential, however, the study was conducted with an irrelevant setup for the administration as profiled here within [22]. We performed initial cell viability studies of the counterion on kidney and liver cells as well as on macrophages and cell viability was affected in the upper µM or lower mM range, indicating a rather benign safety profile which must be substantiated by rigorous pre-clinical toxicology studies.

Conclusion

We detailed the mechanism of the favorable solubility profile of the IL as compared to the free acid, its potassium salt and the prodrug. The counterion of the IL had different effect on the API in the solid *versus* the liquid state. From the solid state, the dissolution was 700 fold faster in comparison to the free acid as a result of reduced lattice energy. Advantages in the liquid state of the IL resulted from increased solubility as well as from a constant increase of the counterion to API ratio with time (counterion remained in solution, API precipitated in part), a mechanism which was demonstrated to increase supersaturation. Ultimately, both mechanisms resulted in an increased transepithelial transport *in vitro*. However, future *in vivo* studies are required to demonstrate whether these promising features of the IL translate into biopharmaceutical advantages.

Materials and Methods

Materials

Dulbecco´s MEM powder and Trypsin powder substance were purchased from Biochrome AG (Berlin, Germany) and Fetal Bovine Serum and RPMI medium from Gibco (Darmstadt, Germany). Caco-2 cells were purchased from DSMZ (Braunschweig, Germany). 4', 6-diamino-2-phenylindole (DAPI) was purchased from Invitrogen (Carlsbad, CA) and Human E-Cadherin MAb (clone 180215) from R&D systems (Minneapolis, MN). Acetonitrile HPLC grade and potassium chloride (KCl) were purchased from VWR (Radnor, PA). Penicillin and streptomycin solution (Pen/Strep), non-essential amino acids (NEA), Hank's Balanced salts powder (without phenol red and sodium hydrogen carbonate), tetrabutylphosphonium hydroxide solution (40% in water v / v; referred to as 'counterion' within this manuscript), trifluoracetic acid (TFA), fluorescein sodium salt, hydrochloric acid 0.5 M, HEPES, glucose and acetic acid (≥ 99.7%) were purchased from Sigma Aldrich (St. Louis, MO). N-[7-Isopropyl-6-(2-methyl-2H-pyrazol-3-yl)-2,4-dioxo-1,4-dihydro-2H-

quinazolin-3-yl]-methanesulfonamide (referred to as 'free acid' within this manuscript) and N-[7-isopropyl-6-(2-methyl-2H-pyrazol-3-yl)-2,4-dioxo-1,4-dihydro-2H-quinazolin-3-yl] N-methylsulfonyl-acetamide (referred to as 'prodrug' within this manuscript) were synthesized by Novartis AG (Basel, Switzerland)[7-9]. Sodium chloride, sodium hydrogen carbonate, sodium dihydrogen phosphate, disodium hydrogen phosphate, formaldehyde, ethanol and methanol were of analytical grade. Deuterated water (D_2O, 99.9% D) was purchased from Deutero GmbH (Kastellaun, Germany), deuterated water (D_2O, 99.9% D) containing 0.05% 3-(trimethylsilyl)propionic-2,2,3,3-d_4 acid-Na (TSP-d_4) from Sigma-Aldrich (Schnelldorf, Germany), hexadeuteriodimethyl sulfoxide (DMSO-d_6, 99.8% D) from Euriso-top (Saarbrücken, Germany), anhydrous dibasic sodium phosphate (99%) from Acros Organics (Geel, Belgium) and AVS Titrinorm 0.1 M hydrochloric acid and 0.1 M sodium hydroxide solution from VWR (Darmstadt, Germany). Standard 5 mm NMR tubes (ST 500) were purchased from Norell (Landisville, PA) and coaxial insert tubes from Wilmad-LabGlass (Vineland, NY). J774.1 cells, HepG2 cells and HEK 293T cells were purchased from ATTC (Manassas, VA).

Methods

Ionic liquid and potassium salt preparation

The ionic liquid (IL) was prepared in analogy to previous reports[23]. Briefly, 1g free acid was suspended in 40 mL acetone, an equimolar amount of the counterion (tetrabutylphosphonium hydroxide) was added and mixed until a clear solution was obtained. Solvents were evaporated at 40 °C, 150 – 300 mbar until approximately 2 ml were left. The liquid was transferred onto a watch crystal and dried at 50 °C *in vacuo* for one day. For the preparation of the potassium salt, 0.5 g acid was suspended in 5 ml ethanol in a round-bottomed flask. The resulting mixture was heated to 40 °C and a solution of 0.083 g of potassium hydroxide in 0.5 ml of water was added continuously over 3 minutes. The solution was cooled to 20-25 °C under stirring. Crystals were collected after 1 hour by filtration with a filter crucible (pore size 4, Winzer, Wertheim, Germany). The filter cake was washed 2 times with 1 ml of ethanol and was dried at 50 °C for 2 hours *in vacuo* to yield 0.45 g salt.

High performance liquid chromatography

Free acid, IL and prodrug samples were analyzed using a HPLC La Chrome Ultra equipped with a diode array detector L2455U, autosampler L-2200U and column oven L-2300 (Hitachi, Schaumburg, IL) on a Zorbax SB-C18 RRHT column (4.6x50mm, 1.8 µm; Agilent, Waldbronn, Germany) at a column temperature of 40 °C. Mobile phase A was 0.1% TFA in water and mobile phase B was 0.1% TFA in acetonitrile with the gradient profile set as follows for mobile phase B: 0

- 3.5 min 15-65%; 3.5-3.7 min 65-15% and 3.7-5 min 15%. The flow rate was set at 1.2 mL/min and detection at λ = 254 nm.

Time lapsed, potentiometrically and photometrically recorded titration experiments for determination solubility, duration of supersaturation, precipitation rate, pka and dissolution rate

Intrinsic and kinetic solubility and the duration of the supersaturation were measured on a Sirius T3 instrument (Sirius Analytical, Forest Row, UK) by potentiometric titration as described before[24, 25]. In brief, typically 10 mg of API were dissolved in 1.5 ml of 0.15 M KCl solution at pH 12 (adjusted with 0.5 M potassium hydroxide). After complete dissolution, the solution was back-titrated by addition of 0.5 M hydrochloric acid until first precipitation occurred and as continuously monitored photometrically (λ = 500 nm). Subsequently, the pH was changed incrementally by repeated addition of minute amounts of acid and base throughout the experiment. After each titrant addition the delayed pH gradient of the API due to precipitation or dissolution was measured and used to extrapolate the equilibrium phase where the pH gradient is zero. The duration of supersaturation is the time interval from the first precipitation (kinetic solubility) to the time when the concentration dropped below the kinetic solubility. Data from analysis with acidity errors larger than 1 mM were excluded. Precipitation and dissolution rates were recorded for the supersaturated and equilibrium phases, respectively. The precipitation rate was calculated as the change in molar concentration over time (dc/dt) after titration of minute amounts of hydrochloride acid (precipitation rate) or potassium hydroxide (dissolution rate), respectively. Concentration changes due to different titrant volume additions were corrected. pKa was determined on the Sirius T3 in potentiometric mode and according to the manufacturer's instruction. Besides by potentiometric titration, duration of supersaturation was determined by real time precipitation experiments with the Sirius T3 instrument. 8µmol potassium salt and IL, respectively, were completely dissolved in 1.5 ml PBS pH 6.8 and pH was monitored over 1 hour for potassium salt and 12 hours for the IL. The change in pH due to precipitation was detected.

Dissolution rates were determined as described earlier[26]. Tablets with defined surface were prepared by compression of 5-10 mg substance in a tablet disc under a weight of 0.18 tonnes for 6 minutes with a manual hydraulic tablet press (Paul Weber Maschienen- und Apparatebau, Stuttgart-Uhlbach, Germany). Tableting is to render the dissolution rate independent of the surface, which was kept constant at 7.07 mm^2 throughout the experiment. Tablets were used for the experiment if these had a smooth surface. Visible cracks or other defects were not observed and solid particles did not detach from the tablet surface during the experiment. Dissolution rates were determined photometrically at room temperature in phosphate buffered saline (PBS) pH 6.8.

X-ray powder diffractometry

Precipitates were collected from the solubility experiments after the first precipitation occurred and subject to X-ray powder diffractometry (XRPD) analysis. These suspensions were filtered through a paper filter (Macherey-Nagel MN 615, 7cm diameter) using a filter crucible *in vacuo*. Precipitates as observed in the equilibrium phase were collected after stable intrinsic solubility concentration was recorded typically for 10 minutes. Powder diffractometric studies were done with a Bruker Discover D8 powder diffractometer (Karlsruhe, Germany) using Cu-Kα radiation (unsplit $K\alpha_1$+$K\alpha_2$ doublet, mean wavelength λ = 154.19 pm) at a power of 40 kV and 40 mA, a focusing Goebel mirror and a 1.0 mm microfocus alignment (1.0 mm pinhole with 1.0 mm snout). Samples were prepared on a flat aluminum surface. Detection of the scattered X-ray beam went through a receiving slit with 7.5 mm opening, a 0.0125 mm nickel foil and a 2.5° axial Soller slit. Detection was done with a LynxEye-1D-Detector (Bruker AXS) using the full detector range of 192 channels. Measurements were done in reflection geometry in coupled two theta/theta mode with a step size of 0.025° in 2θand 0.25 s measurement time per step in the range of 8 – 40° (2θ). Data collection and processing was done with the software packages DIFFRAC.Suite (V2 2.2.690, Bruker AXS 2009-2011, Karlsruhe, Germany) and DIFFRAC.EVA (Version 2.1, Bruker AXS 2012-2012, Karlsruhe, Germany). Simulation of the theoretic pattern of the free acid was done from the cif-file obtained from single crystal analysis with the program Mercury (Mercury 3.1 Development – Build RC5, CCDC 2001-2012, Cambridge, UK).

Differential scanning calorimetry and thermogravimetry

Differential Scanning Calorimetry (DSC) was performed on a DSC 8000 instrument (Perkin Elmer, Waltham, MA) using a scanning rate of 20 K/min. Sample size was 2.10 mg, 5.52 mg, 0.85 mg and 1.67 mg for the free acid, the IL, the potassium salt and the prodrug, respectively. For the IL, the second heating cycle was analyzed to allow removal of residual water during the first heating cycle. Crucibles were weighed before and after measurements. A Q5000 TGA (TA instruments, New Castle, DE) was used for thermo gravimetric analysis. The platinum crucible was tarred first and then loaded with substance. The scan rate was 10 °C / min from 30 °C to 300 °C.

Nuclear magnetic resonance measurement

NMR measurements were performed on a Bruker Avance 400 MHz spectrometer (Karlsruhe, Germany) operating at 400.13 MHz with a BBO BB-H 5mm probe head, and data processing with the TopSpin 3.0 software. The temperature was adjusted with a BCU-05 (Bruker) temperature control unit. Solid-state ^{15}N VACP/MAS NMR spectra were recorded at 22 °C on a Bruker DSX-400 NMR spectrometer with bottom-layer rotors of ZrO_2 (diameter 7 mm) containing

approximately 200 mg of sample. A resonance frequency of ^{15}N 40.6 MHz, referenced to external standard glycine (^{15}N, δ= -342.0) was set with a spinning rate of 6.8-7 kHz, contact time 3 milliseconds, 90° transmitter pulse length of 3.6 microseconds and a repetition time of 4 seconds. 2120 scans were collected for the potassium salt and the free acid and 20,000 scans were collected for the IL. For pKa assignment and characterization of the precipitates by ^{1}H NMR measurements the following acquisition parameters were applied: 16 scans, at a temperature of 300 K, flip angle of 30°, spectral width of 20.55 ppm, and transmitter offset of 6.175 ppm. The acquisition time was set to 3.985 seconds followed by a relaxation delay of 1.0 seconds with collection of 64 K data points at a sample spinning frequency of 20 Hz. Processing parameters were set to an exponential line broadening window function of 0.3 Hz, an automatic baseline correction and manual phasing. For the aggregation assay based on concentration dependent ^{1}H NMR signal shift measurements, 256 scans were collected at a temperature of 300 K using otherwise identical parameters as described above. The spectra were referenced to the external standard of 0.05% sodium trimethylsilylpropionate in D_2O (TSP-d_4) filled in a coaxial insert tube. For sample preparation of the pKa assignment experiment, four samples of 9 mg free acid each were suspended in 10 ml Millipore water. The pH was adapted to 3.57, 5.57, 7.61, and 11.75, respectively, using either 0.1 M aqueous hydrochloric acid or 0.1 M aqueous potassium hydroxide. The samples were lyophilized for 24 h (Christ Lyophilisator Alpha 1-4 LD plus; Osterode, Germany) and dried samples were dissolved in 700 µl DMSO-d_6 before measurement. The sample preparation for the concentration range / aggregation assay was as described before with modification[14]. Briefly, 7.64 mg IL were weighted into a 2 mL Eppendorf tube and dissolved in 1500 µL buffer (8 mM sample; 200 mM dibasic sodium phosphate buffer in D_2O pH 7.4 (pD 7.8). 500 µL of this stock solution was immediately transferred into a 1.5 mL Eppendorf tube and another 500 µL buffer were added yielding a 4 mM solution, and vigorously shaken for two minutes. This dilution step was repeated in order to establish a dilution series of 0.125, 0.25, 0.5, 1, 2, 4, and 8 mM. The 8 mM sample was measured from supernatants collected from the supersaturation and in the equilibrium phase, respectively.

Infrared spectroscopy

The measurements were conducted on Jasco FT/IR-6100 spectrometer from Jasco (Gross-Umstadt, Germany) with diamond attenuated total reflection unit.

Single crystal diffraction

Single crystals of the free acid were obtained by re-crystallization of the product in methanol with access to benzene. The recrystallization of the potassium salt was performed by dissolving 2 mg in 1 mL acetontrile with 2 drops of methanol and evaporating the solvent. Suitable single crystals

were mixed with high viscosity perfluorinated polyalkylether (99.9%, ABCR, 1800 cSt). Selected crystals were mounted and fixed on a plastic quill and instantly cooled in a gas stream of dry, evaporating liquid nitrogen. Data collection for the free acid was performed on a X-ray single crystal diffractometer based on a BRUKER D8 3-axis goniometer with a CCD SMART APEX I detector system (Bruker AXS Inc., Madison, WI) with standard graphite monochromator using sealed tube Mo-Kα radiation (unsplit $K\alpha_1$ λ = 70.93 pm Å + $K\alpha_2$ λ = 71.35 pm doublet, mean λ = 71.073 pm) at a power of 40 kV and 40 mA at a temperature of 168 K (3) K. Operation software was the SMART Suite Software package (v 5.0 Bruker AXS Inc.). Frame acquisition strategy consisted of 2124 frames (512 x 512 pixels, acquisition time 20 s) in 6 runs with ω (0°, 60°, 120°, 180°, 240°, 300°) and a range of 180° ϕ (0.5° steps) for each run. Data collection for the potassium salt was performed on a X-ray single crystal diffractometer based on a BRUKER FR591 κ-goniometer with a CCD APEX II detector system (Bruker AXS Inc.) with Helios multilayer mirror monochromator using rotating anode Mo-Kα radiation (unsplit $K\alpha_1$ λ = 70.93 pm Å + $K\alpha_2$ λ = 71.35 pm doublet, mean λ = 71.073 pm) at a power of 50 kV and 40 mA at 100(2) K. Operation software is the Apex II Suite Software package (v 2012.4-3, Bruker AXS Inc.). Frame acquisition strategy consisted of 1320 frames (512 x 512 pixels, acquisition time 30 s) in 9 runs covering the complete Laue sphere. Both datasets were processed with the Apex II Suite Software package (v 2012.4-3, Bruker AXS Inc.) including the SAINT+ Integration Engine (v 8.18C, Bruker AXS Inc.) for data integration, the SADABS software (v 2008/1, Bruker AXS, Inc.) for absorption correction, XPREP v 2008/2, Bruker AXS Inc.) for the preparation of instruction files and reflection lists. Structure solution via direct methods and structure refinement was made with SHELXS[27] and SHELXL[27] from the software package SHELXTL (v 6.14 8/06/00 Bruker AXS Inc.). Integrity of symmetry was checked with PLATON (v 1.16)[28]). GUIs used for refinement and extraction of crystallographic data are X-SEED (v 2.05)[29] and OLEX 2 (v 1.2)[30]. For all species, all non-hydrogen atoms were refined anisotropically and all hydrogen atoms were refined isotropically on their specified atomic positions by least square methods.

Mass spectrometry

The experiments were conducted as described before with modification[13]. Three solutions of the IL were prepared in Nanopure water:acetonitrile mixtures at a volume ratio of 7:3 and 3:7, respectively, yielding a final concentration of the IL of 1 mmol/L. Samples were directly injected into the an Agilent (Palo Alto, CA) 1100 Series LC/MSD Trap system via ESI-interface with a syringe pump Model 100 (KD scientific, Holliston, MA) at a flow rate of 1 ml/h. The liquid stream was nebulized with nitrogen gas at a flow of 5 L/min and a nebulizer pressure of 15.0 psi. The analysis was done by means of the LC/MSD Trap version 5.3 software (Agilent, Waldbronn, Germany). An ESI ionization method in a negative mode and a scan range from 200 to 4000 m/z

was used. The drying gas temperature was set to 110 °C so that associated molecules of the IL could be transferred into the gas phase. The overall goal was to conserve intermolecular interaction throughout analysis as described before[31].

In vitro permeability through the Caco-2 cell monolayer model

Cells were grown in Dulbecco's modified Eagle's medium high glucose (DMEM) with penicillin and streptomycin (Pen/Strep) as described before[32, 33]. In brief, 500 mL medium were prepared with Dulbecco's modified eagle medium (DMEM) powder containing 4.5 g glucose, 50 mL Fetal Bovine Serum, 5 mL 100x nonessential amino acids (NEA) and 5mL Pen/Strep (penicillin 10,000 U/mL and streptomycin 10 mg mL^{-1} solution 100x). Caco-2 cells were cultured at 37 °C and 5% CO_2 in cell culture medium. 2.7 x 10^5 cells / cm^2 (counted with Neubauer improved hemocytometer; LO-Laboroptik, Friedrichsdorf, Germany) were seeded on polycarbonate filter inserts (diameter 12 mm; 0.4 µm membrane pore size) on 12 well plates (Corning life science, Amsterdam, The Netherlands). Cells typically had 54 -56 passages. The monolayer integrity was monitored by measuring the transepithelial electrical resistance (TEER) and fluorescein added to the apical compartment as a leakage marker. TEER measurements were performed for each cell-seeded filter using a chopstick electrode EVOM2 STX3 electrode and EVOM2 epithelial voltammeter (World Precision Instruments, Sarasota, FL). Specifications for cell-seeded filters required TEER values exceeding 600 (Ω*cm^2)[15, 32, 34]. Sodium fluorescein was applied to two filters of each 12 well plate, following previously published protocols[15, 34]. In brief, 20 µM sodium fluorescein Hank's Buffered Salt Solution (HBSS) buffer solution were applied apically. Samples for reading the fluorescence were taken at all-time points when samples were collected for the API transport study and analyzed on 96 well plates (96F nontreated white microwell SH; Nunc, Penfield, NY) with a LS50B fluorescence spectrometer (Perkin Elmer, Waltham, MA). The apparent permeability coefficients ($P_{app;}$ cm/sec) were calculated as follows: $P_{app} = (dQ/dt)(1/A * c_0)$ and dQ/dt being the steady-state flux [µmol/sec], A being the insert/filter surface area [cm^2] and c_0 being the starting concentration in the apical (donor) chamber [µM]. Transport studies were performed as described before and typically commencing 21-23 days after seeding of the cells on the inserts[33, 35]. For that, HBSS buffer (pH 7.4) was used for sample preparation and as the basolateral (receiving) medium. The APIs were applied apically either as a solution with a concentration of 0.26 mM for the free acid, 0.26 mM for the IL or 0.056 mM for the prodrug (maximal prodrug concentrations after 3 h in solution (0.13 mM at pH 7.4) were lower as those for the IL (2.74 mM at pH 7.4) and the free acid (0.68 mM at pH 7.4) due to solubility limitation). Basolateral API amounts from acid and IL solution experiments were normalized in order to compensate for the higher apical concentrations of acid and IL in comparison to prodrug. Another transport study explored the APIs applied as suspensions to the apical (donor)

compartment. For that, suspensions were prepared in 400µl of HBSS buffer for each filter insert, holding amounts of 1.47 ± 0.08 µmol for the free acid, 1.55 ± 0.05 µmol for the IL or 1.33 ± 0.05 µmol for the prodrug ($n \geq 5$ filter inserts per group). Samples were typically collected from the basolateral (uptake) compartment after 30 minutes. Sodium fluorescein samples were analyzed by fluorescence spectroscopy. The monolayers were further characterized after completion of the transport studies by cell nuclei stain and in representative filters for e-cadherine (cell contacts) labeling. For that, cells on the filters were exposed to 4% formaldehyde in PBS pH 7.4 for 20 minutes and filters were treated with 0.1% Triton X in PBS pH 7.4 for 10 minutes and exposed to 5% BSA in PBS pH 7.4 buffer for 60 minutes, thereafter. Mouse antibody against human e-cadherin was diluted 1:100 in PBS pH 7.4 and applied for 2 hours at room temperature after which a secondary antimouse Alexa Fluor 488 antibody (Life Technologies, Darmstadt, Germany; diluted 1:200 in blocking solution) was applied and subjected to the confocal microscopy, thereafter. Cell nuclei were labeled with 4′,6-diamidine-2-phenylindol (DAPI) and diluted 1:1000 in PBS pH 7.4 according to the manufacturer's protocol and subjected to the confocal microscopy (Leica TCS-SP2, Wetzlar, Germany; lens 63/1.4 oil), thereafter.

Cytotoxicity of counterion

Tetrabutylphosphonium chloride was dissolved and serially diluted in DMSO. For the experiments J774.1 and HepG2 cells were suspended at a concentration $1x10^5$ cells/ml in RPMI medium with 10% FCS and without phenol red. HEK 293T cells were diluted to $2x10^4$ cells/ml in DMEM high glucose medium with 10% FCS and without phenol red. 200 µl of cell suspensions were transferred into 96-well cell culture plates and the API dilutions were added. The final concentration of DMSO was 1%. After 24 h of incubation at 37 °C and 5% CO_2, 10% of AlamarBlue solution were admixed. J774.1 and HepG2 cells were incubated for further 48 hours and HEK 293T cells for 24 hours. The IC_{50} values were calculated, with respect to controls without APIs, from the absorbance values measured at 550 nm, using 630 nm as reference wavelength.

Acknowledgments

This study was funded by Novartis Pharma AG, Basel. T.W., J.B., B.G. are full time associates of Novartis Pharma AG and state a possible conflict of interest. We thank Rüdiger Bertermann for support with the solid state NMR measurements, Elena Katzowitsch for performing the cytotoxicity experiments and Susanne Glowienke for *in silico* toxicology prediction.

Supplementary Information

Supplementary Figures:

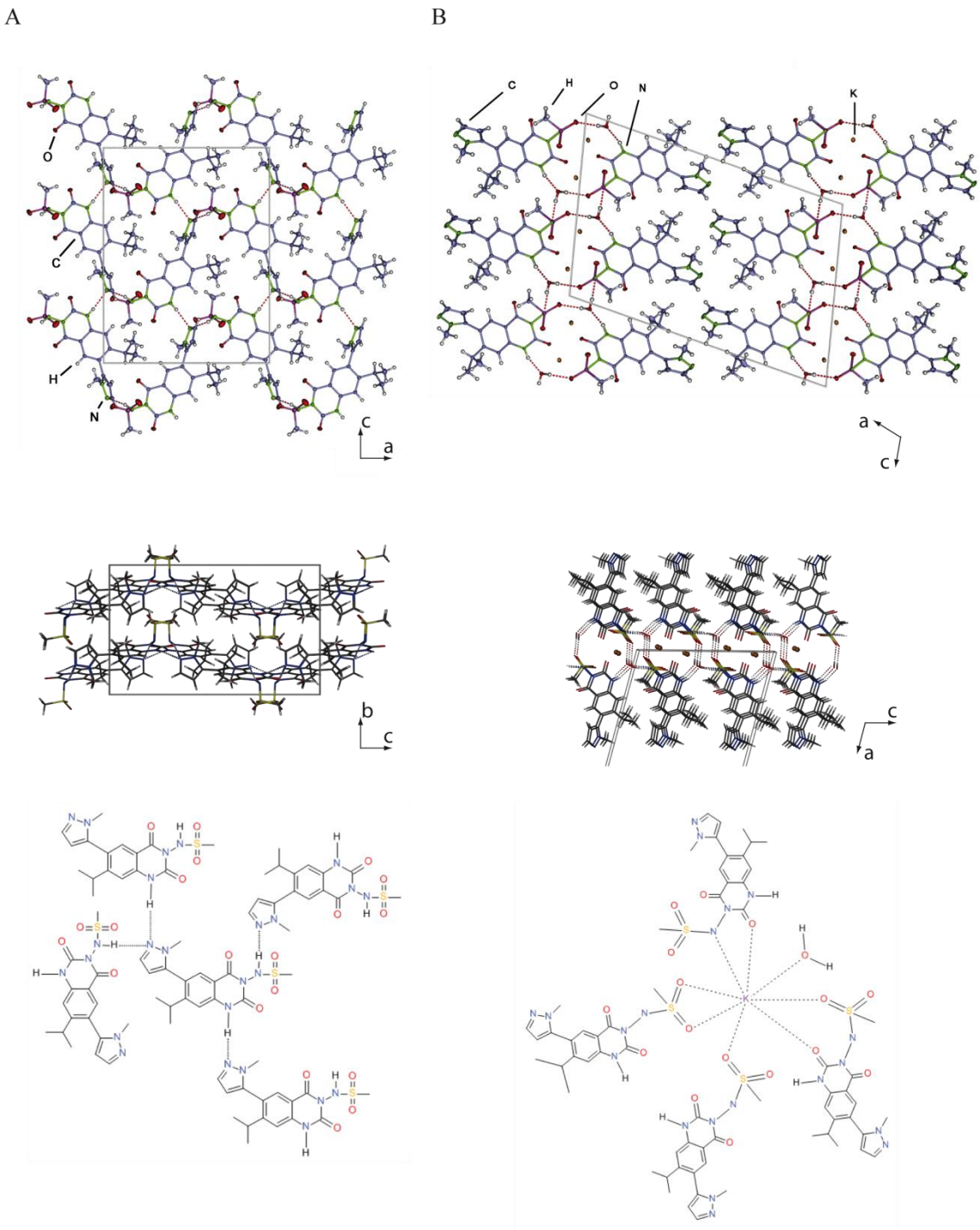

Supplementary Figure 1: (**A**) The crystal structure of the free acid and of the (**B**) potassium salt viewed down the b axis and simplified, respectively. Intermolecular hydrogen bonds are marked as red dotted lines. The thermal ellipsoids depict 50% of the probability levels of the atoms.

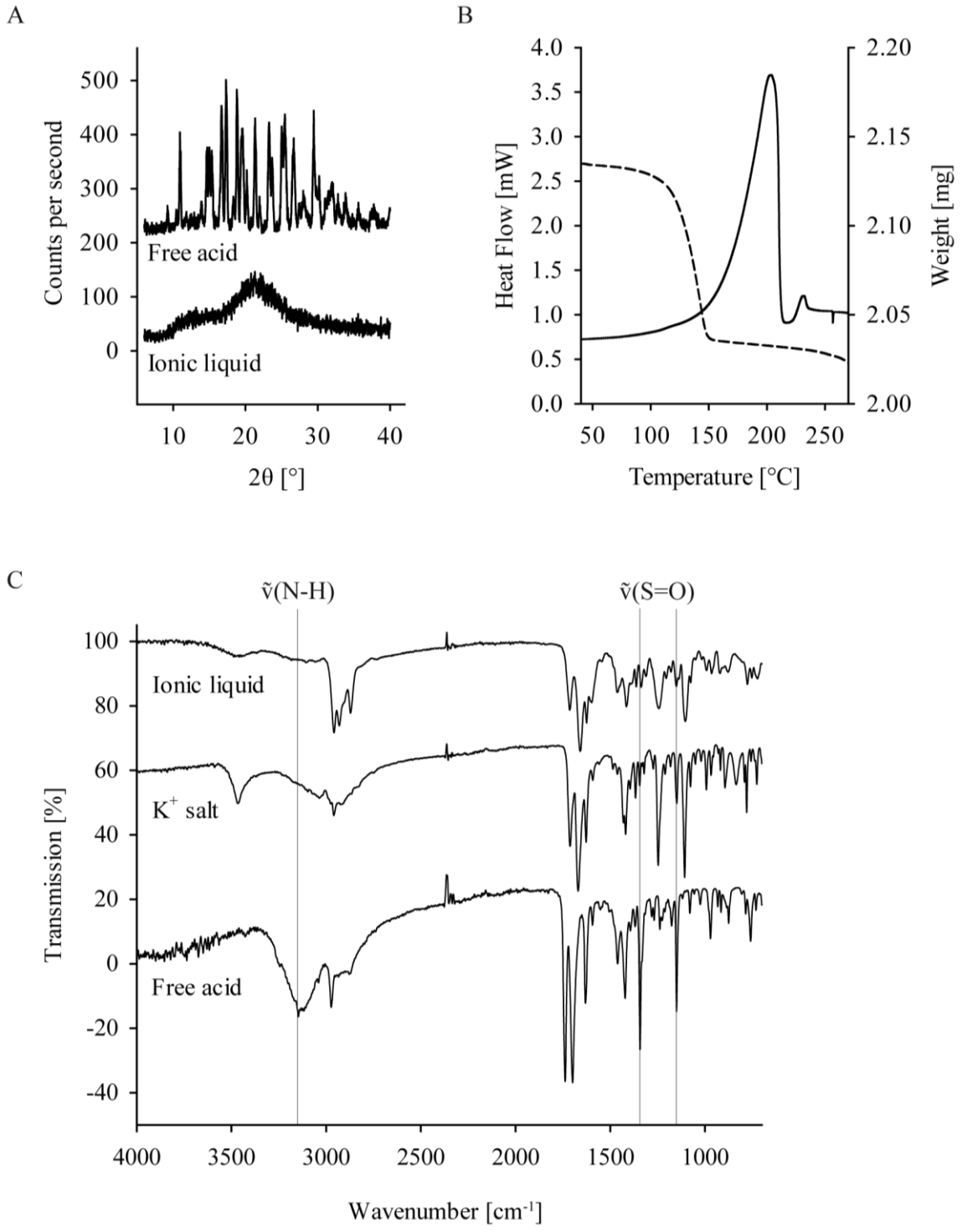

Supplementary Figure 2: (**A**) Powder diffractogram of the free acid and the ionic liquid. (**B**) Heat Flow [mW] and Weight [mg] *vs.* Time profile from DSC and TGA experiments of potassium salt. (**C**) IR spectra of Ionic liquid, potassium salt and free acid.

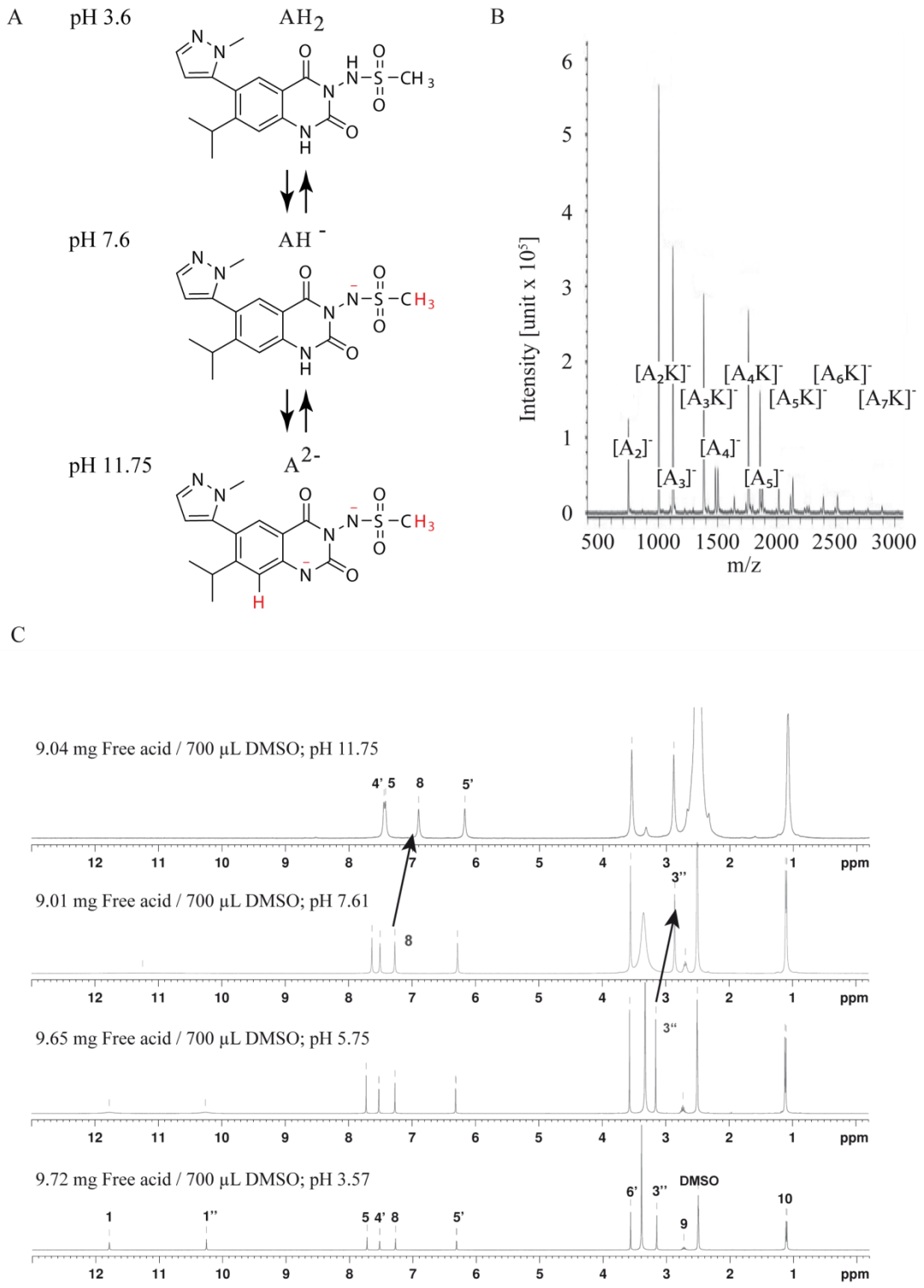

Supplementary Figure 3: (**A**) Assignment of functional groups to pKa values based on signal shifts as highlighted in red at pH 3.6, 7.6 and 11.75, respectively (**Supplementary figure 3C** for details on NMR). (**B**) Electrospray ionization mass spectrum of the ionic liquid dissolved in water. (**C**) ^{1}H NMR spectra of the free acid in DMSO at a pH of 3.57, 5.75, 7.61, and 11.75, respectively. Arrows indicate signal shifts in the signals of the 3'' hydrogens at the methylenesulfone group observed by comparison of the spectra obtained at pH of 5.75 and 7.61, respectively and by the hydrogen in position 8 of the aromatic ring observed in spectra obtained at pH of 7.61 and 11.75, respectively.

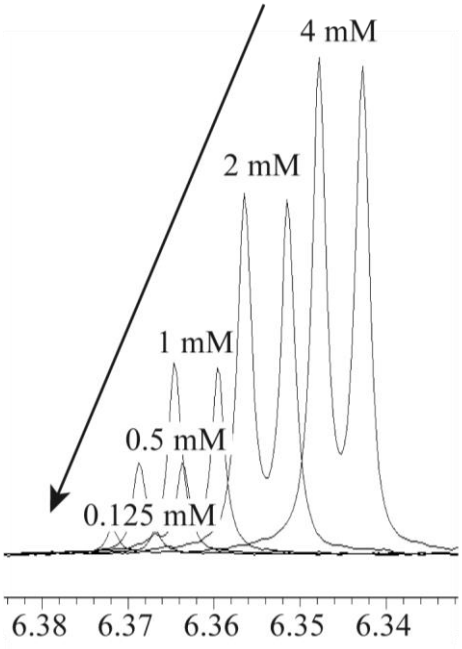

Supplementary Figure 4: ^{1}H NMR spectra obtained from concentration studies of the ionic liquid at 4, 2, 1, 0.5, and 0.125 mM in buffered deuterated water pH 7.4. The arrow highlights the loss in attraction among the free acid molecules with an increase in concentration or the increase of dissociation as a result of dilution.

References

[1] D. A. Miller, A. B. Watts, and R. O. Williams III, *Formulating poorly water soluble drugs*. New York: Springer, 2012.

[2] C. A. Lipinski, F. Lombardo, B. W. Dominy, and P. J. Feeney, "Experimental and computational approaches to estimate solubility and permeability in drug discovery and development settings," *Advanced Drug Delivery Reviews,* vol. 23, pp. 3-25, Jan 15 1997.

[3] K. E. Johnson, "What's an ionic liquid?," *Electrochem. Soc. Interface,* vol. 16, pp. 38-41, 2007.

[4] D. R. MacFarlane, J. M. Pringle, K. M. Johansson, S. A. Forsyth, and M. Forsyth, "Lewis base ionic liquids," *Chem Commun (Camb),* pp. 1905-17, May 14 2006.

[5] W. L. Hough, M. Smiglak, H. Rodriguez, R. P. Swatloski, S. K. Spear, D. T. Daly, *et al.*, "The third evolution of ionic liquids: Active pharmaceutical ingredients," *New J. Chem.,* vol. 31, pp. 1429-1436, 2007.

[6] V. J. Stella and K. W. Nti-Addae, "Prodrug strategies to overcome poor water solubility," *Adv. Drug Delivery Rev.,* vol. 59, pp. 677-694, 2007.

[7] E. Russo, R. Gitto, R. Citraro, A. Chimirri, and S. G. De, "New AMPA antagonists in epilepsy," *Expert Opin. Invest. Drugs,* vol. 21, pp. 1371-1389, 2012.

[8] D. Orain, S. Ofner, M. Koller, D. A. Carcache, W. Froestl, H. Allgeier, *et al.*, "6-Amino quinazolinedione sulfonamides as orally active competitive AMPA receptor antagonists," *Bioorg. Med. Chem. Lett.,* vol. 22, pp. 996-999, 2012.

[9] M. Koller, K. Lingenhoehl, M. Schmutz, I.-T. Vranesic, J. Kallen, Y. P. Auberson, *et al.*, "Quinazolinedione sulfonamides: A novel class of competitive AMPA receptor antagonists with oral activity," *Bioorg. Med. Chem. Lett.,* vol. 21, pp. 3358-3361, 2011.

[10] B. Gomez-Mancilla, R. Brand, T. P. Jurgens, H. Gobel, C. Sommer, A. Straube, *et al.*, "Randomized, multicenter trial to assess the efficacy, safety and tolerability of a single dose of a novel AMPA receptor antagonist BGG492 for the treatment of acute migraine attacks," *Cephalalgia,* 2013.

[11] R. Ahmed, M. Gogal, and J. E. Walsh, "A new rapid and simple non-radioactive assay to monitor and determine the proliferation of lymphocytes: an alternative to [3H]thymidine incorporation assay.," *Journal of immunological methods,* vol. 170, pp. 211-24, 1994.

[12] Y.-L. Hsieh, G. A. Ilevbare, E. B. Van, K. J. Box, M. V. Sanchez-Felix, and L. S. Taylor, "pH-Induced Precipitation Behavior of Weakly Basic Compounds: Determination of Extent and Duration of Supersaturation Using Potentiometric Titration and Correlation to Solid State Properties," *Pharm. Res.,* vol. 29, pp. 2738-2753, 2012.

[13] S. Dorbritz, W. Ruth, and U. Kragl, "Investigation on aggregate formation of ionic liquids," *Adv. Synth. Catal.,* vol. 347, pp. 1273-1279, 2005.

[14] S. R. LaPlante, R. Carson, J. Gillard, N. Aubry, R. Coulombe, S. Bordeleau, *et al.*, "Compound Aggregation in Drug Discovery: Implementing a Practical NMR Assay for Medicinal Chemists," *Journal of Medicinal Chemistry,* vol. 56, pp. 5142-5150, Jun 27 2013.

[15] T. Imai, M. Sakai, H. Ohtake, H. Azuma, and M. Otagiri, "In vitro and in vivo evaluation of the enhancing activity of glycyrrhizin on the intestinal absorption of drugs," *Pharm Res,* vol. 16, pp. 80-6, Jan 1999.

[16] R. J. Davey, S. L. Schroeder, and J. H. ter Horst, "Nucleation of organic crystals--a molecular perspective," *Angew Chem Int Ed Engl,* vol. 52, pp. 2166-79, Feb 18 2013.

[17] M. Volmer and Editor, *Die chemische Reaktion. Bd. IV. Kinetik der Phasenbildung*: J. W. Edwards, 1939.

[18] D. Kashchiev and R. G. M. van, "Review: Nucleation in solutions revisited," *Cryst. Res. Technol.,* vol. 38, pp. 555-574, 2003.

[19] K. Sangwal, "Nucleation: Basic Theory with Applications Edited by Dimo Kashchiev," *Cryst. Res. Technol.,* vol. 36, p. 235, 2001.

[20] N. Rodriguez-Hornedo, D. Lechuga-Ballesteros, and H. J. Wu, "Phase transition and heterogeneous/epitaxial nucleation of hydrated and anhydrous theophylline crystals," *Int. J. Pharm.*, vol. 85, pp. 149-62, 1992.
[21] C. L. Stevenson, D. B. Bennett, and D. Lechuga-Ballesteros, "Pharmaceutical liquid crystals: The relevance of partially ordered systems," *J. Pharm. Sci.*, vol. 94, pp. 1861-1880, 2005.
[22] B. J. Dunn, C. W. Nichols, and S. C. Gad, "Acute dermal toxicity of two quaternary organophosphonium salts in the rabbit," *Toxicology*, vol. 24, pp. 245-50, 1982.
[23] K. Bica, C. Rijksen, M. Nieuwenhuyzen, and R. D. Rogers, "In search of pure liquid salt forms of aspirin: ionic liquid approaches with acetylsalicylic acid and salicylic acid," *Phys Chem Chem Phys*, vol. 12, pp. 2011-7, Feb 28 2010.
[24] M. Stuart and K. Box, "Chasing equilibrium: measuring the intrinsic solubility of weak acids and bases," *Anal Chem*, vol. 77, pp. 983-90, Feb 15 2005.
[25] Y. L. Hsieh, G. A. Ilevbare, B. Van Eerdenbrugh, K. J. Box, M. V. Sanchez-Felix, and L. S. Taylor, "pH-Induced precipitation behavior of weakly basic compounds: determination of extent and duration of supersaturation using potentiometric titration and correlation to solid state properties," *Pharm Res*, vol. 29, pp. 2738-53, Oct 2012.
[26] T. Gravestock, K. Box, J. Comer, E. Frake, S. Judge, and R. Ruiz, "The "GI dissolution" method: a low volume, in vitro apparatus for assessing the dissolution/precipitation behaviour of an active pharmaceutical ingredient under biorelevant conditions," *Anal. Methods*, vol. 3, pp. 560-567, 2011.
[27] G. M. Sheldrick, "A short history of SHELX," *Acta Crystallogr A*, vol. 64, pp. 112-22, Jan 2008.
[28] A. L. Spek, "Structure validation in chemical crystallography," *Acta Crystallogr D Biol Crystallogr*, vol. 65, pp. 148-55, Feb 2009.
[29] L. J. Barbour, "X-seed - a software tool for supramolecular crystallography," *J. Supramol. Chem.*, vol. 1, pp. 189-191, 2003.
[30] O. V. Dolomanov, L. J. Bourhis, R. J. Gildea, J. A. K. Howard, and H. Puschmann, "OLEX2: a complete structure solution, refinement and analysis program," *J. Appl. Cryst.* , vol. 4, pp. 339-341 2009.
[31] F. C. Gozzo, L. S. Santos, R. Augusti, C. S. Consorti, J. Dupont, and M. N. Eberlin, "Gaseous supramolecules of imidazolium ionic liquids: "Magic" numbers and intrinsic strengths of hydrogen bonds," *Chem. - Eur. J.*, vol. 10, pp. 6187-6193, 2004.
[32] H. Jager, L. Meinel, B. Dietz, C. Lapke, R. Bauer, H. P. Merkle, *et al.*, "Transport of alkamides from Echinacea species through Caco-2 monolayers," *Planta Med*, vol. 68, pp. 469-71, May 2002.
[33] I. Hubatsch, E. G. Ragnarsson, and P. Artursson, "Determination of drug permeability and prediction of drug absorption in Caco-2 monolayers," *Nat Protoc*, vol. 2, pp. 2111-9, 2007.
[34] C. Masungi, C. Borremans, B. Willems, J. Mensch, A. Van Dijck, P. Augustijns, *et al.*, "Usefulness of a novel Caco-2 cell perfusion system. I. In vitro prediction of the absorption potential of passively diffused compounds," *J Pharm Sci*, vol. 93, pp. 2507-21, Oct 2004.
[35] K. Hakala, L. Laitinen, A. M. Kuakonen, J. Hirvonen, R. Kostiainen, and T. Kotiaho, "Development of fast LC/MS/MS methods for cocktail dosed Caco-2 samples using atmospheric pressure photoionization (APPI) and electrospray ionization (ESI)," *European Journal of Pharmaceutical Sciences*, vol. 19, pp. S30-S30, Jun 2003.

Chapter 3: Tuning solubility, supersaturation and hygroscopicity by counterion design

Anja Balk[1,§], Johannes Wiest[1,§], Toni Widmer[1,2], Heike Bruhn[3], Benjamin Merget[1], Christoph Sotriffer[1], Bruno Galli[2], Ulrike Holzgrabe[1], and Lorenz Meinel[1]*

[1]Institute for Pharmacy, Am Hubland, University of Würzburg, DE-97074 Würzburg, Germany, [2]Novartis Pharma AG, Lichtstraße 35, CH-4002 Basel, Switzerland, [3]Institute for Molecular Infection Biology, Josef-Schneider-Straße 2, DE-97080 Würzburg, Germany

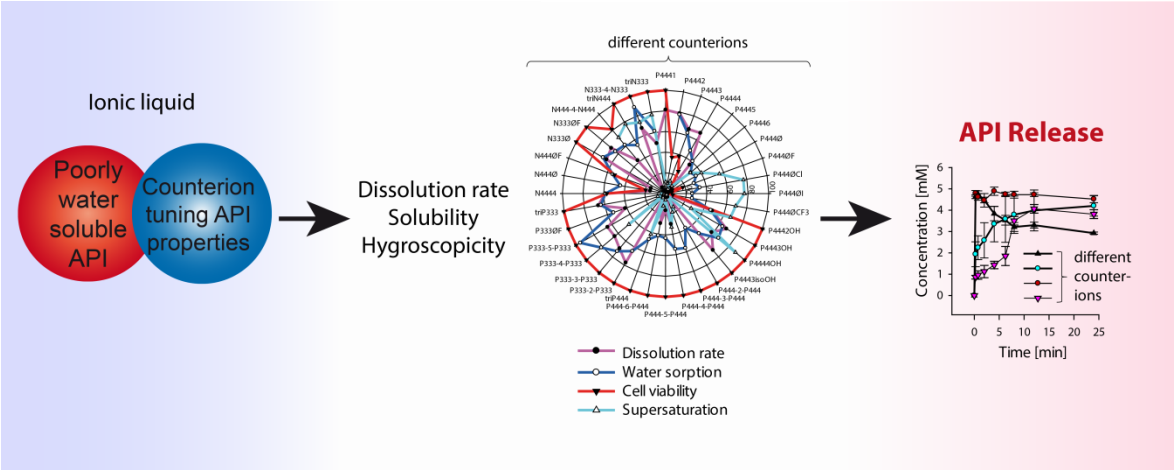

This chapter has not been published.

Introduction

Over the last two decades combinatorial chemistry and high throughput screening in drug discovery resulted in an increasing number of poorly water soluble drug candidates, for these methods tend to identify compounds with large molecular weight and high lipophilicity [1-3]. Potential active pharmaceutical ingredients (API) with low solubility account for about 70% of new drug candidates today [1]. Formulation development for these substances may be challenging as dissolution in biological fluids is low, easily leading to fluctuating pharmacokinetic (PK) parameters within and among patients, respectively. Typical formulation strategies for poorly water soluble drugs (PWSD) comprise the development of prodrugs (for which API structure is changed), or complex formulations including solid dispersions, micellar systems, nanosuspensions, complexation and crystal engineering [2-5]. However, these approaches can be rather time-consuming, cost-intensive or limited by complex manufacturing requirements. One of the most established concepts to overcome low water solubility of weak acids and bases is salt formation [6, 7]. More than 50% of the APIs are marketed as salts [8]. Besides water solubility and dissolution rate, further pharmaceutically relevant physico-chemical properties like hygroscopicity, stability and processability are affected by the preparation of salts [2, 7]. Therefore, these API features can be tuned by proper counterion choice [2]. Solid crystalline salts often display the disadvantage of high lattice forces and the risk of polymorphism [8, 9]. Other API salts are quickly converted back into the unionized form and recrystallization occurs in spite of a rapid dissolution rate [10, 11]. These challenges can be effectively addressed by creation of an ionic liquid (IL) [8, 11-15], with ILs being defined as organic salts composed entirely of ions with a melting point below 100 °C. These special salt forms are instrumental in avoiding polymorphism, increasing the solubility or setting a controlled release profile [8, 16]. Exemplarily, in previous studies we demonstrated for an acidic model compound the metathesis of an amorphous IL leading to a faster, pH-independent dissolution rate, higher solubility and a prolonged duration of supersaturation [11]. However, the study was performed with a single counterion, tetrabutylphosphonium (TBP). Based on these results this study addresses the impact of a suite of rationally designed counterions on the dissolution rate, the supersaturation pattern, the resulting release profile, hygroscopicity and cytotoxicity when forming a salt with the API. The results indicated that all these pharmaceutically important parameters can be tuned within relevant ranges and relevant predictive models were built for a suite of counterions for pharmaceutical parameters effectively demonstrating the powerful possibility to tune APIs through tailor-made counterion design – thereby, avoiding the need to change the API structure.

Results

Synthesis and physico-chemical characterization of the solid state of the LLESs

36 low lattice enthalpy salts (LLESs) were synthesized and classified into six series of salts with structural similar counterions, the alkyl, benzyl, butyl di- and trications, propyl, hydroxyl and ammonium series, respectively (**Figure 1**). For the alkyl series one butyl chain of TBP (a counterion which will be regarded as a reference in this manuscript, as well as its corresponding LLES P_{4444}, representing the API salt with tetrabutylphosphonium) was exchanged by alkyl chains of different length. The benzyl series included TBP derivatives at which one butyl chain was replaced by a differently substituted benzyl group. The butyl di- and trications series contained dications with three butyl chains at one phosphonium center and different alkyl chains between the two phosphonium centers as well as a phosphonium trication with nine butyl substituents. The propyl series was similar to the butyl di- and trications series except the butyl chains were replaced by propyl chains. Counterions of the hydroxyl series contained a hydroxyl moiety at different sites of the counterion. The ammonium series combined counterions of the first four groups with the phosphonium being exchanged by an ammonium ion. All synthesized LLESs were white to slightly yellow and solid substances (data not shown). For all LLESs the purity was more than 95%, apart from P_{4444OH} (78%), $P_{4443isoOH}$ and $N_{444\Theta}$ (91%), respectively, as determined by high performance liquid chromatography with a charged aerosol detector (HPLC-CAD). The deprotonation of the sulfonamide moiety of the APIs was complete, as assessed by infrared spectroscopy (IR) (data not shown). A 1:1 ratio of counterion to API was confirmed for monovalent cations, a 1:2 ratio for dications and 1:3 ratio for trications by nuclear magnetic resonance spectroscopy (NMR). The BGG free acid was crystalline, while all LLES were amorphous, as assessed by X-ray powder diffraction (XRPD) (**Supplementary Figure 1**). For the free acid one sharp endothermic peak, indicating melting at 290 °C was determined by differential scanning calorimetry (DSC), whereas all LLESs had a glass transition but no melting point (**Supplementary Figure 2**). The glass transition temperatures (TG) of LLESs of counterions with one charge ranged from 40 °C to 97 °C, for dications from 81 °C to 124 °C and for trications from 124 °C to 148 °C. For ammonium derivatives TG temperatures were within the same range as phosphonium derivatives or slightly higher.

Dissolution rate

Linear drug release *versus* time profiles were obtained for all LLESs and the dissolution rate was calculated from the resulting slope (**Figure 2**). Within the alkyl series a sigmoidal drop of the dissolution rate was observed for increasing length of one alkyl chain of the P_{4444} derivatives (**Figure 2A**). The dissolution rate of the tributyl-hexyl phosphonium LLES P_{4446} was within the

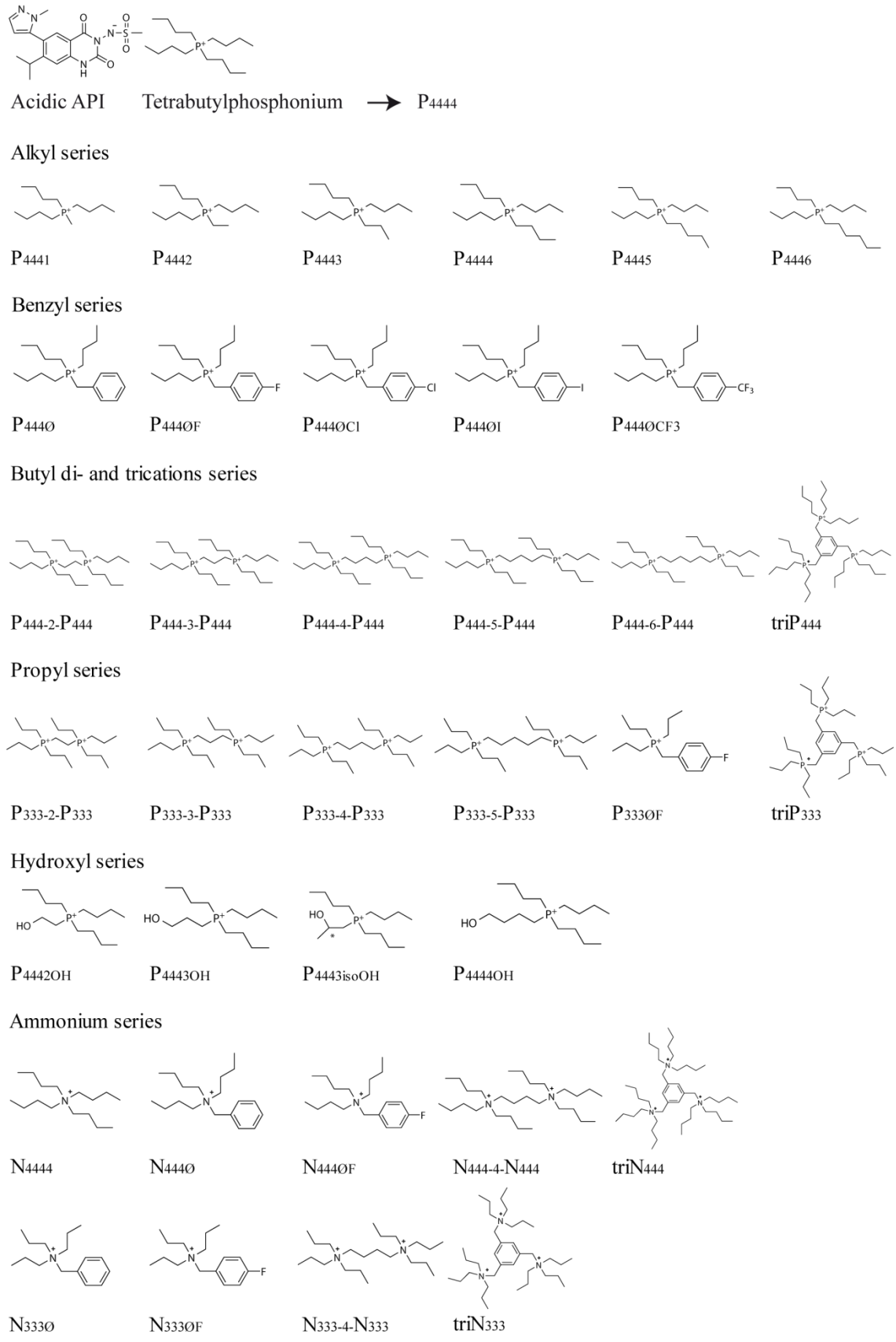

Figure1: Chemical structure of the acidic API and of the counterions. The abbreviations below the counterions refer to the salts being prepared by combination of API and counterion.

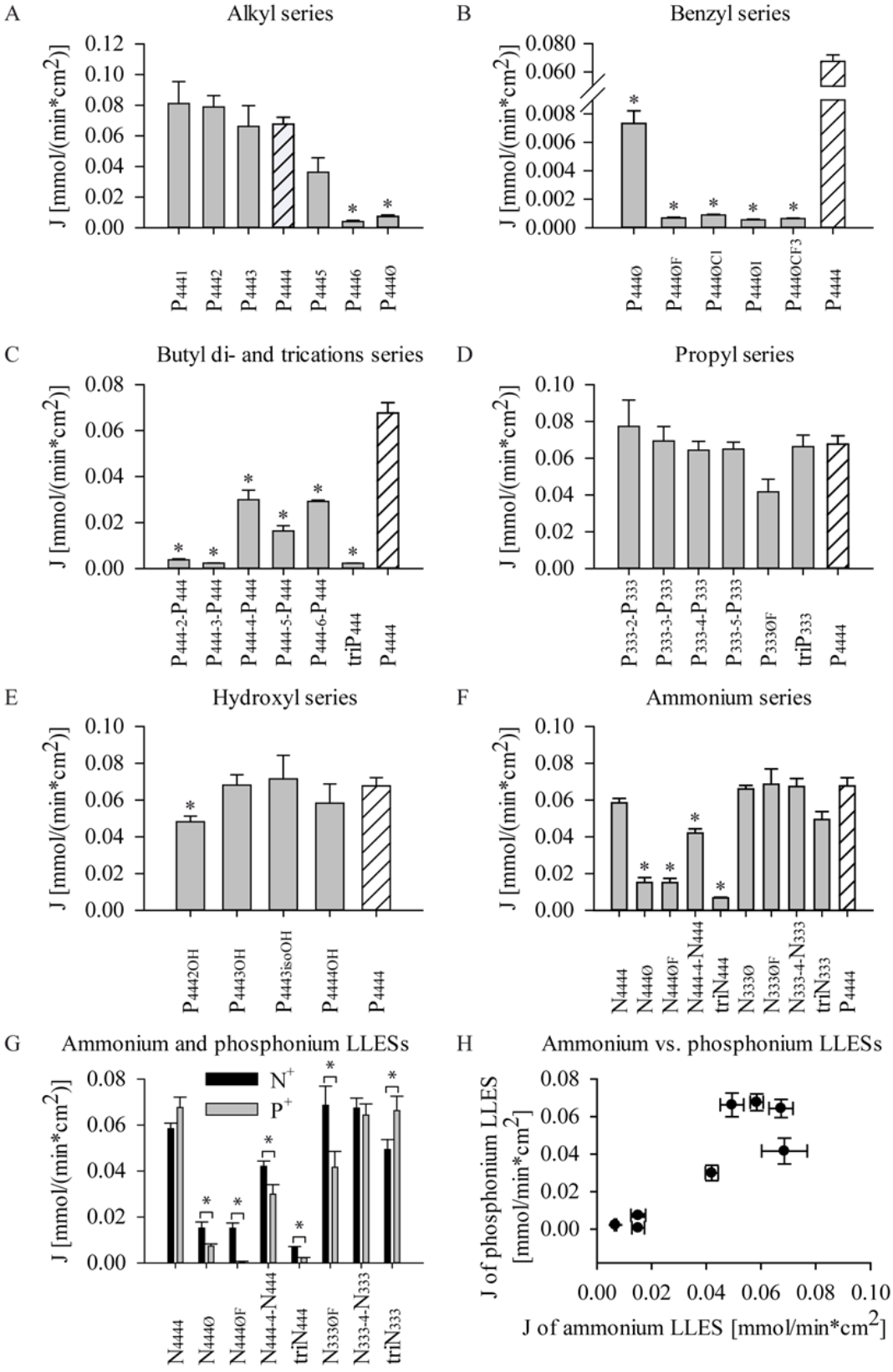

Figure 2: (A-F) Dissolution rate J in mmol/(min*cm^2) of the different LLESs of the distinct series (G) Dissolution rates of the ammonium and the corresponding phosphonium analogues (H) Dissolution rate of the phosphonium LLESs versus the corresponding ammonium analogues.

same order of magnitude as the tributyl-benzyl phosphonium LLES $P_{444Ø}$. While the dissolution rate of the benzyl derivative $P_{444Ø}$ was about 10 times smaller than for P_{4444} (with P_{4444} being the TBP salt serving as reference; see above), fluoro-, chloro-, iodo-, or trifluoromethyl substituents at the benzyl group of the counterion further reduced the dissolution rate to less than 1.3% of what was observed for the P_{4444} (**Figure 2B**). All LLES from the Butyl di-and trications series had significantly lower dissolution rates than P_{4444} (**Figure 2C**). If there were less than three carbon atoms between the two phosphonium atoms of dications dissolution rate was only 5.6% of P_{4444}. If there were more than three carbon atoms, the dissolution rate ranged between 25% and 45% of the rate of P_{4444}. The LLES from the propyl series had no significantly different dissolution rate compared to P_{4444} (**Figure 2D**). There appeared to be no effect of the chain length between the phosphonium ions of the dications on the dissolution pattern. The additional fluorobenzyl substituent of $P_{333ØF}$ did not significantly lower the dissolution rate as compared to P_{4444} (although a trend may be postulated) but was about 50 times higher than for the corresponding butyl counterion $P_{444ØF}$ (**Figure 2D, E**). An introduction of a hydroxyl group into the alkyl based counterions did not significantly impact the dissolution rates as compared to P_{4444}, apart from P_{4442OH} for which the dissolution rate was significantly reduced (**Figure 2E**). Structural modification of the counterion within the hydroxyl series did not correlate with determined the dissolution rates. The results for the ammonium series (**Figure 2F**) were compared to those from the corresponding phosphonium derivatives (**Figure 2G**). Dissolution rates of ammonium derivatives were significantly higher for all ammonium LLESs, apart from N_{4444} and $N_{333\text{-}4}N_{333}$ displaying no significant differences, and the trication $triN_{333}$, which was the only ammonium LLES dissolving significantly slower than the phosphonium analogue. A linear correlation was observed (slope of approximately 1) when plotting the results from the ammonium based counterions to their respective phosphonium analogues (**Figure 2H**).

Duration of Supersaturation

The use of the different counterions allowed for tuning of the durations of supersaturation for the LLESs (**Figure 3**). Within the alkyl series an increasing chain length of one alkyl chain resulted in significantly prolonged supersaturation (**Figure 3A**), e.g. for the hexyl LLES P_{4446} and benzyl LLES $P_{444Ø}$, as compared to P_{4444}. For shorter side chains no significant difference was observed. For the unsubstituted benzyl LLES $P_{444Ø}$ the supersaturation was about 8 times (and significantly) longer than for P_{4444}. Further fluoro-, chloro-, iodo- and trifluoromethyl substituents of the benzyl group resulted in a 16 times longer (and significant) supersaturation, compared to P_{4444} (**Figure 3B**). No general tendency was observed for the effect of the counterion on the duration of supersaturation within the butyl di- and trications series (**Figure 3C**). The trication $triP_{444}$ displayed

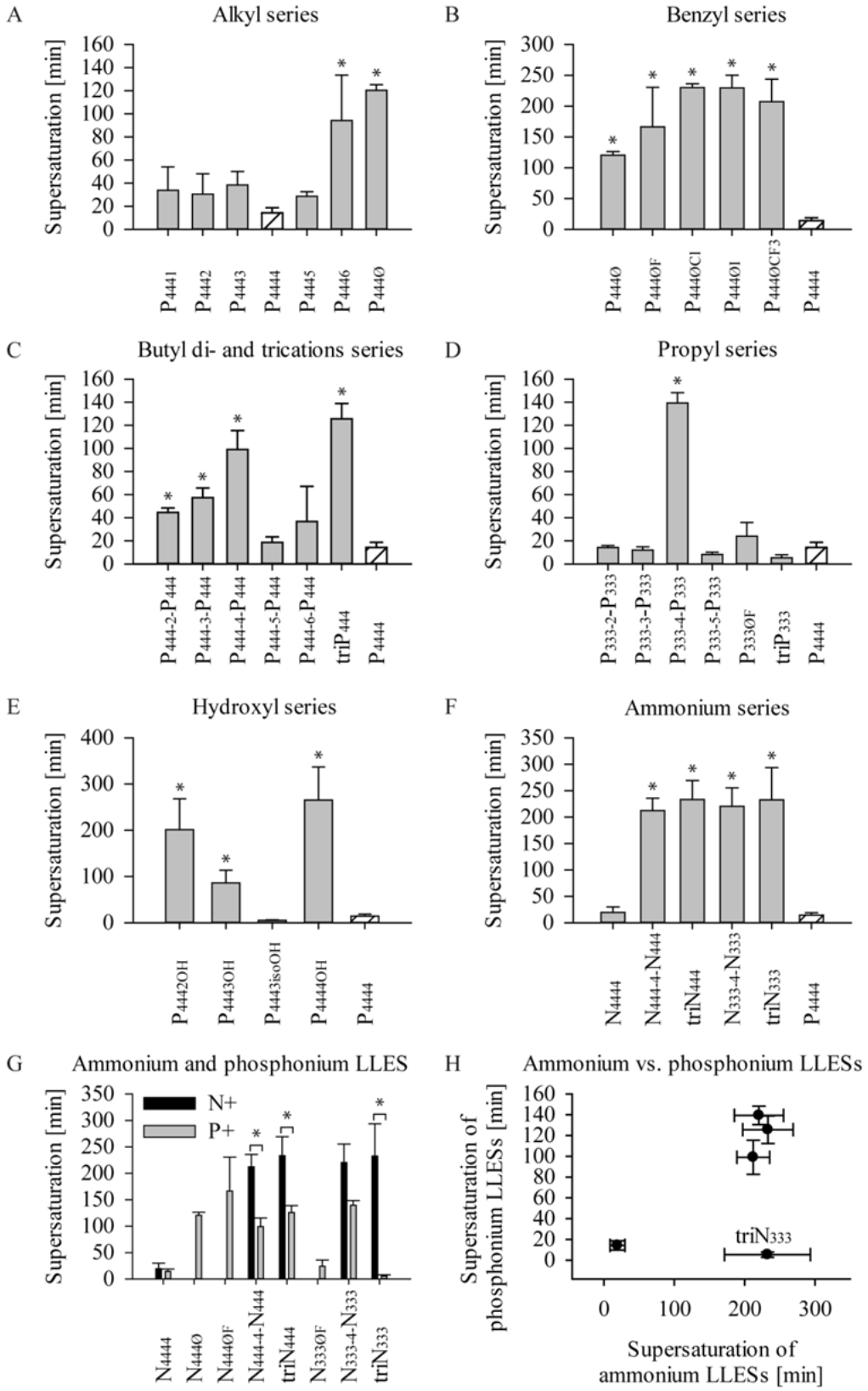

Figure 3: (A-F) Duration of supersaturation in minutes of the different LLESs of the distinct series (G) Duration of supersaturation of the ammonium and the corresponding phosphonium analogues (H) Duration of supersaturation of the phosphonium LLESs versus the corresponding ammonium analogues.

the most lasting supersaturation. The counterions with only two to four CH_2- units between the phosphonium ions had a significantly longer supersaturation duration in comparison to P_{4444}, whereas the counterions with longer alkyl chains in between the phosphonium ions had no significant impact. All counterions of the propyl di- and trications series exhibited a supersaturation pattern comparable to P_{4444} (with the exception of $P_{333\text{-}4\text{-}}P_{333}$ **(Figure 3D)**. For the hydroxyl series no simple correlation between structure and duration of supersaturation was observed (**Figure 3E**). However, if the hydroxyl moiety was not terminal as for $P_{4443isoOH}$, the duration of supersaturation dropped drastically. For the ammonium series only for five of nine LLESs the supersaturation was determined. No supersaturation profile could be detected for ammonium counterions with benzyl substituents, for assay was aborted due to low reaction towards acid and base addition, though detection was possible for the corresponding phosphonium derivatives (**Figure 3F**). While for the ammonium counterion N_{4444} the supersaturation was insignificantly different to P_{4444}, for all ammonium di- and trications no drop of concentration to equilibrium state was detected after 80 extrapolations (**Figure 3F**). Ammonium counterions had a potential yet in some combinations insignificant trend to longer supersaturation in contrast to their phosphonium derivatives. No correlation between ammonium and phosphonium LLES could be developed (**Figure 3H**).

Higher concentrations during the supersaturated state correlated with shorter durations of supersaturation, as observed in the concentration versus time profiles of different LLESs (**Figure 4A**). A negative linear correlation with a negative slope was obtained by plotting the supersaturation ratio S/S_0 against the logarithm of the duration of supersaturation (**Figure 4B**). A linear correlation of the logarithm of the duration of supersaturation was also observed for the pH when first precipitation occurred (**Figure 4C**).

Shake flask experiments

Shake flak experiments were performed for a subseries of 16 LLESs, including P_{4441}, P_{4442}, P_{4444} and P_{4445} from the alkyl series and $P_{444Ø}$, $P_{444ØCl}$ and $P_{444ØCF3}$ from the benzyl series were selected. $P_{444\text{-}4\text{-}}P_{444}$, $P_{444\text{-}5\text{-}}P_{444}$ and $triP_{444}$ were chosen from the Butyl di- and trications series and $P_{333\text{-}4\text{-}}P_{333}$ and $P_{333\text{-}5\text{-}}P_{333}$ from the propyl series. P_{4443OH} and P_{4444OH} represented the hydroxyl series. N_{4444} and $N_{444\text{-}4\text{-}}N_{444}$ were investigated as being part of the ammonium series. Different counterions resulted in distinct release profiles of the LLESs and for four LLESs release profiles are depicted (**Figure 5A**). In some cases as for P_{4444} a fast dissolution within 15 minutes was determined but precipitation was observed after 4 hours and concentration dropped. In other cases a fast dissolution was followed by a stable supersaturation for more than 24 hours, as determined for $P_{333\text{-}4\text{-}}P_{333}$. Besides that, various counterions, like $P_{444ØCF3}$ and $triP_{444,}$ resulted in a prolonged release of API from the LLESs. Duration of supersaturation was defined as time until precipitation was observed and concentration started to drop. Supersaturation determined with shake flask

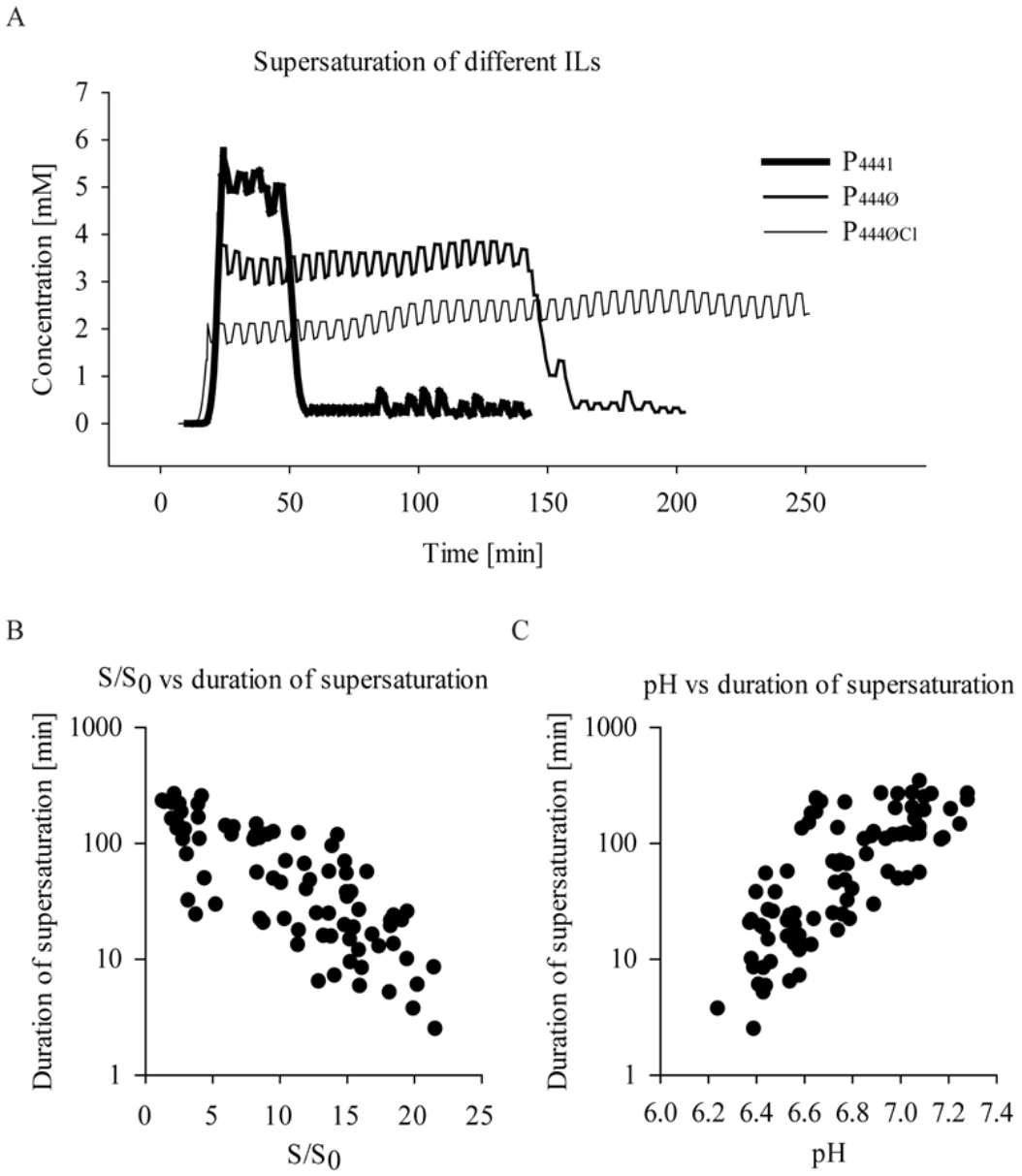

Figure 4: (A) Concentration in mM versus Time in minutes of three different LLESs (B) Duration of supersaturation in minutes versus the Supersaturation ratio (S/S_0) (C) Duration of supersaturation versus the pH value at which supersaturation occurred.

experiments was plotted against the results determined with an autotitrator (**Figure 5B**). In general the duration of supersaturation determined with an autotitrator exceeded 30 minutes for LLESs, for which no precipitation was observed within 24 hours during the powder dissolution experiment. Plotting data with a logarithmic scale for the powder dissolution results, for which precipitation occurred within 24 hours, a linear correlation was observed between the values obtained by shake flask and the autotitrator experiments. The only exception was $P_{444Ø}$. Supersaturation determined with an autotitrator was 2 hours, while precipitation in shake flask experiments was observed after 6.25 hours.

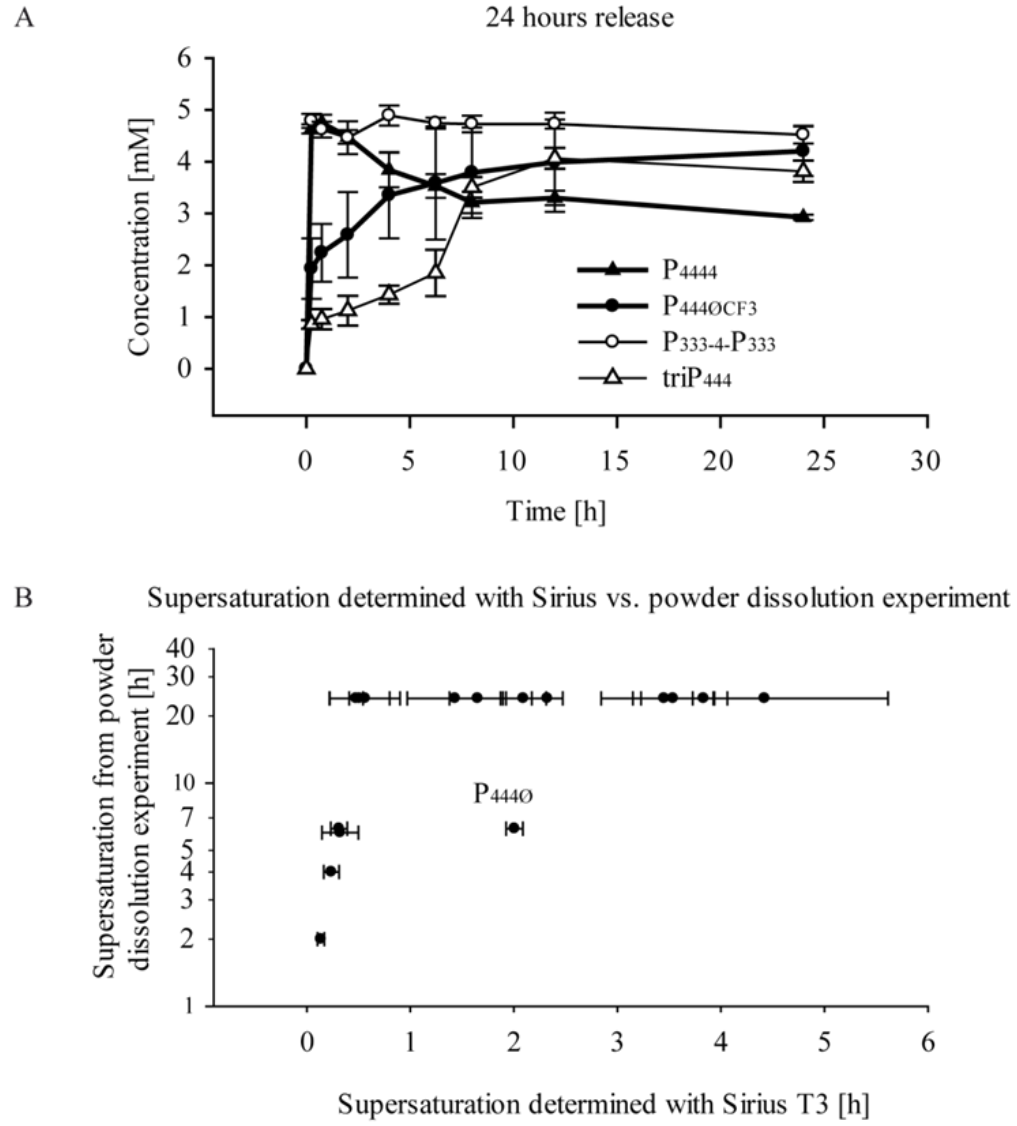

Figure 5: (A) 24 hours release profiles of four selected LLESs (B) Duration of supersaturation in hours determined by powder dissolution experiments versus Duration of supersaturation in hours determined by using an autotitrator.

Dynamic vapor sorption

The hygroscopicity of 36 LLES was assessed from change in mass at different relative humidities (RH) and depicted for 90% RH (**Figure 6, Supplementary Figure 3-5**). Generally at 80% RH values ranged between 5% and 18% change in mass (data not shown) and at 90%RH values between 7% and 32% change in mass were determined. For P_{4441} recrystallization during the experiment was detected, starting at 50% RH and the result was excluded from further analysis. For the alkyl series decreasing water sorption was detected with increasing length of one alkyl chain of the butyl phosphonium counterion (**Figure 6A**). Within the benzyl series, independent of further

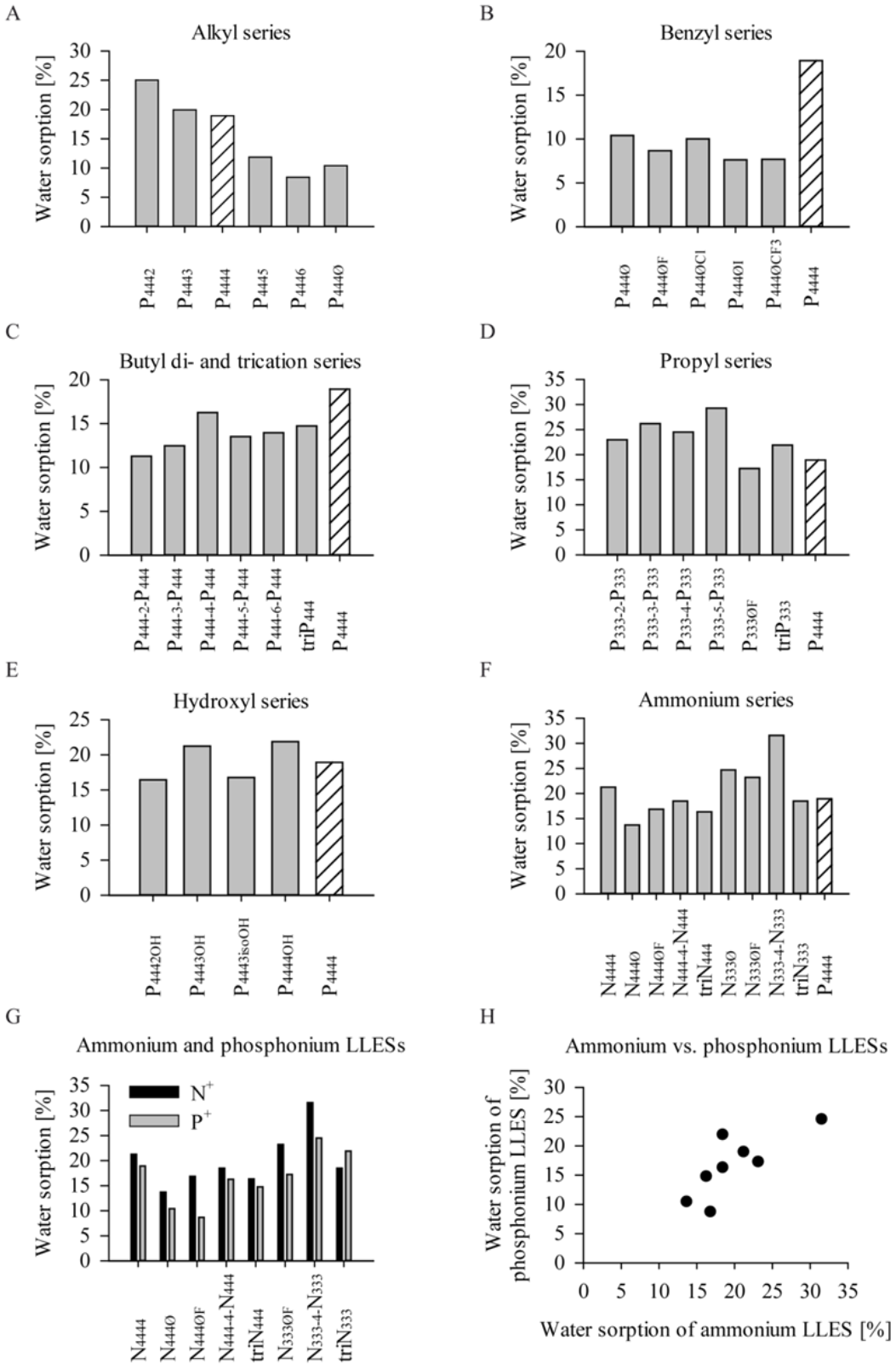

Figure 6: Change in mass in % due to water sorption at 90% RH of the different LLESs of the distinct series (G) Change in mass due to water sorption of the ammonium and the corresponding phosphonium analogues (H) Change in mass due to water sorption of the phosphonium LLESs versus the corresponding ammonium analogues.

halide substituents at the benzyl group, water sorption of about 10% was determined, accounting for about half of the value of P_{4444} (**Figure 6B**). For butyl di-and trications a slightly enhanced water sorption was observed with increasing number of CH_2-units between the phosphonium atoms of the dication, with the exception of $P_{444\text{-}4\text{-}}P_{444}$, which displayed a higher water sorption than the trication (**Figure 6C**). As water sorption experiments were conducted without repetition, we are unable to assess the significance of these results. For propyl dications no correlation between structure and water sorption could be developed within the series, but values were higher than for butyl analogues (**Figure 6D**). While the butyl trication displayed higher water sorption than butyl dications, the value for the propyl trication was lower than for propyl dications. Water sorption of hydroxyl LLESs was comparable to P_{4444} and no general trend was observed within the group (**Figure 6E**). The ammonium LLES displayed generally higher water sorption values than the phosphonium analogues (**Figure 6F and 6G**), apart from $triN_{333}$. For ammonium LLESs a similar correlation of water sorption and structure was observed as for phosphonium counterions (**Figure 6H**).

Cytotoxicity of the counterions

The cell viability of the counterions was determined *in vitro* in human cell lines of hepatic (HepG2) and renal (HEK 293T) origin as well as in murine macrophages (J774.1). For all LLES HEK 293T was the most sensitive cell line. Generally increasing the length of one alkyl chain of the counterions of the alkyl series resulted in a decrease in cell viability, with the exception of P_{4444} counterion in J774.1 cells (**Figure 7A**). IC_{50} values of counterions of the benzyl series are lower than 200 µM for all cell lines apart from $P_{444ØF}$, for which IC_{50} values in the different cell lines range from 200 µM to 400 µM (**Figure 7B**). Butyl di- and trications and counterions of the propyl and hydroxyl series display higher IC_{50} values than 1000 µM in all cell lines (**Figure 7C, 7D and 7E**). For all ammonium counterions IC_{50} values in hepatic cells (HepG2) were higher than 1000 µM. In kidney cells IC_{50} values for the single charged butyl dications were below 600 µM, while they were higher than 800 mM for single charged ammonium counterions (**Figure 7A and 7F**). Ammonium di-and trications display higher values than 1000 µM. In macrophages for all counterions IC_{50} values were higher than 1000 µM apart from the counterions of $N_{444Ø}$, $N_{444ØF}$ and $N_{333\text{-}4\text{-}}N_{333}$ (**Figure 7F**). For the $N_{333\text{-}4\text{-}}N_{333}$ counterion concentrations higher than 200 µM were not applied on J774.1 cells for limited solubility of the counterion in the stock solution and result was therefore excluded from further analysis.

Calculation of models using molecular descriptors

Results for the supersaturation (S), water sorption (WS) and cell viability (V) in HEK 293T cells - the most sensitive of the three cell lines tested - were plotted against the dissolution rate (J)

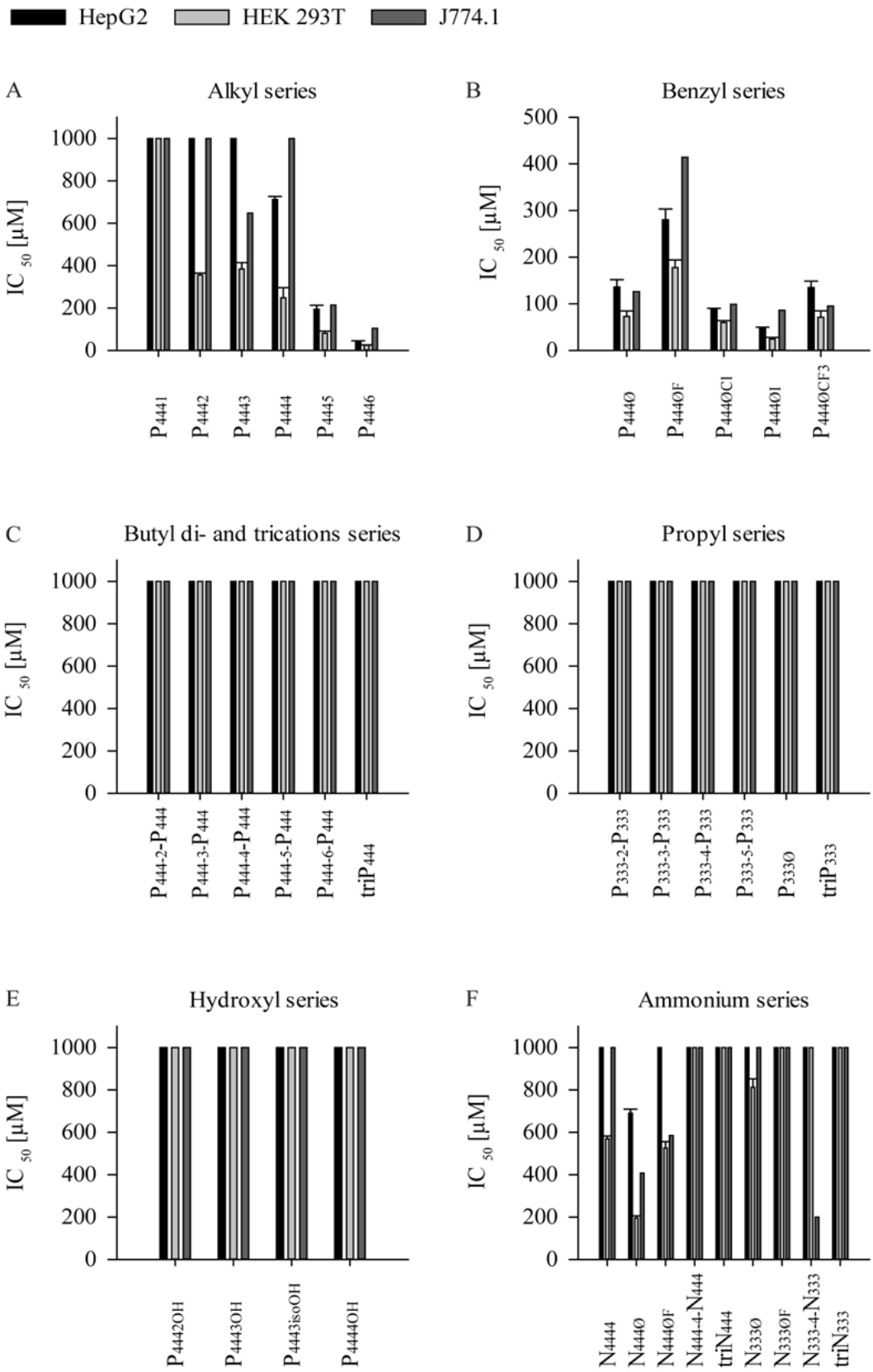

Figure 7: (A-F) Cell viability of the different counterions of the LLESs of the distinct series expressed by half maximal inhibitory concentration (IC_{50}) in µM for the cell lines HepG2, HEK 293T and J774.1.

(**Supplementary Figure 6)**. Correlation of supersaturation and dissolution rate data of hydroxyl series and ammonium counterions did not match the correlation for the four other counterion series. For the alkyl, benzyl, butyl di-and trications and the propyl series a logarithmic correlation between duration of supersaturation and dissolution rate was observed (**Supplementary Figure 6A**). With increasing dissolution rate (J), the duration of supersaturation (S) drops exponentially according to the equation S = 32.8 ln (J) -63.8 (R^2=0.66). $P_{333\text{-}4}$-P_{333} differed strongly from that correlation and displayed an unusual long duration of supersaturation for the high dissolution rate, which was determined for that LLES. A linear correlation was obtained for water sorption (WS) and dissolution rate (J), which can be described by the equation WS = 187.6 J +10.2 (R^2 = 0.74) (**Supplementary Figure 6B**). Cell viability (V) in HEK 293T cells for dications and trications were higher than 1000 µM independent of the dissolution rate. For single charged counterion a rough correlation for the dissolution rate (J) and the cell viability (V) was determined with V = 7922 J + 104 (R^2= 0.47).

Results for the dissolution rate, duration of supersaturation, water sorption and cell viability were calculated using molecular descriptors number of hydrophobic atoms (a_hyd), the graph theoretical diameter (diameter), number of charges (FCharge), number of oxygen atoms (a_nO) and the number of nitrogen atoms (a_nN). Descriptors were calculated only for the counterion of the LLESs and as we confined these studies to one API only, API descriptors could not be developed based on these studies. The dissolution rate (J) of all 36 LLESs can be described by a_hyd, diameter and FCharge according to the equation J = 0.0667 FCharge -0.0054 a_hyd - 0.0054 diameter +0.1134 (R^2= 0.67) and correlation of calculated and measured values is depicted (**Figure 8A**). For the subset of phosphonium counterions without the hydroxyl series and the ammonium counterions it is assumed that the duration of supersaturation (S) can be calculated from dissolution rate (J) according to the logarithmic equation S = -63.8-32.8 log J (R2=0.66) but not by molecular descriptors. Calculated results of supersaturation (S) are plotted against measured values (**Figure 8B**). The Water sorption (WS) results of the 36 LLESs were correlated with the molecular descriptors FCharge and a_hyd. The model WS = 15.1 FCharge-1.3 a_hyd +22.8 (R^2=0.55) was developed (**Figure 8C**). Cell viability (V) in HEK 293T cells was correlated for all 36 counterions with the descriptors FCharge, a_nO and a_hyd according to the equation V = 785 FCharge + 484 a_nO – 38 a_hyd +302 (R^2=0.61). For a subset of single charged counterions without hydroxyl moieties the following equation for cell viability in HEK 293T cells was developed: V = 323 a_nN-78 a_hyd +1678 (R^2=0.49) (**Figure 8D**). The results for the dissolution rate, duration of supersaturation, water sorption and cell viability are summarized one diagram (**Figure 9**).

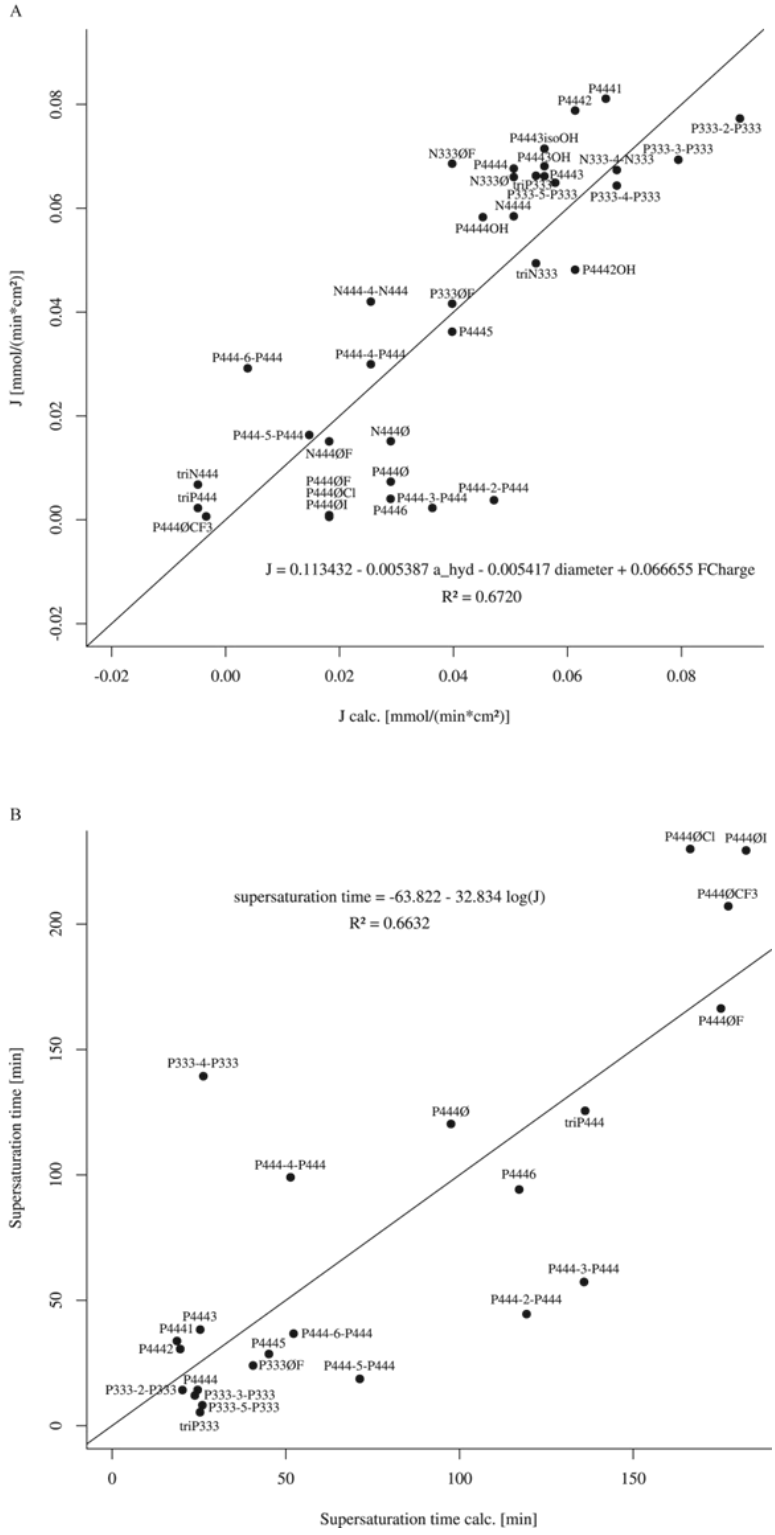

Figure 8: (A) Experimentally determined dissolution rate J in mmol/(min*cm^2) versus the dissolution rate calculated by using the molecular descriptors number of hydrophobic atoms (a_hyd), the graph-theoretical diameter (diameter) and the number of charges of the counterion (FCharge) J_{calc} and the corresponding correlation (B) Experimentally determined duration of supersaturation in minutes versus the duration of supersaturation calculated as a function of the dissolution rate and the corresponding correlation.

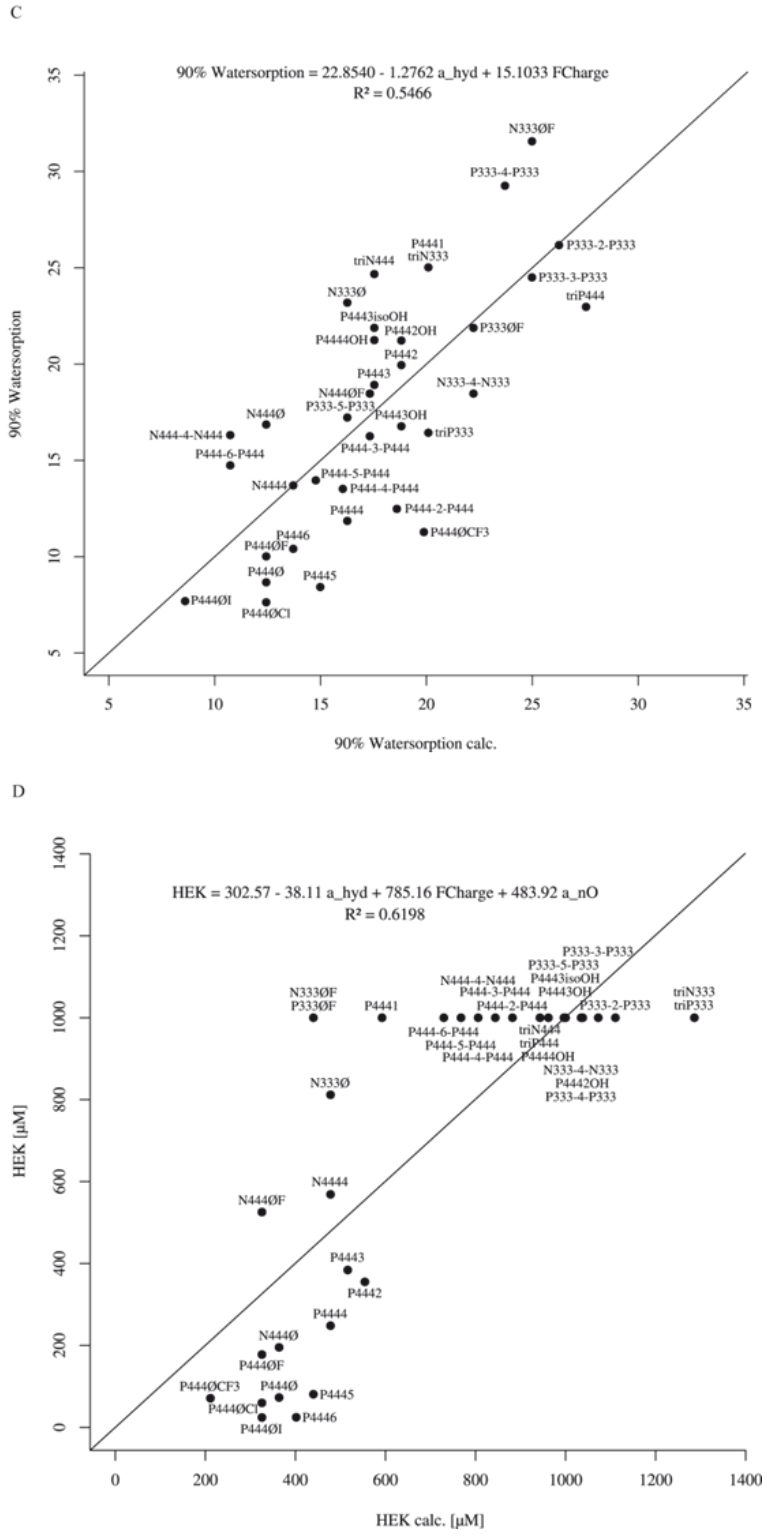

Figure 8: (C) Experimentally determined water sorption expressed as change in mass in % at 90% RH versus the water sorption calculated by using the molecular descriptors number of hydrophobic atoms (a_hyd) and the number of charges of the counterion (FCharge) (90% Watersorption calc.) and the corresponding correlation. (D) Experimental results for Cell viability of the different counterions of the LLESs expressed by half maximal inhibitory concentration (IC_{50}) in µM for the cell line HEK 293T (HEK) versus the calculated values (HEK calc.), using the molecular a_hyd, the number of oxygen atoms (a_nO) and FCharge and the corresponding correlation

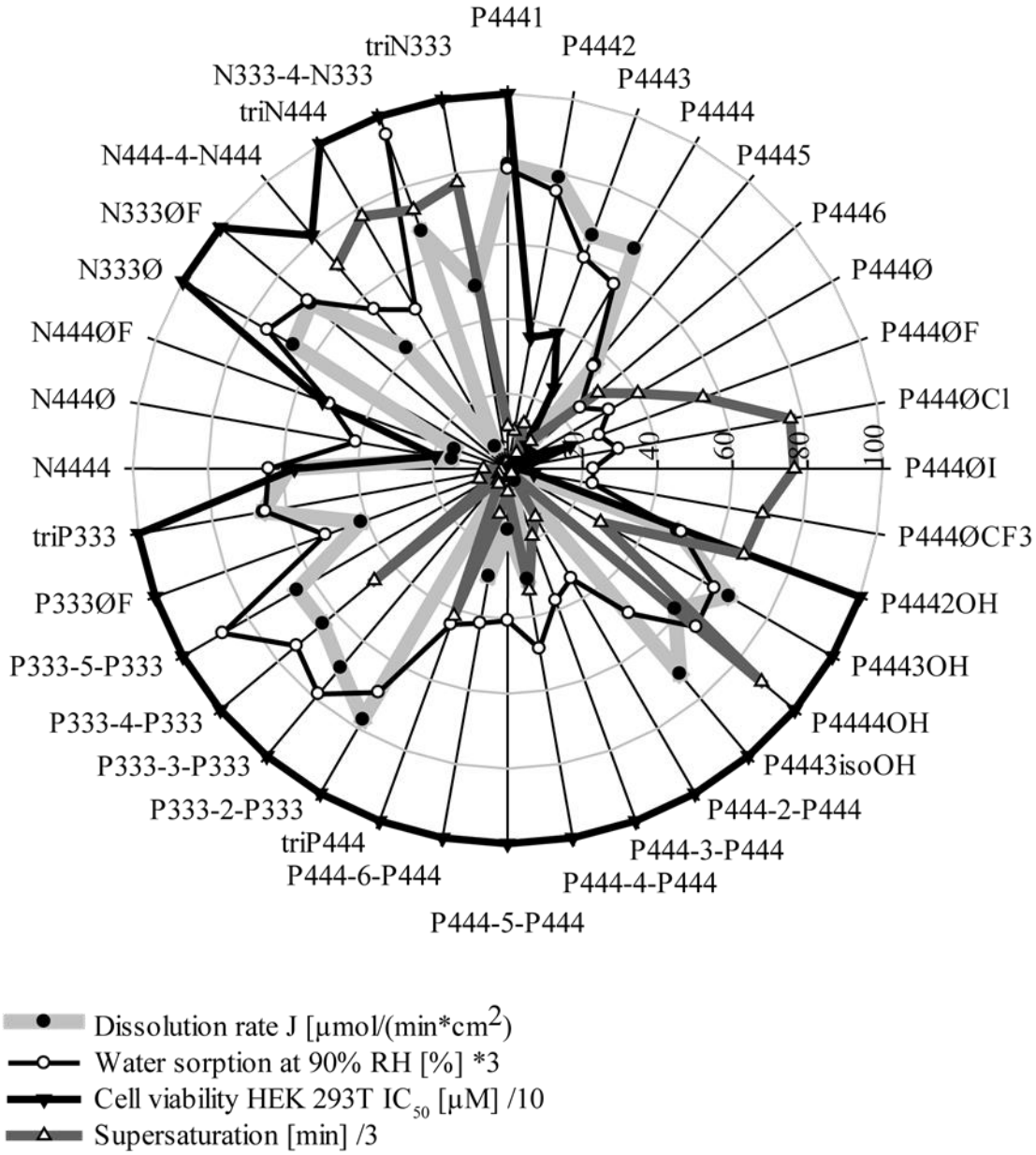

Figure 9: Radar plot, summarizing the results for the dissolution rate, water sorption, cell viability in HEK 293T cell line and the duration of supersaturation.

Discussion

36 LLESs were synthesized with high purity as determined by HPLC-CAD and NMR. The term LLES was chosen, for API and counterions are completely ionized, as determined by NMR and IR, and therefore salts. Moreover, all salts were amorphous and displayed glass transition temperatures from 40 to 148 °C. The amorphous state was accomplished by the choice of bulky counterions with flexible and voluminous side chains and diffused charges [8, 16-18]. This is a typical approach to create ionic liquids (IL). ILs are defined as organic salts with melting points below 100 °C. For the created salts no melting points were observed, but as in some cases TG temperatures were higher than 100 °C (**Supplementary Figure 1**), the definition IL did not match for all of the synthesized salts. Besides the low lattice force, which can be derived from the glass transition temperature, dissolution rate was increased, indicating that molecules can be easily separated against outer pressure. Therefore, the term low lattice enthalpy salt (LLES) was used.

The dissolution rate was modified through counterion choice within a range of 1.3% to 100%, as set for the counterion leading to the fastest dissolving LLES (P_{4441}). According to Yalkowsky solubility primarily depends on the lipophilicity of a substance and the lattice forces [19]. As solubility is correlated with the dissolution rate, the equation is also applicable here [20]. Consequently for improvement of solubility and dissolution these two properties are addressed. As all LLESs were amorphous and displayed similar TG temperatures, lattice forces may be assumed to be negligible for explaining the differences between the LLESs. Lipophilicity is mainly affected by molecular size and hydrogen bonding potential [21]. For a small group of 4 Ampicillin ILs with different counterions an indirect correlation between solubility and lipophilicity had been determined before [22]. Polarity, hydrogen bonding capacity and charge accessibility of the counterion were reported to be the decisive factors, having an impact on solubility [22]. Correlations between solubility and counterion lipophilicity were described before as well for imidazolium-, pyridinium-, pyrrolidinium-, and piperidinium-based ILs [23]. Besides, the mentioned study revealed that the solubility of ILs depends on the ability of cation or anion to develop strong interactions with solvents. The larger the side chains and the higher the molar volume of the counterions were, the lower was the solubility. Similarly within the alkyl and benzyl series it was observed that the more bulky (hence more lipophilic) the substituents of the counterion, the slower was the dissolution rate (**Figure 2A and 2B**). For all LLESs of the butyl di- and trications series, despite for those possessing two charges, dissolution rates were slower than for P_{4444} (**Figure 2C**). Interestingly, if there were only two or three CH_2-units between the phosphonium atoms of the dications, the dissolution rate was slower than for the larger dications for which the phosphonium atoms were separated by longer alkyl chains. This might be explained by the fact, that the charge is less exposed as it is more sterically hindered for shorter chain lengths

between the charged centers. Thus the molecule appears less polar and interaction with water is reduced as has been suggested before [22]. Accordingly, the highly branched trication displayed a low dissolution rate. Less sterically hindered dications with propyl instead of butyl substituents displayed dissolution rates similar to P_{4444} (**Figure 2D**). The strongly lipophilic fluoro-benzyl substituent of $P_{333ØF}$ resulted in a reduced dissolution rate. Additional polar and H-bond forming groups like hydroxyl moieties did not result in an increased dissolution rate (**Figure 2E**). Plotting the outcome from the phosphonium and against the analogous ammonium LLESs, respectively, a slope close to 1 was observed, indicating that the impact of the different counterions on the dissolution rate was independent of the fact, whether ammonium or phosphonium was selected as the center atom (**Figure 2H**). For better comparability of the different groups of counterions, molecular descriptors were identified, providing a possibility to calculate and predict the dissolution rate from structural features of the counterion (**Figure 8A**). An R^2 of 0.67 was obtained for the descriptors charge of the counterion (FCharge), number of hydrophobic atoms (a_hyd) and the graph theoretic diameter (diameter). Thus those properties of the counterion were assumed to be the major factors affecting the dissolution performance of the LLES, with these descriptors mainly describing the lipophilicity as discussed above. Therefore these results nicely build off the discussions by Jain and Yalkowsky for API solubility patterns [19] extending their concept to the use of counterions of APIs. We provided sufficient evidence that by exchanging the counterion, one can modify dissolution pattern of an API without changes in the structure of the compound. This is particularly interesting as the modification of the API structure sometimes leads to an inevitable loss in activity or is accompanied by rather high costs due to additional studies and clinical trials.

Besides the dissolution rate of an API it is also crucial that the dissolved substance remains in solution and does not recrystallize to solid state, preventing absorption of the API. By creation of a TBP-IL of the acidic model compound we already demonstrated a prolonged supersaturation in comparison to the potassium salt [11]. The effect of the modification of the counterion and the impact on the duration of supersaturation was further investigated. Within the alkyl and benzyl series it was observed that with increasing size of one substituent of the counterion the duration of supersaturation was significantly prolonged in comparison to P_{4444} when substituent consisted of more than six carbon atoms (**Figure 3A and 3B**). Thus duration of supersaturation of API in solution appeared to correlate with the lipophilicity of the counterion. For dications the more sterically hindered counterions with four or less CH_2-units between the phosphonium ions displayed a longer duration of supersaturation as compared to the larger dications with five and six CH_2-units between the phosphonium ions (**Figure 3C**). For the smaller and less sterically hindered propyl di- and trications duration of supersaturation was comparable to P_{4444}, with one exception (**Figure 3D**). $P_{333\text{-}4\text{-}}P_{333}$ supersaturated similarly to its butyl analog $P_{444\text{-}4\text{-}}P_{444}$, which cannot be

explained by the structural correlations, developed before. For hydroxyl LLES with terminal hydroxyl moieties a significantly longer supersaturation was determined indicating that the polar group stabilizes the supersaturated state (**Figure 3E**). For a non-terminal hydroxyl moiety no prolonged supersaturation was detected, leading to the hypothesis that hydrogen bonding capacity increases duration of supersaturation, possibly for improved interaction with API and the aqueous medium. Only for five ammonium derivatives it was possible to determine supersaturation with an autotitrator and, therefore, the number of data points was insufficient to build a good estimation of a correlation between structure and supersaturation pattern (**Figure 3H**). Nevertheless, for all which were successfully assessed, the duration of supersaturation was longer for the ammonium as compared to the phosphonium analogues, respectively. Future studies must aim for designing further ammonium counterions to provide broader hence more robust data sets. Similarly to the aforementioned model for the dissolution rate, we aimed for appropriate descriptors suitable for the prediction of the supersaturation pattern from the counterion structure. Especially from the alkyl and benzyl group a correlation of supersaturation and lipophilicity was suggested, as with increasing dissolution rates, which was determined to correlate with the lipophilicity of the counterion, the duration of supersaturation decreased (**Supplementary Figure 6A**). Thus the same molecular descriptors as for the dissolution rate were chosen. However, for all LLESs no good correlation was received. For both the LLESs from the ammonium series and the hydroxyl series the supersaturation did not seem to depend on the descriptors used before, further indicating that counterion lipophilicity did not serve as a good approximate for supersaturation duration of all series or that the design space in terms of structural heterogeneity of the counterion is by far smaller as compared to the dissolution rate. In fact, if only the data of the alkyl, benzyl, butyl-di and trications and propyl series were used, a R^2 of 0.66 was received for the correlation between duration of supersaturation and the logarithm of the dissolution rate, which is a measure for the hydrophilicity at the same time (**Figure 8B**). A possible explanation might be that API and counterion form aggregates in solution during the supersaturated state. By interaction of the counterion and the API upon dissolution, hence incomplete dissociation, the API is stabilized in its ionized form and this is driving the lengths of the supersaturation. Mechanistically, the accessibility for protons to the API might be hindered by the presence of the counterion, reducing the API propensity for protonation, hence neutralization, hence aggregation and ultimately precipitation/crystallization. The existence of these aggregates during supersaturation has been confirmed for P_{4444} [11]. Arguably, from a mechanistic perspective, one may conclude that as long as the dissociation of the API and the counterion are less favored, the protonation of the API is delayed, hence as long as the dissociation constant (K_d) is lowered one will obtain a longer supersaturation. Likely, the K_d is at least in part driven by the entropy gain of the dissociated counterion with surrounding water molecules (assuming one works in the pharmaceutically

relevant aqueous environment). Therefore, an increasing counterion lipophilicity will hamper the counterions ability to disturb the water clusters, leading to an increase in the standard Gibbs energy ($\Delta G°$) and the natural logarithm of the equilibrium constant (lnK) for counterions with increasing lipophilicity, respectively (assuming pressure and temperature remain constant). This mechanistic explanation was used before for imidazolium-, pyridinium-, pyrrolidinium- and piperidinium-based ILs for which their solubility was linked to the capacity of the anion or cation to interact with the solvent, which was associated with small hydrophilic counterions [23]. In essence, the tendency of the API-counterion salt for dissociation is reduced with increasing lipophilicity of the counterion. Therefore, more lipophilic counterions form more stable aggregates and supersaturate for a longer period of time. For the counterions with terminal hydroxyl group an interaction with the API molecule, possibly by an H-bond, was assumed that stabilizes aggregates of API and counterion in aqueous solution and therefore prolongs the supersaturation. For LLES with non-terminal hydroxyl moiety the interaction is not possible and therefore no prolonged supersaturation is observed. For ammonium series too few data was available for developing a theory.

Besides the effect of the structure of the counterions on the supersaturation also the impact of the supersaturation ratio and the pH during supersaturation were analyzed. For P_{4444} an exponential correlation was reported between the duration of supersaturation and the ratio of kinetic to equilibrium solubility [11]. The concentration versus time profiles of LLESs (**Figure 4A**) suggested a similar correlation. The duration of supersaturation was logarithmically plotted against the ratio of supersaturation S/S_0 (**Figure 4B**). A linear correlation was obtained indicating that the lower the concentration during the supersaturation process is, with reference to its equilibrium solubility, the longer the duration of supersaturation. This correlation was observed before for the API with different ratios of supersaturation being accomplished by different ratios of counterion to API [11]. The observation was linked to the classical nucleation theory with the ratio of supersaturation (S/S_0) correlation exponentially with the rate of crystal formation (j) which is assumed to be the rate limiting step for the recrystallization [24, 25].

The pH, when first precipitation occurred, was also plotted against the logarithmic duration of supersaturation (**Figure 4C**). As before, a linear correlation was obtained. A possible interpretation is that the lower the pH and the more protons are available and the faster the API is protonated initiating the collapse of the supersaturated state. Combining all results for supersaturation it can be concluded that the more lipophilic the counterion, the longer is the duration of supersaturation.

The experiments with the autotitrator are designed to obtain rapid insight into the dissolution rate and solubility profiles of new compounds. The system is analyzing and extrapolating from a non-equilibrium state to an equilibrium state, saving time while, allowing useful pharmaceutical interpretation and valid prediction of equilibrium conditions. Nevertheless, corroboration of these results with real time experiments is advantageous. Therefore, real time experiments in shake flasks

were conducted. A good correlation between the autotitrator and shake flask experiments was obtained for supersaturation (**Figure 5B**), such that a supersaturation duration of more than 30 min in as observed in the autotitrator corresponded to a supersaturation of more than 24 hours in the shake flask experiment. Only exception was $P_{444Ø}$, which displayed precipitation after 6.25 hours. This exception may be linked to the different setup of the autotitrator versus the shake flask experiments. The autotitrator first completely dissolves the API and counterion by appropriate pH setting followed by carefully titrating the solution into a pH range within which the autotitrator detects first precipitation. This initial precipitate is back-and forward titrated with the addition of tiny amounts of bases and acids as appropriate and from this state the algorithm extrapolates to solubility. In contrast, the shake flask experiments start with a slurry of the API/counterion. The quite substantial difference is that the autotitrator results are obtained after the substance was completely dissolved, whereas for the shake flask setup the experiments started with the undissolved substance. One may speculate that as $P_{444Ø}$ was only partly dissolved in shake flak experiment when first precipitation was observed, the counterion concentration was lower than during the autotitrator experiments. From earlier results it is known that a linear correlation existed between the concentration of one counterion in solution and the duration of supersaturation and potentially, this may have happened here [11]. However, further experiments are required to substantiate this hypothesis.

The shake flask experiments demonstrated that by proper choice of the counterions, immediate and prolonged release profiles were obtained, correlating also well with the results for dissolution rate, as for LLESs with low dissolution rates a slow release was observed and for high dissolution rates a fast release, respectively (**Figure 5A**). This proves that only by choice of counterion the drug release of a compound can be modified in a significant way without any structural changes of the API, which is accompanied by additional costs as discussed before.

Water sorption affects many physico-chemical properties of solids, like chemical stability, powder flow, compactibility, lubricity and dissolution rate [26, 27]. Especially for the preparation of pharmaceutical solid dosage forms these properties are decisive and need to be controlled to assure a constant quality. For amorphous substances water uptake results in reduction of glass transition temperatures according to the Kelley-Büche equation.

$$TG_{mix} = [(w_1 * TG_1) + (K * w_2 * TG_2)]/[w_1 + (K * w_2)] \text{ with } K = (\rho_1 * \Delta\alpha_2)/(\rho_2 * \Delta\alpha_1)$$

TG is the glass transition temperature, w the weight fraction, Δα the change in thermal expansivity and ρ is the true density [28, 29]. With a TG of <136 K [30] water is an efficient plasticizer and substantially increases molecular mobility, which can result in undesired liquefaction and recrystallization for substances with low glass transition temperatures. In amorphous forms the solid state is disordered and water can permeate into the solid, such that the effective surfaces for

water adsorption is much higher as compared to crystalline states [27]. Consequently, most amorphous or liquid APIs and, therefore, most ILs are reported to be hygroscopic [31-33]. It is known that the more polar a substance is, the higher is the water sorption [26, 34]. Polarity as determined by Nile Red assay was reported to correlate with the initial water sorption rate for 9 ILs [34]. For ILs the interaction with water is enhanced with increasing counterion charge, while it is reduced with increasing delocalization of the charge and size of the counterion, e.g. by larger alkyl chains [23, 31-33, 35]. The percentage change in mass at 90% RH was determined as a measure for hygroscopicity. Within the alkyl series with increasing length of one alkyl chain of counterion the water sorption was reduced from about 25% to 9%, which we link to the increasing lipophilicity of counterion with larger size of the apolar moiety (*vide supra*, **Figure 6A**). Counterions of the benzyl series displayed similarly low hygroscopicity as tributylhexyl phosphonium but, differently to dissolution rate and supersaturation, further halide moieties at the benzyl group had no additional effect (**Figure 6B**). Counterions of the butyl di- and trication series were less hygroscopic as the more polar propyl analogues (**Figure 6C and 6D**). Hydroxyl moieties, though increasing polarity, did not result in a substantial change in hygroscopicity (**Figure 6E**). Ammonium analogues were more hygroscopic than phosphonium counterions which might be explained by the larger size of the phosphonium ion and therefore more diffused charge in comparison to the ammonium ion (**Figure 6F**). Generally for all LLESs at 80% RH values ranged between 5% and 18% change in mass was determined. According to the hygroscopicity classification scheme by the European Pharmacopeia all LLESs have to be regarded as moderately to very hygroscopic [36]. This drawback of increased hygroscopicity is a consequence of increased hydrophilicity of the LLESs which at the same time leads to an increased dissolution rate (**Supplementary Figured 3B**). Formulation strategies to address this challenge have been described before [37]. As for both water sorption and dissolution rate the interaction of water with the substance is decisive, correlation between hygroscopicity and dissolution rate was determined and a high coefficient of determination of 0.74 was obtained (**Supplementary Figure 6B**). As it was possible to calculate the dissolution rate of the LLESs by molecular descriptors of the counterions, the approach was used for the water sorption data, as well. A good correlation with R^2 of 0.55 for measured and calculated water sorption was obtained, using the molecular descriptors charge (FCharge) and number of hydrophobic atoms (a_hyd) (**Figure 8C**). The diameter was no significant factor in the equation. With the prefactor of the charge being about 10 times higher than for the number of hydrophobic atoms the importance of the charges of the counterion for the hygroscopicity is revealed. The developed correlation can be used to estimate the hygroscopicity of the LLESs by calculable descriptors of the counterion.

During development of ionic liquids and LLESs for pharmaceutical use, the assessment of toxicity is a crucial step. For an IL with the counterion TBP low cytotoxicity in 60 cell lines was already

reported and by comparison to a tributyldodecyl phosphonium ($P_{444\ 12}$) IL it was assumed that one longer alkyl chain leads to an increased cytotoxicity [38]. Similarly, for ILs with guanidinium cations and choline phosphate ILs it was reported that cytotoxicity enhanced, with longer and/or branched alkyl chains and increasing anion mass size [39, 40]. The higher lipophilicity due to side chains or formation of neutral ion-pairs is supposed to result in a reduced interaction with the aqueous medium and an improved proclivity to intercalate with cell membranes [40]. Therefore, the correlation of cytotoxicity and structure was studied. Generally data of the alkyl series corroborate the theory that prolonged alkyl chains result in higher cytotoxicities (**Figure 7A**). More apolar and larger benzyl substituents of the tributyl cations result in comparable cytotoxicities as for P_{4446} (**Figure 7B**). On the other hand more polar propyl benzyl cation $P_{333Ø}$ is less toxic (**Figure 7D**). More polar dications and trications, independent of phosphonium or ammonium as center atom, and hydroxyl counterions resulted in cell viabilities higher than the maximum value that was determined (**Figure 7C-7F**). Comparison of ammonium counterions with the phosphonium analogues was only possible for four counterions which do not display maximum IC_{50} values. Ammonium counterions appear to be slightly less cytotoxic than phosphonium counterions, however, the data set is limited to only four observations (**Figure 7F**). The results seem to be in good accordance with the theory linking larger and more lipophilic species interaction with cell membranes and cytoplasmic uptake is enhanced, leading to a higher cytotoxicity [39-41]. From the calculation of the cytotoxicity for HEK 293T cell line a good correlation was obtained with the molecular descriptors charge of counterion (FCharge), number of oxygen groups (a_nO) and the number of hydrophobic atoms (a_hyd). These descriptors were chosen as for the investigated counterions the number oxygen atoms equals the number of hydroxyl moieties and therefore the hydrogen bonding capacity. The number of hydrophobic atoms is a parameter for molecular size and lipophilicity, while the charge is a parameter for hydrophilicity. From the prefactors of charge and number of oxygen atoms it can be concluded that the positive impact of them on cell viability is about ten times higher than the negative effect of hydrophobic atoms. For no higher concentrations than 1000 µM were tested – and as this threshold suggested absence of cytotoxicity - it was not possible to seize a distinction between all di- and trications as well as the hydroxyl set counterions. Therefore, even better coefficient of determination might be obtained for experiments exceeding the 1000 µM threshold (**Figure 8D**).

By summarizing the results for the dissolution rate, the duration of supersaturation, the water sorption and the cell viability in one diagram an overview of the correlations mentioned above is obtained (**Figure 9**). Starting at the top of the radar plot in clockwise direction the counterion lipophilicity increases from P_{4441} to $P_{444ØCF3}$ being associated with a decrease in dissolution rate, water sorption and cell viability as well as an increase in duration of supersaturation. With decreasing counterion lipophilicity by introduction of hydroxyl moieties and more charges per

counterion higher dissolution rates, water sorption, cell viability and lower supersaturation durations are observed, though some values differed from the general trend. With propyl instead of butyl chains even less lipophilic counterions were obtained, resulting in dissolution rates comparable to P_{4441}. Besides the similarities between the phosphonium LLES and their corresponding ammonium analogues are illustrated. Impressively, this overview elucidates the large variety of physico-chemical and biological properties which can be achieved for the very same API, simply by choice of one counterion of the developed library. Future studies are needed to assess the effect of the API structure on the properties of the LLES, combining a large variety of acidic APIs with a large number of counterions. Besides, by determination of descriptors for calculation of the LLESs properties predictions may be envisioned, allowing for the selection of a counterion for a specific API, in order to obtain the desired release profile of the API.

Conclusion

36 LLESs were synthesized of a poorly water soluble drug. By choice of counterion it was possible to deliberately tune the dissolution rate, duration of supersaturation and hygroscopicity. For the dissolution rate, hygroscopicity and cytotoxicities, correlations were determined for measured results and values calculated by simple molecular descriptors. Thereby, the calculations allow a prediction of the properties of a LLES or counterion to a certain extent even before synthesis and characterization. Besides, for hydroxyl free phosphonium LLESs a correlation between duration of supersaturation and dissolution rate was determined, revealing the impact of counterion lipophilicity on the supersaturation of an API. In summary, a counterion library was synthesized, offering the possibility to deliberately change the release profile of an API from immediate to prolonged release over 12 hours. This study illustrated the huge impact of counterions on pharmaceutically relevant features of an API salt, proving preparation of LLESs with API optimized counterions a beneficial concept to overcome formulation challenges.

Materials and methods

Materials

N-[7-Isopropyl-6-(2-methyl-2H-pyrazol-3-yl)-2,4-dioxo-1,4-dihydro-2H-quinazolin-3-yl]-methanesulfonamide (referred to as ‘acid’ or ‘free acid’ within this manuscript) was synthesized by Novartis AG (Basel, Switzerland) [42-44]). Tetrabutylphosphonium hydroxide solution (40% in water v / v; referred to as TBP within this manuscript), hydrochloric acid 0.5 M and potassium hydroxide concentrate for preparation of 0.5M potassium hydroxide solution, tripropylphosphine 97% and tributylphosphine ≥93.5% were purchased from Sigma Aldrich (Schnelldorf, Germany). Sodium chloride, potassium chloride, sodium hydrogen carbonate, sodium dihydrogen phosphate,

disodium hydrogen phosphate were of analytical grade. HPLC grade acetonitrile and methanol and ammonium acetate HiPerSolv Chromanorm were purchased from VWR (Darmstadt, Germany), hexadeuteriodimethyl sulfoxide (DMSO-d6, 99.8% D) from Euriso-top (Saarbrücken, Germany). HPLC grade water was obtained by in-house Millipore system from Merck (Darmstadt, Germany). The further chemicals and solvents for synthesis were purchased from Alfa-Aesar (Karlsruhe, Germany), Fisher Scientific (Schwerte, Germany), Fluka (Buchs, Switzerland), Merck (Darmstadt, Germany), Sigma-Aldrich (Schnelldorf, Germany) and VWR International (Darmstadt, Germany). J774.1 cells, HepG2 cells and HEK 293T cells were purchased from ATTC (Manassas, VA). All LLESs were synthesized and confirmed by NMR and IR by Johannes Wiest.

Methods

Synthesis of counterions and LLES

Synthesis of the counterions and LLES followed a general way of preparation. Briefly, the counterions were synthesized by a reaction of tertiary phosphines and amines with alkyl halides and dihalides to phosphonium and ammonium halides, respectively. After purification, the halides were exchanged by hydroxide quantitatively with anion exchange resin [45, 46]. The concentrations of the phosphonium or ammonium hydroxide solutions were determined by quantitative NMR spectroscopy. For LLES synthesis equivalent amount of counterion hydroxide solution was added to the free form of the acidic API, dissolved in methanol. The ratio of monocation to API was 1:1, dication 1:2 and trication 1:3. After removal of solvents *in vacuo*, the LLES were dried for 48 h at 55 °C *in vacuo*.

Nuclear Magnetic Resonance measurement (NMR)

NMR measurements were performed using a Bruker Avance III 400 MHz spectrometer (Bruker BioSpin, Karlsruhe, Germany) and the data were processed with the TopSpin 3.0 software from Bruker. The samples were dissolved in deuterated DMSO-d6, filled in standard 5 mm NMR tubes (ST 500) purchased from Norell (Landisville, USA) and the spectra were referenced to the residual solvent signal of DMSO (2.5 ppm/39.52 ppm).

Infrared Spectroscopy (IR)

The IR spectra were measured using a Jasco FT/IR-6100 spectrometer from Jasco (Gross-Umstadt, Germany) with diamond attenuated total reflection unit.

High performance liquid chromatography with charged aerosol detector (HPLC-CAD)

Analytical HPLC analyses were performed using an Agilent Technologies 1100 series systems (Waldbronn, Germany) consisting of a binary pump, a degasser, an autosampler, a column thermostat, a diode-array UV detector and a Corona® charged aerosol (CAD) detector from Dionex Corporation (Sunnyvale, USA). An Acclaim Trinity P1 column (3.0 x 50 mm, 3µm) from Dionex Corporation (Sunnyvale, USA) was used. For each sample 0.5 mg compound was weighted by a micro scales in a 10 ml volumetric flask and 1.5 ml was centrifuged with 13.000 rpm ten minutes by an EBA 12 centrifuge of Hettich (Tuttlingen, Germany) in an Eppendorf cap. The supernatant was transferred into a HPLC vial from Phenomenex (Aschaffenburg, Germany). The separation was carried out using a Acclaim Trinity P1 column and a gradient of A: 10 mM ammonium acetate buffer pH 5.0 and acetonitrile (80:20/V:V) (A) and B: 200 mM ammonium acetate buffer pH 5.0 and acetonitrile (50:50/V:V) with a flow of 0.5 ml/min. The elution started with 100% A going up to 100% B in 15 min, then hold 5 min 100% B, going back to 100% A in 0.1 min and then conditioned for 5 min with 100% A. For determination of the purity of the ionic Liquids and counterions the normalization method described in the European Pharmacopeia was applied using the area under signals detected by charged aerosol detector.

X-ray powder diffractometry (XRPD)

Dry substances were applied on silicon single crystal zero background specimen holder and analyzed with a Bruker Discover D8 powder diffractometer (Karlsruhe, Germany) using Cu-Kα radiation (unsplit $K\alpha_1$+$K\alpha_2$ doublet, mean wavelength λ = 154.19 pm) at a power of 40 kV and 40 mA, a focusing Goebel mirror and a 1.0 mm microfocus alignment (1.0 mm pinhole with 1.0 mm snout). Scattered X-ray beam went through a receiving slit with 7.5 mm opening, a 0.0125 mm nickel foil and a 2.5° axial Soller slit. Detection was done with a LynxEye-1D-Detector (Bruker AXS) using the full detector range of 192 channels. Measurements were performed in reflection geometry in coupled two theta/theta mode with a step size of 0.025° in 2θ and 0.25 s measurement time per step in the range of 8 – 40° (2θ). Data collection and processing was done with the software packages DIFFRAC.Suite (V2 2.2.690, Bruker AXS 2009-2011, Karlsruhe, Germany) and DIFFRAC.EVA (Version 2.1, Bruker AXS 2012-2012, Karlsruhe, Germany).

Differential scanning Calorimetry (DSC)

Substances were weighed out into aluminium pans with a pinhole in the lid, enabling residual solvents to evaporate. 2-7 mg of samples were analyzed with DSC 8000 (Perkin Elmer, Waltham, MA) at a scanning rate of 20K/min from -50 °C to 200 °C.

Determination of dissolution rate

Dissolution rates were determined as described earlier using a Sirius T3 intrument (Sirius Analytical, Forest Row, UK) [47]. Tablets with surface area of 0.07 cm^2 were prepared in a tablet disc by compression of 5-10 mg substance under a weight of 0.18 tonnes for 6 minutes with a manual hydraulic tablet press (Paul Weber Maschienen- und Apparatebau, Stuttgart-Uhlbach, Germany). Dissolution rates were determined photometrically at room temperature in phosphate buffered saline pH 6.8 following manufacturer's instructions. Each LLES was measured three times.

Determination of duration of supersaturation with autotitrator

Intrinsic solubility during supersaturated and equilibrium state as well as the duration of the supersaturation were measured with a Sirius T3 (Sirius Analytical, Forest Row, UK) as described before [48, 49]. 13-16 µmol of the compounds were dissolved in 1.5 ml of 0.15 M KCl solution at pH 12 (adjusted with 0.5 M potassium hydroxide). After complete dissolution, the solution was back-titrated by addition of 0.5 M hydrochloric acid until first precipitation occurred and was detected photometrically (λ = 500 nm). Subsequently, the pH was changed incrementally by repeated addition of minute amounts of acid and base. The delayed pH gradient of the compounds, due to precipitation or dissolution, was used to extrapolate the equilibrium phase where the pH gradient was zero. Solubility was calculated from pH of this extrapolated point. A maximum number of 80 extrapolations were performed during one experiment. The duration of supersaturation was calculated from the time interval from the first precipitation (kinetic solubility) to the time when the concentration dropped below the kinetic solubility. Data from analysis with acidity errors larger than 1 mM were excluded. For each LLES three assays were performed. Supersaturation ratio S/S_0 was calculated by dividing the concentration during supersaturation by the concentration during the equilibrium state.

Shake flask experiments

For powder dissolution shake flask experiments 4.74 µmol ± 0,14 µmol dry substance was weighed into an 1.5 ml tube. From each substance three samples were prepared: To the dry substance 1 ml PBS buffer pH 6.8 was added and samples were incubated at 37 °C at 400rpm. Samples of 50 µl were drawn after certain time intervals (15 min, 45 min 2 h, 4 h, 6 h, 8 h, 12 h, 24 h), transferred into Eppendorf tubes and centrifuged 5 minutes at 13000 rpm. 10 µl of supernatant were diluted with 990µl PBS buffer 6.8 and concentrations were determined photometrically at 254 nm.

Dynamic vapor sorption (DVS)

For detection of moisture sorption isotherms at 25 °C of different substances a DVS HT instrument (Surface Measurement Systems Ltd., London, UK) was used. Measurements were performed after

initial drying at 10% RH. Equilibrium state was assumed to be reached, when change in mass was less than 0.02 mg per minute. In steps of 10% RH relative humidity was increased after equilibrium state was reached. Moisture sorption isotherms were measured from 10% to 90% RH.

Cytotoxicity of counterion

Cytotoxicity was tested in human embryonic kidney 293 cells (HEK 293T), human hepatoma HepG2 cell (HepG2) and murine macrophage cell line J774.1 (J774.1) as described before[11]. Serial dilutions of the counterion salts in DMSO were prepared. All salts were bromide salts apart from 6 exceptions. The counterions of P_{4441} and P_{4442} were iodide salts; the counterions of P_{4444}, N_{4444}, P_{4443OH} and $P_{4443isoOH}$ were chloride salts. For the experiments J774.1 and HepG2 cells were suspended in RPMI medium with 10% FCS and without phenol red at a concentration 1x105 cells/ml. For HEK 293T cells a concentration of 2x104 cells/ml in DMEM high glucose medium with 10% FCS and without phenol red was applied. 200 µl of cell suspensions were transferred into 96-well cell culture plates and the compound dilutions were admixed. The final DMSO concentration was 1%. After 24 h of incubation at 37 °C and 5%CO2, 10% of AlamarBlue solution were added. J774.1 and HepG2 cells were incubated for further 48 hours and HEK 293T cells for 24 hours. The IC_{50} values were calculated, using controls without compound. The absorbance was measured at 550 nm, using 630 nm as reference wavelength.

Calculation of models using molecular descriptors

All counter ion structures were de-salted and protonated using the Wash plugin of MOE (Molecular Operating Environment MOE), 2012.10; Chemical Computing Group Inc., 1010 Sherbooke St. West, Suite 910, Montreal, QC, Canada, H3A 2R7, 2012), followed by a short energy minimization in the MMFF94x force field using default settings. Subsequently, MOE was employed to calculate the used molecular descriptors. All statistical analyses were carried out with the statistical framework R (R Core Team, 2013, R Foundation for Statistical Computing, Vienna, Austria).

Statistics

All results were analyzed using Minitab Statistical Software (Minitab Inc., PA, USA). The results of the dissolution rate and duration of supersaturation for the LLES series were analyzed with one-way ANOVA, considering p-values of 0.05 as significant. For the comparison of a phosphonium LLES with its ammonium analogue two-sample t-Test was applied, considering p-values of 0.05 as significant.

Acknowledgments

We gratefully acknowledge the financial support by the Bayerische Forschungsstiftung project “Springs and parachutes”.

Supplementary Figures

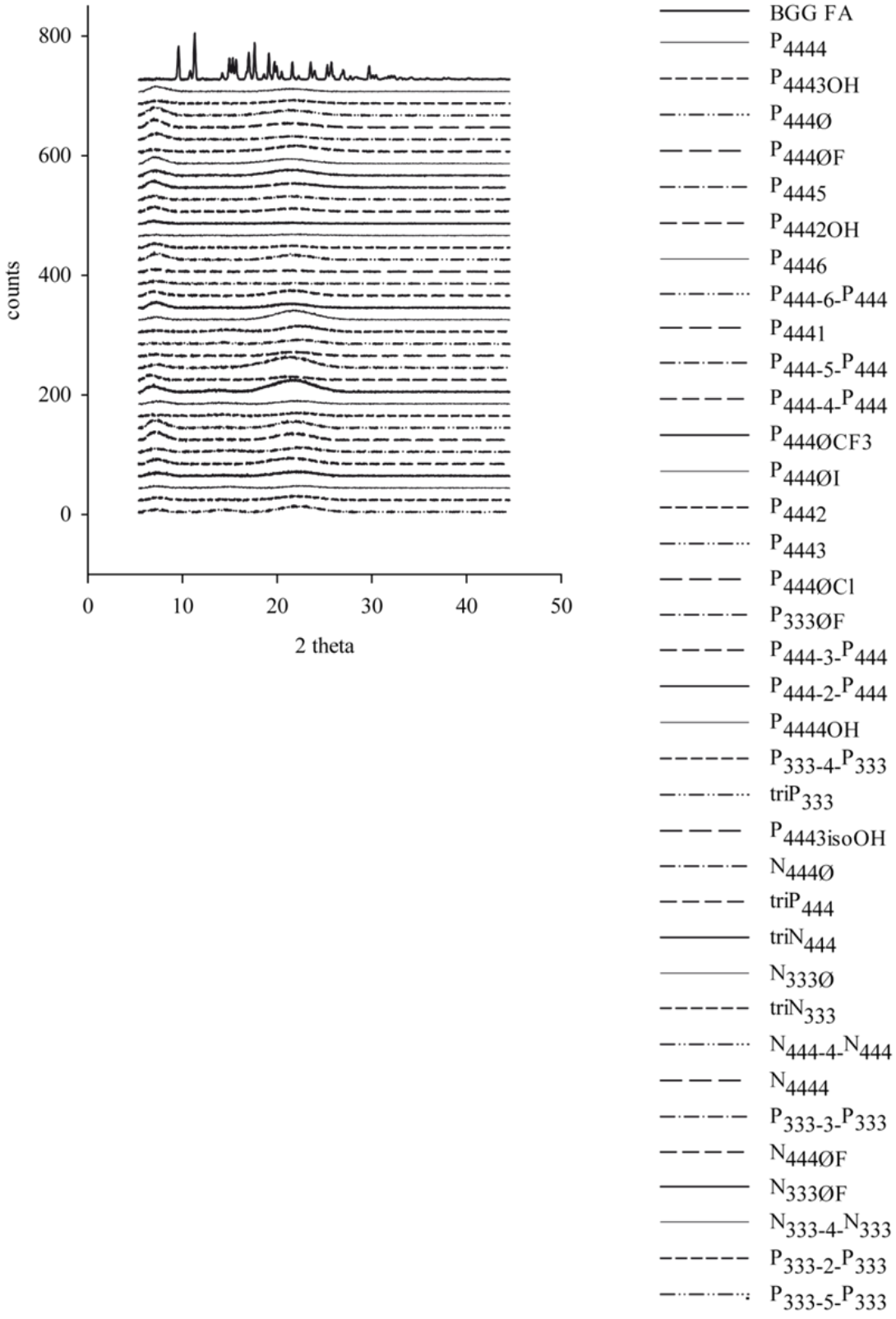

Supplementary Figure 1: Results of XRPD analysis of the different LLESs

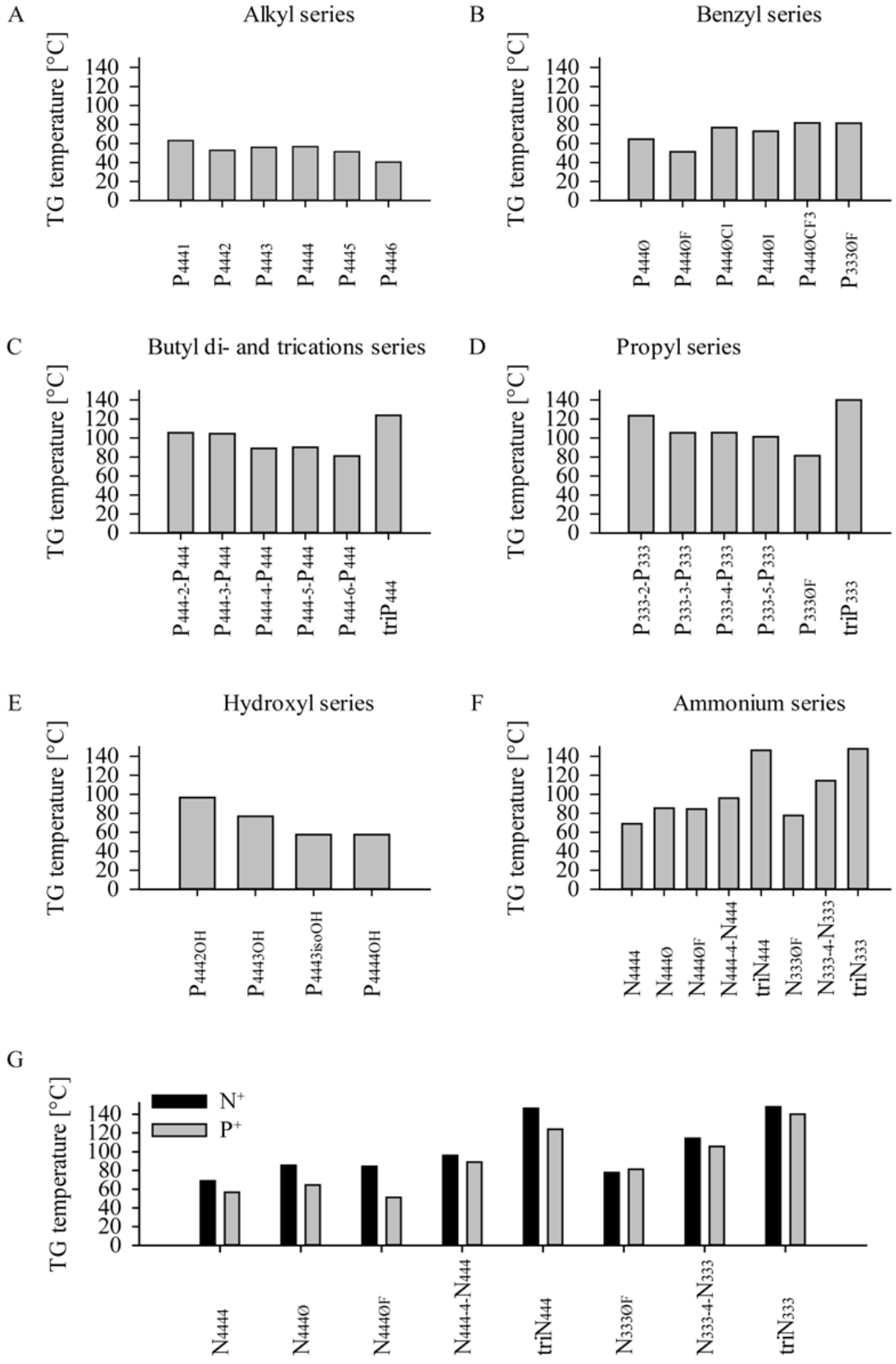

Supplementary Figure 2: (A-F) Glass transition (TG) temperatures of the different LLES of the distinct series (G) TG temperatures of the ammonium LLESs and the corresponding phosphonium LLESs.

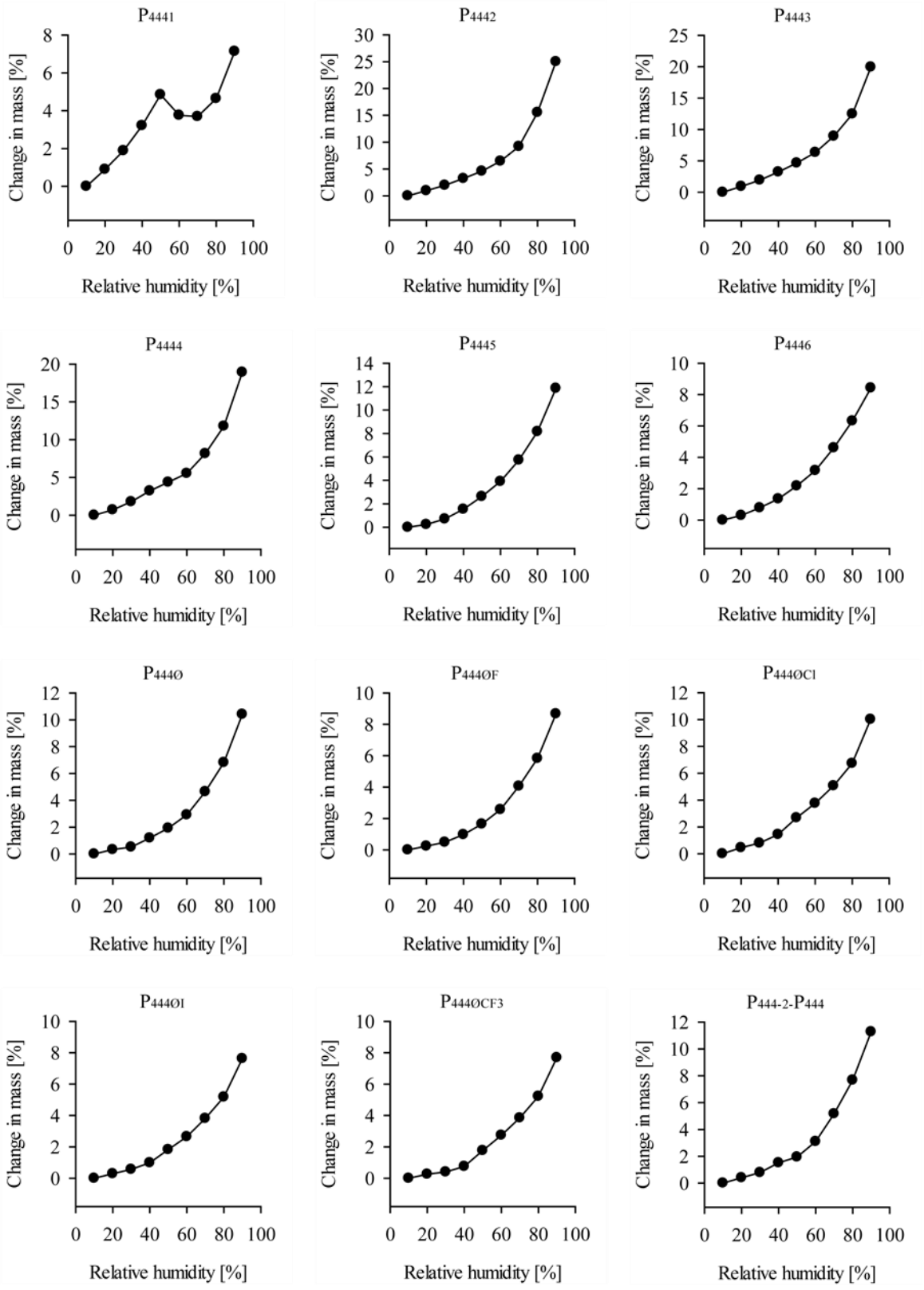

Supplementary Figure 3: Dynamic vapor sorption data (part 1)

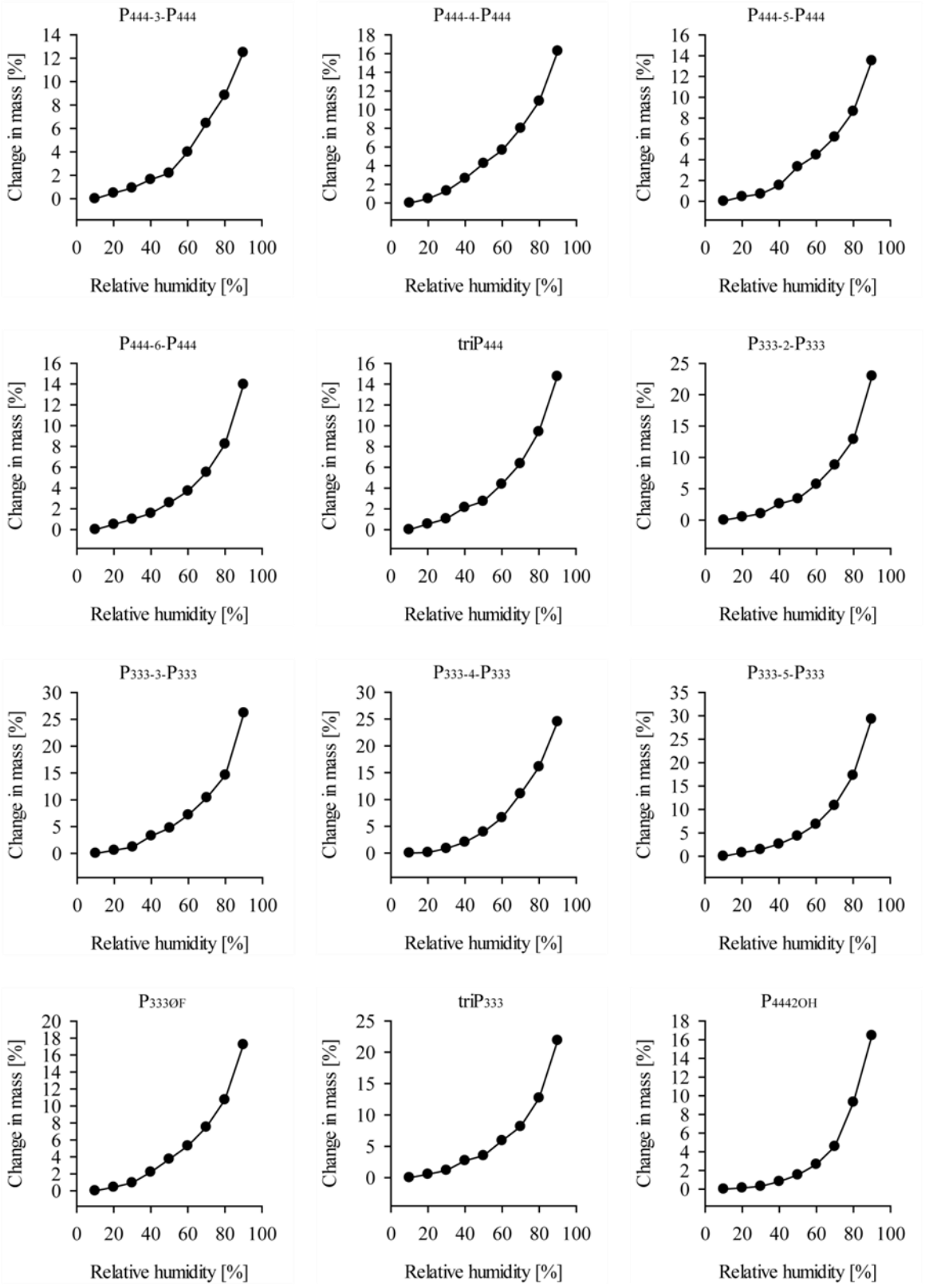

Supplementary Figure 4: Dynamic vapor sorption data (part 2)

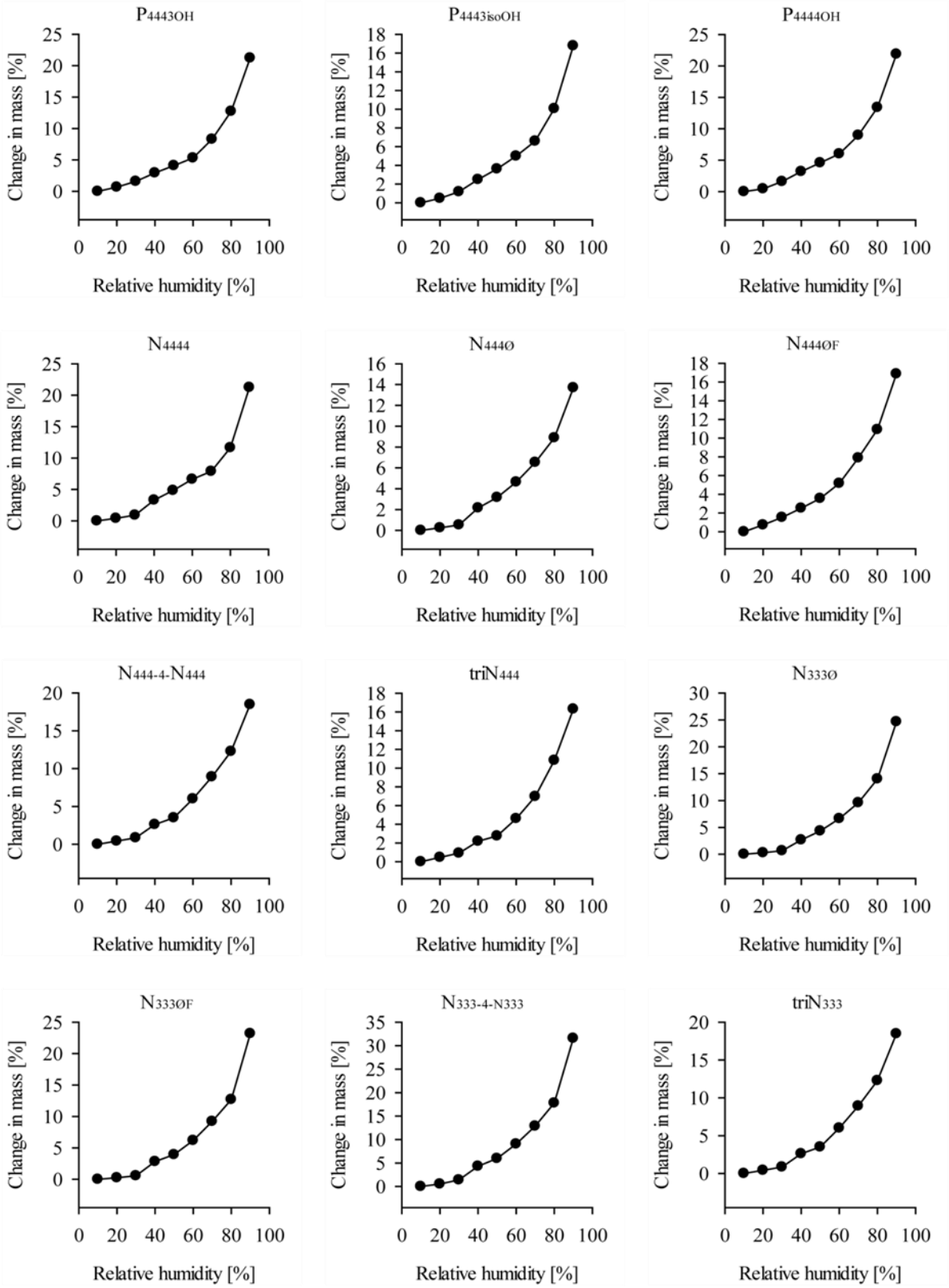

Supplementary Figure 5: Dynamic vapor sorption data (part 3)

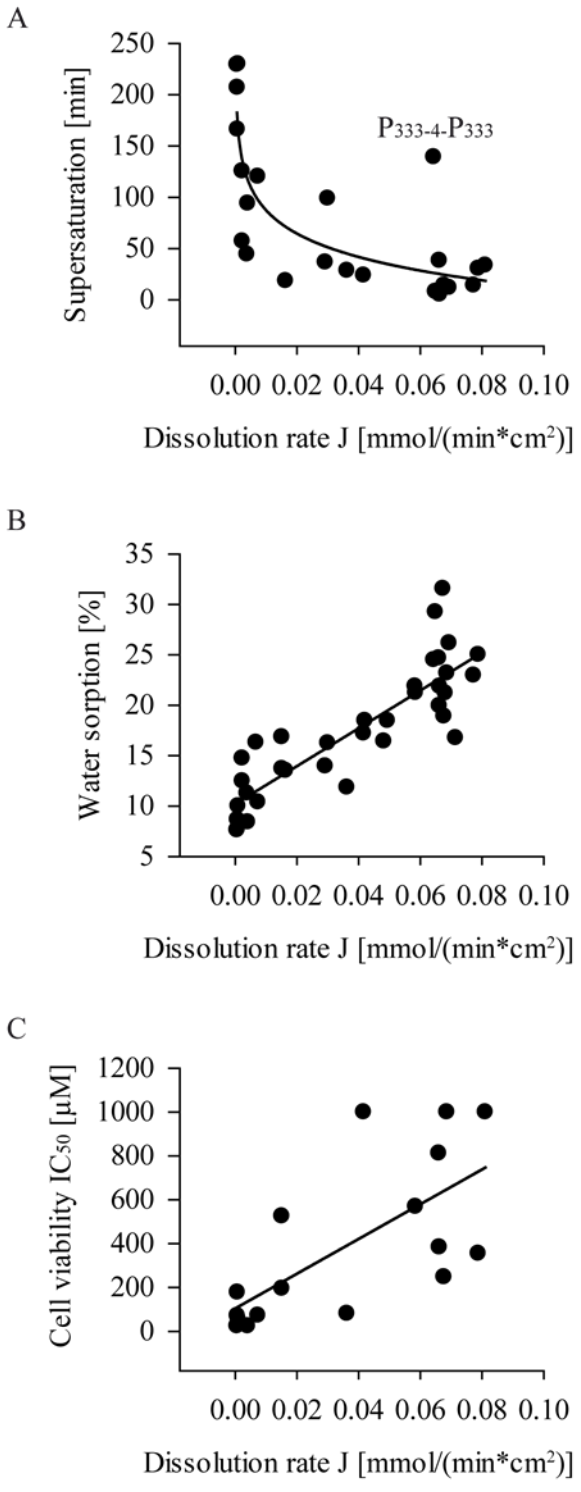

Supplementary Figure 6: (A) Duration of supersaturation in minutes of all LLESs versus the dissolution rate J in mmol/(min*cm^2) (B) Water sorption expressed as change in mass in % at 90% RH versus the dissolution rate J in mmol/(min*cm^2) (C) Cell viability results of the single charged counterions expressed by half maximal inhibitory concentration (IC_{50}) in µM for the cell lines HEK 293T versus the dissolution rate J in mmol/(min*cm^2).

References

[1] Y. Kawabata, K. Wada, M. Nakatani, S. Yamada, and S. Onoue, "Formulation design for poorly water-soluble drugs based on biopharmaceutics classification system: basic approaches and practical applications," *Int J Pharm*, vol. 420, pp. 1-10, Nov 25 2011.

[2] R. O. Williams III, A. B. Watts, and D. A. Miller, *Formulating Poorly Water Soluble Drugs* vol. 3. New York, NY: Springer New York, 2012.

[3] A. Fahr and X. Liu, "Drug delivery strategies for poorly water-soluble drugs," *Expert Opin Drug Deliv*, vol. 4, pp. 403-16, Jul 2007.

[4] V. J. Stella and K. W. Nti-Addae, "Prodrug strategies to overcome poor water solubility," *Adv Drug Deliv Rev*, vol. 59, pp. 677-94, Jul 30 2007.

[5] P. M. Dean, J. Turanjanin, M. Yoshizawa-Fujita, D. R. MacFarlane, and J. L. Scott, "Exploring an Anti-Crystal Engineering Approach to the Preparation of Pharmaceutically Active Ionic Liquids," *Crystal Growth & Design*, vol. 9, pp. 1137-1145, Feb 2009.

[6] A. T. Serajuddin, "Salt formation to improve drug solubility," *Adv Drug Deliv Rev*, vol. 59, pp. 603-16, Jul 30 2007.

[7] P. H. Stahl, C. G. Wermuth, and I. U. o. P. a. A. Chemistry, *Handbook of Pharmaceutical Salts Properties, Selection, and Use*, 2 ed. Zürich: VHVA; Weinheim:Wiley-VCH, 2011.

[8] J. Stoimenovski, D. R. MacFarlane, K. Bica, and R. D. Rogers, "Crystalline vs. ionic liquid salt forms of active pharmaceutical ingredients: a position paper," *Pharm Res*, vol. 27, pp. 521-6, Apr 2010.

[9] B. Rodriguez-Spong, C. P. Price, A. Jayasankar, A. J. Matzger, and N. Rodriguez-Hornedo, "General principles of pharmaceutical solid polymorphism: a supramolecular perspective," *Adv Drug Deliv Rev*, vol. 56, pp. 241-74, Feb 23 2004.

[10] R. N. Gursoy and S. Benita, "Self-emulsifying drug delivery systems (SEDDS) for improved oral delivery of lipophilic drugs," *Biomed Pharmacother*, vol. 58, pp. 173-82, Apr 2004.

[11] A. Balk, T. Widmer, J. Wiest, H. Bruhn, J. C. Rybak, P. Matthes, *et al.*, "Ionic liquid versus prodrug strategy to address formulation challenges," *Pharm Res*, vol. 32, pp. 2154-67, Jun 2015.

[12] J. L. Shamshina, P. S. Barber, and R. D. Rogers, "Ionic liquids in drug delivery," *Expert Opin Drug Deliv*, vol. 10, pp. 1367-81, Oct 2013.

[13] I. M. Marrucho, L. C. Branco, and L. P. Rebelo, "Ionic liquids in pharmaceutical applications," *Annu Rev Chem Biomol Eng*, vol. 5, pp. 527-46, 2014.

[14] C. P. Frizzo, I. M. Gindri, A. Z. Tier, and L. Buriol, "Pharmaceutical Salts: Solids to Liquids by Using Ionic Liquid Design," K. Jun-ichi, Ed., ed: InTech, 2013, pp. 557-579.

[15] R. Ferraz, L. C. Branco, C. Prudencio, J. P. Noronha, and Z. Petrovski, "Ionic liquids as active pharmaceutical ingredients," *ChemMedChem*, vol. 6, pp. 975-85, Jun 6 2011.

[16] W. L. Hough, M. Smiglak, H. Rodriguez, R. P. Swatloski, S. K. Spear, D. T. Daly, *et al.*, "The third evolution of ionic liquids: active pharmaceutical ingredients," *New Journal of Chemistry*, vol. 31, pp. 1429-1436, 2007.

[17] K. Bica and R. D. Rogers, "Confused ionic liquid ions-a "liquification" and dosage strategy for pharmaceutically active salts," *Chem Commun (Camb)*, vol. 46, pp. 1215-7, Feb 28 2010.

[18] K. J. Fraser, E. I. Izgorodina, M. Forsyth, J. L. Scott, and D. R. MacFarlane, "Liquids intermediate between "molecular" and "ionic" liquids: Liquid Ion Pairs?," *Chem Commun*, pp. 3817-3819, 2007.

[19] N. Jain, G. Yang, S. G. Machatha, and S. H. Yalkowsky, "Estimation of the aqueous solubility of weak electrolytes," *Int J Pharm*, vol. 319, pp. 169-171, Aug 17 2006.

[20] A. M. Persson, A. Sokolowski, and C. Pettersson, "Correlation of in vitro dissolution rate and apparent solubility in buffered media using a miniaturized rotating disk equipment: Part I. Comparison with a traditional USP rotating disk apparatus," *Drug Discov Ther*, vol. 3, pp. 104-13, 2009.

[21] H. van de Waterbeemd, G. Camenisch, G. Folkers, J. R. Chretien, and O. A. Raevsky, "Estimation of blood-brain barrier crossing of drugs using molecular size and shape, and H-bonding descriptors," *J Drug Target,* vol. 6, pp. 151-65, 1998.

[22] C. Florindo, J. M. Araujo, F. Alves, C. Matos, R. Ferraz, C. Prudencio, *et al.*, "Evaluation of solubility and partition properties of ampicillin-based ionic liquids," *Int J Pharm,* vol. 456, pp. 553-9, Nov 18 2013.

[23] M. G. Freire, C. M. Neves, P. J. Carvalho, R. L. Gardas, A. M. Fernandes, I. M. Marrucho, *et al.*, "Mutual solubilities of water and hydrophobic ionic liquids," *J Phys Chem B,* vol. 111, pp. 13082-9, Nov 15 2007.

[24] R. J. Davey, S. L. Schroeder, and J. H. ter Horst, "Nucleation of organic crystals--a molecular perspective," *Angew Chem Int Ed Engl,* vol. 52, pp. 2166-79, Feb 18 2013.

[25] D. Kashchiev and G. M. van Rosmalen, "Review: Nucleation in solutions revisited," *Crystal Research and Technology,* vol. 38, pp. 555-574, 2003.

[26] G. Zografi, "States of Water Associated with Solids," *Drug Development and Industrial Pharmacy,* vol. 14, pp. 1905-1926, 1988.

[27] C. Ahlneck and G. Zografi, "The Molecular-Basis of Moisture Effects on the Physical and Chemical-Stability of Drugs in the Solid-State," *International Journal of Pharmaceutics,* vol. 62, pp. 87-95, Jul 31 1990.

[28] F. N. Kelley and F. Bueche, "Viscosity and glass temperature relations for polymer-diluent systems," *Journal of Polymer Science,* vol. 50, pp. 549-556, 1961.

[29] B. Hancock and G. Zografi, "The Relationship Between the Glass Transition Temperature and the Water Content of Amorphous Pharmaceutical Solids," *Pharmaceutical Research,* vol. 11, pp. 471-477, 1994/04/01 1994.

[30] K. Amann-Winkel, C. Gainaru, P. H. Handle, M. Seidl, H. Nelson, R. Bohmer, *et al.*, "Water's second glass transition," *Proc Natl Acad Sci U S A,* vol. 110, pp. 17720-5, Oct 29 2013.

[31] Y. Cao, Y. Chen, X. Sun, Z. Zhang, and T. Mu, "Water sorption in ionic liquids: kinetics, mechanisms and hydrophilicity," *Phys Chem Chem Phys,* vol. 14, pp. 12252-62, Sep 21 2012.

[32] S. Cuadrado-Prado, M. Dominguez-Perez, E. Rilo, S. Garcia-Garabal, L. Segade, C. Franjo, *et al.*, "Experimental measurement of the hygroscopic grade on eight imidazolium based ionic liquids," *Fluid Phase Equilibria,* vol. 278, pp. 36-40, Apr 15 2009.

[33] F. D. Francesco, N. Calisi, M. Creatini, B. Melai, P. Salvo, and C. Chiappe, "Water sorption by anhydrous ionic liquids," *Green Chemistry,* vol. 13, pp. 1712-1717, 2011.

[34] Y. Chen, Y. Cao, X. Lu, C. Zhao, C. Yan, and T. Mu, "Water sorption in protic ionic liquids: correlation between hygroscopicity and polarity," *New Journal of Chemistry,* vol. 37, p. 1959, 2013.

[35] M. Klahn, C. Stuber, A. Seduraman, and P. Wu, "What determines the miscibility of ionic liquids with water? Identification of the underlying factors to enable a straightforward prediction," *J Phys Chem B,* vol. 114, pp. 2856-68, Mar 4 2010.

[36] A. W. Newman, S. M. Reutzel-Edens, and G. Zografi, "Characterization of the "hygroscopic" properties of active pharmaceutical ingredients," *J Pharm Sci,* vol. 97, pp. 1047-59, Mar 2008.

[37] A. Balk, U. Holzgrabe, and L. Meinel, "'Pro et contra' Ionic liquid drugs - challenges and opportunities for pharmaceutical translation," *Eur J Pharm Biopharm,* 2015.

[38] V. Kumar and S. V. Malhotra, "Study on the potential anti-cancer activity of phosphonium and ammonium-based ionic liquids," *Bioorg Med Chem Lett,* vol. 19, pp. 4643-6, Aug 15 2009.

[39] R. F. M. Frade, A. A. Rosatella, C. S. Marques, L. C. Branco, P. S. Kulkarni, N. M. M. Mateus, *et al.*, "Toxicological evaluation on human colon carcinoma cell line (CaCo-2) of ionic liquids based on imidazolium, guanidinium, ammonium, phosphonium, pyridinium and pyrrolidinium cations," *Green Chemistry,* vol. 11, pp. 1660-1665, 2009.

[40] K. D. Weaver, H. J. Kim, J. Z. Sun, D. R. MacFarlane, and G. D. Elliott, "Cyto-toxicity and biocompatibility of a family of choline phosphate ionic liquids designed for pharmaceutical applications," *Green Chemistry*, vol. 12, pp. 507-513, 2010.

[41] R. A. Kumar, N. Papaiconomou, J. M. Lee, J. Salminen, D. S. Clark, and J. M. Prausnitz, "In vitro cytotoxicities of ionic liquids: effect of cation rings, functional groups, and anions," *Environ Toxicol*, vol. 24, pp. 388-95, Aug 2009.

[42] E. Russo, R. Gitto, R. Citraro, A. Chimirri, and G. De Sarro, "New AMPA antagonists in epilepsy," *Expert Opin Investig Drugs*, vol. 21, pp. 1371-89, Sep 2012.

[43] D. Orain, S. Ofner, M. Koller, D. A. Carcache, W. Froestl, H. Allgeier, *et al.*, "6-Amino quinazolinedione sulfonamides as orally active competitive AMPA receptor antagonists," *Bioorg Med Chem Lett*, vol. 22, pp. 996-9, Jan 15 2012.

[44] M. Koller, K. Lingenhoehl, M. Schmutz, I. T. Vranesic, J. Kallen, Y. P. Auberson, *et al.*, "Quinazolinedione sulfonamides: a novel class of competitive AMPA receptor antagonists with oral activity," *Bioorg Med Chem Lett*, vol. 21, pp. 3358-61, Jun 1 2011.

[45] M. Umeno and S. Takita, "Preparation process of quaternary phosphonium hydroxide," US Patent Number 4761493, 1988.

[46] Y. Zhang, S. Zhang, X. Lu, Q. Zhou, W. Fan, and X. Zhang, "Dual amino-functionalised phosphonium ionic liquids for CO2 capture," *Chemistry*, vol. 15, pp. 3003-11, 2009.

[47] T. Gravestock, K. Box, J. Comer, E. Frake, S. Judge, and R. Ruiz, "The “GI dissolution” method: a low volume, in vitro apparatus for assessing the dissolution/precipitation behaviour of an active pharmaceutical ingredient under biorelevant conditions," *Analytical Methods*, vol. 3, p. 560, 2011.

[48] M. Stuart and K. Box, "Chasing equilibrium: measuring the intrinsic solubility of weak acids and bases," *Anal Chem*, vol. 77, pp. 983-90, Feb 15 2005.

[49] Y. L. Hsieh, G. A. Ilevbare, B. Van Eerdenbrugh, K. J. Box, M. V. Sanchez-Felix, and L. S. Taylor, "pH-Induced precipitation behavior of weakly basic compounds: determination of extent and duration of supersaturation using potentiometric titration and correlation to solid state properties," *Pharm Res*, vol. 29, pp. 2738-53, Oct 2012.

Chapter 4: Transformation of acidic poorly water soluble drugs into ionic liquids

Anja Balk[1], Johannes Wiest[1], Toni Widmer[1,2],
Bruno Galli[2], Ulrike Holzgrabe[1], Lorenz Meinel[1,*]

[1]Institute for Pharmacy and Food Chemistry, University of Würzburg, Am Hubland, University of Würzburg, DE-97074 Würzburg, Germany, [2]Novartis Pharma AG, Lichtstraße 35, CH-4002 Basel, Switzerland

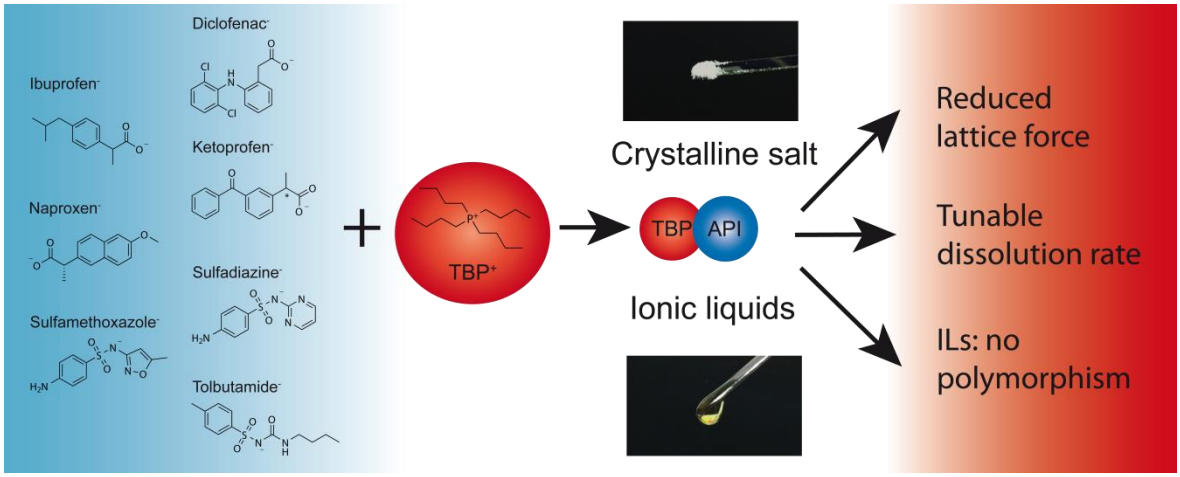

This chapter was originally published in European journal of pharmaceutics and biopharmaceutics, vol. 94, pp. 73-82, 2015; DOI: 10.1016/j.ejpb.2015.04.034, with permission of Elsevier, License number 3638781483368.

Introduction

Oral dosage forms of active pharmaceutical ingredients (API) are a preferred image for drug administration. Oral delivery typically requires (nearly) complete dissolution of the API at its absorption site and prevention of precipitation during gastrointestinal transit until complete absorption, a process typically lasting about four hours [1]. This poses specific challenges, especially for poorly water soluble drugs with low solubility (with solubility being defined as the molar concentration of API in ionized and unionized form in equilibrium state or not) driving poor bioavailability and often unacceptable pharmacokinetic variability [1]. Pharmaceutical strategies addressing these challenges without modification of the chemical structure of the API include particle size reduction, cocrystal formation, polymorph selection, complexation, salt formation, solubilization or presentation in amorphous form, e.g. as molecular dispersions in polymer carriers thereby reducing the interaction between the API molecules [2]. These dosage forms may result in improved dissolution rates but are typically challenged by solution stability with potential precipitation before the API is adequately absorbed. A simple concept combining salt formation and a reduction of the interaction between the API molecules is the preparation of an ionic liquid (IL). The approach has been demonstrated to stabilize dissolved APIs in supersaturated states for several hours following dissolution from an amorphous, solid state [3].

ILs are defined as organic salts with melting points below 100 °C [4]. Those ILs which are liquid at ambient temperature and pressure are referred to as room temperature ILs (RT-ILs) [5]. During the last years the application of ILs was extended from solvents in ('green') chemistry and catalysts for synthesis to pharmaceutical application with the ultimate goal to improve API dissolution, solubility and bioavailability and to prevent polymorphism [4],[6-14].

Tetrabutylphosphonium (TBP) has already been used for the preparation of an IL with Salicylic acid and Ibuprofen [11, 13]. However no detailed solubility data were provided. Another study reported a TBP IL of an anti-migraine drug and determined a faster dissolution and supersaturation in solution leading to improved transport kinetics *in vitro* in comparison to the free acid and the API's potassium salt [3].

In this study we detailed the potential of transforming 7 commonly used acidic APIs into TBP salts and compared them to their respective sodium salts. These TBP salts were characterized with ^{1}H Nuclear magnetic resonance (NMR) and Infrared spectroscopy (IR), X-ray powder diffraction (XRPD) and Differential scanning calorimetry (DSC). Hygroscopicity was assessed by dynamic vapor sorption (DVS). Dissolution rate, saturation concentrations and 24 hours solubility profiles were determined photometrically.

Results

Salt metathesis and physico-chemical characteristics of TBP salts

TBP salts of drugs with one carboxylic acid group, in the case of Diclofenac, Ibuprofen, Ketoprofen, and Naproxen, and with one sulfonamide group, as in Sulfadiazine, Sulfamethoxazole, and Tolbutamide, were prepared from the corresponding free acids (**Figure 1**). TPB salts of Ibuprofen, Ketoprofen, Naproxen and Sulfamethoxazole were clear, slightly yellow viscous liquids at room temperature and RT-ILs, whereas TBP salts of Diclofenac, Sulfadiazine and Tolbutamide were slightly yellow solids.

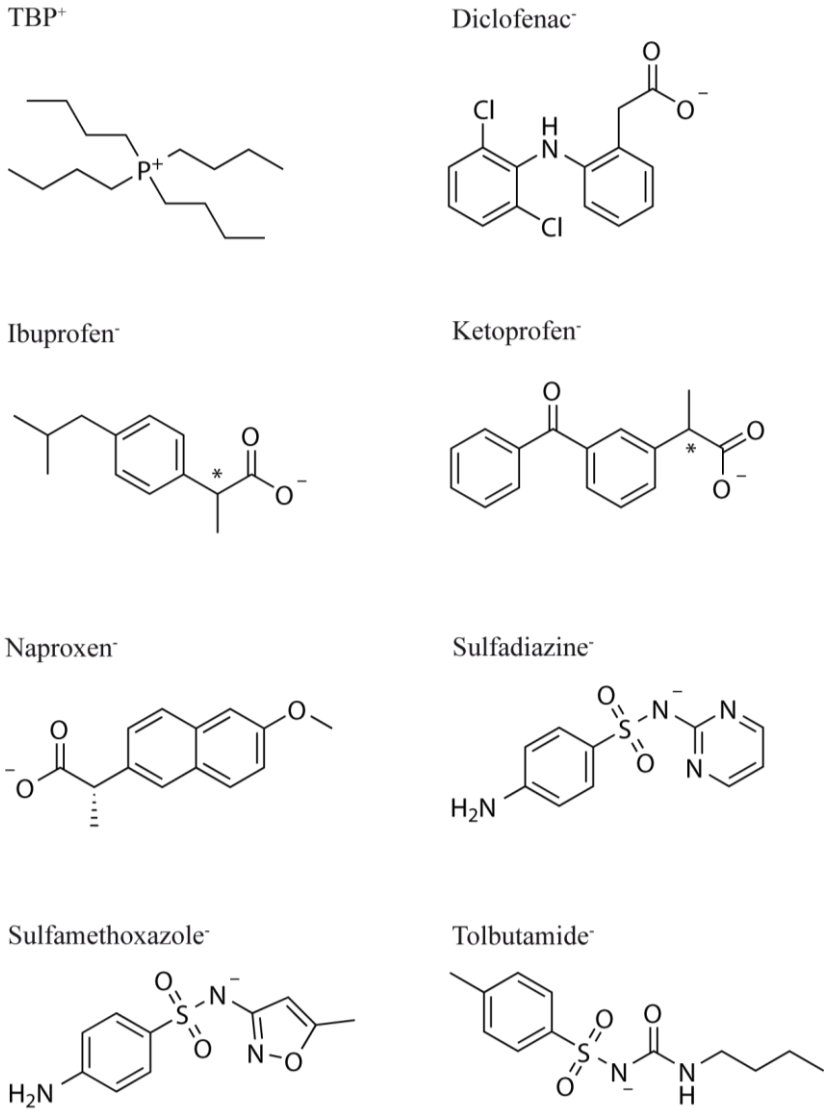

Figure 1: Structures of the counterion tetrabutylphosphonium (TBP+) and the ionized APIs Diclofenac, Ibuprofen, Ketoprofen, Naproxen, Sulfadiazine, Sulfamethoxazole and Tolbutamide.

Moisture content of TBP salts was determined by Karl Fischer Coulometer directly following production and found to be 0.5% for Ibuprofen (RT-IL), 0.2% for Ketoprofen (RT-IL) and Naproxen (RT-IL), and less than 0.2% for all other TBP salts (data not shown).

The free acids and their corresponding TBP salts were analyzed by ^{1}H-NMR, ^{13}C-NMR and IR spectroscopy (**Supplementary Figure 1**). Since the salt formation is characterized by a loss of the acidic proton, the corresponding ^{1}H NMR signal at 10 - 12.5 ppm disappears upon IL formation (all NMR spectra are provided as **Supplementary Information 1**). The proton signals for TBP were recorded at 0.9 - 2.3 ppm and included a signal for the 12 protons of its terminal methyl groups at δ = 0.92 ppm (t, ^{3}J = 7.1), 16 protons recorded for its intermediate ethylene groups at δ = 1.55 - 1.30 ppm and 8 for the methylene groups next to the phosphonium δ = 2.30 – 2.10 ppm. The integration of these signals for TBP and comparison with the integrals of the signals recorded for the respective APIs confirmed a 1:1 stoichiometry for all ILs tested. Apart from signals from the acid and the counterion no further signals were observed for any of the TBP salts, indicating the good stability of the API during salt formation.

Signals for Diclofenac differed slightly from the generally observed pattern recorded for the other APIs: Diclofenac signals at δ = 12.7 ppm and 7.2 ppm represented the proton of the free acid and of the amine proton, respectively (**Supplementary Information 1)**. Whereas the signal of the carboxylic proton disappeared upon TBP salt formation as expected, the amine signal shifted to 10.9 ppm in the TBP salt, suggesting the formation of an intramolecular H-bond between the amine proton and the (deprotonated) carboxyl moiety.

The ionic nature of the TBP salts was further supported by IR spectroscopy (**Supplementary Figure 1**). For APIs with a carboxylic function the typical O-H and C=O stretching vibrations were observed at 2885 cm^{-1} and 1690 cm^{-1} (Diclofenac), 2954 cm^{-1} and 1709 cm^{-1} (Ibuprofen), 2938 cm^{-1} and 1694 cm^{-1} (Ketoprofen), and 3162 cm^{-1} and 1726 cm^{-1} (Naproxen)[15]. Following deprotonation, symmetric and anti-symmetric stretching vibration for carboxylic anions were observed at 1575 cm^{-1} and 1346 cm^{-1} (Diclofenac TBP), 1580 cm^{-1} and 1376 cm^{-1} (Ibuprofen TBP), 1592 cm^{-1} and 1372 cm^{-1} (Ketoprofen TBP), and 1588 cm^{-1} and 1369 cm^{-1} (Naproxen TBP) along with missing O-H stretching vibration[15]. The broad bands between 3330 cm^{-1} and 3290 cm^{-1} for Ibuprofen TBP, Naproxen TBP, Ketoprofen TBP were assigned to residual water[15]. For the sulfonamide groups of Sulfadiazine, Sulfamethoxazole and Tolbutamide, deprotonation was detected by a shift of the two typical sulfuric bands from 1324 cm^{-1} and 1149 cm^{-1} to 1235 cm^{-1} and 1122 cm^{-1} (Sulfadiazine), from 1303 cm^{-1} and 1142 cm^{-1} to 1232 cm^{-1} and 1123 cm^{-1} (Sulfamethoxazole) from 1316 cm^{-1} and 1177 cm^{-1} to 1243 cm^{-1} and 1124 cm^{-1}, respectively

(Tolbutamide; **Supplementary Figure 1**). From NMR and IR data it can be stated that all APIs were ionized and formed TBP salts.

Sodium salts of the APIs were selected for comparison with the TBP salts. Sodium salts of Ketoprofen, Sulfamethoxazole and Tolbutamide were prepared in house and quality of the resulting white crystalline powders was confirmed by elementary analysis. Sodium salts of Diclofenac, Ibuprofen, Naproxen and Sulfadiazine were purchased. For all sodium salts deprotonation was assessed by ^{1}H NMR and IR. Based on the elementary analysis, NMR and IR data sodium salt formation could be confirmed.

Melting points and glass transition temperatures were determined by DSC (**Figure 2**). For all TBP salts the melting point and glass transition temperature, respectively, were lower than the melting point of the corresponding free acid and sodium salt. All liquid TBP salts (Ibuprofen RT-IL, Ketoprofen RT-IL, Naproxen RT-IL and Sulfamethoxazole RT-IL) had glass transition temperatures below 0 °C. The melting point of the solid and crystalline (*vide infra*) Tolbutamide TBP salt was 56 °C. TBP salts of Diclofenac and Sulfadiazine TBP salts were crystalline (*vide infra*) with melting points exceeding 100 °C; hence, they did not fulfill the definition of an ionic liquid. All melting points of all sodium salts were exceeding 100 °C and exceeded those of the corresponding free acids, with one exception only: for Tolbutamide the melting points of the free acid and the sodium salt were almost identical (**Figure 2**).

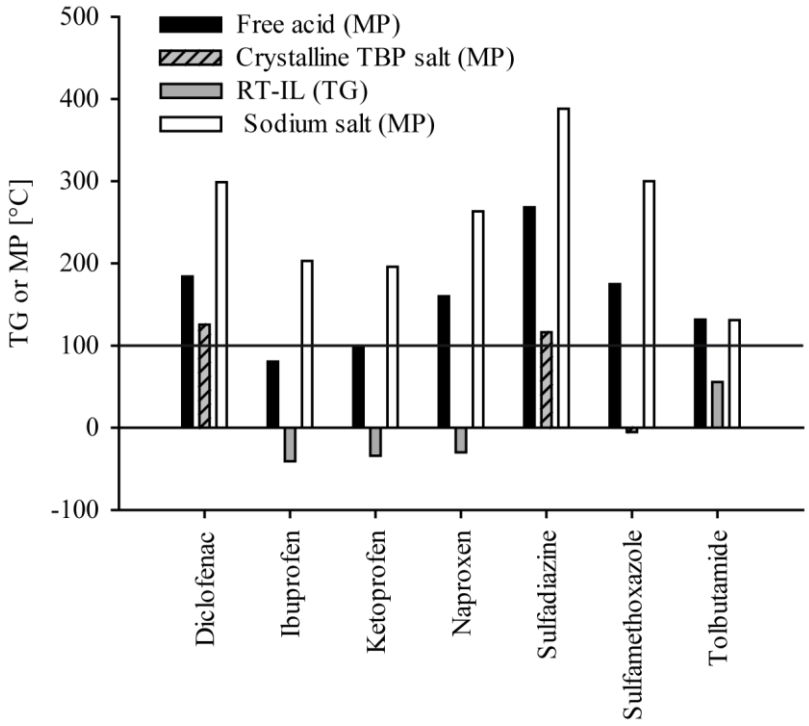

Figure 2: Melting points (MP) and glass transition temperatures (TG) of free acids, TBP salts and sodium salts.

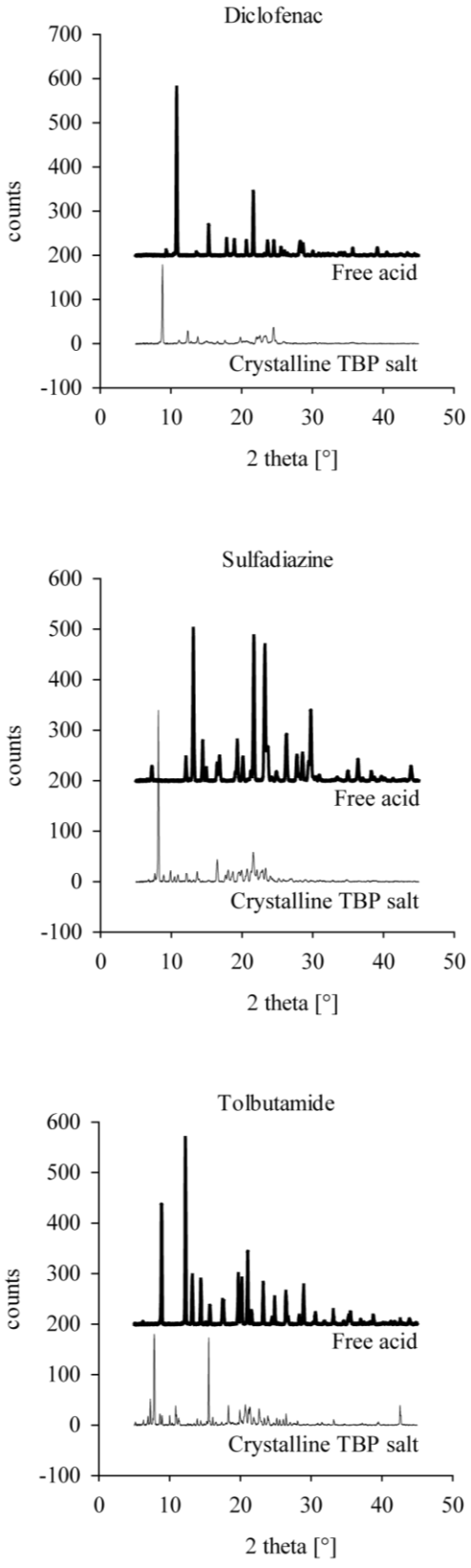

Figure 3: XRPD diffraction patterns of Diclofenac, Sulfadiazine, Tolbutamide and corresponding crystalline TBP salts.

The diffraction pattern of the free acids and the solid TBP salts (Diclofenac, Sulfadiazine, Tolbutamide) was collected by XRPD. All solid substances were crystalline. Different diffraction patterns were observed for the TBP salts as compared to the corresponding free acids, reflecting changes in crystal structure as a result of salt formation (**Figure 3**).

The free acids, the corresponding sodium salts and TBP salts were exposed to different relative humidities (r.H.) in order to check the extent of hygroscopicity (**Supplementary Figure 2, 3**). The mass changes are reported for 80% r.H. (**Table 1**). The free acids of Sulfamethoxazole (2.5%), Naproxen (0.9%) and Diclofenac (0.8%) had the highest changes in mass, whereas all others had changes less than 0.05%. The water sorption was higher for all TBP salts as compared to their corresponding free acids, with Ibuprofen RT-IL, Ketoprofen RT-IL and Naproxen RT-IL having water sorptions ranging from 17.3% to 27.4%, Diclofenac TBP salt, Sulfamethoxazole RT-IL and Tolbutamide TBP salt ranging from 10.4% to 14.5%, and Sulfadiazine TBP salt having 2.7%. For sodium salts of the carboxylic acids Diclofenac, Ibuprofen, Ketoprofen and Naproxen water sorption ranged from 15.9% to 28.4% while for sodium salts of sulfonamides Sulfadiazine, Sulfamethoxazole and Tolbutamide water sorption was below 1.7%. Surface activity of TBPOH in water was determined and no micelle formation was detected (data not shown).

Water sorption at 80% r.H. [%]			
API	Free acids	TBP salts	Sodium salts
Diclofenac	0.84	14.48	26.27
Ibuprofen	0.02	17.33	15.89
Ketoprofen	0.04	18.42	35.32
Naproxen	0.91	27.39	28.39
Sulfadiazine	0.03	2.74	0.85
Sulfamethoxazole	2.48	10.50	0.31
Tolbutamide	0.05	10.42	1.69

Table 1: Change in mass in % due to water sorption at 80% r.H. of the acidic APIs and the corresponding TBP and sodium salts.

Dissolution rate and 24 hour solubility

The dissolution rate was determined for all free acids, their corresponding TBP salts and the sodium salts. All TBP salts had significantly faster dissolution rates than their corresponding free acids (**Figure 4**). Faster kinetics were particularly observed for the *liquid* TBP salts, all having dissolution rates > 0.2 mmol/(min*cm^2). Ibuprofen RT-IL had a 900-fold, Ketoprofen RT-IL a 250-fold, Naproxen RT-IL a 1000-fold, and Sulfamethoxazole RT-IL 20-fold increased dissolution rate as compared to their free acid. The dissolution rates of the *solid* TBP salts (Diclofenac, Sulfadiazine, Tolbutamide) were lower as compared to *liquid* TBP salts with values less than 0.12 mmol/(min*cm^2). The dissolution rates of the solid TBP salts increased for Diclofenac 80-fold, Sulfadiazine 200-fold, and Tolbutamide 40-fold as compared to their free acids, respectively (**Figure 4**). Interestingly, the differences in dissolution kinetics were generally less pronounced when comparing the TBP salts with the respective sodium salts. The dissolution rate of the TBP salt of Diclofenac was 4-fold, Ibuprofen 14-fold, Ketoprofen 6-fold, and Naproxen 3-fold faster in comparison with the sodium salt. For sulfonamides a reverse pattern was observed, with the sodium salts having faster dissolution kinetics as compared to the TBP salts. Sulfadiazine sodium had a dissolution rate being 4-fold faster, Sulfamethoxazole sodium 2-fold faster, and Tolbutamide sodium 6-fold faster as than the TBP salt (**Figure 4**).

24 hour solubility profiles were recorded for comparison of the free acids (**Figure 5A, B**) and the TBP salts (**Figure 5 C, D**). For these experiments, conditions were set such that each salt could have yielded a theoretical concentration of up to 5 mM when completely dissolved (**Figure 5 A – D**). Plateau concentrations were achieved within 2 -10 hours for all carboxylic acids (**Figure 5A**) and all TBP salts of the carboxylic acids rapidly plateaued within 2 hours (**Figure 5C**). More heterogeneous results were obtained for the sulfonamide acids. In analogy to the carboxylic acids, several hours were required for Tolbutamide to reach its solubility plateau while both Sulfadiazine and Sulfamethoxazole leveled off within 2 hours (**Figure 5B**). On the contrary, the dissolution

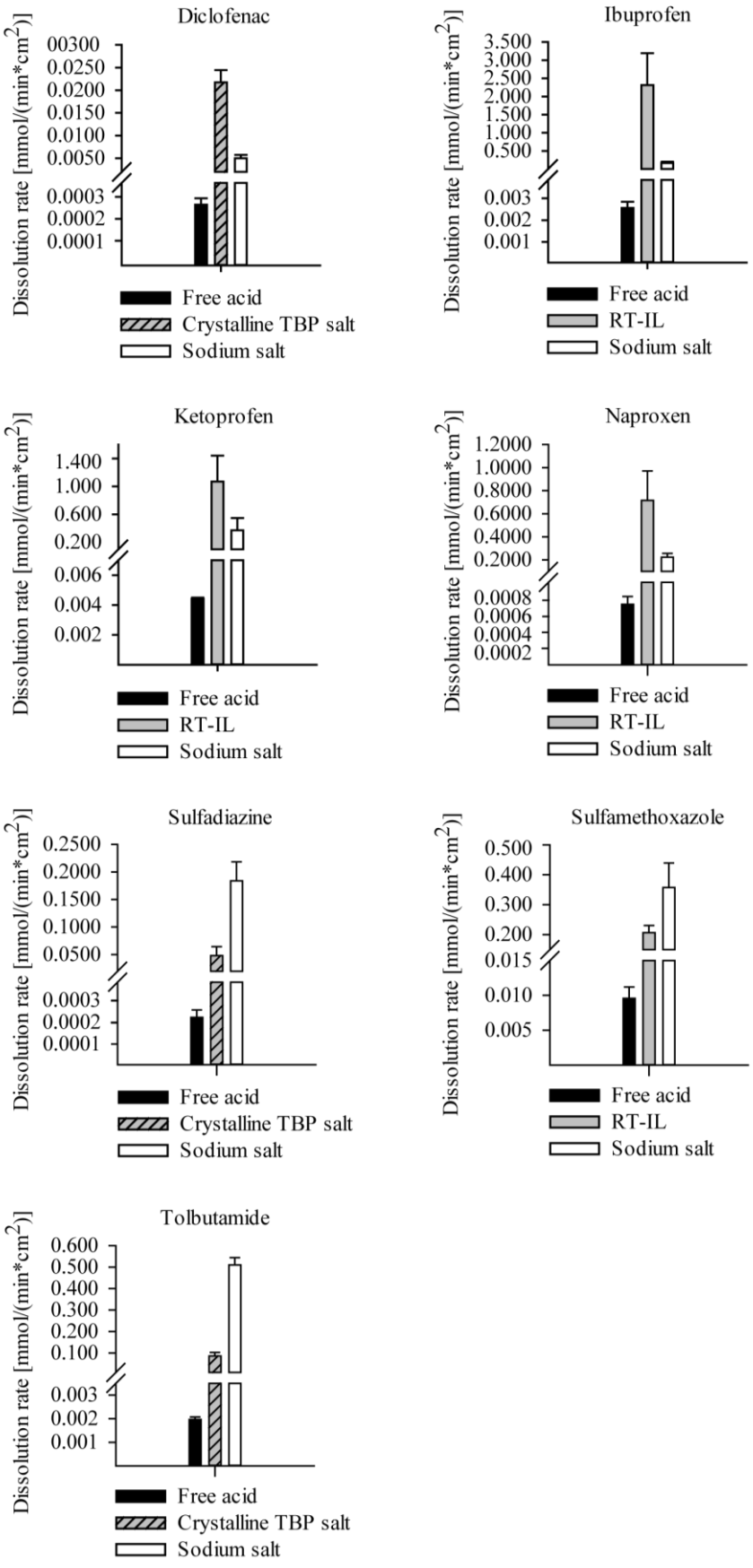

Figure 4: Dissolution rate in mmol/(min*cm^2) of acidic API, corresponding TBP and sodium salts.

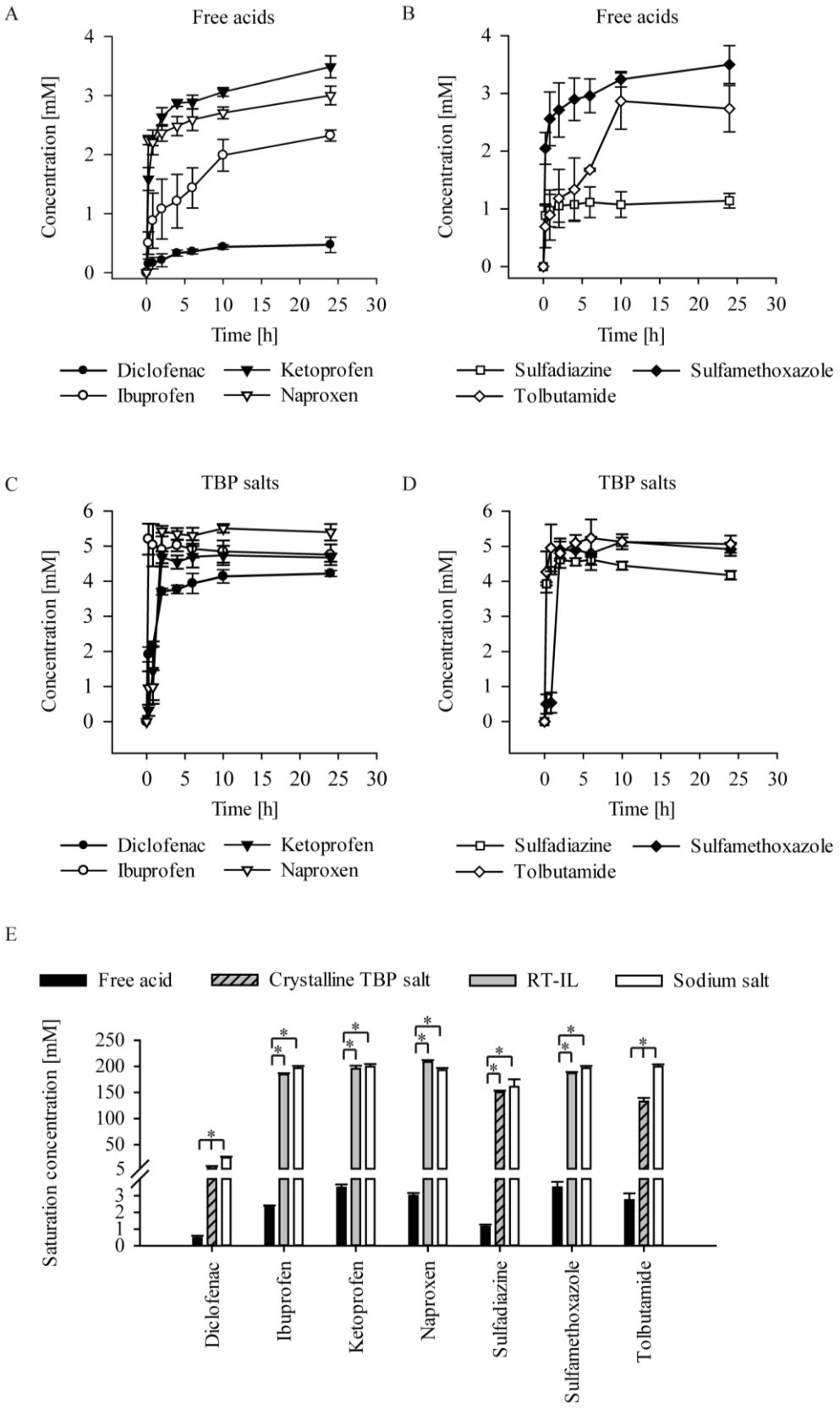

Figure 5: Concentration in mM versus time in hours profiles of acidic APIs and corresponding TBP salts over 24 hours and saturation concentration in mM for acidic APIs, corresponding TBP and sodium salts after 24 hours.

kinetics were much faster for all TBP salts of the sulfonamides, plateauing in less than 2 hours (**Figure 5D**). No recrystallization or decrease in concentration was observed for the TBP salts within 24 hours. For all salts for which a solubility exceeding 5 mM was observed, a second experiment was run. For this, conditions were set such that these salts could have yielded a theoretical concentration of up to 200 mM when completely dissolved (**Figure 5E**). In this second experiment, significantly higher maximum concentrations (**Figure 5E**) were reached within 24 hours for all TBP salts as compared to their free acids, with Ibuprofen (≥ 80-fold), Ketoprofen (≥ 60-fold), Naproxen (≥ 70-fold;), Sulfadiazine (130-fold), Sulfamethoxazole (≥ 50 time), Tolbutamide (30-fold) and Diclofenac (20-fold). Some salts displayed a solubility exceeding 200 mM and were reported as '≥' in the brackets for the fact that these were completely dissolved at the maximal possible concentration of 200 mM. The salts being completely dissolved included the TBP and sodium salts of Ibuprofen, Ketoprofen, Naproxen and Sulfamethoxazole as well as the sodium salt of Tolbutamide. Experiments aiming for higher theoretical concentrations than 200 mM were jeopardized by experimental constraints, as aspiration of solid and suspended salt could not be avoided. The TBP and sodium salts of Sulfadiazine were incompletely dissolved and the saturation concentrations were not significantly different. For the Diclofenac sodium salt the saturation concentration was 3-fold higher than for the TBP salt and the undissolved substance observed for Diclofenac sodium was crystalline whereas the TBP salt formed two liquid phases. Besides for the TBP salt of Diclofenac, a phase separation into two liquid phases was observed for the TBP salt of Tolbutamide. For both salts an emulsion was readily formed with gentle shaking.

Discussion

Biopharmaceutically acceptable absorption of orally administered APIs require both, sufficient aqueous solubility and permeability through gastrointestinal mucosa [1]. BCS Class II (BCS 2) compounds are defined by a low solubility and high permeability. Therefore, formulation strategies for compounds of this class target a solubility improvement in an effort to optimize their biopharmaceutical profiles [1, 16, 17]. Consequently, we selected the BCS 2 APIs Diclofenac, Ibuprofen, Ketoprofen, Naproxen, Sulfadiazine, Sulfamethoxazole and Tolbutamide for this study [18-22]. Frequently, solubility improvement of ionizable APIs is subject to salt screening, with sodium being the most commonly used counterion for acidic APIs [1] and therefore, sodium salts were used as a control group. TBP was chosen as a counterion, as in previous studies IL formation with APIs was reported [3, 11, 13] and a quite benign cytotoxicity profile as assessed in three cell lines with IC_{50} values ranging from 250 to 1000 µM [3].

Previous studies detailed the manufacturing constraints for TBP salts, which are limited to APIs with a stability at pH 7-9 for at least one hour [3]. Salt formation is particularly effective for free

acid–counterion pairs with pK_a differences of at least 3 units, in order to assure a complete proton transfer [23]. Therefore, TBPOH- a strong base - is a particularly suitable counterion for salt formation of a broad range of APIs. For the tested APIs, the process of TBP salt formation did not result in API degradation or of the counterion (as detected by ^{1}H-NMR). The ionic state of the resulting salts / liquid salts was confirmed by ^{1}H-NMR and IR spectroscopy (**Supplementary Figure 1**). The diffractograms of the TBP salts were different from the corresponding free acids (**Figure 3**) as were melting points and glass transition temperatures, respectively (**Figure 2**). TBP salts of Ibuprofen, Ketoprofen, Naproxen and Sulfamethoxazole were room temperature ILs (RT-ILs) whereas the melting points of the TBP salts of Diclofenac and Sulfadiazine exceeded 100 °C (hence no ILs), indicating that the ability to form RT-IL is as dependent on the API as it is on the counterion. The TBP salt of Tolbutamide was an ionic liquid (no RT-IL; melting point > 25 °C) even though crystalline.

One of the reported advantages of RT-ILs is to circumvent polymorphism challenges, including dynamic changes of solubility, stability and hygroscopicity during storage [14, 24], as previously reported for the Ibuprofen sodium salt [25] and for the Naproxen sodium salt (pseudo-polymorphism) [26]. None of the RT-ILs precipitated throughout 9 months (data not shown). However, more research is required regarding bulk stability with regard to precipitation and to the feasibility for processing these RT-ILs challenged by their viscosity, compressibility, or thermal stability or hygroscopicity.

According to the criteria of the European Pharmacopoeia (EP), substances are classified ‘slightly hygroscopic’ if water sorption after 24 hours at 80% r.H. and 25 °C ranges between 0.2% and 2%, ‘hygroscopic’ for 2-15% and ‘very hygroscopic’ if exceeding 15% [27]. Transforming the APIs into TBP salts generally increased their hygroscopicity as indicated for Diclofenac (slightly hygroscopic → hygroscopic), Naproxen (slightly hygroscopic → hygroscopic), Ibuprofen (not hygroscopic → hygroscopic), Ketoprofen (not hygroscopic → hygroscopic), Sulfadiazine (not hygroscopic → hygroscopic) and Tolbutamide (not hygroscopic → hygroscopic; exception Sulfamethoxazole; hygroscopic → hygroscopic)). RT-ILs of Ibuprofen, Ketoprofen and Naproxen were very hygroscopic. This pattern followed the general trend that amorphous solids or liquids adsorb water within their bulk and their surfaces, in contrast to crystalline forms in which water adsorption is restricted to the crystal surfaces [28]. However, crystalline sodium salts of carboxylic acids displayed high values of water sorption, particularly for Diclofenac and Ketoprofen sodium salts which were even more hygroscopic than the TBP salts and transformed into tetrahydrates and Ibuprofen sodium into a dihydrate as reported before [29-31]. Sulfonamide sodium salts were only slightly hygroscopic and did not form hydrates. These hydrates or pseudopolymorphs require

particular attentions, as these may display quite different physico-chemical properties as compared to the anhydrous forms.

Water sorption may be a concern limiting dosing accuracy, the chemical stability, powder flow, compatibility and general processability [32]. Therefore, the benefit of the improved dissolution rate for the sodium salts and RT-ILs is at least in part at the expense of increased water sorption and high viscosity, challenging straightforward manufacturing. Current studies aim at tailoring the hygroscopicity of the counterion and thereby the hygroscopicity of the counterion / API salt. These studies need to provide a library of homologous counterions as well as new counterion structures to balance low hygroscopicity and long stability against high dissolution rates.

One main motivation of salification (including IL formation) is increasing the dissolution rate, which is in most cases sufficiently described by a simple diffusion layer model following Fick's laws, consisting of the solid API surface, an adjacent so called aqueous boundary layer (ABL) and the bulk solution [33]. It is hard to predict to which extent the choice of the counterion will impact the dissolution rate (i.e. if a small, hydrophilic or large, lipophilic is more effective in boosting dissolution). The dissolution rate depends on the diffusion rate of the molecules from the thin ABL into the bulk of the dissolution medium in all cases in which the diffusion rate is slower than the dissolution rate from the solid phase. Based on Fick's laws, the dissolution rate is directly proportional to the concentration gradient between the thin layer at the API surface and the concentration in the bulk (sink conditions may be assumed in most relevant conditions) [1, 34], thereby linking the concentration at the solid API / ABL interface to the dissolution rate. Within this layer the process of dissolution involves (i) breaking of the interactions of molecules from the salt, (ii) breaking the interaction of the solute molecules, (iii) the separation of the solvent molecules (cavitation), and (iv) the formation of interactions between the solvent and the solute molecules. The interaction among the solute molecules in solid state correlates with the crystallinity of the solid substance. For all tested APIs, the bulky TBP counterion with its voluminous alkyl side chains reduced the melting points as compared to the free acids and the sodium salts, suggesting a reduced packing efficiency and lattice enthalpy, respectively [9, 35]. In addition to these basic qualitative and thermodynamic considerations, the frequency of API detachment from the solid state has been correlated to the activation energy for detachment, which can be indirectly derived from relating the activation energy for attachment of dissolved API to the solid form and the work required for the formation of the drug-drug cluster under isobaric and isothermal conditions. Thereby, the frequency of API detachment (a kinetic parameter) is linked to a thermodynamic criterion, the work for cluster formation [36]. The work for cluster formation is linked to the free enthalpy of the solid, which in return may be (crudely) assessed in many cases by the melting point. Consequently, these qualitative considerations link the reduced melting point of

the TBP salts as compared to the free acids to the increased rate of detachment, hence increased dissolution rate. As pointed out before, another driving force is the interaction of solute and solvent molecules within the ABL, as described in aqueous solutions by the hydration enthalpy and entropy. The presentation of the APIs in ionized form as TBP and sodium salts, respectively, builds off the increased potential for hydrogen bonding and hydration (**Supplementary Figure 1**), potentially driving higher dissolution rates than for the free acids (**Figure 4**). For imidazolium ILs, increasing anion-cation interaction correlated with increased interaction with water. Furthermore it was found, that the interaction with water was reduced with increasing delocalization of the charge and size of the counterion, e.g. by larger alkyl chains [37]. In analogy to these studies one may assume that the TBP with its lipophilic alky chains and its more diffuse charge as compared to the sodium ion might result in a reduced interaction with water for TBP as compared to the sodium cation. These considerations provide a qualitative insight why the prediction of the dissolution rate is challenging. On the one hand, the depression of the melting point by increasing the counterion size favors dissolution while on the other hand the reduced interaction of such counterions with water due to the increased lipophilicity lower the dissolution rate and as it has been found before [38]. Experiments conducted as outlined in this manuscript are essential to assess to which extent the use of a small counterion (such as the sodium cation particularly driving the dissolution rate by effective interaction with water molecules) or a larger lipophilic one (such as the TBP, driving the dissolution rate through a reduction of the interactions within the solid state) favors the dissolution rate for a given API. The difficulty to predict the outcome from these studies is readily demonstrated by the faster dissolution rates of the TBP salts as compared to the sodium salts of the carboxylic acids Diclofenac, Ibuprofen, Ketoprofen and Naproxen in contrast to the sulfonamides Sulfadiazine, Sulfamethoxazole and Tolbutamide for which the opposite was qualitatively observed (**Figure 4**) and in contrast to another sulfonamide [3]. This data indicated that the increase of the dissolution rate is not necessarily a function of the respective acidic functional group (carboxylic acid *versus* sulfonamide). TBP did not form micelles and, therefore, it is unlikely that the dissolution rate was a result of a solubilization effect by TBP. Therefore the explanation for the observed difference in dissolution rate of sodium and TBP salts is the difference of melting points and the lipophilicity of the counterion. The data provided here along with previous results suggested that the extent to which the two factors impact the dissolution rate is mainly driven by the API and cannot be limited to a functional group which is deprotonated. Therefore, each API requires a precisely tailored counterion to optimize the dissolution rate.

The differences in the dissolution rates measured with rapid stirring (**Figure 4**) translated into substantially different release profiles (**Figure 5**) under shake flask conditions. However, the solubility for some TBP and sodium salts was in fact exceeding 200 mM, which was the maximum theoretical concentration possible for this experimental setting as any higher amount resulted in

inevitable aspiration of solid and suspended salt as we conducted the experiments. For these, the solubility is reported as ≥ 200 mM. However, the actual solubility may even exceed these values (**Figure 5E**).For the Diclofenac and Tolbutamide TBP salts a liquid-liquid phase separation (LLPS) was observed during the solubility determination. LLPS in the case of these TBP salts is likely linked to supersaturated aqueous API solutions in which crystal nucleation kinetics are rate limiting in comparison with the LLPS and as reported before [39-41]. Previous studies suggested that the solute rich phase may be applicable as a drug reservoir [42].

The approaches outlined here within for acidic APIs require enteric coated formulations for administration. This is as the solubility of a weakly acidic API depends on the degree of ionization and, therefore, on the pKa of the API and the pH of the surrounding medium. The API salts are considerably protonated at pH values < pka favoring the conversion into the free acid, hence recrystallization. Thus for an oral application both sodium and TBP salts should be presented in appropriate formulations avoiding exposure to the acidic gastric fluids after dissolution, resulting in recrystallization.

Conclusion

TBP salts were successfully prepared for several acidic APIs resulting in lower melting points and glass transition temperatures, respectively, with four liquids and three crystalline solid salts. The dissolution rates and solubilities were effectively impacted by forming ionic liquids, particularly when room temperature ionic liquids (RT-IL) were obtained. However, presenting the APIs as RT-ILs was at the price of increased hygroscopicity and future studies aim at controlling these features by alternative counterions.

The data reported here supported the fascinating potential of extended salt screening programs, including the synthesis of tailor-made counterions for optimal pharmaceutical outcome.

Materials and Methods

Materials

Potassium chloride (KCl) was purchased from VWR (Radnor, PA). Tetrabutylphosphonium hydroxide solution (40% in water v / v), hydrochloric acid 0.5 M, Sulfadiazine (minimum 99%), Naproxen (USP specification), Ibuprofen sodium salt, Naproxen sodium salt, Sulfadiazine sodium salt, Sulfamethoxazole were purchased from Sigma Aldrich (St. Louis, MO). Sodium chloride, sodium hydroxide, sodium hydrogen carbonate, sodium dihydrogen phosphate, disodium hydrogen phosphate, methanol, ethanol, Diclofenac, Ibuprofen, Ketoprofen, Tolbutamide and Diclofenac sodium salt, were of analytical grade. Quality of the free forms of the APIs was assured by ^{1}H

NMR. Hexadeuteriodimethyl sulfoxide (DMSO-d_6, 99.8% D) from Euriso-top (Saarbrücken, Germany) was used. Standard 5 mm NMR tubes (ST 500) were purchased from Norell (Landisville, PA).

Methods

Preparation of ionic liquids and low melting salts

Ionic liquids (IL) and crystalline TBP salts were prepared in analogy to previous reports [13]. Briefly, 100 mg free acid was suspended in 5 mL methanol, an equimolar amount of the counterion (tetrabutylphosphonium hydroxide) was added and mixed until a clear solution was obtained. Solvents were evaporated at 40 °C, 150 – 300 mbar until approximately 2 ml were left. The liquid was transferred onto a watch glass and dried at 55 °C *in vacuo* for two days. Substances were stored in a desiccator. Moisture content was determined with Mettler Toledo DL37 KF Coulometer.

Sodium salt preparation

Ketoprofen sodium salt was prepared according to the method described by Hildebrand and Müller-Goymann [43]. In short, Ketoprofen free acid was dissolved in methanol p.a.. Dried sodium hydroxide was dissolved in water and an equimolar amount of sodium hydroxide solution was added to the free acid. Solvent was evaporated at 50 °C *in vacuo* and dried for one day. The resulting salt was dissolved in ethanol at 50 °C and solvent was evaporated *in vacuo* at room temperature until precipitation of salt occurred. After 1 day suspension was filtered and salt was dried for 1 day *in vacuo* at 50 °C. Sulfamethoxazole and Tolbutamide sodium salts were prepared in a similar way. For Tolbutamide seed crystals were needed for crystallization which were prepared by gradual ethanol evaporation under ambient conditions.

Nuclear magnetic resonance measurement

NMR measurements were performed on a Bruker Avance 400 MHz spectrometer (Karlsruhe, Germany) operating at 400.13 MHz with a BBO BB-H 5mm probe head, and data processing with the TopSpin 3.0 software. The temperature was adjusted with a BCU-05 (Bruker) temperature control unit.

Infrared spectroscopy

The measurements were conducted on Jasco FT/IR-6100 spectrometer from Jasco (Gross-Umstadt, Germany) with diamond attenuated total reflection unit.

X-ray powder diffractometry

Free acids and solid TBP salts were transferred onto a silicon single crystal zero background specimen holder, covering an area with a diameter of approximately 5 mm. Powder diffractometric studies were done with a Bruker Discover D8 powder diffractometer (Karlsruhe, Germany) using Cu-Kα radiation (unsplit $K\alpha_1$+$K\alpha_2$ doublet, mean wavelength λ = 154.19 pm) at a power of 40 kV and 40 mA, a focusing Goebel mirror and a 1.0 mm microfocus alignment (1.0 mm pinhole with 1.0 mm snout). Detection of the scattered X-ray beam went through a receiving slit with 7.5 mm opening, a 0.0125 mm nickel foil and a 2.5° axial Soller slit. Detection was done with a LynxEye-1D-Detector (Bruker AXS) using the full detector range of 192 channels. Measurements were done in reflection geometry in coupled two theta/theta mode with a step size of 0.025° in 2θ and 0.33 s measurement time per step in the range of 5 – 45° (2θ). Data collection and processing was done with the software packages DIFFRAC.Suite (V2 2.2.690, Bruker AXS 2009-2011, Karlsruhe, Germany) and DIFFRAC.EVA (Version 2.1, Bruker AXS 2012-2012, Karlsruhe, Germany). Conversion of measurement data into universally readable ASCII format was done with the Bruker AXS File Exchange software (2.2.40.1, Bruker AXS 2009-2012, Karlsruhe, Germany).

Differential scanning calorimetry

Differential Scanning Calorimetry (DSC) was performed on a DSC 8000 instrument (Perkin Elmer, Waltham, MA) using a scanning rate of 20 K/min. Sample size was 2.5 mg to 6.7 mg. For free acids melting point was determined from one heating cycle. For the ILs and LLESs three heating and cooling cycles were performed and the second and third heating cycles were analyzed to allow removal of residual water during the first heating cycle.

Dynamic vapor sorption

Moisture sorption isotherms of different substances were measured at 25 °C using a DVS Advantage 1 instrument (Surface Measurement Systems Ltd., London, UK). Initially, samples were dried at 10% r.H. until the change in mass was less than 0.02 mg per minute and equilibrium state was supposed to be reached. Thereafter, the relative humidity was increased by steps of 10% r.H. when equilibrium state was reached and the next step was only initiated when the mass change was less than 0.02 mg per minute. Moisture sorption was measured from 10% to 90% r.H.

Surface tension

Tensiometer K12 (Krüss GmbH, Hamburg, Germany) was used with a Wilhelmy plate (platinum) for surface tension determination. Temperature of 80 ml of Millipore water was adjusted to 25 °C. Small volumes of TBPOH 40% in water were added manually with an Eppendorf pipette. After addition of TPBOH solution is stirred for 3 minutes. Consequently, solution was left untouched for

another minute for micelle formation. For each data point 10 measurements were made within 40 seconds.

Photometrical determination of dissolution rate

Dissolution rates were measured with a Sirius T3 instrument (Sirius Analytical, Forest Row, UK) as described earlier [44]. Tablets with defined surfaces were prepared by compression of 5-10 mg substance in a tablet disc (diameter of the tablet disk was 0.07 cm^2 and is provided by the manufacturer of the machine) under a weight of 0.18 tonnes for 6 minutes with a manual hydraulic tablet press (Paul Weber, Stuttgart, Germany), and as described before [44]. Ibuprofen RT-IL, Ketoprofen RT-IL, Naproxen RT-IL and Sulfamethoxazole RT-IL – all of which being viscous liquids at room temperature - were filled into the identical tablet disk and obviously did not require compression as these were liquids. The release of drug substance from these tablet disc allows data collection with a standardized surface area (0.07 cm^2), which is required to fit the data for calculation of the dissolution rate [44]. Dissolution rates were determined photometrically at room temperature in phosphate buffered saline (PBS) pH 6.8 at a stirring speed of 4800 rpm following manufacturer's instructions. The linear part of the release profile was used for calculation of the dissolution rate (dissolved substance per time and surface area).

24-hours solubility profiles

4.8 µmol (sdv <0.25) dry substance was transferred into an 1.5 ml tube, 1ml PBS buffer pH 6.8 were added and tubes was incubated at 37 °C while being shaken at 400 rpm. For all substances triplicates were performed. After 15 min, 45 min, 2 hours, 4 hours, 6 hours, 10 hours and 24 hours 50 µl samples of solutions were transferred into a separate tube and centrifuged for 5 min at 13000 rpm. Concentration of compound in supernatant was determined photometrically at 270 nm. For those TBP salts and sodium salts which were completely dissolved at 5 mM a second experiment was run using higher amounts of salt such that a theoretical maximum concentration of 200 mM could be achieved if all salt is dissolved after 24 hours. For those salts even exceeding the solubility of 200 mM, no further experiments were conducted as retrieving supernatant from these suspensions was impossible without aspirating solid and suspended salt. For all experiments (5 mM or 200 mM) the pH was controlled after 24 hours and was 6.8 ± < 0.2.

Acknowledgments

The funding by the Bayerische Forschungsstiftung (grant 'Springs and Parachutes') is gratefully acknowledged. B.G. and T.W. are full time employees of Novartis and state a possible conflict of interest.

Supplementary Information

Supplementary Figures:

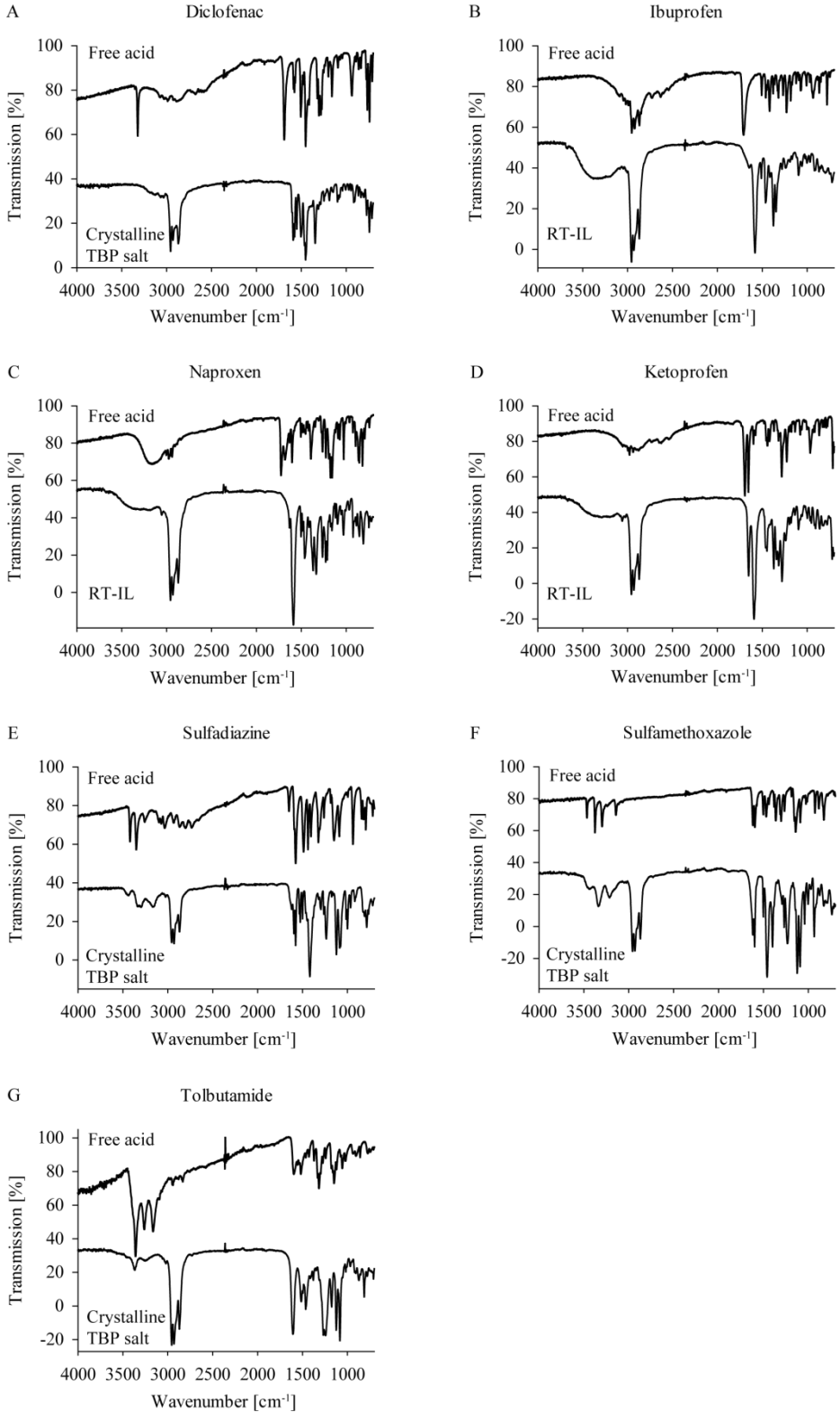

Supplementary Figure 1: IR spectra of acidic APIs and corresponding TBP salts.

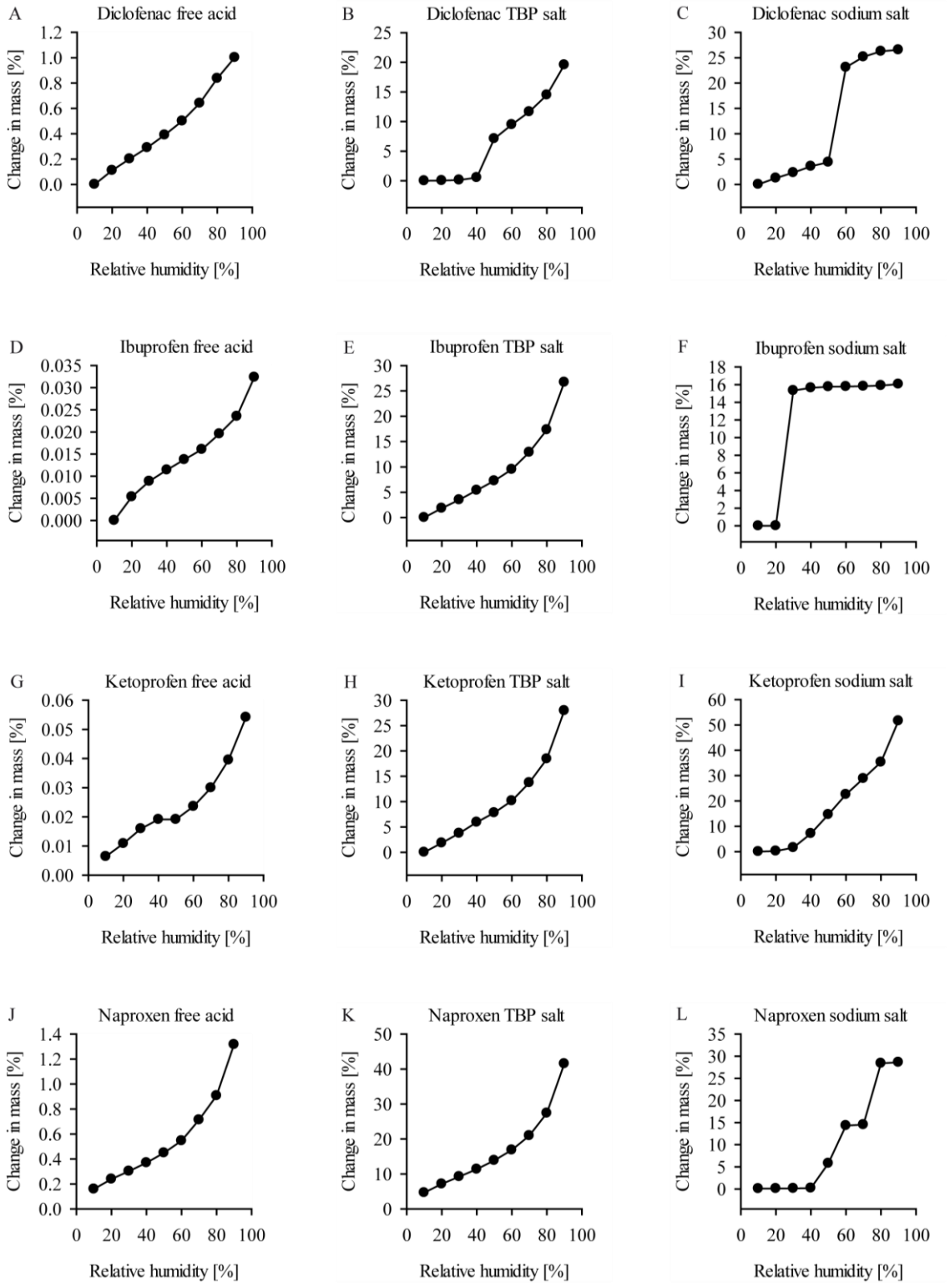

Supplementary Figure 2: Dynamic vapor sorption data of free acids, TBP salts and sodium salts of Diclofenac, Ibuprofen, Ketoprofen and Naproxen.

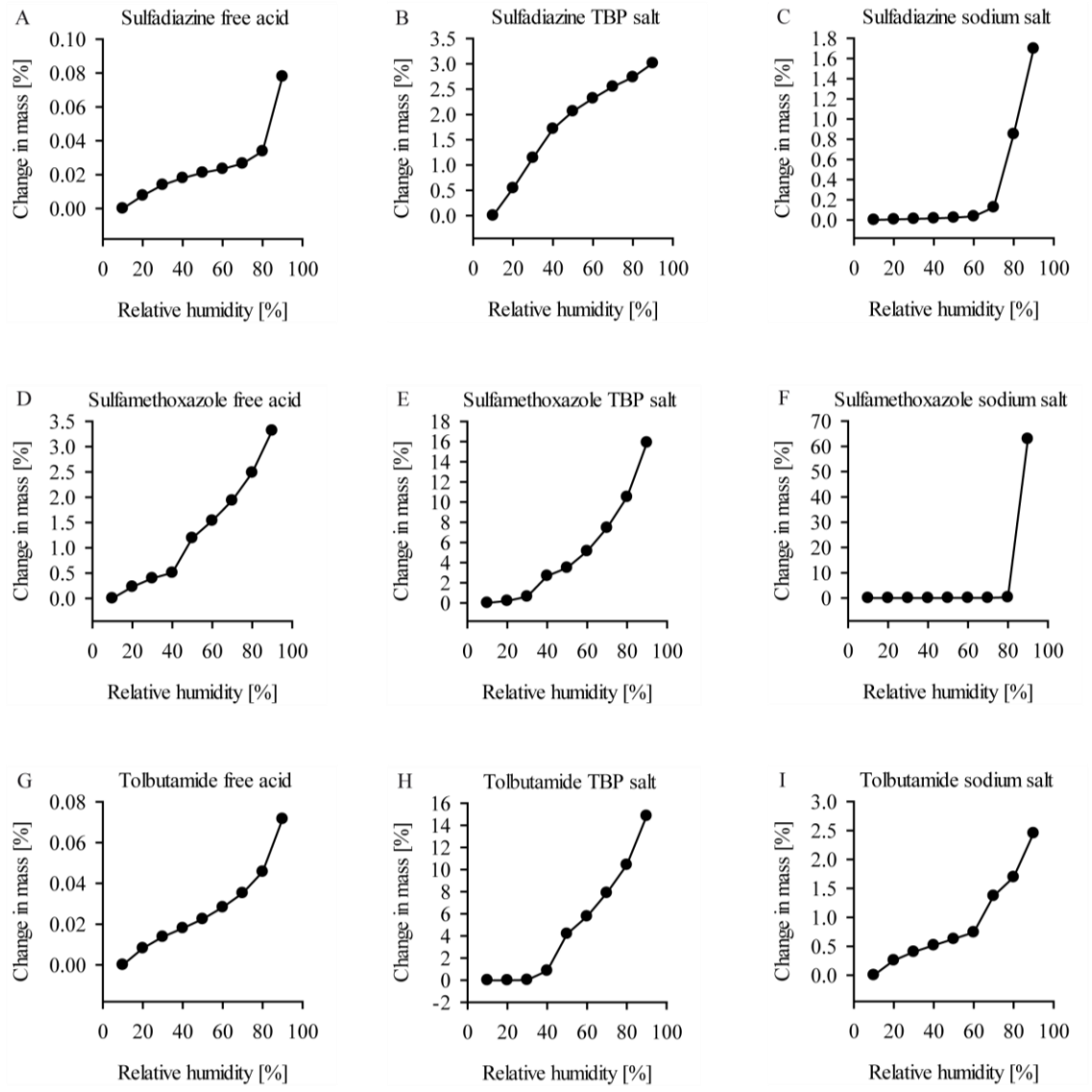

Supplementary Figure 3: Dynamic vapor sorption data of free acids, TBP salts and sodium salts of Sulfadiazine, Sulfamethoxazole and Tolbutamide.

Supplementary Information: IR and NMR data.

Diclofenac-TBP:

IR (ATR) $\tilde{\nu}$ [cm^{-1}]: 3033, 2956, 2929, 2871, 1575, 1551, 1504, 1465, 1453, 1346, 1096, 743, 714.

^{1}H-NMR (DMSO-d_6, δ [ppm], J [Hz]): 10.95 (s, 1H), 7.42 (d, 2H, J = 8), 7.03 (t, 1H, J = 8.0), 6.98 (dd, 1H, J = 7.4, J = 1.4), 6.88 (dt, 1H, J = 7.6, J = 1.6), 6.69 (dt, 1H, J = 7.3, J = 1.2), 6.20 (dd, 1H, J = 7.9, J = 0.9), 3.29 (s, 2H), 2.28 – 2.06 (m, 8H), 1.59 (m, 16H), 0.91 (t, 12H, J = 7.2).

^{13}C-NMR (DMSO-d_6, δ [ppm], J [Hz]): 173.2, 143.6, 138.4, 129.8, 129.1, 129.0, 128.9. 125.2, 123.4, 119.3, 115.2, 45.8, 23.3 (d, 4C, $^{3}J_{C,P}$ = 15.6), 22.6 (d, 4C, $^{2}J_{C,P}$ = 4.5), 17.3 (d, 4C, $^{1}J_{C,P}$ = 47.7), 13.2 (s, 4C).

Diclofenac-sodium:

IR (ATR) $\tilde{\nu}$ [cm^{-1}]: 3385, 3258, 1574, 1498, 1452, 1398, 745.

^{1}H-NMR (DMSO-d_6, δ [ppm], J [Hz]): 10.36 (s, 1H), 7.43 (d, 2H, J = 8), 7.04 (t, 1H, J = 8.0), 7.03 (dd, 1H, J = 7.4, J = 1.4), 6.91 (dt, 1H, J = 7.6, J = 1.5), 6.72 (dt, 1H, J = 7.4, J = 1.1), 6.22 (dd, 1H, J = 7.9, J = 0.9), 3.35 (s, 2H).

^{13}C-NMR (DMSO-d_6, δ [ppm], J [Hz]): 174.7, 143.4, 138.3, 130.1, 129.1, 129.0, 128.7. 125.6, 123.8, 119.7, 115.4, 44.9.

Diclofenac:

IR (ATR) $\tilde{\nu}$ [cm^{-1}]: 3322, 2885, 1690, 1506, 1452, 937, 741.

^{1}H-NMR (DMSO-d_6, δ [ppm], J [Hz]): 12.68 (s, 1H), 7.52 (d, 2H, J = 8.1), 7.23 (s, 1H), 7.21 (dd, 1H, J = 7.5, J = 1.4), 7.19 (t, 1H, J = 8.3), 7.06 (dt, 1H, J = 7.8, J = 1.4), 6.86 (dt, 1H, J = 7.4, J = 1.2), 6.29 (dd, 1H, J = 8.1, J = 0.9) 3.70 (s, 2H).

^{13}C-NMR (DMSO-d_6, δ [ppm], J [Hz]): 173.3, 142.7, 137.1, 130.9, 130.0, 129.2, 127.5, 125.6, 123.9, 120.8, 116.0, 37.7.

Ibuprofen-TBP:

IR (ATR) $\tilde{\nu}$ [cm^{-1}]: 2956, 2930, 2870, 1580, 1464, 1376, 1347, 1096, 723.

^{1}H-NMR (DMSO-d_6, δ [ppm], J [Hz]): 7.13 (m, 2H), 6.94 (m, 2H), 3.15 (q, 1H, J = 7.1), 2.36 (d, 2H, J = 7.1), 2.29 – 2.10 (m, 8H), 1.78 (nonet, 1H, J = 6.7), 1.55 – 1.31 (m, 16H), 1.17 (d, 3H, J = 7.1), 0.91 (t, 12H, J = 7.2), 0.85 (d, 6H, J = 6.6).

^{13}C-NMR (DMSO-d_6, δ [ppm], J [Hz]): 174.8, 144.1, 136.9, 127.8, 127.1, 49.3, 44.4, 29.7, 23.3 (d, 4C, $^{3}J_{C,P}$ = 15.6), 22.6 (d, 4C, $^{2}J_{C,P}$ = 4.4), 22.2, 20.4, 17.3 (d, 4C, $^{1}J_{C,P}$ = 47.7), 13.2 (s, 4C).

Ibuprofen-sodium:

IR (ATR) $\tilde{\nu}$ [cm^{-1}]: 2961, 1546, 1406, 1363, 1293, 1058, 786.

^{1}H-NMR (DMSO-d_6, δ [ppm], J [Hz]): 7.17 (m, 2H), 6.96 (m, 2H), 3.22 (q, 1H, J = 7.1), 2.37 (d, 2H, J = 7.1), 1.78 (nonet, 1H, J = 6.7), 1.22 (d, 3H, J = 7.1), 0.85 (d, 6H, J = 6.6).

^{13}C-NMR (DMSO-d_6, δ [ppm], J [Hz]): 177.7, 143.8, 137.9, 128.5, 127.7, 49.0, 44.8, 30.2, 22.7, 20.7.

Ibuprofen:

IR (ATR) $\tilde{\nu}$ [cm^{-1}]: 2953, 1709, 1418, 1229, 1183, 779.

^{1}H-NMR (DMSO-d_6, δ [ppm], J [Hz]): 12.22 (s, 1H), 7.19 (m, 2H), 7.10 (m, 2H), 3.62 (q, 1H, J = 7.1), 2.41 (d, 2H, J = 7.1), 1.81 (nonet, 1H, J = 6.8), 1.34 (d, 3H, J = 7.2), 0.85 (d, 6H, J = 6.6).

^{13}C-NMR (DMSO-d_6, δ [ppm], J [Hz]): 175.4, 139.5, 138.5, 128.9, 127.1, 44.3, 44.2, 29.6, 22.2, 18.5.

Ketoprofen-TBP:

IR (ATR) $\tilde{\nu}$ [cm^{-1}]: 2957, 2930, 2872, 1652, 1592, 1447, 1372, 1281, 1097, 721, 704.

^{1}H-NMR (DMSO-d_6, δ [ppm], J [Hz]): 7.88 – 7.27 (m, 9H), 3.24 (q, 1H, J = 7.1), 2.29 – 2.07 (m, 8H), 1.55 – 1.32 (m, 16H), 1.23 (d, 3H, J = 7.1), 0.91 (t, 12H, J = 7.1).

^{13}C-NMR (DMSO-d_6, δ [ppm], J [Hz]): 196.2, 174.0, 147.3, 137.5, 136.1, 132.3, 132.0, 129.5, 128.8, 128.4, 127.4, 126.2, 49.6, 23.3 (d, 4C, $^{3}J_{C,P}$ = 15.6), 22.6 (d, 4C, $^{2}J_{C,P}$ = 4.4), 20.2, 17.3 (d, 4C, $^{1}J_{C,P}$ = 47.7), 13.2 (s, 4C).

Ketoprofen Sodium:

IR (ATR) $\tilde{\nu}$ [cm^{-1}]: 1659, 1579, 1571, 1398, 1321, 1277, 720, 689.

^{1}H-NMR (DMSO-d_6, δ [ppm], J [Hz]): 7.88 – 7.27 (m, 9H), 3.35 (q, 1H, J = 7.1), 1.28 (d, 3H, J = 7.1).

^{13}C-NMR (DMSO-d_6, δ [ppm], J [Hz]): 196.1, 176.7, 146.3, 137.4, 136.3, 132.4, 132.1, 129.5, 128.8, 128.5, 127.7, 126.7, 48.7, 20.0

Ketoprofen:

IR (ATR) $\tilde{\nu}$ [cm^{-1}]: 2938, 1694, 1654, 1283, 1228, 715, 690.

^{1}H-NMR (DMSO-d_6, δ [ppm], J [Hz]): 12.45 (s, 1H), 7.80 – 7.40 (m, 9 H), 3.82 (q, 1H, J = 7.1), 1.40 (d, 3H, J = 7.2).

^{13}C-NMR (DMSO-d_6, δ [ppm], J [Hz]): 195.6, 175.1, 141.8, 137.1, 137.0, 132.7, 131.9, 129.6, 128.7, 128.6, 128.5, 128.3, 44.4, 18.5.

Naproxen-TBP:

IR (ATR) $\tilde{\nu}$ [cm^{-1}]: 2957, 2930, 2872, 1588, 1463, 1369, 1334, 1264, 1228, 1211, 1031, 809.

^{1}H-NMR (DMSO-d_6, δ [ppm], J [Hz]): 7.68 (d, 1H, J = 7.7), 7.61 (d, 1H, J = 8.5), 7.6 (m, 1H), 7.46 (dd, 1H, J = 8.5, J = 1.7), 7.21 (d, 1H, J = 2.5), 7.06 (dd, 1H, J = 8.9, J = 2.6), 3.84 (s, 3H), 3.29 (q, 1H, J = 7.1), 2.30 – 2.08 (m, 8H), 1.56 – 1.32 (m, 16H), 1.28 (d, 3H, J = 7.1), 0.91 (t, 12H, J = 7.1).

^{13}C-NMR (DMSO-d_6, δ [ppm], J [Hz]): 174.7, 156.2, 142.2, 132.3, 128.7, 128.5, 127.8, 125.3, 124.5, 117.7, 105.6, 55.0, 49.6, 23.3 (d, 4C, $^{3}J_{C,P}$ = 15.6), 22.6 (d, 4C, $^{2}J_{C,P}$ = 4.4), 20.3, 17.3 (d, 4C, $^{1}J_{C,P}$ = 47.7), 13.2 (s, 4C).

Naproxen-sodium:

IR (ATR) $\tilde{\nu}$ [cm^{-1}]: 1584, 1390, 1364, 1251, 1210, 1161, 1029.

^{1}H-NMR (DMSO-d_6, δ [ppm], J [Hz]): 7.70 (d, 1H, J = 9.0), 7.63 (d, 1H, J = 8.6), 7.61 (m, 1H), 7.47 (dd, 1H, J = 8.4, J = 1.7), 7.21 (d, 1H, J = 2.6), 7.07 (dd, 1H, J = 8.9, J = 2.6), 3.84 (s, 3H), 3.39 (q, 1H, J = 7.1), 1.32 (d, 3H, J = 7.1).

^{13}C-NMR (DMSO-d_6, δ [ppm], J [Hz]): 176.9, 156.3, 141.3, 132.4, 128.8, 128.5, 127.7, 125.6, 124.7, 117.9, 105.6, 55.0, 48.9, 20.2.

Naproxen:

IR (ATR) $\tilde{\nu}$ [cm^{-1}]: 3162, 1726, 1393, 1175, 1157, 819.

^{1}H-NMR (DMSO-d_6, δ [ppm], J [Hz]): 12.30 (s, 1H), 7.78 (t, 2H, J = 9.4), 7.71 (d, 1H, J = 0.9), 7.40 (dd, 1H, J = 8.4, J = 1.8), 7.29 (d, 1H, J = 2.5), 7.15 (dd, 1H, J = 8.7, J = 2.6), 3.86 (s, 3H), 3.80 (q, 1H, J = 7.1), 1.44 (d, 3H, J = 7.1).

^{13}C-NMR (DMSO-d_6, δ [ppm], J [Hz]): 175.4, 157.1, 136.3, 133.2, 129.1, 128.4, 126.8, 126.4, 125.5, 118.7, 105.7, 55.1, 44.6, 18.4.

Sulfadiazine-TBP:

IR (ATR) $\tilde{\nu}$ [cm^{-1}]: 2957, 2930, 2871, 1578, 1499, 1418, 1235, 1122, 1086, 675.

^{1}H-NMR (DMSO-d_6, δ [ppm], J [Hz]): 8.04 (d, 2H, J = 4.6), 7.60 – 7.20 (m, 2H), 6.56 – 6.34 (m, 2H), 6.29 (t, 1H, J = 4.6), 5.25 (s, 2H), 2.32 – 2.03 (m, 8H), 1.66 – 1.28 (m, 16H), 0.91 (t, 12H, J = 7.1).

^{13}C-NMR (DMSO-d_6, δ [ppm], J [Hz]): 164.5, 156.8, 149.4, 134.3, 128.2, 111.7, 108.6, 23.3 (d, 4C, $^{3}J_{C,P}$ = 15.6), 22.6 (d, 4C, $^{2}J_{C,P}$ = 4.4), 17.3 (d, 4C, $^{1}J_{C,P}$ = 47.7), 13.2 (s, 4C).

Sulfadiazine-sodium:

IR (ATR) $\tilde{\nu}$ [cm^{-1}]: 1599, 1582, 1542, 1416, 1239, 1125, 1079, 800, 676.

^{1}H-NMR (DMSO-d_6, δ [ppm], J [Hz]): 8.10 (d, 2H, J = 4.7), 7.60 – 7.40 (m, 2H), 6.50 – 6.42 (m, 2H), 6.37 (t, 1H, J = 4.7), 5.33 (s, 2H).

^{13}C-NMR (DMSO-d_6, δ [ppm], J [Hz]): 164.5, 157.2, 149.9, 133.4, 128.2, 111.9, 109.0.

Sulfadiazine:

IR (ATR) $\tilde{\nu}$ [cm^{-1}]: 1577, 1488, 1324, 1149, 938, 680.

^{1}H-NMR (DMSO-d_6, δ [ppm], J [Hz]): 11.24 (s, 1H), 8.55 – 8.39 (m, 2H), 7.67 – 7.52 (m, 2H), 6.99 (t, 1H, J = 4.9), 6.62 – 6.50 (m, 2H), 5.99 (s, 2H).

^{13}C-NMR (DMSO-d_6, δ [ppm], J [Hz]): 158.2, 157.2, 153.0, 129.8, 124.9, 115.5, 112.1.

Sulfamethoxazole-TPB:

IR (ATR) $\tilde{\nu}$ [cm^{-1}]: 3431, 3338, 3214, 2957, 2930, 2872, 1618, 1598, 1500, 1459, 1398, 1232, 1123, 1093, 1002, 934, 827.

^{1}H-NMR (DMSO-d_6, δ [ppm], J [Hz]): 7.40 – 7.20 (m, 2H), 6.58 – 6.27 (m, 2H), 5.71 (d, 1H, 4J = 0.8 Hz), 5.27 (s, 2H), 2.32 – 2.03 (m, 8H), 2.08 (d, 3H, 4J = 0.8 Hz), 1.66 – 1.28 (m, 16H), 0.91 (t, 12H, J = 7.1).

^{13}C-NMR (DMSO-d_6, δ [ppm], J [Hz]): 166.7, 164.8, 149.4, 135.1, 127,2, 112.2, 97.0, 23.3 (d, 4C, $^{3}J_{C,P}$ = 15.6), 22.6 (d, 4C, $^{2}J_{C,P}$ = 4.4), 17.3 (d, 4C, $^{1}J_{C,P}$ = 47.7), 13.2 (s, 4C), 12.2.

Sulfamethoxazole Sodium:

IR (ATR) $\tilde{\nu}$ [cm^{-1}]: 3485, 3466, 3374, 1619, 1597, 1502, 1469, 1412, 1211, 1166, 1118, 1091, 798, 753.

^{1}H-NMR (DMSO-d_6, δ [ppm], J [Hz]): 7.40 – 7.20 (m, 2H), 6.58 – 6.27 (m, 2H), 5.73 (d, 1H, J = 0.8 Hz), 5.32 (s, 2H), 2.09 (d, 3H, J = 0.8 Hz).

^{13}C-NMR (DMSO-d_6, δ [ppm], J [Hz]): 165.9, 165.5, 149.9, 133.7, 127,5, 112.2, 97.0, 12.2.

Sulfamethoxazole:

IR (ATR) $\tilde{\nu}$ [cm^{-1}]: 3466, 3376, 3297, 1617, 1595, 1501, 1363, 1303, 1142, 827.

^{1}H-NMR (DMSO-d_6, δ [ppm], J [Hz]): 10.90 (s, 1H), 7.60 – 7.30 (m, 2H), 6.74 – 6.46 (m, 2H), 6.09 (d, 1H, J = 0.9), 6.06 (s, 2H), 2.28 (d, 3H, J = 0.8).

^{13}C-NMR (DMSO-d_6, δ [ppm], J [Hz]): 169.8, 157.9, 153.3, 128.8, 124.2, 112.6, 95.3, 12.0.

Tolbutamide-TBP:

IR (ATR) $\tilde{\nu}$ [cm^{-1}]: 3368, 2956, 2930, 2872, 1606, 1514, 1465, 1267, 1243, 1124, 1083, 813.

^{1}H-NMR (DMSO-d_6, δ [ppm], J [Hz]): 7.69 – 7.48 (m, 2H), 7.22 – 6.99 (m, 2H), 5.61 (s, 1H), 2.96 – 2.69 (m, 2H), 2.29 (s, 3H), 2.25 – 2.07 (m, 8H), 1.60 – 1.32 (m, 16H), 1.32 – 1.12 (m, 4H), 0.91 (t, 12H, J = 7.1), 0.82 (t, 3H, J = 7.2).

^{13}C-NMR (DMSO-d_6, δ [ppm], J [Hz]): 160.3, 145.5, 138.1, 127.7, 126.3, 32.3, 23.3 (d, 4C, $^{3}J_{C,P}$ = 15.6), 22.6 (d, 4C, $^{2}J_{C,P}$ = 4.4), 20.8, 19.7, 17.3 (d, 4C, $^{1}J_{C,P}$ = 47.7), 13.8, 13.2 (s, 4C).

Tolbutamide-TBP:

IR (ATR) $\tilde{\nu}$ [cm^{-1}]: 3368, 2956, 2930, 2872, 1606, 1514, 1465, 1267, 1243, 1124, 1083, 813.

^{1}H-NMR (DMSO-d_6, δ [ppm], J [Hz]): 7.69 – 7.48 (m, 2H), 7.22 – 6.99 (m, 2H), 5.61 (s, 1H), 2.96 – 2.69 (m, 2H), 2.29 (s, 3H), 2.25 – 2.07 (m, 8H), 1.60 – 1.32 (m, 16H), 1.32 – 1.12 (m, 4H), 0.91 (t, 12H, J = 7.1), 0.82 (t, 3H, J = 7.2).

^{13}C-NMR (DMSO-d_6, δ [ppm], J [Hz]): 160.3, 145.5, 138.1, 127.7, 126.3, 32.3, 23.3 (d, 4C, $^{3}J_{C,P}$ = 15.6), 22.6 (d, 4C, $^{2}J_{C,P}$ = 4.4), 20.8, 19.7, 17.3 (d, 4C, $^{1}J_{C,P}$ = 47.7), 13.8, 13.2 (s, 4C).

Tolbutamide:

IR (ATR) $\tilde{\nu}$ [cm^{-1}]: 3358, 3262, 3165, 1595, 1519, 1316, 1177.

^{1}H-NMR (DMSO-d_6, δ [ppm], J [Hz]): 10.44 (s, 1H), 7.91 – 7.67 (m, 2H), 7.46 – 7.32 (m, 2H), 6.42 (t, 1H, J = 5.4), 2.98 – 2.88 (m, 2H), 2.38 (s, 3H), 1.35 – 1.23 (m, 2H), 1.23 – 1.10 (m, 2H), 0.81 (t, 3H, J = 7.3).

^{13}C-NMR (DMSO-d_6, δ [ppm], J [Hz]): 151.3, 143.5, 137.5, 129.4, 127.2, 31.3, 21.0, 19.3, 13.5.

References

[1] R. O. Williams III, A. B. Watts, and D. A. Miller, *Formulating Poorly Water Soluble Drugs* vol. 3. New York, NY: Springer New York, 2012.

[2] A. Fahr and X. Liu, "Drug delivery strategies for poorly water-soluble drugs," *Expert Opin Drug Deliv,* vol. 4, pp. 403-16, Jul 2007.

[3] A. Balk, T. Widmer, J. Wiest, H. Bruhn, J. C. Rybak, P. Matthes, *et al.*, "Ionic liquid versus prodrug strategy to address formulation challenges," *Pharm Res,* vol. 32, pp. 2154-67, Jun 2015.

[4] R. Ferraz, L. C. Branco, C. Prudencio, J. P. Noronha, and Z. Petrovski, "Ionic liquids as active pharmaceutical ingredients," *ChemMedChem,* vol. 6, pp. 975-85, Jun 6 2011.

[5] H. Mizuuchi, V. Jaitely, S. Murdan, and A. T. Florence, "Room temperature ionic liquids and their mixtures: potential pharmaceutical solvents," *Eur J Pharm Sci,* vol. 33, pp. 326-31, Apr 23 2008.

[6] W. L. Hough and R. D. Rogers, "Ionic liquids then and now: From solvents to materials to active pharmaceutical ingredients," *Bulletin of the Chemical Society of Japan,* vol. 80, pp. 2262-2269, Dec 15 2007.

[7] K. Bica and R. D. Rogers, "Confused ionic liquid ions-a "liquification" and dosage strategy for pharmaceutically active salts," *Chem Commun (Camb),* vol. 46, pp. 1215-7, Feb 28 2010.

[8] J. Stoimenovski and D. R. MacFarlane, "Enhanced membrane transport of pharmaceutically active protic ionic liquids," *Chem Commun (Camb),* vol. 47, pp. 11429-31, Nov 7 2011.

[9] J. Stoimenovski, D. R. MacFarlane, K. Bica, and R. D. Rogers, "Crystalline vs. ionic liquid salt forms of active pharmaceutical ingredients: a position paper," *Pharm Res,* vol. 27, pp. 521-6, Apr 2010.

[10] P. M. Dean, J. Turanjanin, M. Yoshizawa-Fujita, D. R. MacFarlane, and J. L. Scott, "Exploring an Anti-Crystal Engineering Approach to the Preparation of Pharmaceutically Active Ionic Liquids," *Crystal Growth & Design,* vol. 9, pp. 1137-1145, Feb 2009.

[11] K. Bica, H. Rodriguez, G. Gurau, O. A. Cojocaru, A. Riisager, R. Fehrmann, *et al.*, "Pharmaceutically active ionic liquids with solids handling, enhanced thermal stability, and fast release," *Chem Commun (Camb),* vol. 48, pp. 5422-4, Jun 4 2012.

[12] W. L. Hough, M. Smiglak, H. Rodriguez, R. P. Swatloski, S. K. Spear, D. T. Daly, *et al.*, "The third evolution of ionic liquids: active pharmaceutical ingredients," *New Journal of Chemistry,* vol. 31, pp. 1429-1436, 2007.

[13] K. Bica, C. Rijksen, M. Nieuwenhuyzen, and R. D. Rogers, "In search of pure liquid salt forms of aspirin: ionic liquid approaches with acetylsalicylic acid and salicylic acid," *Phys Chem Chem Phys,* vol. 12, pp. 2011-7, Feb 28 2010.

[14] I. M. Marrucho, L. C. Branco, and L. P. Rebelo, "Ionic liquids in pharmaceutical applications," *Annu Rev Chem Biomol Eng,* vol. 5, pp. 527-46, 2014.

[15] M. Hesse, H. Meiner, and B. Zeeh, *Spektroskopische Methoden in der organischen Chemie,* 7 ed. vol. 323. Stuttgart: Georg Thieme Verlag, 2005.

[16] G. L. Amidon, H. Lennernas, V. P. Shah, and J. R. Crison, "A theoretical basis for a biopharmaceutic drug classification: the correlation of in vitro drug product dissolution and in vivo bioavailability," *Pharm Res,* vol. 12, pp. 413-20, Mar 1995.

[17] A. Dahan, J. M. Miller, and G. L. Amidon, "Prediction of solubility and permeability class membership: provisional BCS classification of the world's top oral drugs," *AAPS J,* vol. 11, pp. 740-6, Dec 2009.

[18] B. Chuasuwan, V. Binjesoh, J. E. Polli, H. Zhang, G. L. Amidon, H. E. Junginger, *et al.*, "Biowaiver monographs for immediate release solid oral dosage forms: diclofenac sodium and diclofenac potassium," *J Pharm Sci,* vol. 98, pp. 1206-19, Apr 2009.

[19] C. Alvarez, I. Nunez, J. J. Torrado, J. Gordon, H. Potthast, and A. Garcia-Arieta, "Investigation on the possibility of biowaivers for ibuprofen," *J Pharm Sci*, vol. 100, pp. 2343-9, Jun 2011.
[20] I. E. Shohin, J. I. Kulinich, G. V. Ramenskaya, B. Abrahamsson, S. Kopp, P. Langguth, *et al.*, "Biowaiver monographs for immediate-release solid oral dosage forms: ketoprofen," *J Pharm Sci*, vol. 101, pp. 3593-603, Oct 2012.
[21] M. Alleso, N. Chieng, S. Rehder, J. Rantanen, T. Rades, and J. Aaltonen, "Enhanced dissolution rate and synchronized release of drugs in binary systems through formulation: Amorphous naproxen-cimetidine mixtures prepared by mechanical activation," *J Control Release*, vol. 136, pp. 45-53, May 21 2009.
[22] N. A. Kasim, M. Whitehouse, C. Ramachandran, M. Bermejo, H. Lennernas, A. S. Hussain, *et al.*, "Molecular properties of WHO essential drugs and provisional biopharmaceutical classification," *Mol Pharm*, vol. 1, pp. 85-96, Jan 12 2004.
[23] R. J. Bastin, M. J. Bowker, and B. J. Slater, "Salt selection and optimisation procedures for pharmaceutical new chemical entities," *Organic Process Research & Development*, vol. 4, pp. 427-435, Sep-Oct 2000.
[24] S. Byrn, R. Pfeiffer, M. Ganey, C. Hoiberg, and G. Poochikian, "Pharmaceutical solids: a strategic approach to regulatory considerations," *Pharm Res*, vol. 12, pp. 945-54, Jul 1995.
[25] G. G. Zhang, S. Y. Paspal, R. Suryanarayanan, and D. J. Grant, "Racemic species of sodium ibuprofen: characterization and polymorphic relationships," *J Pharm Sci*, vol. 92, pp. 1356-66, Jul 2003.
[26] P. Di Martino, C. Barthelemy, G. F. Palmieri, and S. Martelli, "Physical characterization of naproxen sodium hydrate and anhydrate forms," *Eur J Pharm Sci*, vol. 14, pp. 293-300, Dec 2001.
[27] V. Murikipudi, P. Gupta, and V. Sihorkar, "Efficient throughput method for hygroscopicity classification of active and inactive pharmaceutical ingredients by water vapor sorption analysis," *Pharm Dev Technol*, vol. 18, pp. 348-58, Mar-Apr 2013.
[28] C. Ahlneck and G. Zografi, "The Molecular-Basis of Moisture Effects on the Physical and Chemical-Stability of Drugs in the Solid-State," *International Journal of Pharmaceutics*, vol. 62, pp. 87-95, Jul 31 1990.
[29] M. Bartolomei, P. Bertocchi, E. Antoniella, and A. Rodomonte, "Physico-chemical characterisation and intrinsic dissolution studies of a new hydrate form of diclofenac sodium: comparison with anhydrous form," *J Pharm Biomed Anal*, vol. 40, pp. 1105-13, Mar 18 2006.
[30] P. Rossi, E. Macedi, P. Paoli, L. Bernazzani, E. Carignani, S. Borsacchi, *et al.*, "Solid–Solid Transition between Hydrated Racemic Compound and Anhydrous Conglomerate in Na-Ibuprofen: A Combined X-ray Diffraction, Solid-State NMR, Calorimetric, and Computational Study," *Crystal Growth & Design*, vol. 14, pp. 2441-2452, 2014.
[31] P. Di Martino, C. Barthelemy, E. Joiris, D. Capsoni, A. Masic, V. Massarotti, *et al.*, "A new tetrahydrated form of sodium naproxen," *J Pharm Sci*, vol. 96, pp. 156-67, Jan 2007.
[32] G. Zografi, "States of Water Associated with Solids," *Drug Development and Industrial Pharmacy*, vol. 14, pp. 1905-1926, 1988.
[33] P. H. Stahl, C. G. Wermuth, and I. U. o. P. a. A. Chemistry, *Handbook of Pharmaceutical Salts Properties, Selection, and Use*, 2 ed. Zürich: VHVA; Weinheim:Wiley-VCH, 2011.
[34] A. A. Noyes and W. R. Whitney, "The Rate of Solution of Solid Substances in Their Own Solutions," *Journal of the American Chemical Society*, vol. 19, pp. 930-934, 1897.
[35] P. M. Dean, J. M. Pringle, and D. R. MacFarlane, "Structural analysis of low melting organic salts: perspectives on ionic liquids," *Phys Chem Chem Phys*, vol. 12, pp. 9144-53, Aug 28 2010.
[36] D. Kashchiev, "Chapter 10 - Transition frequencies," in *Nucleation*, D. Kashchiev, Ed., ed Oxford: Butterworth-Heinemann, 2000, pp. 136-173.
[37] M. G. Freire, C. M. Neves, P. J. Carvalho, R. L. Gardas, A. M. Fernandes, I. M. Marrucho, *et al.*, "Mutual solubilities of water and hydrophobic ionic liquids," *J Phys Chem B*, vol. 111, pp. 13082-9, Nov 15 2007.

[38] F. Alves, F. S. Oliveira, B. Schroder, C. Matos, and I. M. Marrucho, "Synthesis, characterization, and liposome partition of a novel tetracycline derivative using the ionic liquids framework," *J Pharm Sci*, vol. 102, pp. 1504-12, May 2013.

[39] G. A. Ilevbare and L. S. Taylor, "Liquid–Liquid Phase Separation in Highly Supersaturated Aqueous Solutions of Poorly Water-Soluble Drugs: Implications for Solubility Enhancing Formulations," *Cryst. Growth Des.*, vol. 13, pp. 1497-1509, 2013.

[40] L. Lafferrère, C. Hoff, and S. Veesler, "Study of liquid–liquid demixing from drug solution," *J. Cryst. Growth* vol. 269, pp. 550-557, 2004.

[41] S. Veesler, L. Lafferrere, E. Garcia, and C. Hoff, "Phase transitions in supersaturated drug solution," *Organic Process Research & Development*, vol. 7, pp. 983-989, Nov-Dec 2003.

[42] L. I. Mosquera-Giraldo and L. S. Taylor, "Glass-liquid phase separation in highly supersaturated aqueous solutions of telaprevir," *Mol Pharm*, vol. 12, pp. 496-503, Feb 2 2015.

[43] G. E. Hildebrand and C. C. Muller-Goymann, "Ketoprofen sodium: preparation and its formation of mixed crystals with ketoprofen," *J Pharm Sci*, vol. 86, pp. 854-7, Jul 1997.

[44] T. Gravestock, K. Box, J. Comer, E. Frake, S. Judge, and R. Ruiz, "The "GI dissolution" method: a low volume, in vitro apparatus for assessing the dissolution/precipitation behaviour of an active pharmaceutical ingredient under biorelevant conditions," *Analytical Methods*, vol. 3, p. 560, 2011.

Conclusion and outlook

Ionic liquids (IL) and Low lattice enthalpy salts (LLES) proved a versatile tool for formulation scientists to tune the crucial parameters for drug release and bioavailability. ILs were prepared for several acidic APIs by combination with bulky voluminous counterions. With the delocalization of charges and introduction of side-chains into the counterion, hindering its interaction with the API, ILs or at least salts with a low lattice force were effectively designed [1, 2]. The liquid state at room temperature is especially interesting as no crystalline structures and hence no polymorphs may be formed, respectively, quite regularly imposing hurdles on pharmaceutical development programs. Various examples have been presented leading to Room temperature ionic liquids (RT-ILs), due to their stable liquid state avoiding polymorphism [1, 3-5]. However, studies also detailed, that in some cases such RT-ILs may transform into crystalline, hence solid hydrates [6]. Within the presented studies the ratio of API and counterion was 1:1 in all cases. As liquefaction of ILs was observed for increasing API to counterion ratios, non-stoichiometric salts could be interesting to be further investigated [7]. Other options aiming to reduce the formation of a strong lattice structure include the combination of one API with two or even more different counterions in a 1:1 or other ratio of the API to counterion(s).

The IL concept is particularly addressing the challenges around solubility or dissolution rate, quite frequently observed for poorly water soluble drugs (PWSD). For ILs and LLESs the choice of the counterion had a strong impact on the dissolution rate. Due to ionization, the salts and ILs generally dissolve faster than the corresponding free acids, as the interaction with the aqueous medium is increased. The dissolution rate of the salts and ILs depended on the melting point and the lipophilicity of the counterion. ILs and LLESs generally displayed lower melting points than the respective sodium or potassium salts; however, this did not generally translate into faster dissolution rates. Arguably the desired impact on the dissolution rate by reducing the melting point (hence increasing the lattice enthalpy) by larger, sterically demanding counterions was counterbalanced by a concomitant increase of these counterions' lipophilicity which was negatively impacting the dissolution rate. These data sets provided evidence, that a strategy solely focusing on a reduction of the melting point alone is insufficient in meeting the goal of accelerated dissolution rates. This was studied in detail for ILs of one API with similar melting points, revealing that the dissolution rate correlated with the lipophilicity of the counterion. These insights will be quite instrumental in custom-designed counterions of the future allowing for a precise tuning of the dissolution rate and at the same time for tuning the release profiles for poorly water soluble APIs. Immediate to prolonged release of an API may be accomplished simply by the choice of counterion, complementing of perhaps sometimes challenging the need for complex, polymer based formulations to meet these goals.

Another aspect which should be taken into consideration when designing counterions for poorly water soluble, weak acids with pKa values of 5-7 is that protons present in dissolution media or intestinal fluids drive (partial) protonation of the acid, hence charge neutralization resulting in recrystallization of the free form. However, IL preparation was observed to stabilize the API in solution by aggregate formation, as determined by NMR aggregation assay, thus preventing precipitation of the free form as it occurred for the corresponding potassium salt. The relative amount of counterion almost linearly prolonged the duration of supersaturation. By determination of supersaturation of an API with several counterions an indirect correlation between dissolution rate and duration of supersaturation was detected. A hypothesis was developed in that the more hydrophilic the counterion, the better it interacts with the aqueous medium and the less aggregates are formed protecting the acid API from protonation and consequently recrystallization. To prove this hypothesis further experiments are required. Future studies on the aggregation pattern of the API with different counterions will elucidate whether larger or more aggregates are formed with more lipophilic counterions. Instrumentally, this can be addressed by NMR aggregation assay [8, 9], viscosity and conductivity measurements (Walden plots) [10] and electrospray ionization mass spectrometry (ESI-MS) [11, 12] of ILs with systematically altered counterions e.g. with one alkyl chain increasing systematically by one or more methyl unit, resulting in an increased size and lipophilicity of the counterion. Besides, the interaction of the ILs or the different counterions with the aqueous medium could be further investigated using titration calorimetry and determining the heat of dissolution.

For one IL the transport through Caco-2 cell layers was determined in comparison to the free acid and a prodrug, with the acidic group being acetylated, rendering the prodrug more lipophilic than the free acid. Applied as suspensions the better permeable prodrug was outperformed by the IL as it was much better soluble. Interestingly and in contrast to some observations reported previously for other APIs, the ILs prepared in the studies reported here within did not affect the permeability through epithelial model membranes of the API [2, 9, 13, 14], in spite of various mechanistic explanations linking the formation of neutral ion pairs or larger aggregates to improved permeation [15-18]. Our observations based on Caco-2 assay results, clearly linked the advantageous impact of the IL as compared to the prodrug and the free acid on its increase in kinetic solubility resulting in a higher concentration gradient between the apical and basolateral compartments, respectively. We did not collect evidence that this enhanced transepithelial transport rate was at least in part a result of enhanced permeability of IL aggregates for the case studied here within. However, for the fascinating potential of manipulating pharmaceutical properties to an extent outlined here within, the IL approach appears to be an alternative to prodrug formation, with the great advantage that no structural changes of the API are required.

A concern with ILs as pharmaceutical formulations is the unknown toxicity of the new counterions. In the studies presented here the cytotoxicity was assessed *in vitro* in three cell lines. An increase in cytotoxicity correlated with an increase in the counterion lipophilicity, in particular with the number of hydrophobic atoms the number of charges per molecule and the number of hydroxyl moieties of the counterion, corroborating previous reports linking counterion lipophilicity and cytotoxicity. These studies explained the observation by different interaction with lipophilic cell membranes and cytoplasmic uptake, inducing unfavorable cellular responses including apoptosis [19-22]. Novel counterions will always be exposed to the challenge of potential toxicity. One approach to mitigate this risk *a priori* is to confine ones IL strategy to counterions which have been already proven safe including amino or fatty acids [23-26] and ideally listed 'as generally recognized as safe' substances (GRAS) [4, 27-29]. Alternatively, one may target for counterions which are not absorbed when e.g. taken orally and, therefore, may not cause any harm, at least systemically. Typically ionized molecules may not be transported through lipid membranes of the epithelial barriers, apart from those being small enough to pass 'aqueous pores' [30, 31]. Thus counterions could be prepared with a low ion-pairing capacity, which are strongly charged but too large for a transport through pores, hence not absorbed.

Besides for toxicological reasons, future *in vivo* studies are also needed to study the effect of different counterions on the pharmacokinetic profiles. In particular for the LLESs presented in the third chapter animal trials have already been planned to elucidate to which extent the distinct physicochemical properties of the different LLESs may result in relevant changes of the biopharmaceutical parameters of an API. For this upcoming first proof of concept both, small highly charged hydrophilic counterions and large voluminous lipophilic counterions are particularly interesting. For an oral application it has to be considered that ILs of acidic APIs (pka > 2) are not stable in gastric fluids as the API will be protonated and the substance will recrystallize. One approach to solve this dilemma is by presenting these in enterically coated capsules. Possibly, these capsules may be prepared without any excipients for these proof of concept studies, but future studies must demonstrate to which extent this is feasible, particularly as the dosing accuracy is challenging or potential release challenges may arise from IL being confined within incompletely dissolving gelatin nests during disintegration of the (gelatin) hard capsules. The beauty of excipient-free filling of the capsules is that co-formulated excipients may impact the dissolution and solubility profiles, thereby masking or at least potentially confounding the impact of the ILs. However, should powder mixtures be required for successful formulation of such capsules, one should pay particular attention to the hygroscopic nature of some of these ILs, and associated challenges on the stability of the capsules and water uptake of the powder blend with associated chemical stability challenges during storage. Other options include the use of gastro-resistant matrixes for IL protection. However, the presence of polymer for matrix formation, within

which the ILs are embedded, may however, confound the observations, as pointed out before for the powder blends.

As mentioned above, the mayor drawback of ILs and LLESs for preparation of solid oral dosage forms is the rather high hygroscopicity, which is typical for some of these salts and may only partly be controlled by lipophilic counterions, with their negative impact on the dissolution rate of solubility profiles being the limiting factor. The more lipophilic the counterion was, the lower was the hygroscopicity of the IL of LLES, with the number of hydrophobic atoms and the number of charges per molecule being identified as the major parameters driving its features. However, even ILs of lipophilic counterions were hygroscopic to a certain extend. Some possibilities to face this problem have been presented in the first chapter like working under defined relative humidity or embedding the ILs and LLESs in lipophilic water soluble matrixes. Similar concepts need to be developed for the ILs and LLESs presented in the chapters before.

Besides the hygroscopicity, formulations need to be optimized to assure long-time stability of ILs and LLESs. Regarding the shelf life of ILs and LLES a plentitude of information is available; however not from a pharmaceutical point of view. Stability and impurities need to be determined according to the guidelines ‘Stability Testing of New Drug Substances and Products’ and ‘Impurities in New Drug Products’ by the International Conference on Harmonisation of Technical Requirements for Registration of Pharmaceutics for human use (ICH) [32, 33]. To detect the low amounts of decomposition products, which can significantly impair health, adequate and precise analytical methods need to be developed to assure a consistent high quality during storage. Such methods could be liquid chromatography - mass spectrometry (LC-MS) or liquid chromatography followed by charged aerosol detection (HPLC-CAD).

In this contribution, the IL concept was confined to acidic APIs. The promising results suggest expanding the investigations to bases as APIs for IL preparation. However, the motivation of using ILs for basic APIs is slightly different than from what was presented for acidic APIs. Bases are ionized in the acidic gastric fluids after oral administration and their dissolution and apparent solubility are favored. Therefore, deploying ILs for bases may be motivated in an effort to stabilize these against precipitation in cases of higher pH environments or when controlled release profiles are sought.

The focus of the presented studies was an oral application of API-ILs. However, the concept of ILs may obviously be extended to other routes of application. In particular for a transdermal application promising results were presented before [3], though in most of the presented studies no API-ILs were applied but the API was dissolved in an IL, which served as a solvent vehicle in the delivery system [28, 34, 35]. Due to the possibility to tune the permeability by proper counterion

choice, the drug transport through skin may be favorably adapted when transforming an API into an IL and by means of adjustment with lipophilic counterions. Furthermore, controlled API release profiles can be targeted by rational counterion design, which may be desirable when the application frequency of dosing regimens is to be reduced. Other potential routes include trans-epithelial, nasal or trans-corneal, ocular administration, respectively. Highly viscous sticky RT-ILs could offer the possibility to apply high concentrations of API topically minimizing the need for excipients in this delivery system. For an intramuscular application ILs could offer the possibility to inject highly concentrated liquid formulations as well as to provide API release kinetics leading to sustained release [36]. Thus ILs might be used as injectable drug delivery systems with a prolonged release.

In conclusion, ILs were demonstrated to offer a great option for formulation scientist to deliberately adjust the parameters for drug release and bioavailability to the therapeutic needs of patients. At the same time the full pharmaceutical potential of ILs has not even nearly been recognized by the pharmaceutical industry to date. The studies presented here may be regarded as a starting point for this novel formulation platform, leading to a better insight of ILs as a formulation strategy and promising new IL based drug delivery systems.

References

[1] J. Stoimenovski, D. R. MacFarlane, K. Bica, and R. D. Rogers, "Crystalline vs. ionic liquid salt forms of active pharmaceutical ingredients: a position paper," *Pharm Res,* vol. 27, pp. 521-6, Apr 2010.

[2] A. S. Prakash, "The counter ion: expanding excipient functionality," *J. Excipients and Food Chem.*, vol. 2, pp. 28-40, 2011 2011.

[3] W. L. Hough, M. Smiglak, H. Rodriguez, R. P. Swatloski, S. K. Spear, D. T. Daly, *et al.*, "The third evolution of ionic liquids: active pharmaceutical ingredients," *New Journal of Chemistry,* vol. 31, pp. 1429-1436, 2007.

[4] P. M. Dean, J. Turanjanin, M. Yoshizawa-Fujita, D. R. MacFarlane, and J. L. Scott, "Exploring an Anti-Crystal Engineering Approach to the Preparation of Pharmaceutically Active Ionic Liquids," *Crystal Growth & Design,* vol. 9, pp. 1137-1145, Feb 2009.

[5] K. Bica, H. Rodriguez, G. Gurau, O. A. Cojocaru, A. Riisager, R. Fehrmann, *et al.*, "Pharmaceutically active ionic liquids with solids handling, enhanced thermal stability, and fast release," *Chem Commun (Camb),* vol. 48, pp. 5422-4, Jun 4 2012.

[6] O. A. Cojocaru, S. P. Kelley, G. Gurau, and R. D. Rogers, "Procainium Acetate Versus Procainium Acetate Dihydrate: Irreversible Crystallization of a Room-Temperature Active Pharmaceutical-Ingredient Ionic Liquid upon Hydration," *Crystal Growth & Design,* vol. 13, pp. 3290-3293, Aug 2013.

[7] K. Bica and R. D. Rogers, "Confused ionic liquid ions-a "liquification" and dosage strategy for pharmaceutically active salts," *Chem Commun (Camb),* vol. 46, pp. 1215-7, Feb 28 2010.

[8] S. R. Laplante, R. Carson, J. Gillard, N. Aubry, R. Coulombe, S. Bordeleau, *et al.*, "Compound Aggregation in Drug Discovery : Implementing a Practical," 2013.

[9] A. Balk, T. Widmer, J. Wiest, H. Bruhn, J. C. Rybak, P. Matthes, *et al.*, "Ionic liquid versus prodrug strategy to address formulation challenges," *Pharm Res,* vol. 32, pp. 2154-67, Jun 2015.

[10] D. R. MacFarlane, M. Forsyth, E. I. Izgorodina, A. P. Abbott, G. Annat, and K. Fraser, "On the concept of ionicity in ionic liquids," *Phys Chem Chem Phys,* vol. 11, pp. 4962-7, Jul 7 2009.

[11] R. Bini, O. Bortolini, C. Chiappe, D. Pieraccini, and T. Siciliano, "Development of cation/anion "interaction" scales for ionic liquids through ESI-MS measurements," *J Phys Chem B,* vol. 111, pp. 598-604, Jan 25 2007.

[12] S. Dorbritz, W. Ruth, and U. Kragl, "Investigation on aggregate formation of ionic liquids," *Advanced Synthesis & Catalysis,* vol. 347, pp. 1273-1279, Jul 2005.

[13] E. K. Esbjorner, P. Lincoln, and B. Norden, "Counterion-mediated membrane penetration: cationic cell-penetrating peptides overcome Born energy barrier by ion-pairing with phospholipids," *Biochim Biophys Acta,* vol. 1768, pp. 1550-8, Jun 2007.

[14] S. P. Vincent, J. M. Lehn, J. Lazarte, and C. Nicolau, "Transport of the highly charged myo-inositol hexakisphosphate molecule across the red blood cell membrane: a phase transfer and biological study," *Bioorg Med Chem,* vol. 10, pp. 2825-34, Sep 2002.

[15] M. R. Cole, M. Li, B. El-Zahab, M. E. Janes, D. Hayes, and I. M. Warner, "Design, synthesis, and biological evaluation of beta-lactam antibiotic-based imidazolium- and pyridinium-type ionic liquids," *Chem Biol Drug Des,* vol. 78, pp. 33-41, Jul 2011.

[16] R. Ferraz, V. Teixeira, E. Rodrigues, R. Fernandes, C. Prudencio, J. P. Noronha, *et al.*, "Antibacterial activity of Ionic Liquids based on ampicillin against resistant bacteria," *Rsc Advances,* vol. 4, pp. 4301-4307, 2014.

[17] C. Florindo, J. M. Araujo, F. Alves, C. Matos, R. Ferraz, C. Prudencio, *et al.*, "Evaluation of solubility and partition properties of ampicillin-based ionic liquids," *Int J Pharm,* vol. 456, pp. 553-9, Nov 18 2013.

[18] P. C. A. G. Pinto, D. M. G. P. Ribeiro, A. M. O. Azevedo, V. Dela Justina, E. Cunha, K. Bica, *et al.*, "Active pharmaceutical ingredients based on salicylate ionic liquids: insights

into the evaluation of pharmaceutical profiles," *New Journal of Chemistry,* vol. 37, pp. 4095-4102, 2013.

[19] R. A. Kumar, N. Papaiconomou, J. M. Lee, J. Salminen, D. S. Clark, and J. M. Prausnitz, "In vitro cytotoxicities of ionic liquids: effect of cation rings, functional groups, and anions," *Environ Toxicol,* vol. 24, pp. 388-95, Aug 2009.

[20] R. F. M. Frade, A. A. Rosatella, C. S. Marques, L. C. Branco, P. S. Kulkarni, N. M. M. Mateus, *et al.*, "Toxicological evaluation on human colon carcinoma cell line (CaCo-2) of ionic liquids based on imidazolium, guanidinium, ammonium, phosphonium, pyridinium and pyrrolidinium cations," *Green Chemistry,* vol. 11, pp. 1660-1665, 2009.

[21] K. D. Weaver, H. J. Kim, J. Z. Sun, D. R. MacFarlane, and G. D. Elliott, "Cyto-toxicity and biocompatibility of a family of choline phosphate ionic liquids designed for pharmaceutical applications," *Green Chemistry,* vol. 12, pp. 507-513, 2010.

[22] R. Konsoula and F. A. Barile, "Correlation of in vitro cytotoxicity with paracellular permeability in Caco-2 cells," *Toxicol In Vitro,* vol. 19, pp. 675-84, Aug 2005.

[23] K. Fukumoto, M. Yoshizawa, and H. Ohno, "Room temperature ionic liquids from 20 natural amino acids," *J Am Chem Soc,* vol. 127, pp. 2398-9, Mar 2 2005.

[24] H. Ohno and K. Fukumoto, "Amino acid ionic liquids," *Acc Chem Res,* vol. 40, pp. 1122-9, Nov 2007.

[25] J. Kagimoto, K. Fukumoto, and H. Ohno, "Effect of tetrabutylphosphonium cation on the physico-chemical properties of amino-acid ionic liquids," *Chem Commun (Camb),* pp. 2254-6, Jun 4 2006.

[26] P. D. McCrary, P. A. Beasley, G. Gurau, A. Narita, P. S. Barber, O. A. Cojocaru, *et al.*, "Drug specific, tuning of an ionic liquid's hydrophilic–lipophilic balance to improve water solubility of poorly soluble active pharmaceutical ingredients," *New Journal of Chemistry,* vol. 37, pp. 2196-2202, 2013.

[27] P. M. Dean, J. M. Pringle, and D. R. MacFarlane, "Structural analysis of low melting organic salts: perspectives on ionic liquids," *Phys Chem Chem Phys,* vol. 12, pp. 9144-53, Aug 28 2010.

[28] M. Zakrewsky, K. S. Lovejoy, T. L. Kern, T. E. Miller, V. Le, A. Nagy, *et al.*, "Ionic liquids as a class of materials for transdermal delivery and pathogen neutralization," *Proc Natl Acad Sci U S A,* vol. 111, pp. 13313-8, Sep 16 2014.

[29] J. M. M. Araújo, C. Florindo, A. B. Pereiro, N. S. M. Vieira, A. A. Matias, C. M. M. Duarte, *et al.*, "Cholinium-based ionic liquids with pharmaceutically active anions," *RSC Advances,* vol. 4, pp. 28126-28132, 2014.

[30] P. H. Stahl, C. G. Wermuth, and I. U. o. P. a. A. Chemistry, *Handbook of Pharmaceutical Salts Properties, Selection, and Use,* 2 ed. Zürich: VHVA; Weinheim:Wiley-VCH, 2011.

[31] S. D. Kramer, "Absorption prediction from physicochemical parameters," *Pharm Sci Technolo Today,* vol. 2, pp. 373-380, Sep 1999.

[32] "Stability Testing of New Drug Substances and Products Q1A(R2)," vol. 68, ed. US FDA Federal Register: International Conference on Harmonisation (ICH), 2003, pp. 65717-18.

[33] "Impurities of New Drug Products Q3B(R2)," vol. 68, ed. US FDA Federal Register: International Conference of Harmonisation (ICH), 2003, pp. 64628-9.

[34] D. Dobler, T. Schmidts, I. Klingenhofer, and F. Runkel, "Ionic liquids as ingredients in topical drug delivery systems," *Int J Pharm,* vol. 441, pp. 620-7, Jan 30 2013.

[35] M. Moniruzzaman, Y. Tahara, M. Tamura, N. Kamiya, and M. Goto, "Ionic liquid-assisted transdermal delivery of sparingly soluble drugs," *Chem Commun (Camb),* vol. 46, pp. 1452-4, Mar 7 2010.

[36] J. Zuidema, F. Kadir, H. A. C. Titulaer, and C. Oussoren, "Release and absorption rates of intramuscularly and subcutaneously injected pharmaceuticals (II)," *International Journal of Pharmaceutics,* vol. 105, pp. 189-207, 1994.

Abbreviations

A^-	Deprotonated acid
a_nN	Number of nitrogen atoms
a_nO	Number of oxygen atoms
ABL	Aqueous boundary layer
AH	Free acid
ahyd	Number of hydrophobic atoms
AMPA	α-amino-3-hydroxy-5-methyl-4-isoxazolepropionic acid receptor
API	Active pharmaceutical ingredient
B	Free base
BH^+	Protonated base
c	Concentration
$C_{16}M_2Im$	Hexadecyldimethylimidazolium
C_2MIM	1-ethyl-3-methylimidazoium
C_2OHMIM	1-hydroxy-ethyl-3-methylimidazolium
CAD	Charged aerosol detector
C_nMIm	1-Alkyl-3-methyl-imidazolium derivative
CP	Cetylpyridinium
DAPI	4′,6-diamidine-2-phenylindol
DMEM	Dulbecco’s modified Eagle’s medium
DMSO	Dimethyl sulfoxide
DSC	Differential scanning calorimetry
DTA	Differential thermal analysis
DVS	Dynamic vapor sorption
E	Equilibrium
ESI-MS	Electrospray ionization mass spectrometry
FCharge	Number of charges
FDA	Food and Drug Administration
ΔG°	Standard Gibbs energy
GRAS	Generally regarded as safe substance
HBSS	Hank's Buffered Salt Solution
HPLC	High performance liquid chromatography
HTS	High throughput screening
IC_{50}	Half maximal inhibitory concentration

ICH	International Conference on Harmonisation of Technical Requirements for Registration of Pharmaceutics for human use
IL	Ionic liquid
IR	Infrared spectroscopy
j	Crystal formation rate
J	Dissolution rate
lnK	Natural logarithm of the equilibrium constant
K_a	Acid dissociation constant
KCl	Potassium chloride
K_d	Dissociation constant
K_{sp}	Solubility product
LC-MS	Liquid chromatography - mass spectrometry
[Lid][Ibu]	Complex of ibuprofen and lidocaine
LLES	Low lattice enthalpy salt
LLPS	Liquid-liquid state phase separation
logP	Logarithm of the octanol/water partition coefficient
MOE	Molecular Operating Environment
MP	Melting point
NEA	Nonessential amino acids
NMR	Nuclear Magnetic Resonance spectroscopy
NOE	Nuclear Overhauser Enhancement
N_TH_3Sal)	2-amino heptane salicylate
PAMPA	Parallel artificial membrane permeation assay
P_{app}	Apparent permeability coefficients
PBS	Phosphate buffered saline
Pen/Strep	Penicillin and streptomycin
pH_{max}	pH of maximum solubility
PK	Pharmacokinetic
Δ pka	pka difference
PWSD	Poorly water soluble drug
QSAR	Quantitative structure–activity relationship
R^2	Coefficient of determination
RT-IL	Room temperature ionic liquid
S	Supersaturation
S/S_0	Supersaturation ratio
SDS	Sodium dodecylsulfate

T	Temperature
t	Time
TAPH	Tetraalkylphosphonium hexanoate
TAPO	Tetraalkylphosphonium oleate
TBP	Tetrabutylphosphonium
TEA	Tetraethylammonium
TEER	Transepithelial electrical resistance
TFA	Trifluoracetic acid
TG	Glass transition temperature
TGA	Thermal gravimetric analysis
t_{max}	Time to maximum plasma concentration
TSP	3-(trimethylsilyl)propionic acid
UV	Ultraviolet
V	Cell viability
w	weight fraction
WS	Water sorption
XRD	X-ray-diffraction
XRPD	X-ray powder diffractometry
$\Delta\ \alpha$	change in thermal expansivity
λ	Wavelength
ρ	True density
f	Frequency of attachment of unit blocks to a nucleus

Curriculum vitae

Publications:

A. Balk, U. Holzgrabe, L. Meinel, "'Pro et contra' ionic liquid drugs - Challenges and opportunities for pharmaceutical translation," Eur J Pharm Biopharm, 2015, Accepted manuscript.

A. Balk, J. Wiest, T. Widmer, B. Galli, U. Holzgrabe, L. Meinel, "Transformation of acidic poorly water soluble drugs into ionic liquids," Eur J Pharm Biopharm, vol. 94, pp. 73-82, May 2015.

A. Balk, T. Widmer, J. Wiest, H. Bruhn, J. C. Rybak, P. Matthes, et al., "Ionic liquid versus prodrug strategy to address formulation challenges," Pharm Res, vol. 32, pp. 2154-67, Jun 2015.

Acknowledgments

I would like to sincerely thank Prof. Dr. Dr. Lorenz Meinel for giving me the opportunity to perform my thesis in the interesting and versatile area of poorly water soluble drugs, for the possibility to get access to a plentitude of scientific methods and for his helpful advice and support, in particular with the manuscripts.

Furthermore, I would like to express my gratitude to Prof. Ulrike Holzgrabe for the great collaboration with her and her group and for her contribution to the manuscripts.

I am very grateful to Dr. Bruno Galli for the interesting ideas and conversations, his contributions to the manuscripts as well as for the coordination of the cooperation with Novartis, which I greatly acknowledge.

I also would like to thank Prof. Dr. Christoph Sotriffer for the support with the calculations using molecular descriptors.

Special thanks go to Toni Widmer and Johannes Wiest for the great cooperation, for the exchange of ideas and inspiring conversations, for supporting me with regard to NMR, IR, DVS and further analytical techniques, for the contributions to the manuscripts and the nice time we spent together.

I am very grateful to Benjamin Merget for the support with the calculations using molecular descriptors, to PD Dr. Heike Bruhn for the cytotoxicity assessment, to Dr. Christoph Rybak for the support with the XRPD measurements, Dr. Tessa Lühmann for the CLMS pictures of the Caco-2 layers, Dr. Philipp Matthes and Prof. Dr. Klaus Müller-Buschbaum for the single crystal measurements, as well as Dr. Jörg Berghausen and Dr. Anastasios Sakalis. I really would like to thank them for their contributions to the manuscripts.

I would like to mention Sebastian Puhl, Gabriel Jones, Dr. Georg Hiltensperger, Isabel Schulz, Vera Kohl, Dr. Sascha Zügner, Christine Schneider, Cornelia Heindl, Doris Moret and Prof. Dr. Oliver Germershaus and thank them for their support in particular during the first weeks of my work but also later on. Furthermore I would like to thank all members of the group of Prof. Dr. Meinel.

Finally, I would like to thank my family - I am deeply grateful for their constant and immeasurable support.

Documentation of authorship

This section contains a list of the individual contribution for each author to the publications reprinted in this thesis. Unpublished manuscripts are handled, accordingly.

P1	**Balk A, Holzgrabe U, Meinel L** (2015) 'Pro et contra' Ionic liquid drugs – challenges and opportunities for pharmaceutical translation. European journal of pharmaceutics and biopharmaceutics Accepted manuscript

Author	**1**	**2**	**3**										
Study design/concept development	x		x										
Literature analysis and interpretation	x	x											
Manuscript planning	x		x										
Manuscript writing	x	x	x										
Correction of manuscript	x	x	x										
Supervision of Anja Balk			x										

P2	**Balk A, Widmer T, Wiest J, Bruhn H, Rybak J-C, Matthes P, Müller-Buschbaum K, Sakalis A, Lühmann T, Berghausen J, Holzgrabe U, Galli B, Meinel L** (2015) Ionic liquid versus prodrug strategy to address formulation challenges. Pharmaceutical Research **32**(6): 2154-2167

Author	**1**	**2**	**3**	**4**	**5**	**6**	**7**	**8**	**9**	**10**	**11**	**12**	**13**
Ionic liquid and salt preparation	x	x											
High performance liquid chromatography	x	x											
Time lapsed, potentiometrically and photometrically recorded titration experiments for determination of solubility, duration of supersaturation, precipitation rate, pka and dissolution rate	x												
X-ray powder diffractometry	x	x			x								
Differential scanning calorimetry and thermogravimetry	x	x											
Nuclear Magnetic Resonance Measurement			x										
Infrared spectroscopy			x										
Single crystal diffraction	x		x			x	x						
Mass spectrometry								x					
In vitro permeability through the Caco-2 cell monolayer model	x								x				
Cytotoxicity of counterion				x									
Study design/concept development	x	x								x	x	x	x
Data analysis and interpretation	x	x	x								x		x
Manuscript planning	x	x					x			x	x		x
Manuscript writing	x												x
Correction of manuscript	x										x		x
Supervision of Anja Balk													x

P3	**Balk A, Wiest J, Widmer T, Bruhn H, Merget B, Sotriffer C, Galli B, Holzgrabe U, Meinel L** Tuning dissolution , supersaturation and hygroscopicity of an API by counterion design. Unpublished manuscript

Author	**1**	**2**	**3**	**4**	**5**	**6**	**7**	**8**	**9**				
Synthesis of counterions and LLES		x											
Nuclear Magnetic Resonance Measurement		x											
Infrared spectroscopy		x											
High performance liquid chromatography with charged aerosol detector		x											
X-ray powder diffractometry	x												
Differential scanning calorimetry	x												
Determination of dissolution rate	x												
Determination of duration of supersaturation with autotitrator	x												
Shake flask experiments	x												
Dynamic vapor sorption			x										
Cytotoxicity of counterion				x									
Calculation of models using descriptors	x				x								
Statistics	x												
Study design/concept development	x	x					x	x	x				
Data analysis and interpretation	x	x				x		x	x				
Manuscript planning	x							x	x				
Manuscript writing	x								x				
Correction of manuscript	x					x			x				
Supervision of Anja Balk									x				

P4	**Balk A, Wiest J, Widmer T, Galli B, Holzgrabe U, Meinel L** (2015) Transformation of acidic poorly water soluble drugs into ionic liquids. European journal of pharmaceutics and biopharmaceutics **94**: 73–82

Author	**1**	**2**	**3**	**4**	**5**	**6**							
Preparation of ionic liquids and low melting salts	x												
Sodium salt preparation	x												
Nuclear magnetic resonance measurement		x											
Infrared spectroscopy	x	x											
X-ray powder diffractometry	x												
Differential scanning calorimetry	x												
Dynamic vapor sorption			x										
Surface tension	x												
Photometrical determination of dissolution rate	x												
24-h solubility profiles	x												
Study design/concept development	x			x		x							
Data analysis and interpretation	x	x			x	x							
Manuscript planning	x					x							
Manuscript writing	x					x							
Correction of manuscript	x				x	x							
Supervision of Anja Balk						x							

Erklärung zu den Eigenanteilen des Doktoranden sowie der weiteren Doktoranden als Koautoren an Publikationen und Zweitpublikationsrechten bei einer kumulativen Dissertation.

Für alle in dieser kumulativen Dissertation verwendeten Manuskripte liegen die notwendigen Genehmigungen der Verlage (‚reprint permission') für die Zweitpublikation vor, außer das betreffende Kapitel ist noch gar nicht publiziert. Dieser Umstand wird einerseits durch die genaue Angabe der Literaturstelle der Erstpublikation auf der ersten Seite des betreffenden Kapitels deutlich gemacht oder die bisherige Nichtveröffentlichung durch den Vermerk „unpublished" oder „nicht veröffentlicht" gekennzeichnet.

Die Mitautoren der in dieser kumulativen Dissertation verwendeten Manuskripte sind sowohl über die Nutzung als auch über die oben angegebenen Eigenanteile informiert und stimmen dem zu.

Die Anteile der Mitautoren an den Publikationen sind in den vorausgehenden Tabellen aufgeführt.

Prof. Dr. Dr. Lorenz Meinel	05. Juni 2015	Unterschrift
Anja Balk	05. Juni 2015	Unterschrift